

ROYAL HOLLOWAY UNIVERSITY OF LONDON
School of Biological Sciences

**INFLUENCE OF THE BENGUELA CURRENT IN
GENETIC SUB-STRUCTURING OF COMMERCIALY
EXPLOITED FISH SPECIES**

by

Romina Paula Novo Lopes Henriques

Thesis submitted as part of the requirements for the awarding of the degree
of Doctor of Philosophy

November 2011

Declaration of Work

I, Romina Paula Novo Lopes Henriques, hereby declare that all the work presented in this thesis is from my authorship, with the exception of the laboratory techniques employed to isolate microsatellite markers (described in Chapter 2.2.4) that were performed by my colleague Dr Niall McKeown.

Name: 

Date: 18th November 2011

Acknowledgments

The present work would not have been possible without the valuable help of numerous people throughout these last 4 years.

First, and foremost, I would like to thank my supervisor, Paul Shaw, for giving me the opportunity to study such fascinating oceanographic system and its impact on species evolution. Thank you for all the help, guidance and insightful comments that made me learn so much. Also, I would like to thank the Portuguese FCT (Fundação para a Ciência e Tecnologia) that funded this work through a PhD scholarship (SFRH/BD/36176/2007).

This work would not have been the same without the never-ending efforts of Warren Potts and Warwick Sauer. I owe you many of my samples, a lot of my knowledge on life history, and amazing field trips to southern Angola that made my life happier.

Thank you as well to my colleagues: Yoko, Niall, Olgaç and Janek. Your help was very much appreciated in times of trouble and despair. Thank you to the “ancient DNA” people: Ian Barnes, Selina Brace, Jessica Thomas and Peter Heintzman that helped me innumerable times throughout this thesis and provided invaluable conversations about the evolution of species.

In Angola, I would like to thank Prof. Carmen Santos (Universidade Agostinho Neto – Luanda), the Flamingo and Cunene River Mouth Lodge people, Paulo Carqueja, Cabeça, Tim, and Jerry, and the fishing companies Pesca Sede and Sicopal for all the help, all the consideration and all the efforts that made my fieldtrips easier.

Especially, I would like to thank my uncles Manuel and Cassiano Henriques, and cousins Jaime and Elizabeth Novo that took me in, fed me and helped me get to some dodgy places to collect fins at the most unearthly hours. I will never forget all that you have done.

In addition, some of the samples used in this work were collected by local collaborators, to who I am deeply grateful: Tiago Peixoto (*Diplodus* spp); Nuno Prista (*A. regius*);

João Pereira (*D. vulgaris*); Spyker (*A. inodorus*); Michael Steer (*A. japonicus*), and Alejandro de Vera Hernández (*A. aequidens*).

Finally, to all my friends (that are too many to name) that helped me through this journey and kept me sane. Also, many, many thanks to Nuno, for the patience and love, and my family (mom, dad, sis') that stayed by me, and endured hours of random babbling about fish. I love you all very much.

Abstract

Oceanographic features such as currents, fronts and upwelling cells have been recognised as possible factors driving population differentiation within species. The Benguela Current is one of the oldest upwelling systems in the world, located off the west coast of Southern Africa, and represents a biogeographical boundary between the Atlantic and Indo-Pacific Oceans. Previous studies have reported the influence of this system in isolating several marine taxa between the two oceans. However, few have been conducted within the Benguela Current boundaries, in order to understand its role in shaping population genetic structure of fish species at a regional level. The present study documents the influence of the Benguela Current oceanographic features on the genetic differentiation, population connectivity and evolutionary history of five coastal fish species (*Diplodus capensis*, *Argyrosomus inodorus*, *Argyrosomus coronus*, *Atractoscion aequidens* and *Lichia amia*), and one oceanic pelagic fish species (*Thunnus albacares*). Results for both mitochondrial and nuclear marker variation in all coastal species revealed a similar geographical pattern of population genetic structuring despite distinct differences in life history features. The oceanic species exhibited shallow population differentiation between Atlantic and Indian Oceans. For coastal species, different depths of differentiation were observed, ranging from speciation events (*A. aequidens*, *A. coronus* and *A. japonicus*) to shallow structuring (*A. inodorus* and *T. albacares*). Furthermore, in these cases, population structures were coincident with the Benguela Current oceanographic features, suggesting that the system may represent a vicariant barrier to dispersal of coastal fish species. Congruence between mitochondrial and nuclear markers suggests that population isolation was not a single historical event, but has persisted over large timescales and is still active. The existence of cryptic speciation events, and the high levels of genetic diversity and differentiation documented make the Benguela Current a natural laboratory to study evolutionary mechanisms shaping biodiversity and genetic population structure of marine fish species.

Table of Contents

Declaration of Work	2
Acknowledgments	3
Abstract	5
Table of Contents	6
List of Tables	10
List of Figures	17
INTRODUCTION	23
<i>CHAPTER 1: Introduction and State of the Art</i>	<i>24</i>
1.1. The Benguela Current	24
1.1.1. Oceanographic features	24
1.1.2. Changes in the Benguela Current through time	29
1.1.3. The Benguela ecosystem	31
1.2. Population genetics and evolutionary history of marine species	33
1.2.1. Population genetics in marine species: principles and general concepts	33
1.2.2. Molecular markers	34
Mitochondrial DNA and nuclear DNA sequences	35
Microsatellites	36
1.2.3. Usefulness of molecular markers in fisheries management	38
1.3. Influence of oceanographic features in marine fish population structure	40
1.4. The study species	43
1.4.1. <i>Diplodus capensis</i> (Smith, 1844) - Blacktail	44
1.4.2. <i>Argyrosomus</i> spp.	46
<i>Argyrosomus coronus</i> Griffiths & Heemstra 1995 – West coast dusky kob	46
<i>Argyrosomus inodorus</i> Griffiths & Heemstra 1995 – Silver kob	47
<i>Argyrosomus japonicus</i> (Temminck & Schlegel, 1843) – Dusky kob	48
1.4.3. <i>Atractoscion aequidens</i> (Cuvier, 1830) - Geelbeck	49
1.4.4. <i>Lichia amia</i> (L. 1758) - Leerfish	51
1.4.5. <i>Thunnus albacares</i> (Bonaterre, 1890) – Yellowfin tuna	51
1.5. Aims and objectives	53
METHODS	55
<i>CHAPTER 2: General Methodology</i>	<i>56</i>

2.1. Sampling	56
2.2. Molecular techniques	58
2.2.1. DNA extraction	58
2.2.2. PCR amplification and sequencing of mitochondrial and nuclear DNA loci	58
2.2.3. Amplification and screening of microsatellite DNA markers	60
<i>Diplodus capensis</i>	60
<i>Argyrosomus coronus</i> / <i>A. inodorus</i>	61
<i>Thunnus albacares</i>	61
<i>Atractoscion aequidens</i>	62
2.2.4. Isolation of 12 microsatellite markers for <i>Atractoscion aequidens</i> (Cuvier, 1830), Sciaenidae: an overexploited marine fish	63
2.3. Statistical analyses	66
2.3.1. Mitochondrial DNA	66
Population structure and phylogeographic patterns	66
Evolutionary history	67
2.3.2. Microsatellites	70
Population structure	70
Demographic history	71
RESULTS	73
<i>CHAPTER 3: Diplodus capensis</i>	<i>74</i>
3.1. Population structure and evolutionary history of <i>Diplodus capensis</i> (Smith 1844) in a heterogeneous environment: the Benguela Current	74
3.1.1. Introduction	74
3.1.2. Methods	76
3.1.3. Results	80
3.1.4. Discussion	91
<i>CHAPTER 4: Argyrosomus spp.</i>	<i>101</i>
4.1. Tempo and mode of evolution of <i>Argyrosomus</i> spp. (Perciformes, Sciaenidae) in the eastern Atlantic: evidence of Pleistocene origins	101
4.1.1. Introduction	101
4.1.2. Methods	103
4.1.3. Results	106
4.1.4. Discussion	115

4.2. First evidence of climate-induced shifts in dominant species in the Benguela Current: <i>Argyrosomus coronus</i> and <i>Argyrosomus inodorus</i>	123
4.2.1. Introduction	123
4.2.2. Methods	125
4.2.3. Results	129
4.2.4. Discussion	134
4.3. Evolutionary history of <i>Argyrosomus coronus</i> (Perciformes: Sciaenidae) in a highly unstable oceanographic system, the Angola-Benguela Front	141
4.3.1. Introduction	141
4.3.2. Methods	143
4.3.3. Results	147
4.3.4. Discussion	156
<i>CHAPTER 5: Atractoscion aequidens</i>	163
5.1. Population structure and evolutionary history of <i>Atractoscion aequidens</i> (Cuvier, 1830) across the Benguela Current region	163
5.1.1. Introduction	163
5.1.2. Methods	164
5.1.3. Results	167
5.1.4. Discussion	175
5.2. Marine population evolution across the Benguela Current system: molecular evidence for allopatric speciation in a Sciaenid fish, <i>Atractoscion aequidens</i> (Cuvier 1830)	183
5.2.1. Introduction	183
5.2.2. Methods	185
5.2.3. Results	188
5.2.4. Discussion	194
<i>CHAPTER 6: Lichia amia</i>	200
6.1. Population structure and evolutionary history of a coastal pelagic fish in the Benguela Current: <i>Lichia amia</i> (L.1758)	200
6.1.1. Introduction	200
6.1.2. Methods	201
6.1.3. Results	203
6.1.4. Discussion	207
<i>CHAPTER 7: Thunnus albacares</i>	211

7.1. Population and phylogeographic structuring of <i>Thunnus albacares</i> (Bonnaterre, 1788) around southern Africa: implications for fisheries management and conservation	211
7.1.1. Introduction	211
7.1.2. Methods	213
7.1.3. Results	217
7.1.4. Discussion	225
DISCUSSION	231
<i>CHAPTER 8: General Discussion and Conclusions</i>	232
8.1. Limitations of the present work	232
8.1.1. Sampling	233
8.1.2. Markers and statistical analyses	233
8.2. Contributions to the knowledge of genetic population sub-structuring of marine species	235
8.2.1. Genetic diversity and population structure of the study species	235
8.2.2. Comparison of patterns of genetic diversity between the Benguela Current and other oceanographic systems of the world	242
8.3. Contributions to the knowledge of evolutionary and demographic history in marine species	244
8.3.1. Evolutionary history of the study species	244
8.3.2. Demographic history of the study species	248
8.4. Implications of climate change	250
8.5. Implications for fisheries and conservation	252
8.6. Future work	254
8.7. Conclusion	255
BIBLIOGRAPHY	256

List of Tables

- Table 2.1:** Sampling locations around southern Africa for each of the study species: country, region and region code, sample size and latitude/longitude coordinates. 57
- Table 2.2:** Mitochondrial and nuclear DNA loci sequenced, primers utilised, total number of individuals per site sequenced and optimal annealing temperatures (T_a) for each species. 59
- Table 2.3:** Microsatellite loci used to screen genetic variation in *Diplodus capensis*, *Argyrosomus* spp. and *Thunnus albacares*: repeat type, optimised amplification conditions (annealing temperature and number of cycles) and dye labels used. 62
- Table 2.4:** Primer sequences (GenBank accession numbers JF927900-JF927911) and characteristics of 12 microsatellite loci developed for *Atractoscion aequidens*: optimal annealing temperature (T_a); allele numbers (N_a) and size range, observed (H_O) / expected (H_E) heterozygosity. Values in bold were significant following Bonferroni correction. 65
- Table 3.1:** Sampling strategy for *D. capensis* across the Benguela Current region: sampling locations, sample code, sample size and latitude/longitude coordinates. 76
- Table 3.2:** Mitochondrial genetic diversity levels and neutrality tests for *D. capensis* COI region: **n** – number of individuals; **H** – number of haplotypes; **h** – haplotype diversity; π - nucleotide diversity; **F** – Ewens-Waterson neutrality test; **D** – Tajima neutrality test; **F_S** – Fu neutrality test. Statistically significant results ($p < 0.05$) in bold. 81
- Table 3.3:** Pairwise F_{ST} values based on mtDNA COI data, between *D. capensis* samples (see Table 3.1 for sample codes). Statistical significant results in bold ($p < 0.05$). 81
- Table 3.4:** Analysis of molecular variance (AMOVA) results based on COI data, for the three population differentiation scenarios tested. Statistically significant results ($p < 0.005$) in bold. 82
- Table 3.5:** *Diplodus capensis* genetic demographic history for northern and southern Benguela sub-system populations, based on mtDNA COI sequence variation: genetic diversity levels (h and π); neutrality tests (Tajima's D and Fu's F_S); mismatch distribution parameters: σ - time since expansion in mutation units, θ_0 -

population size before expansion, θ_1 – population size after expansion; and time since expansion (T in KY). 83

Table 3.6: Genetic diversity at 8 cross-specific microsatellite loci in *D. capensis* samples: n – number of individuals genotyped; Na – number of alleles; AR – allelic richness (minimum of 16 individuals); H_E – expected heterozygosity; H_O – observed heterozygosity; F_{IS} – inbreeding coefficient. Significant deviations to Hardy-Weinberg expectations in bold. 88

Table 3.7: Pairwise F_{ST} values between *D. capensis* samples based on 8 microsatellite loci. Values significantly greater than zero ($p < 0.05$) in bold. 89

Table 3.8: Analysis of molecular variance (AMOVA) results based on 8 microsatellite loci, for the three population differentiation scenarios tested. Statistically significant results ($p < 0.05$) in bold. 89

Table 3.9: Pairwise F_{ST} values between *D. capensis* samples based on 6 microsatellite loci (potentially selected loci Dvul4 and Dvul33 removed). Values significantly greater than zero ($p < 0.05$) in bold. 90

Table 3.10: Demographic history of *D. capensis* populations in the northern and southern Benguela sub-systems: probability of significant departure from equilibrium population size (i.e. a bottleneck) and estimates of effective population size (N_e + 95% confidence intervals). 91

Table 4.1: Comparison of life history features between *Argyrosomus* species in the eastern Atlantic (adapted from Potts et al. 2010). 102

Table 4.2: Sampling strategy for *Argyrosomus* spp. in the eastern Atlantic, including country, region, sample size, and latitude/longitude coordinates. 103

Table 4.3: Uncorrected pairwise distances between *Argyrosomus* species: concatenated mtDNA-nDNA dataset above diagonal, separate mtDNA / nDNA datasets below diagonal. 107

Table 4.4: Uncorrected pairwise distances between *Argyrosomus* species for individual mtDNA loci: cytb / COI sequence data above diagonal; CR sequence data below diagonal. 107

Table 4.5: Estimates of convergence of run parameters for the three datasets used: split frequencies of standard deviations ($StDev < 0.01$), effective sample size ($ESS > 200$) and potential scale reduction factor ($PSRF \approx 1$). 107

Table 4.6: Estimates of tempo of evolution of *Argyrosomus* spp. in the Benguela Current: $Ln(Likelihood)$ - posterior probabilities of calibration method employed;

tmrca- estimated time since most recent common ancestor (95% HPD in brackets).

115

Table 4.7: Estimates of tempo of evolution of *Argyrosomus* spp. in the Benguela Current for the three mtDNA regions sequenced (CR, COI and cytb): *Ln(Likelihood)* - posterior probabilities of calibration method employed; *tmrca*- estimated time since most recent common ancestor (95% HPD in brackets). 115

Table 4.8: Mitochondrial genetic diversity levels and neutrality tests for *A. inodorus* CR: **n** – number of individuals; **H** – number of haplotypes; **h** – haplotype diversity; π - nucleotide diversity; **F** – Ewens-Waterson neutrality test; **D** – Tajima neutrality test; **F_S** – Fu neutrality test. Statistically significant results ($p < 0.05$) in bold. 130

Table 4.9: *Argyrosomus inodorus* genetic demographic history for northern and southern Benguela sub-system populations, based on mtDNA CR sequence variation: mismatch distribution parameters: σ - time since expansion in mutation units, θ_0 - population size before expansion, θ_1 – population size after expansion; and time since expansion (T in thousand years - KY). Statistical significant results ($p < 0.05$) in bold. 132

Table 4.10: Genetic diversity at 6 cross-specific microsatellite loci in *A. inodorus* samples: **n** – number of individuals genotyped; **Na** – number of alleles; **AR** – allelic richness (minimum of 39 individuals); **H_E** – expected heterozygosity; **H_O** – observed heterozygosity; **F_{IS}** – inbreeding coefficient. Significant deviations to Hardy-Weinberg expectations in bold. 133

Table 4.11: Sampling strategy for *A. coronus* across the northern Benguela sub-system: sampling locations, sample code, sample size and latitude/longitude coordinates 143

Table 4.12: Mitochondrial genetic diversity levels and neutrality tests for *A. coronus* CR: **n** – number of individuals; **H** – number of haplotypes; **h** – haplotype diversity; π - nucleotide diversity; **F** – Ewens-Waterson neutrality test; **D** – Tajima neutrality test; **F_S** – Fu neutrality test. Statistically significant results ($p < 0.05$) in bold. 148

Table 4.13: Pairwise F_{ST} values based on mtDNA CR data, between *A. coronus* samples (see Table 4.11 for sample codes). Values significantly greater than zero ($p < 0.05$) in bold. 148

Table 4.14: *A. coronus* genetic demographic history, based on mtDNA CR sequence variation: genetic diversity levels (**h** and π); neutrality tests (Tajima's **D** and Fu's **F_S**); mismatch distribution parameters: σ - time since expansion in mutation units,

- θ_0 - population size before expansion, θ_1 – population size after expansion; and time since expansion (**T** in KY). Statistical significant results ($p < 0.05$) in bold. 149
- Table 4.15:** Genetic diversity at 6 cross-specific microsatellite loci in *A. coronus* across 5 sites in the northern Benguela sub-system: **n** – number of individuals genotyped; **Na** – number of alleles; **AR** – allelic richness (minimum of 16 individuals); **H_E** – expected heterozygosity; **H_O** – observed heterozygosity; **F_{IS}** – inbreeding coefficient. Significant deviations to Hardy-Weinberg expectations in bold ($p < 0.05$). 151
- Table 4.16:** Pairwise F_{ST} values between *A. coronus* samples based on 6 microsatellite loci (see Table 4.11 for sample codes). Values significantly greater than zero ($p < 0.05$) in bold. 153
- Table 4.17:** Demographic history of the *A. coronus* population in the northern Benguela sub-system: probability of significant departure from equilibrium population size (i.e. a bottleneck) and estimates of effective population size (N_e + 95% confidence intervals). 154
- Table 4.18:** Comparison of genetic diversity at 6 microsatellite loci in obtained for *A. coronus* and Namibian *A. inodorus*: **n** – number of individuals; **Na** – number of alleles; **AR** – allelic richness (minimum of 40 individuals). 154
- Table 4.19:** *A. coronus* (KNA – Namibia, and KA – Angola) and *A. inodorus* (KN) individuals showing evidence of introgressive hybridization as diagnosed by morphology, mtDNA CR sequence data and microsatellite genotypic assignments using STRUCTURE and NewHybrids. 156
- Table 5.1:** Sampling strategy for *A. aequidens* across the Benguela Current region: sampling locations, sample code, sample size and latitude/longitude coordinates. 164
- Table 5.2:** Mitochondrial genetic diversity levels and neutrality tests for *A. aequidens* CR: **n** – number of individuals; **H** – number of haplotypes; **h** – haplotype diversity; π - nucleotide diversity; **F** – Ewens-Watson neutrality test; **D** – Tajima neutrality test; **F_S** – Fu neutrality test. Statistically significant results ($p < 0.05$) in bold. 168
- Table 5.3:** Pairwise F_{ST} values based on mtDNA CR data, between *A. aequidens* samples (see Table 5.1 for sample codes). Values significantly greater than zero ($p < 0.05$) in bold. 169
- Table 5.4:** Analysis of molecular variance (AMOVA) results based on CR data, for the two population differentiation scenarios tested. Statistically significant results ($p < 0.05$) in bold. 169

- Table 5.5:** *Atractoscion aequidens* genetic demographic history for northern and southern Benguela sub-system populations, based on mtDNA COI sequence variation: genetic diversity levels (h and π); neutrality tests (Tajima's D and Fu's F_S); mismatch distribution parameters: σ - time since expansion in mutation units, θ_0 - population size before expansion, θ_1 - population size after expansion; and time since expansion (T in KY). Statistical significant results ($p < 0.05$) in bold. 171
- Table 5.6:** Genetic diversity at 8 microsatellite loci in *A. aequidens* samples: n - number of individuals genotyped; N_a - number of alleles; AR - allelic richness (minimum of 47 individuals); H_E - expected heterozygosity; H_O - observed heterozygosity; F_{IS} - inbreeding coefficient. Significant deviations to Hardy-Weinberg expectations in bold (corrected $p < 0.001$). 173
- Table 5.7:** Pairwise F_{ST} values between *A. aequidens* samples based on 8 microsatellite loci. Values significantly greater than zero (corrected $p < 0.001$) in bold. 174
- Table 5.8:** Analysis of molecular variance (AMOVA) results based on 8 microsatellite loci, for the two population differentiation scenarios tested. Statistically significant results ($p < 0.05$) in bold. 174
- Table 5.9:** Demographic history of *A. aequidens* populations in the northern and southern Benguela sub-systems: probability of departure from equilibrium population size (i.e. a bottleneck) and estimates of effective population size (N_e + 95% confidence intervals). 175
- Table 5.10:** Sampling strategy for *A. aequidens* phylogenetic study: sampling locations, sample code, sample size and latitude/longitude coordinates. 185
- Table 5.11:** Uncorrected pairwise distances calculated for concatenated mtDNA, mtDNA-nDNA and nDNA datasets, between northern (GA) and southern (GSA) clades of *A. aequidens* and different *Argyrosomus* species (see Table 5.10 for species codes). 192
- Table 5.12:** Uncorrected pairwise distances calculated for concatenated mtDNA, mtDNA-nDNA and nDNA datasets, within northern (GA) and southern (GSA) clades of *A. aequidens* and different *Argyrosomus* species (see Table 5.10 for species codes). 192
- Table 5.13:** Genetic differentiation (pairwise F_{ST}) and gene flow (effective migration, N_{em}), calculated for concatenated mtDNA and nDNA datasets, between northern (GA) and southern (GSA) clades of *A. aequidens* and different *Argyrosomus* species (see Table 5.10 for species codes). Values significantly greater than zero ($p < 0.05$) in bold. 193

- Table 5.14:** Estimates of time since divergence for the northern (GA) and southern (GSA) *A. aequidens* clades and *Argyrosomus* spp. (see Table 5.10 for species codes) in the Benguela Current region: Ln(Likelihood) = posterior likelihood of calibration method employed, and estimated time since most recent common ancestor (MY). 193
- Table 6.1:** Sampling strategy for *L.amia* across the Benguela Current: sampling sites, sample codes, sample size and geographical coordinates. 201
- Table 6.2:** Mitochondrial genetic diversity levels and neutrality tests for *L. amia* CR sequences: **n** – number of individuals; **H** – number of haplotypes; **h** – haplotype diversity; π - nucleotide diversity; **F** – Ewens-Waterson neutrality test; **D** – Tajima neutrality test; **F_S** – Fu neutrality test. Statistically significant results (p<0.05) in bold. 204
- Table 6.3:** Pairwise F_{ST} values based on mtDNA CR data, between *L.amia* samples (see Table 6.1 for sample codes). Values significantly different from zero (p<0.005) in bold. 205
- Table 6.4:** *Lichia amia* genetic demographic history for northern and southern Benguela sub-system populations, based on mtDNA CR sequence variation: genetic diversity levels (*h* and π); neutrality tests (Tajima’s D and Fu’s F_S); mismatch distribution parameters: σ - time since expansion, in mutation units; θ_0 - population size before expansion; θ_1 – population size after expansion; and time since expansion (T in KY). Statistical significant results (p<0.05) in bold. 206
- Table 6.5:** Estimates of time since most recent common ancestor for *L. amia* in the Benguela Current based on CR sequences, including 95% highest posterior probabilities (HPD in brackets). 207
- Table 7.1:** Sampling strategy for *T. albacares*: sampling locations, sample code, sample size and latitude/longitude coordinates. 213
- Table 7.2:** Mitochondrial genetic diversity and neutrality tests for *T. albacares* COI region: **n** – number of individuals; **H** – number of haplotypes; **h** – haplotype diversity; π - nucleotide diversity; **F** – Ewens-Waterson neutrality test; **D** – Tajima neutrality test; **F_S** – Fu neutrality test. Statistically significant results (p<0.05) in bold. 218
- Table 7.3:** Pairwise F_{ST} values based on mtDNA COI data, between *T. albacares* samples (see Table 7.1 for sample codes). Values significantly greater than zero (p<0.001) in bold. 219

- Table 7.4:** Analysis of molecular variance (AMOVA) results based on COI data, for the two population differentiation scenarios tested. Statistically significant results ($p < 0.005$) in bold. 219
- Table 7.5:** *Thunnus albacares* genetic demographic history for Atlantic Ocean and Indian Ocean populations, based on mtDNA COI sequence variation: genetic diversity levels (h and π); neutrality tests (Tajima's D and Fu's F_S); mismatch distribution parameters: σ - time since expansion in mutation units, θ_0 - population size before expansion, θ_1 - population size after expansion; and time since expansion (T in KY). Statistical significant results ($p < 0.05$) in bold. 220
- Table 7.6:** Genetic diversity at 6 cross-specific microsatellite loci in *T. albacares* samples: n - number of individuals genotyped; N_a - number of alleles; AR - allelic richness for a minimum of 57 individuals; H_E - expected heterozygosity; H_O - observed heterozygosity; F_{IS} - inbreeding coefficient. Significant deviations to Hardy-Weinberg expectations in bold. 222
- Table 7.7:** Genic and genotypic χ^2 tests, above and below diagonal respectively, between *T. albacares* samples based on 6 microsatellite loci. Statistically significant comparisons after Bonferroni corrections in bold ($p < 0.005$). 223
- Table 7.8:** Pairwise F_{ST} values for *T. albacares* obtained with FreeNA, based on 6 microsatellite loci. Uncorrected values are displayed above the diagonal, values corrected by the ENA method are displayed below the diagonal. Significant results in bold ($\alpha = 0.005$). 223
- Table 7.9:** Demographic history of *T. albacares* populations in the northern and southern Benguela sub-systems: probability of significant departure from equilibrium population size (i.e. a bottleneck) and estimates of effective population size (N_e + 95% confidence intervals). 225

List of Figures

- Figure 1.1:** The Benguela Current system (adapted from Shillington et al. 2004) 26
- Figure 1.2:** *Diplodus capensis* - adapted from Heemstra & Heemstra (2004) 44
- Figure 1.3:** *A. indodorus* - adapted from Griffiths & Heemstra (1995) 47
- Figure 1.4:** *A. japonicus*- adapted from Griffiths & Heemstra (1995) 48
- Figure 1.5:** *A. aequidens* - adapted from Heemstra & Heemstra (2004) 49
- Figure 1.6:** *Licha amia* – adaptated from Heemstra & Heemstra (2004) 51
- Figure 2.1:** Main sampling locations around Southern Africa: Angola, Namibia, and South Africa (see Table 2.1 for details). 56
- Figure 3.1:** Sampling strategy for *D. capensis* across the Benguela Current, highlighting sampling sites, and their position relative to the major oceanographic features of the system: the Benguela, Angola and Agulhas Currents; position of the Angola-Benguela Front; central Namibia upwelling cell; continental shelf width. 77
- Figure 3.2:** Reconstruction of haplotype network for *D. capensis* across the Benguela Current, based on 619bp of mtDNA COI. Node sizes are proportional to the number of haplotypes. Red dots correspond to missing haplotypes. 82
- Figure 3.3:** Mismatch distribution histograms for northern and southern Benguela sub-system *D. capensis* populations, based on mtDNA COI sequences. Filled bars indicate the observed frequency of pairwise differences and the grey line indicates the expected distribution under a model of rapid demographic expansion. 84
- Figure 3.4:** Reconstruction of phylogenetic relationships among COI haplotypes from northern (BA and BN) and southern (BSA) populations of *D. capensis*, plus *D. sargus* (DS) and *D. vulgaris* (DV); posterior probabilities above branches. Units in number of changes per year. 85
- Figure 3.5:** Chronograms of time since divergence (MYA, above nodes) among COI haplotype clades from *D. capensis*, *D. sargus* (DS) and *D. vulgaris* (DV) (grey bars = 95% highest posterior density intervals), using a sequence mutation rate of 1.5% per MY. 86
- Figure 3.6:** Bayesian analysis of individual multi-locus genotype clustering (STRUCTURE) hidden population structure, and admixture levels for *D. capensis* across the Benguela Current region. 90
- Figure 4.1:** Reconstruction of phylogenetic relationships within *Argyrosomus* spp. using the concatenated mtDNA dataset. Statistical support for nodes is given for

both Bayesian (posterior probabilities, above branches) and ML analyses (aRLT values, below branches). Outgroup = *C. nebulosus*. 108

Figure 4.2: Reconstruction of phylogenetic relationships within *Argyrosomus* spp. using the nDNA dataset. Statistical support for nodes is given for both Bayesian (posterior probabilities, above branches) and ML analyses (aRLT values, below branches). Outgroup = *C. nebulosus*. 109

Figure 4.3: Reconstruction of phylogenetic relationships within *Argyrosomus* spp. using the concatenated mtDNA-nDNA dataset. Statistical support for nodes is given for both Bayesian (posterior probabilities, above branches) and ML analyses (aRLT values, below branches). Outgroup = *C. nebulosus*. 109

Figure 4.4: Chronogram of time since divergence estimated for *Argyrosomus* spp., for the mtDNA dataset, using a fixed mutation rate. Grey bars over branches represent 95% highest posterior density (HPD). 111

Figure 4.5: Chronogram of time since divergence estimated for *Argyrosomus* spp., for the mtDNA dataset, applying an internal node calibration point (~ 2 MYA). Grey bars over branches represent 95% highest posterior density (HPD). 111

Figure 4.6: Chronogram of time since divergence estimated for *Argyrosomus* spp., for the mtDNA-nDNA dataset, using a fixed mutation rate. Grey bars over branches represent 95% highest posterior density (HPD). 112

Figure 4.7: Chronogram of time since divergence estimated for *Argyrosomus* spp., for the mtDNA-nDNA dataset, applying an internal node calibration point (~ 2 MYA). Grey bars over branches represent 95% highest posterior density (HPD). 112

Figure 4.8: Chronogram of time since divergence estimated for *Argyrosomus* spp., for the nDNA dataset, using a fixed mutation rate. Grey bars over branches represent 95% highest posterior density (HPD). 113

Figure 4.9: Chronogram of time since divergence estimated for *Argyrosomus* spp., for the nDNA dataset, applying an internal node calibration point (~ 2 MYA). Grey bars over branches represent 95% highest posterior density (HPD). 113

Figure 4.10: Sampling strategy for *A. inodorus* across the Benguela Current region, highlighting sampling sites, and their position relative to the major oceanographic features of the system: position of the Benguela and Agulhas Currents, central Namibia upwelling cell, and continental shelf width. 126

Figure 4.11: HaeIII restriction profiles from COI PCR products of *A. coronus* (lanes 3, 4, 7 and 8) and *A. inodorus* (lanes 5, 6, 9 and 10), plus the unrestricted PCR

product (lane 2) and DNA size ladder Hyperladder II (bright bands = 300bp and 1000bp). 129

Figure 4.12: Reconstruction of haplotype network for *A. inodorus* across the Benguela Current, based on 794bp of mtDNA CR sequences. Node sizes are proportional to the number of haplotypes. Red dots correspond to missing haplotypes. 131

Figure 4.13: Mismatch distribution histograms for northern and southern Benguela sub-system *A. inodorus* populations, based on mtDNA CR sequences. Filled bars indicate the observed frequency of pairwise distribution, grey line indicates the expected distribution under a model of sudden demographic expansion. 132

Figure 4.14: Map of posterior probability of population membership of geo-referenced *A. inodorus* samples, based on 6 microsatellite loci: HEN and EastC. Dark colors delineate areas of higher probability of population membership. Black isolines represent the level of genetic. 134

Figure 4.15: Sampling strategy for *A. coronus* across the northern Benguela sub-system, highlighting sampling sites and their position relative to the major oceanographic features of the system: the Benguela and Angola Currents; position of the Angola-Benguela Front; the major upwelling cell in central Namibia; continental shelf width. 143

Figure 4.16: Reconstruction of haplotype network for *A. coronus* across the northern Benguela sub-system, based on 524bp of mtDNA CR sequences, in samples from 5 sites. Node sizes are proportional to the number of individuals possessing that haplotype. Red dots correspond to missing haplotypes. 149

Figure 4.17: MtDNA CR sequence mismatch distribution histograms for the *A. coronus* population. Filled bars indicate the observed frequency of pairwise distribution, grey line indicates the expected distribution under a model of demographic expansion. 150

Figure 4.18: Allelic frequencies of diagnostic alleles at the six microsatellite loci used to genotype *A. coronus* and *A. inodorus*. 152

Figure 4.19: Factorial Components Analysis for *A. coronus* microsatellite genotypes. Marked circles correspond to outlier individuals: 1 = KA270 (CUN), 2 = KNA19 (HEN), 3 = KA190 (LUC) and 4 = KA258 (LUA). 152

Figure 4.20: Multilocus assignment tests performed in STRUCTURE for hybrid identification based on 6 microsatellite loci: black bars indicate *A. coronus* genotypes, grey bars indicate *A. inodorus* genotypes (see Table 4.17 for individual identification). Dashed lines indicate probability of assignment to each species: $q >$

0.9 – pure *A. coronus*; $q < 0.1$ – pure *A. inodorus*; $0.1 < q < 0.9$ – putative hybrid.

155

Figure 5.1: Sampling strategy for *A. aequidens* across the Benguela Current region, highlighting sampling sites, and their position relative to the major oceanographic features of the system: position of the Benguela and Agulhas Currents, central Namibia upwelling cell, and continental shelf width.

165

Figure 5.2: Reconstruction of haplotype network for *A. aequidens* across the northern Benguela sub-system, based on 578bp of mtDNA CR sequences. Node sizes are proportional to the number of haplotypes. Red dots correspond to missing haplotypes.

170

Figure 5.3: Reconstruction of haplotype network for *A. aequidens* across the southern Benguela sub-system, based on 578bp of mtDNA CR sequences. Node sizes are proportional to the number of haplotypes. Red dots correspond to missing haplotypes.

170

Figure 5.4: Mismatch distribution histograms for northern and southern Benguela sub-system *A. aequidens* populations, based on mtDNA CR sequences. Filled bars indicate the observed frequencies of pairwise mutational differences, grey line indicates the expected distribution under a model of sudden demographic expansion.

171

Figure 5.5: Bayesian analysis of individual multi-locus genotype clustering (STRUCTURE) cryptic population structure, and admixture levels for *A. aequidens* across the Benguela Current region.

175

Figure 5.6: Reconstruction of phylogenetic relationships within *A. aequidens* (GA + GN – northern; GSA – southern Benguela sub-systems) and among *Argyrosomus* species (see Table 5.10 for species codes) from the Benguela region and *Argyrosomus regius* (KP) from Europe, using concatenated mtDNA (CR+COI=cytb) data. Statistical support for nodes is given for both Bayesian (posterior probabilities above branches) and ML analyses (aRLT values below branches). Outgroup: Cneb (*C. nebulosus*).

190

Figure 5.7: Reconstruction of phylogenetic relationships within *A. aequidens* (GA + GN – northern; GSA – southern Benguela sub-systems), using mtDNA-nDNA dataset. Statistical support for nodes is given for both Bayesian (posterior probabilities above branches) and ML analyses (aRLT values below branches). Outgroup: Cneb (*C. nebulosus*).

190

- Figure 5.8:** Reconstruction of phylogenetic relationships within *A. aequidens* (GA + GN – northern; GSA – southern Benguela sub-systems) using nDNA. Statistical support for nodes is given for both Bayesian (posterior probabilities above branches) and ML analyses (aRLT values below branches). Outgroup: Cneb (*C. nebulosus*). 191
- Figure 5.9:** Reconstruction of phylogenetic relationships among *Argyrosomus* species from the Benguela region, and *Argyrosomus regius* (KP) from Europe (see Table 5.10 for species codes), using nDNA data. Statistical support for nodes is given for both Bayesian (posterior probabilities above branches) and ML analyses (aRLT values below branches). Outgroup: Cneb (*C. nebulosus*). 191
- Figure 5.10:** Estimated chronogram of time since divergence for *A. aequidens* clades and *Argyrosomus* species across the Benguela Current region, based on the concatenated mtDNA dataset. Grey bars correspond to the 95% highest posterior probabilities for each estimate (see Table 5.10 for clade and species codes). 194
- Figure 6.1:** Sampling strategy for *L. amia* across the Benguela Current, highlighting sampling sites, and their position relative to the major oceanographic features of the system: the Benguela, Angola and Agulhas Currents; position of the Angola-Benguela Front; central Namibia upwelling cell; continental shelf width. 201
- Figure 6.2:** Reconstruction of haplotype network for *L. amia* across the Benguela Current, based on 581bp of mtDNA CR sequences. Node sizes are proportional to the number of haplotypes. Red dots correspond to missing haplotypes. 204
- Figure 6.3:** Map of posterior probability of population membership of geo-referenced *L. amia* samples, based on mtDNA CR data: FLA (left) and South Africa (right). Dark colors delineate areas of higher probability of population membership. Black isolines represent the level of genetic divergence. 205
- Figure 6.4:** Mismatch distribution histograms for northern and southern Benguela sub-system *L. amia* populations, based on mtDNA CR sequences. Filled bars indicate the observed frequency of pairwise distribution, grey line indicates the expected distribution under a model of sudden demographic expansion. 206
- Figure 7.1:** Reconstruction of haplotype network for *T. albacares*, based on 700bp of mtDNA COI sequences. Branch lengths are proportional to the number of differences, and node sizes are proportional to the number of haplotypes. 218
- Figure 7.2:** Mismatch distribution histograms for Atlantic Ocean and Indian Ocean *T. albacares* populations, based on mtDNA COI sequences. Filled bars indicate the

observed frequency of sequence differences, grey line indicates the expected distribution under a model of rapid demographic expansion. 220

Figure 7.3: Map of posterior probability of population membership of geo-referenced *T. albacares* samples, based on 6 microsatellite loci: Indian Ocean (IO - left) and Atlantic Ocean (BRA - right). Dark colors delineate areas of higher probability of population membership. Black isolines represent the level of genetic differentiation. 224

INTRODUCTION

CHAPTER 1: Introduction and State of the Art

1.1. The Benguela Current

1.1.1. Oceanographic features

The Benguela Cold Current Large Marine Ecosystem is a highly productive upwelling system ($>180 \text{ gCm}^{-2}\text{year}^{-1}$) located off the coast of southwestern Africa (Figure 1.1), from South Africa to Angola (Shannon 1985; Fennel 1999; Boyer et al. 2000). Regional southerly and southeasterly trade winds drive an offshore surface drift that promotes the coastal uprising of cold, nutrient-rich South Atlantic Central water from depths of 200-300m (Krammer et al. 2006). The upwelling system is thought to have begun around 10 million years ago (MYA) (Diester-Haass et al. 1988; Diester-Hass 1990; Krammer et al. 2006). However, the system became fully developed only in the late Miocene or beginning of the Pliocene (6 MYA), and the present oceanographic features were established about 2 MYA (Krammer et al. 2006), making the Benguela Current one of the oldest upwelling systems of the world (Shannon 1985). Currently, the main area of upwelling extends from the Angola-Benguela Front to the Cape of Good Hope, and intermittently as far as the Nelson Mandela Metropole (Port Elizabeth) in eastern South Africa (Shannon 1985) (Figure 1.1.). The system modulates the climate of the nearby coast by restricting the amount of evaporation available for precipitation, and thus the coastal area is a desert region with the Orange River on the Namibian-South African border being the only perennial freshwater body (Marlow et al. 2000).

The Benguela Current is bounded to both north and south by warm tropical currents, the Angola and the Agulhas Currents respectively (Shannon 1985) (Figure 1.1). The Angola current forms the east section of the Guinea gyre (17-24°S), and exhibits a seasonal displacement, contracting northwards during the austral winter and spreading south in the spring (Gyory et al. 2005). The Angola-Benguela Front (ABF) results from the interaction between the Angola and the Benguela currents, and is characterized by eddies with nutrient-rich upwelled water (Fennel 1999; Jahn et al. 2003). Convergence between the two systems takes place approximately off the coast of the Cunene River mouth in southern Angola (16°S) (Shillington et al. 2004; Hutchings et al. 2009). However, the ABF position is linked with the South Atlantic Anticyclone (SAA), and

exhibits seasonal displacement. During the austral summer the SAA spreads south, and the Angola Current flow is at its maximum, resulting in the southwards displacement of the ABF, which may reach Walvis Bay in central Namibia (23°S). Conversely, during austral winter and early spring the SAA moves north, the upwelling intensity off central Namibia increases, and the ABF is displaced northwards, as far as Benguela in central Angola (12°S) (Jahn et al. 2003; Shillington et al. 2004; Hutchings et al. 2009).

The Agulhas current forms the western boundary of the Indian Ocean gyre, flowing down the east coast of Africa (27°-40°S) (Shillington et al. 2004). Once it reaches the southern extremity of the continental shelf (Cape Agulhas) it retroflects and flows eastwards, constituting the Agulhas Return Current (Figure 1.1). One special trait of the Agulhas retroflection is the periodic emission of anticyclonic rings (gyres) of warm, saline Indian Ocean water into the South Atlantic region. The rings maintain their thermal characteristics, hence forming a link between the two oceans, which might have a strong influence in global climate patterns (Gyory et al. 2005).

The major oceanographic features of the Benguela system include (Figure 1.1):

- three boundary regions: two subtropical boundaries off Angola and the Agulhas Bank (South Africa), and a colder boundary in central Namibia;
- the Angola Current, flowing southwards and interacting with the Benguela Current, forming the Angola-Benguela Front;
- a predominantly north-south coastal orientation, from Cape Frio (Namibia) to Cape Agulhas (South Africa), with a north-east trend to the north in southern Angola, and then a north-west trend in central Angola (Benguela);
- three large embayments located at Lobito (central Angola), Walvis Bay (central Namibia), and St. Helena Bay (western South Africa);
- a main upwelling zone between Cape Frio and Cape Agulhas, with a strong perennial upwelling cell off the coast of central Namibia (Lüderitz) that partially separates the system into two sub-systems: northern and southern Benguela;
- multiple and smaller upwelling cells, which occur throughout the region, due to the combination of continental shelf width and coastal topography;
- strongly pulsed upwelling events in cyclic intervals of 3 to 10 days, particularly in southern Benguela, which greatly influence the short-term variability in productivity and fish recruitment;

- cold, highly-productive water occurring in a narrow coastal band between Cape Frio and Cape Agulhas, expanding northwards with movements of the Angola-Benguela Front;
- cold, productive water occurring in the eastern Agulhas Bank, where the Agulhas Current diverges from the coast, and on the central Bank;
- warm, saline Indian Ocean waters injected into the South Atlantic region (Agulhas Rings);
- a poorly-defined outer boundary in the south, due to the presence of the South Atlantic gyre (Hutchings et al. 2009).

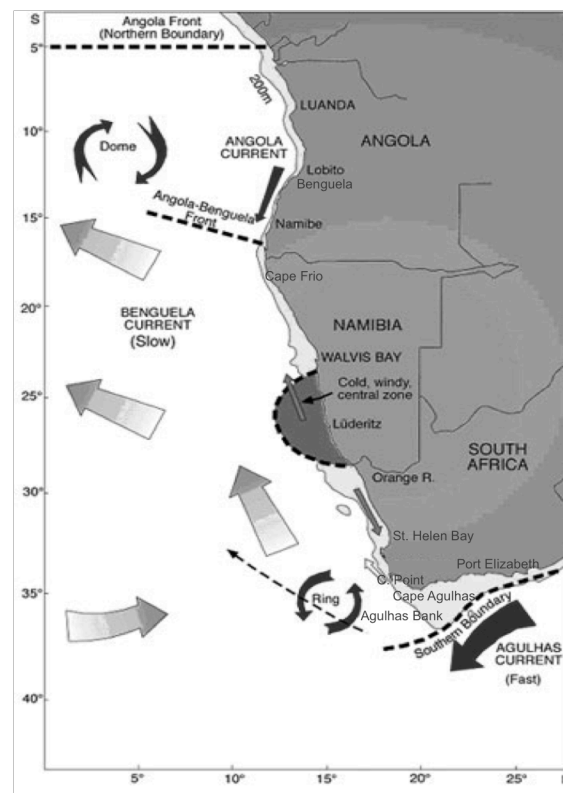


Figure 1.1: The Benguela Current system (adapted from Shillington et al. 2004)

Three main upwelling cells occur within the Benguela Current system in regions of narrower continental shelf and stronger southerly winds: Cape Frio (Namibia), Lüderitz (Namibia) and Cape Point (South Africa) (Hutchings et al. 2009). Despite the upwelling cell at Cape Frio primary productivity in northern Namibia is lower than in the central region, due to the intrusion of warm, nutrient-poor Angolan Current water every austral summer (Hutchings et al. 2009). Since upwelling intensity is closely related to the magnitude of southerly winds and local bathymetry, the northern Benguela sub-system is characterized by a year-round coastal upwelling whilst the southern sub-system

presents seasonal upwelling periods (Sakko 1998; Boyer et al. 2000). Upwelling peaks occur out of phase between the two sub-systems, being recorded during late winter / early spring in the northern sub-system, and during summer / autumn in the southern sub-system (Hutchings et al. 2009). The proximity and interaction with tropical currents, combined with the perennial upwelling cell and colder sea surface temperatures distinguish the Benguela Current from the remaining Large Marine Ecosystems of the world (Boyer et al. 2000; Shillington et al. 2004).

The Benguela Current system can thus be divided in four major regions, each exhibiting distinct oceanographic features: the Angolan subtropical zone; the northern Benguela sub-system; the upwelling area off Lüderitz; and the southern Benguela sub-system (Hutchings et al. 2009).

Angolan subtropical zone: extends from northern to central Angola, and is characterized by severe seasonal sea surface temperature changes, which appear to be influenced by the emission of Kelvin waves by the Equatorial Atlantic waters. The warm season occurs in the austral summer months (December-March), and exhibits highly stratified water and deeper thermocline. The cold season extends from July to September, where the thermocline is closer to the surface (Ostrowski et al. 2009). Wind-driven upwelling occurs between August and September, mainly at the southern boundary (Hutchings et al. 2009).

Northern Benguela sub-system: extends from central Angola to central Namibia and main features include: seasonal movements of the Angola Current; seasonal displacement of the Angola-Benguela Front; low oxygen water bodies and upwelling cells off Cape Frio and Lüderitz (Sakko 1998; Boyer et al. 2000). Large scale, multi-year climatic changes in this region have been observed, and are characterized by either anomalously warm or cold water periods (Boyer et al. 2000; Shillington et al. 2004; Hutchings et al. 2009). Warm water anomalies are thought to originate due to atmospheric changes in the western tropical Atlantic – known as Benguela Niños. In such years the ABF moves further south and warm and saline water advects as far south as Walvis Bay in central Namibia. These intrusions push the thermocline deeper, resulting in low-nutrient upwelling years, and were reported in 1963, 1984 and 1995 (Boyer et al. 2000; Shillington et al. 2004; Hutchings et al. 2009). During colder years, the ABF moves northwards, and colder southern Atlantic water spreads through the system. Reported events (1982, 1986, 1992, 1997) coincide with strong El Niño Southern Oscillation (ENSO) years in the Pacific, and may reflect changes in the South

Atlantic circulation patterns (Hutchings et al. 2009). The occurrence of low-oxygen water results from the interaction of multiple processes such as the intrusion of oxygen-depleted Angolan waters; local decay of biological matter; influx of relatively oxygenated water from Cape Basin due to upwelling off Lüderitz, and stratification of shelf waters (Sakko 1998; Hutchings et al. 2009). The intensity of the oxygen depletion in this region will depend on the interaction of upwelling events at Lüderitz and Cape Frio. A shift towards more oxygenated water has been reported over the last 8 years, which may be related with a decrease in phytoplankton concentrations in the region (Hutchings et al. 2009).

Lüderitz upwelling area: is characterized by strong trade winds resulting in high turbulence, offshore transport and low phytoplankton levels (Sakko 1998; Hutchings et al. 2009). It is considered that the region may represent a potential barrier to dispersal of pelagic phases of multiple fish species, due to disruption of longshore transport (Lett et al. 2007), but that mesopelagic and demersal fishes may not be affected so strongly (Hutchings et al. 2009). As observed in the northern Benguela sub-system, the upwelling cell exhibits cyclic variability, which occurs at an annual and decadal scale, and is related to changes in the South Atlantic cyclone (Sakko 1998; Hutchings et al. 2009).

Southern Benguela sub-system: extends from central Namibia to Nelson Mandela Metropole (Port Elizabeth) in South Africa. As observed in the northern sub-system, the region is characterized by oxygen-depleted waters, which result from the decay of biological matter, but do not reach the same levels observed in northern Benguela. However, a decrease in oxygen has been reported for the last decades, contrary to what is being observed in the northern region (Hutchings et al. 2009). Upwelling intensity is very variable in the South African west coast, and appears to peak in the late summer/autumn (Hutchings et al. 2009).

Upwelling systems, such as the Benguela Current are unstable environments with continuous changes in physical, chemical and biological features (Sakko 1998). Environmental conditions vary both in time and space, resulting in a dynamic ecosystem characterized by times of high but unpredictable primary productivity, thus supporting a low diversity of species (Sakko 1998). Therefore, oceanographic processes inherent to this region play a major role in influencing productivity, which will significantly affect survival of pelagic eggs, larvae and juvenile fish, having a severe impact throughout the trophic web (Cole & McGlade 1998).

1.1.2. Changes in the Benguela Current through time

The Miocene (23-6 MYA) was a time of profound changes in the world atmospheric and oceanic circulation patterns. In particular, during mid- to late-Miocene (12.7-7.7 MYA) major climatic changes occurred due to the beginning of the uplift of the Isthmus of Panama and expansion of Antarctic ice sheets, that led to a generalized cooling of surface and deep water masses (Krammer et al. 2006). In the southern Atlantic these changes led to the establishment of the Benguela Current, about 12 MYA (Siesser 1980; Diester-Haass 1990; Krammer et al. 2006), and were followed by an increase in upwelling intensity around 10 MYA (Diester-Haass 1990; Krammer et al. 2006). Glacial and inter-glacial cycles during the late-Miocene and beginning of the Pliocene resulted in changes in both the Benguela Current circulation patterns and upwelling productivity, which were documented by cyclic depositions of light-dark sediment in the sea floor in the region, changes in the nutrient content of core-sediments, changes in fossil community assemblies and shifts in the dominant calcareous nanoplankton fossil species (Diester-Haass 1990; Krammer et al. 2006). In particular, calcareous nanoplankton assemblies are known to respond quickly to fluctuations in climate as well as alterations in surface-water conditions, and shifts of the dominant species commonly reflect changes in sea surface temperatures, salinity, light and nutrient availability (Krammer et al. 2006).

Lithological changes in the Benguela Current region in the last 12 MY, in particular cyclic depositions of light-dark sediment, are thought to reflect glacial-interglacial cycles and to indicate shifts in the course of the Benguela Current main flow (Krammer et al. 2006). During Antarctic glacial periods, the Benguela system shifted northwards, and in interglacial periods, the system turned westwards into Cape Basin (Krammer et al. 2006). Therefore the position, location of upwelling cells, and circulation patterns of the modern Benguela Current are thought to have progressively migrated northwards during the late Miocene/beginning of the Pliocene (Diester-Haass 1990; Krammer et al. 2006).

In the mid-Miocene steep decreases in carbonate (the carbonate crashes) have been reported all over the globe, particularly in the equatorial regions of Pacific, Indian and Atlantic Oceans (Diester-Haass et al. 2004). The carbonate crashes were also documented in the Benguela region, between 9.6-9 MYA, and were possibly related to

an increase in sediment deposition from the Orange River, which may have reduced oxygen levels and resulted in severe decreases in paleoproductivity (Diester-Haass et al. 2004). These events were then followed by an increase in paleoproductivity by the late Miocene (7-6 MYA) (Krammer et al. 2006).

Changes in the Benguela Current during the Miocene were not limited to productivity levels, circulation patterns and upwelling intensity, but also involved changing sea levels. During the establishment of the Benguela Current, 12 MYA, sea levels were roughly 250m above those of today (Siesser 1980). However, a sudden lowering in sea level occurred at the beginning of the Pliocene (~6 MYA), and by the Pliocene-Pleistocene transition (2 MYA) sea levels had dropped to -300m compared to present day levels (Siesser 1980).

The Pliocene-Pleistocene transition (3-2 MYA) was influenced by the closure of the Central American Seaway (3 MYA), which resulted in the establishment of the north Atlantic deepwater, and the intensification of the northern hemisphere glaciation (Marlow et al. 2000). The establishment of the north Atlantic deepwater led to heat transfer between northern and southern Atlantic, resulting in a generalized cooling in the latter (Marlow et al. 2000). In the Benguela region the Pliocene-Pleistocene transition was accompanied by upwelling intensification (2.9-1.2 MYA) (Marlow et al. 2000), with 5 different phases identified:

- i)** mid-Pliocene (4.6-3.2 MYA): warmer sea surface temperatures, around 26°C, with three cooling events (1-2°C) at 4.1, 3.7 and 3.2 MYA, possibly related with an increase in the Antarctic ice sheets;
- ii)** late Pliocene (3.2-2.1 MYA): gradual cooling, coincident with the onset of the northern hemisphere glaciation. Two major cooling events were reported at 2.8 and 2.5 MYA, with a decrease in sea surface temperatures of up to 2°C;
- iii)** Pleistocene (2-1.4 MYA): rapid decrease in sea surface temperatures (2-3°C at 2.1 and 1.9 MYA);
- iv)** mid-Pleistocene (1.3-0.6 MYA): sea surface temperatures lowered dramatically, coinciding with further intensification of ice sheets during glacial phases, and transition to fluctuating sea surface temperatures similar to the Quaternary glacial-interglacial cycles;
- v)** late Pleistocene (0.5-0.1 MYA): establishment of the Quaternary glacial-interglacial 40 – 100 thousand year (KY) cycles.

During the Pleistocene the Atlantic frontal systems, including the Southern Atlantic Anticyclone and the Subtropical Convergence Zone, were displaced and actively influenced the circulation patterns of the Benguela Current (Marlow et al. 2000; Jahn et al. 2003). The increase in the northern hemisphere ice sheets resulted in a southwards displacement of the South Atlantic Anticyclone, which led to a southern expansion of the Angola-Benguela Front and a decrease in upwelling intensity in the northern Benguela region (Jahn et al. 2003). During the mid-Pleistocene Revolution (0.9-0.4 MYA), the Benguela system entered an unstable mode, which was reflected in the position of the Angola-Benguela Front (Jahn et al. 2003).

Variability of the oceanographic features of the Benguela system occurred throughout the Quaternary, with increased upwelling episodes and colder sea surface waters around 60 and 18 KYA (Kirst et al. 1999).

The Pleistocene age in the Benguela Current was, thus, characterized by abrupt changes in circulation patterns, decreased sea surface temperatures and sea levels that greatly influenced upwelling intensity and productivity (Kirst et al. 1999; Marlow et al. 2000; Jahn et al. 2003).

1.1.3. The Benguela ecosystem

The Benguela Current Large Marine Ecosystem, one of the most productive ecosystems in the world, supports large fish stocks, but exhibits low biodiversity levels (Sakko 1998). Due to high productivity the most abundant fish species are small pelagics such as mullet (*Mugillus* spp.) and horse mackerel (*Trachurus* spp.) (Sakko 1998; Bianchi et al. 1999; Boyer et al. 2000; Hutchings et al. 2009). In the demersal habitat, the ecosystem is dominated by hake (*Merluccius* spp.), goby (*Sufflogobius bibarbatus*), squid and cuttlefish (Sakko 1998; Bianchi et al. 1999). Top fish predators in the region include Cape fur seal (*Arctocephalus pusillus pusillus*), Cape gannets (*Morus capensis*) and penguins (*Spheniscus demersus*) (Sakko 1998; Bianchi et al. 1999; Boyer et al. 2000; Hutchings et al. 2009).

Heavy fisheries exploitation in the last century has led to important changes in the ecosystem structure, particularly in the northern region, with decreases in overall biomass and changes in the dominant species (Heymans et al. 2004; Freon et al. 2005). Sardines (*Sardinops* sp.) and anchovies (*Engraulis capensis*) dominated the pelagic fisheries in the northern Benguela region until 1950. However fishery and climate induced crashes led the populations to very low biomass levels, and resulted in their

replacement mainly by horse mackerel, jellyfish and gobies (Sakko 1998; Heymans et al. 2004; Freon et al. 2005; Hutchings et al. 2009). Additionally, Cape fur seals appear to be increasing in numbers in the region, since they are generalist predators and can easily change target species (Hutchings et al. 2009). In southern Benguela, the ecosystem appears to have remained relatively stable in the last decades, with some changes consisting on the replacement of sardines by anchovies as the most abundant pelagic species in 1960 and 2000s, due to poor-recruitment years for sardines and over-fishing, which resulted in two bursts of abundance and a stabilization of the number of predators (Hutchings et al. 2009).

These obvious differences in the ecosystem composition and reaction to external forces clearly highlight the environmental differentiation between the northern and southern Benguela regions, and the importance of ecosystem-environment interactions.

1.2. Population genetics and evolutionary history of marine species

1.2.1. Population genetics in marine species: principles and general concepts

A continuous challenge in evolutionary biology is to understand the processes by which populations become genetically distinct. Given the apparent absence of physical barriers to dispersion, and the high dispersal potential either as adults or as pelagic eggs/larvae, it was generally considered that marine species were panmictic (Palumbi 1992). However, marine fauna may exhibit significant population sub-structuring, that can be driven by several different forces such as mutation, genetic drift, gene flow and natural selection (Palumbi 1992; Waples 1998; Riginos & Nachman 2001; Hemmer-Hansen et al. 2007).

A species population structure is composed of two parts: demographic structure, that includes biological features associated with life history; and genetic structure, which is determined by the actual population structure but also by mutation, selection and evolution (Sunnucks 2000; Beebee & Rowe 2005; Heddrick 2005). Therefore, one of the main goals of population genetics is to understand the relation between demographic features (such as mating system, rates of births and deaths, etc.) and the distribution of molecular genetic diversity (Sunnucks 2000). Variability in life history features is normally a good indicator of a species genetic sub-structuring patterns (e.g. Graves 1998; Bargelloni et al. 2005; Gaggiotti et al. 2009; Galarza et al. 2009; Gonzalez-Wanguemert et al. 2010).

However, to fully understand population sub-structuring and speciation it is necessary to investigate the “nature, efficacy and timing of barriers to gene flow” between populations (Lessios et al. 2003). For marine organisms such identification has proven to be difficult, as physical barriers are not as easily identifiable as in the terrestrial environment. Nevertheless, several evolutionary mechanisms have been identified as responsible for shaping population genetic sub-structure in different marine species, such as historical climatic fluctuations (Janko et al. 2007; Kenchington et al. 2009; Bester-van der Merwe et al. 2011), biogeographical discontinuities (Joyeux et al. 2001; Lessios et al. 2003; Floeter et al. 2008; Gaither et al. 2010; Sivasundar & Palumbi 2010), oceanographic features (McCartney et al. 2000; Bargelloni et al. 2005; Ravago-Gotanco et al. 2007), environmental gradients leading to local adaptation (Rocha et al. 2005; Taylor & Hellberg 2005; McCairns & Bernatchez 2008) and physical distance

(Gold et al. 2001; Domingues et al. 2007; Medina et al. 2007). In particular, oceanographic features such as fronts, eddies and upwelling cells have recently been identified as playing a major role in genetic sub-structuring of populations, since they can disrupt gene flow between adjacent populations and induce local larval retention (e.g. Waters & Roy 2004; York et al. 2008; Galarza et al. 2009; Vinas et al. 2010; White et al. 2010). The incorporation of oceanographic information into genetic analyses has been termed “seascape genetics”, and derives from the landscape genetics concept designed to test the influence of 2-D environmental factors in spatial genetic sub-structuring (Hansen & Hemmer-Hansen 2007).

1.2.2. Molecular markers

The amount and type of genetic variation in a population are potentially affected by a number of factors such as selection, inbreeding, genetic drift, gene flow and mutation (Sunnucks 2000; Beebee & Rowe 2005; Heddrick 2005). The extent and pattern of molecular variation within a population is generally consistent with neutral variation, which represents a balance between loss of variation by genetic drift and gain by mutational processes (Heddrick 2005). Generally, neutrality of genetic variants can be assumed when the selection coefficient s (either the selective disadvantage of a deleterious allele or the advantage of an adaptive one) is $< 1/(2N_e)$, where N_e stands for the effective population size. Therefore, neutral molecular markers are appropriate to describe demographic history and population evolution (Heddrick 2005). Although marine species traditionally exhibit large census population size, it has been suggested that the effective population size is much smaller (Hauser & Carvalho 2008), and thus neutral markers are also suitable to be applied in such cases.

Genetic markers are heritable characters with multiple states in each character, reflecting modifications in the DNA sequence. In a diploid organism each individual might have one or two different states (alleles/nucleotides) for each character (*locus*). Therefore, separate *loci* can provide an independent test of hypotheses, and the combination of several *loci* can yield extreme sensitivity (Sunnucks 2000). The genetic markers used in population genetics have developed rapidly in recent years, from alloenzymes, RAPD (Randomly Amplified Polymorphic DNA), RFLP (Restriction Fragment Length Polymorphism) and AFLP (Amplification Fragment Length

Polymorphism), to DNA sequencing, DNA microsatellites and SNPs (Single Nucleotide Polymorphism) (DeSalle & Amato 2004).

Mitochondrial DNA and nuclear DNA sequences

The mitochondrial genome consists of a circular DNA “chromosome”, which contains a non-coding region (Control Region or D-loop) plus thirty-six to thirty-seven genes: two ribosomal RNAs, twenty-two transfer RNAs and twelve/thirteen subunits for multimeric proteins of the inner membrane of mitochondria (Brown & Simpson 1979). The Control Region plays an important role in replication and transcription. Mitochondrial DNA (mtDNA) exhibits a limited ability to repair DNA mismatches and it lacks histones. Therefore mutation-fixation rates are ten times higher than those observed in the nuclear genome. High evolution rates affect primarily the protein-coding genes, being lower in the ribosomal RNA genes (Brown & Simpson 1979).

Several models of nucleotide evolution have been described for mtDNA, based on frequency and nucleotide substitution rates. The simplest model is the one described by Jukes & Cantor (1969), which considers equal frequencies for the four nucleotides and equal substitution rates. Other models allow the manipulation of frequencies and/or the substitution rates between transitions and transversions (Beebee & Rowe 2005).

Mitochondrial DNA has been used to investigate phylogenetic and taxonomic relationships at various evolutionary depths due to its unique properties: strictly orthologous genes; lack of recombination; a higher substitution rate compared to the one observed for the nuclear genome; easy isolation; and a smaller effective population size, when compared with the nuclear genome (Awise et al. 1987). Due to its clonal inheritance mode, the effective population size of mtDNA is a quarter of that for nuclear genes (Awise et al. 1987). Under neutrality, the time until the most recent common ancestor (the coalescent process) is proportional to the effective population size, and thus the coalescent process will proceed faster for mitochondrial loci than for alleles at nuclear genes (Awise 2000). As so, mtDNA phylogenetic trees are more likely to reflect the “true” species trees, as events such as complete lineage sorting and reciprocal monophyly will be recorded first in the mtDNA genome than in the nuclear genome (Awise 2000).

In fish species, the Control Region is commonly used in phylogenetic and phylogeographic assessments due to higher mutation rates and polymorphism (Tang et al. 2006). However, although the Control Region is useful in inferring phylogeographic

patterns at a microevolutionary timescale of tens of thousands of years (Avice 2000), homoplasy can confound distance estimation and phylogenetic inference over longer timescales (Tamura & Nei 1993). Because of this, several other mtDNA regions with lower mutation rates have been used such as cytochrome *b*, nicotinamide adenine dinucleotide dehydrogenase subunit 2 (NADH2), cytochrome *c* oxidase I (COI), and the ribosomal RNA 12S and 16S subunits (e.g. Chen et al. 2003; Bernardi & Lape 2005; Ward et al. 2005; Tang et al. 2006; Koblmuller et al. 2007; Chiba et al. 2009; Lakra et al. 2009). Currently the use of the COI gene as a phylogenetic/taxonomic marker is extremely widespread, due to the Barcode of Life Initiative (Hebert et al. 2003). This consortium proposes the use of a 648 base pairs (bp) sequence, defined in relation to the mouse mtDNA genome, as this short DNA sequence gives enough information in terms of nucleotide polymorphism to distinguish between congeneric species, despite the fact that there is only an average of 2% sequence divergence between 98% of congeneric fish species (Hebert et al. 2003; Sevilla et al. 2007).

When dealing with phylogenetic and species identification issues the best option is to use non-contiguous genes that ensure the recovery of accurate phylogenetic patterns. The most common approach is to combine different mitochondrial genes, however the strict dependence on mtDNA, which is maternally inherited, may bias the resulting phylogenetic inference. Maternal inheritance of genes may result in dubious species or supraspecific grouping due to cases of hybridization and introgression, that may cause the “gene tree” not to reflect the “species tree” (Beebee & Rowe 2005). Additionally, due to the circular nature of the mitochondrial genome, the true independence of the genes cannot be assumed, and thus their utility in phylogenetic analysis may be compromised (He et al. 2008). Therefore, use of the nuclear genome (nDNA) for taxonomic/phylogenetic purposes is rising. Genes such as ribosomal 28S and S7, and rhodopsin have been used increasingly in evolutionary studies (Collin 2003; Lavoue et al. 2003; Near & Cheng 2008; Waters et al. 2010).

In conclusion, combining both mtDNA and nDNA analyses may be the best approach when trying to correctly identify phylogenetic or taxonomic relationships.

Microsatellites

Of all nuclear markers, microsatellites are the most commonly used in population studies (Selkoe & Toonen 2006). They consist of tandem repetitions of one to six nucleotides, dispersed in high frequencies (10^4 to 10^5 copies) throughout the nuclear

genome, and are organized in uninterrupted, interrupted or compound loci, e.g. $(AG)_n$, $(GC)_nAT(GC)_n$, and $(GC)_n(AT)_n(GT)_n$ respectively (Estoup & Cornuet 1999).

Microsatellites with small repeat unit patterns (mono- or dinucleotides) occur more frequently, which may be related to slippage of bases during replication. Slippage is thought to occur within the protein complex that mediates DNA replication, as a consequence of mispairing between the original and the newly synthesized DNA strand (Bennett 2000). The resulting region of unpaired DNA is then forced to “loop out”, and if this loop is on the new strand the overall effect is addition of a repeat unit; if it is on the template strand it is removed by enzymes and the overall effect is the loss of a repeat unit (Estoup & Cornuet 1999). Larger repeat units require one strand to slip further before the bases could pair correctly again, and would potentially explain why they are less common in the genome and often more stable (less variable). The rate at which this slippage occurs is not the same as mutation rate, since most “loops” are correctly repaired by the DNA mismatch repair system (Bennett 2000). In addition nucleotide insertions, deletions or substitutions are also responsible for originating new microsatellites (Estoup & Cornuet 1999).

Microsatellites are codominant markers that exhibit Mendelian heritability, which allows distinguishing of heterozygote and homozygote individuals for the same locus (Selkoe & Toonen 2006). Consequently, it is possible to analyze genetic relationships and structure not only at the population level (through allelic frequencies) but also at the individual level (with genotypes) (Selkoe & Toonen 2006). Due to their high mutation rate, which can be five times higher than that observed for other parts of the genome, it is possible to assess recent genetic changes in population structure, thus making these markers extremely useful for population studies (Hedrick 2005). Contrary to multilocus dominant markers (AFLPs, RFLPs), microsatellites are flexible, and they can be analyzed as genotypic arrays, allelic frequencies or gene genealogies (Sunnucks 2000). Furthermore, microsatellites exhibit a highly conserved adjacent sequence region (flank region), which can be used for the siting of DNA primers that will guide amplification reactions (Selkoe & Toonen 2006). The automation of amplification protocols, and the possibility of multiplexing (amplifying different microsatellite loci in one single reaction) with polymerase chain reaction (PCR) have allowed screening of several loci simultaneously and the use of small amounts of tissue, further enhancing the advantages of these markers in population biology and thus contributing for their widespread use (Beaumont 1999; Selkoe & Toonen 2006).

1.2.3. Usefulness of molecular markers in fisheries management

Genetic markers are now being used increasingly in fisheries management for species assignments, definition of stocks and/or assessment of population structure, identification of phylogeographic patterns, and understanding population evolutionary history (Carvalho & Hauser 1994; Coyle 1997; Ward 2000; Cochrane & Doulman 2005). Although allozymes have been used in the past, mitochondrial and nuclear DNA analyses are currently widespread due to the simplicity of the protocols and the emergence of PCR, which allows fast and reliable amplification of small amounts of DNA (Ward 2000).

Due to their faster mutation rate, compared with the nuclear genome, mitochondrial markers are commonly used to investigate phylogeographic patterns (e.g. Avise 2000; Bowen et al. 2006; Diaz-Jaimes et al. 2010; Karl et al. 2011), levels of genetic diversity and population connectivity (e.g. Bremer et al. 1998; Gold & Richardson 1998; Ely et al. 2005; Bester-van der Merwe et al. 2011), and evolutionary history (e.g. von der Heyden et al. 2007; Worheide et al. 2008; Chiba et al. 2009; Corrigan & Beheregaray 2009) in marine species. In particular, these genetic markers are very useful for correct species identification and assignment of individuals, which should be the first step to achieve effective fisheries management (e.g. Bowen et al. 2001; Colborn et al. 2001; Santos et al. 2006; McCairns & Bernatchez 2008; Griffiths et al. 2010). Reconstruction of phylogenetic relationships and phylogeographic patterns using mtDNA markers have revealed interspecific relations and colonization routes throughout the globe, providing valuable insights for conservation and fisheries management (e.g. Bowen et al. 1994; Bowen & Grant 1997; Bowen et al. 2001; Lessios et al. 2003; Waters & Roy 2004; Bowen et al. 2006; Diaz-Jaimes et al. 2010; Chaves-Campos et al. 2011; Karl et al. 2011; Ruzzante et al. 2011)

In marine biology, microsatellites have traditionally been used in the assessment of contemporary stock and population structure for establishing accurate management measures. Genetic studies have provided valuable insights into the genetic sub-structuring of commercially exploited species, subsequently revealing in a number of cases that stocks were composed of more than one genetic population, and so should be managed in different ways. For example king mackerel (*Scomberomorus cavalla*) fisheries were managed as two independent stocks, one in the Atlantic and the other in the Gulf of Florida, but based on capture-recapture data extensive mixing was thought to occur in the summer. Therefore, the boundaries of each stock changed according to

the season. The results obtained for microsatellite markers revealed that Atlantic and Gulf populations were isolated, presenting insignificant gene flow between them, and thus seasonal boundaries were irrelevant and even prejudicial for stock management (Gold et al. 2002). On the other hand Florin & Hoglund (2007) found no evidences of genetic substructuring in turbot (*Psetta maxima*) in the Baltic Sea, despite the highly sedentary life history of the adults. Thus, genetic evidence is essential for the establishment of accurate management measures that will promote the maintenance of stock viability, genetic diversity and, hence, evolutionary potential for exploited marine species.

As such, due to high polymorphism and codominance, microsatellite loci are currently one of the most powerful methods to investigate population structure (Balloux & Lugon-Moulin 2002). Nevertheless, the combination of multiple markers with different mutation rates and inheritance models will provide a more comprehensive picture in the investigation of population structure and evolutionary history of species (Beebee & Rowe 2005). Currently, most studies on genetic diversity and population sub-structuring employ a combination of both mtDNA markers and nDNA microsatellite markers (e.g. Sunnucks 2000, DeSalle & Amato 2004). Due to a clonal inheritance mode, mtDNA retains more historical information than nDNA, and so can be used to assess older processes influencing gene flow and evolution of populations, while nDNA microsatellites exhibit faster mutation rates and are commonly used to document more recent (or “contemporary”) gene flow levels and population dynamics/evolution.

1.3. Influence of oceanographic features in marine fish population structure

Biological populations can be subdivided into smaller clusters (demes) that can have different arrangements in space, time, ecology, etc. (Hedrick 2005). In terms of genetic structure, population subdivision implies that individuals do not mate at random and populations are not panmictic, which can result in different levels of apparent inbreeding when all demes are pooled together (Hedrick 2005). Departures from panmixia can create a correlation between genes in uniting gametes relative to a pair of genes taken at random from the population (Hedrick 2005). Using this concept, Wright (1965) proposed different moment estimators (F statistics) to describe population structure and quantify the effects of inbreeding. The F statistics are commonly defined as a function of observed and expected heterozygosity within demes and populations. A common statistic used in the study of genetic differentiation is F_{ST} – this is a measure of observed genetic diversity within sub-populations relative to observed genetic diversity between sub-populations, and can vary between 0 (no genetic differentiation) and 1 (complete genetic differentiation) (Wright 1965).

Population substructuring in biological species is mainly influenced by barriers to dispersion both in the terrestrial and marine environments. However, in the marine realm average levels of genetic divergence for widespread teleosts are commonly small (average $F_{ST} = 0.020$ for nuclear microsatellites), and lower than those observed for freshwater (average $F_{ST} = 0.144$) or anadromous (average $F_{ST} = 0.081$) species (Ward et al. 1994b; but see Waples 1998). Lower levels of genetic differentiation in marine species are commonly related with higher dispersal potential (as adults or larvae) and historically higher effective population sizes: e.g. *Thunnus thynnus* (mtDNA $F_{ST} = 0.023$; nDNA $F_{ST} = 0.002$ - Carlsson et al. 2004), *Thunnus obesus* (nDNA $F_{ST} = 0.000$ to 0.003 - Gonzalez et al. 2008), or *Coryphaena hippurus* (mtDNA $F_{ST} = 0.000$ to 0.571 - Diaz-Jaimes et al. 2010),

An increasing number of studies have revealed evidence of deep genetic structuring in several widespread marine teleosts (Lakra et al. 2007; Alves-Costa et al. 2008; Han et al. 2008; Lakra et al. 2009), including the highly migratory *Thunnus thynnus* (Carlsson et al. 2004; Reeb 2010; Riccioni et al. 2010). Most patterns of genetic population structuring appear to be related to major biogeographical barriers, such as the Isthmus of Panama (e.g. McCartney et al. 2000; Lessios et al. 2003; Taylor & Hellberg 2005),

the Pacific great divide (e.g. Lessios et al. 1999), or the freshwater output of the Amazon River (e.g. Joyeux et al. 2001).

Environmental conditions can also play a major role in shaping genetic population structure and evolutionary history of marine species at smaller, regional scales. Since most fish species exhibit at least one pelagic phase during their life-cycle, oceanographic features such as currents, fronts, eddies, jets and upwelling cells can also act as effective barriers to dispersion either by limiting adult dispersal, or the transport of pelagic eggs and larvae, promoting local retention and thus restricting gene flow between adjacent populations (Galarza et al. 2009; White et al. 2010). For example, a number of studies have shown genetic population sub-structuring in marine fish linked to oceanographic features such as the Antarctic-Polar Front (*Dissostichus eleginoides* – Shaw et al. 2004); the Balearic and the Almeria-Oran Fronts in the western Mediterranean (*Diplodus sargus*, *Oblada melanura* and *Mullus surmuletus* – Galarza et al. 2009); the Humboldt Current in the eastern Pacific (*Dosidicus gigas* – Sandoval-Castellano et al. 2007); and an upwelling cell off the coast of New Zealand (*Patiriella regularis* – Waters & Roy 2004).

In particular, the Benguela Current is considered one of the major biogeographical barriers in the Atlantic Ocean, and has played an important part in isolating tropical and warm-temperate marine species between the Atlantic and Indo-Pacific Oceans (Floeter et al. 2008). At a regional level the oceanographic features of the system appear to have influenced the evolutionary history of several marine species, namely Cape Hake and hake (*Merluccius capensis* and *M. paradoxus* – von der Heyden et al. 2007, von der Heyden et al. 2010, respectively), Cape fur seal (*Arctocephalus pusillus pusillus* – Matthee et al. 2006), rocky lobster (*Jasus lalandii* – Matthee et al. 2007), and lobster (*Palinurus delagoae* – Gopal et al. 2006). Few studies have shown evidence of genetic population sub-structuring within the Benguela Current system (e.g. Teske et al. 2006; von der Heyden et al. 2007), however, these were mainly conducted in the southern Benguela sub-system, and to date no comprehensive study has been conducted across the Benguela Current region, to compare levels of genetic diversity and population connectivity between populations in the northern and southern sub-systems.

It is easier to identify the influence on genetic diversity of external, environmental factors by comparing several species with identical distribution ranges and biological features (Hickey et al. 2009). Even if species exhibit different life histories, such as different migration abilities and/or different durations of pelagic phases of the life cycle,

it is possible to retrieve common population structure and/or phylogeographic patterns, thus inferring the influence of the environment on population structure and evolutionary history (Hickey et al. 2009). Therefore, in the present study four commercially exploited fish species (*Diplodus capensis*, *Atractoscion aequidens*, *Lichia amia* and *Thunnus albacares*) and one species complex (kob – *Argyrosomus* spp.), presenting different life histories, were used to evaluate the influence of oceanographic features of the Benguela Current in population connectivity, genetic sub-structuring and evolutionary history.

1.4. The study species

The oceanographic processes inherent to the Benguela Current system may be crucial in shaping population structure of local fish species (Hemmer-Hansen et al. 2007; Alemany et al. 2009; Galarza et al. 2009; White et al. 2010). The complex nature of the upwelling regime, including years where there is complete disruption (the Benguela Niños), has a severe influence on productivity which significantly impacts pelagic species by affecting survival of eggs, larvae and juvenile fish (Cole & McGlade 1998). In addition, the perennial upwelling cell off Lüderitz may act as a semi-permanent physical environmental barrier to the longshore transport of pelagic fish eggs and larvae (Lett et al. 2007). Upwelling cells may drive pelagic eggs and larvae offshore, where environmental conditions are unsuitable both for development and survival, thus disrupting recruitment and gene flow between adjacent populations (Waters & Roy 2004). Also the observed distribution and seasonal variation of sea surface temperatures may play an important role in shaping distribution and/or structure of local populations, as most fish species exhibit different optimal temperature preferences throughout their life cycle, presenting specific distribution, spawning seasons and migratory patterns accordingly (Griffiths & Hecht 1995; Griffiths 1997a; Kirchner & Holtzhausen 2001; Potts et al. 2010).

In order to understand the influence of the Benguela Current oceanographic features on population sub-structuring of local fish species, the study species were chosen based on the following criteria: *i*) distribution and migration patterns spanning across the Benguela Current region; *ii*) life history features, namely different optimal temperature preferences, presence and duration of pelagic phases, and differential migration abilities; and *iii*) importance for both commercial fishing industries and local communities. Four of the five chosen species are regional and coastal benthopelagics, whereas one is a cosmopolitan oceanic pelagic. Coastal species are geelbeck (*Atractoscion aequidens*), kob (*Argyrosomus spp.*), blacktail (*Diplodus capensis*) and leerfish (*Lichia amia*), while yellowfin tuna (*Thunnus albacares*) is the oceanic pelagic. All the coastal species are primary targets of recreational and subsistence fisheries in the surf zone, whereas commercial linefish vessels also target *Argyrosomus spp.* and *A. aequidens*, hence creating a multi-user fishery difficult to regulate (Kirchner 1998; Hutton et al. 2001; Heemstra & Heemstra 2004; Potts et al. 2008; Potts et al. 2009; Potts et al. 2010; Richardson 2010). The absence of accurate scientific information and

adequate fishery controls has resulted in signs of over-fishing across the Benguela Current region over the last two decades (Sakko 1998; Bianchi et al. 1999; Hutchings et al. 2009).

1.4.1. *Diplodus capensis* (Smith, 1844) - Blacktail

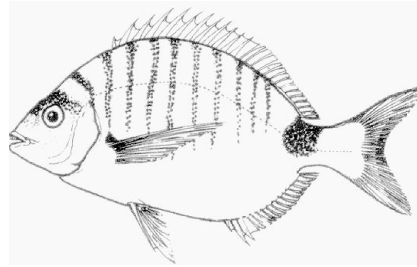


Figure 1.2: *Diplodus capensis* - adapted from Heemstra & Heemstra (2004)

Diplodus capensis (blacktail) belongs to the Sparidae family, and exhibits a tropical-temperate distribution around southern Africa, from Angola to Mozambique (Bianchi et al. 1999; Heemstra & Heemstra 2004). The systematic status of *D. capensis* appears to be unresolved. Based on morphological features De la Paz et al. (1973, in Bargelloni et al. 2005) suggested that the species belongs to a complex also including *Diplodus sargus sargus* in the Mediterranean, *D. sargus cadenatii* in the eastern Atlantic, and *D. sargus lineatus* in the Cape Verde Islands. In a phylogenetic study by Summerer et al. (2001) the complex emerges as a cohesive clade with *D. sargus lineatus* and *D. sargus capensis* in basal positions, although the authors failed to note that the observed genetic differentiation between *D. sargus capensis* and *D. sargus sargus* seems to be high enough to class them as different species. In 2004 Heemstra & Heemstra proposed a change from sub-specific status (*D. sargus capensis*) to species status (*D. capensis*) without additional supporting evidence. Heemstra & Heemstra (2004) also referred to a morphological differentiation between Namibian and South African populations, implying that these populations also may be different species. Finally, Bargelloni et al. (2005) suggested that *D. sargus sargus* and *D. sargus cadenatii* were the same species due to lack of genetic differentiation at nuclear markers (microsatellites). As so, at the moment, *Diplodus capensis* is considered an independent species from the European *D. sargus*, although no further evidence has been brought forward since the genetic survey of Summerer et al. (2001).

Like most sparids, *Diplodus capensis* is a slow growing, long-lived and late maturing species (Heemstra & Heemstra 2004), with maximum reported size for the South African population at 45 cm fork length, corresponding to 3 kg and 21-year old individuals (Mann & Buxton 1997; Mann & Buxton 1998). This species is a generalized benthic carnivore, able to feed in waters with temperatures equal to or colder than 13°C (Lechanteur & Griffiths 2003). Adults are rudimentary protandric hermaphrodites (Mann & Buxton 1998; Richardson 2010), and tend to occur on shallow rocky and sand substrates, whilst juveniles prefer estuaries and tide pools (Heemstra & Heemstra 2004). The eggs and larvae are pelagic, and larvae settle at an average length of 12mm. Patrick & Strydom (2009) demonstrated that *D. capensis* larvae are able to swim up to 32.4km without feeding and at speeds up to 35.2 cm.s⁻¹, a value greater than any previously obtained for other temperate Sparidae larvae. Tagging studies in southern Angola revealed a high degree of adult residency (Richardson 2010), and a recent survey of biological features of southern Angola *D. capensis* revealed significant differences between populations from Angola (northern Benguela sub-system) and South Africa (southern Benguela sub-system) (Richardson 2010). Angolan *D. capensis* appears to grow more slowly (maximum age 31 years) and mature later (15 cm / 5 years) than South African *D. capensis* (maximum age 21 years; mature at 22 cm / 4 years) (Mann & Buxton 1997; Mann & Buxton 1998; Richardson 2010). In addition, morphological studies revealed significant differentiation between the two populations, suggesting that Angolan and South African *D. capensis* may represent isolated populations (Richardson 2010). Spawning season varies between locations, extending from June to October in southern Angola, July to September in KwaZulu-Natal (South Africa), and October to December in Eastern Cape (South Africa) appearing to be linked with local sea surface temperatures of 17-20°C (Mann & Buxton 1997; Mann & Buxton 1998; Richardson 2010).

Diplodus capensis is a valuable fishery resource in southern Angola, representing 87% of total catches from artisanal and subsistence fisheries (Richardson 2010). Based on spawner biomass-per-recruit values for samples caught in protected and un-protected areas Richardson (2010) reported a steep decline, in which exploitation appears to have reduced the species biomass in unprotected areas to 20% of its pristine values. These results highlight the species vulnerability to exploitation, even at local and subsistence levels.

1.4.2. *Argyrosomus* spp.

Argyrosomus spp. (kob) belong to the Sciaenidae family (Sasaki 1989; Griffiths & Heemstra 1995). Kob species are distributed throughout the world, and several species have been described from the Benguela Current region. *Argyrosomus coronus* Griffiths & Heemstra, 1995 occurs from Angola to central Namibia; *A. inodorus* Griffiths & Heemstra, 1995 ranges from northern Namibia to eastern South Africa; and *A. japonicus* (Temminck & Schlegel, 1843) is distributed throughout South Africa (Griffiths & Heemstra 1995). The species originally described from this region, *A. hololepidotus* (Lacepede, 1801) was subsequently found to be endemic to Madagascar (Griffiths & Heemstra 1995). Description of *A. coronus* and *A. inodorus* was based on morphological features such as otoliths and number of swimbladder appendages (Griffiths & Heemstra 1995).

Argyrosomus coronus Griffiths & Heemstra 1995 – West coast dusky kob

The species occurs from northern Angola to southern Namibia, and has been caught as far south as St. Helen Bay in western South Africa (Griffiths & Heemstra 1995; Potts et al. 2010). It is more abundant in northern regions, showing a preference for warmer waters. It may be found in estuaries, surf zones and further offshore, with depth range varying from 20m to 100m (Griffiths & Heemstra 1995; Potts et al. 2010).

Biological features reveal fast growth, with maximum reported size at 190 cm, corresponding to 13 years of age. Size at maturity is estimated at 82cm for males and 90.4 cm for females (4.4 / 4.3 years), and spawning takes place in late spring (November) off the coast of southern Angola (Potts et al. 2010). Although juveniles and sub-adults are commonly found in the region of the Cunene River mouth, the species is not considered to be estuarine dependent due to the absence of permanent estuaries in southern Angola (Griffiths & Heemstra 1995).

Tagging studies revealed that *A. coronus* adults undertake an annual return migration, which appears to be related to the seasonal displacement of the Angola-Benguela Front, migrating northwards during winter and southwards in early spring / summer (Potts et al. 2010). Therefore, it is considered that *A. coronus* is composed of one single panmitic population in Angolan waters. The species life history characteristics are extremely similar to those of other *Argyrosomus* species, namely *A. regius*, from the northeastern

Atlantic and *A. japonicus* from South Africa (Potts et al. 2010). Due to variations in seasonal distribution, *A. coronus* is not frequently caught by the commercial fishery industry, but represents a valuable seasonal target in inshore artisanal and recreational fisheries (Potts et al. 2010). A recent decline in catches has been reported, suggesting that the species may be showing signs of overexploitation (Potts et al. 2010).

Argyrosomus inodorus Griffiths & Heemstra 1995 – Silver kob

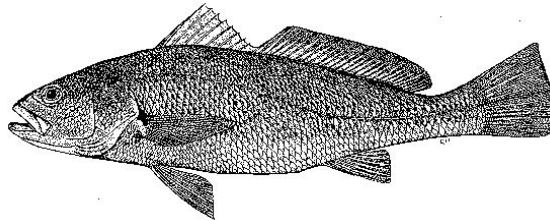


Figure 1.3: *A. inodorus* - adapted from Griffiths & Heemstra (1995)

Argyrosomus inodorus occurs from northern Namibia to the Kei River in South Africa (Griffiths & Heemstra 1995). Depth range varies from 20m to 100m (Griffiths & Heemstra 1995; Kirchner 1998). In eastern South Africa *A. inodorus* rarely enters estuaries or surf zones (Griffiths 1997a), however in more western and cooler areas the species is more abundant in the surf zone (Griffiths & Heemstra 1995; Kirchner 1998). As it does not commonly occur between southern Namibia and Central Point in South Africa, the Namibian population may be isolated from the South African population (Griffiths & Heemstra 1995; Griffiths 1997a; Kirchner & Holtzhausen 2001). Despite reaching similar maximum size (105 cm), growth rates appear to vary between Namibian and South African *A. inodorus*, with maximum reported age of 19 and 25 years, respectively (Griffiths 1997a; Kirchner 1998). In both populations, spawning occurs during the austral spring and early summer (September-December), and maturity is reached at 35-40 cm (~2.4 years) (Griffiths 1997a; Kirchner 1998).

In South African waters *A. inodorus* is divided into three discrete stocks: Western Cape, Southern Cape, and Eastern Cape (Griffiths 1997a). Stocks were identified based on the existence of three different spawning and nursery grounds; observed differences in size at maturity and sex-ratios; growth rate; otolith dimension and length (Griffiths 1997a). In addition, tagging-recapture experiments have shown that there was little migration between the Western and Southern stocks, and virtually none between these and the Eastern stock. In all three stocks, adults exhibited offshore migration during winter,

which might be related to specific temperature preferences of 13-16°C (Griffiths 1997a).

In Namibian waters there is evidence of only one stock (Kirchner 1998), confirmed by the preliminary genetic study of van der Bank & Kirchner (1997), and the tagging-recapture work of Kirchner & Holtzhausen (2001). Namibian *A. inodorus* appears to exhibit a seasonal return migration for spawning for according to Kirchner & Holtzhausen (2001) adults migrate in the beginning of austral summer (January-April) towards southern Namibia to spawn (Meob Bay), then return to the feeding sites in northern Namibia. The eggs and larvae are thought to drift northwards with the Benguela Current until they reach nursery grounds in central Namibia. As juveniles reach two years, they migrate northwards to join the adults on the feeding grounds (Kirchner & Holtzhausen 2001). Although adults can reproduce from a size of 40cm (2.4 years of age), only older adults (6-7 years) undertake the annual return migration (Kirchner & Holtzhausen 2001).

Argyrosomus inodorus is a highly valuable fishery resource throughout its distribution, being targeted by multiple fishery industries (Griffiths 1997a; Kirchner 1998). In Namibia the species is mainly caught by recreational anglers inshore while commercial line-fisheries target it beyond the surf-zone (Kirchner 1998). In South Africa, the species is most commonly caught by the line-fishery industry off the Eastern Cape (Griffiths 1997a).

Argyrosomus japonicus (Temminck & Schlegel, 1843) – Dusky kob

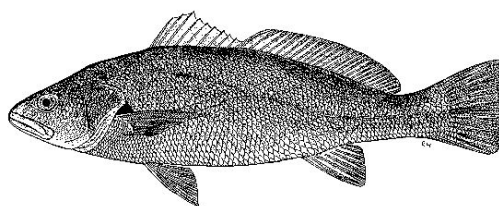


Figure 1.4: *A. japonicus*- adapted from Griffiths & Heemstra (1995)

Argyrosomus japonicus is distributed around southern Africa from the Cape of Good Hope to southern Mozambique, and in the Indo-Pacific Ocean (Sasaki 1989; Griffiths & Heemstra 1995). In South Africa it is found in estuaries, the surf zone and nearshore, to depths of about 50 m. Species abundance is low in the cold waters between the Cape of Good Hope and Namibia (Griffiths 1996, 1997b). Like *A. coronus*, *A. japonicus* is a

large sciaenid, reaching a maximum size of 181 cm, corresponding to 75 kg and 42 years of age (Griffiths 1996).

In South Africa there is strong evidence of migratory behaviour towards the spawning grounds located off KwaZulu-Natal during austral spring, although reproductive activity is also observed, at a lower level, in Western and Eastern Cape Provinces (Griffiths 1996). Spawning season varies with location, occurring in early spring in KwaZulu-Natal (August-November), and in late spring in the Western and Eastern Cape Provinces (October-January) (Griffiths 1996). Size and age at maturity varies between females and males: 110 cm / 6 years, and 92 cm / 5 years, respectively (Griffiths 1996). Adult fish are mainly found in the nearshore environment, juveniles remain exclusively in inshore habitats (surf zone and estuaries), and small juveniles occur only in estuaries (Griffiths 1996). Despite the existence of three different spawning grounds, tagging studies revealed evidence of only one population throughout South Africa, but with a limited individual migration range – the majority of recaptured individuals were within 10 km from the tagging site (Griffiths 1996). Both eggs and larvae are pelagic (Silberschneider & Gray 2008), and experiments by Clark et al. (2005) revealed that settlement occurs on average one month after spawning. Although adults appear to be resident, *A. japonicus* larvae have the ability to disperse over large distances (22.4 km at velocities up to $16.6 \text{ cm}\cdot\text{s}^{-1}$ – Clark et al. 2005).

In South Africa, *A. japonicus* is a valuable prize fish, being predominantly targeted by inshore, recreational anglers (Heemstra & Heemstra 2004).

1.4.3. *Atractoscion aequidens* (Cuvier, 1830) - Geelbeck

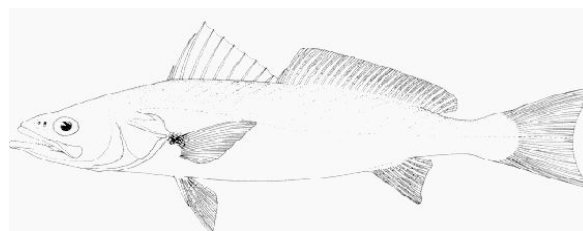


Figure 1.5: *A. aequidens* - adapted from Heemstra & Heemstra (2004)

Atractoscion aequidens (Cuvier, 1830) belongs to the Sciaenidae family (Sasaki 1989). The species occurs mainly in the southeastern Atlantic, from the Gulf of Guinea to South Africa, and in the Indo-Pacific from South Africa to southern Mozambique and in Australia (Bianchi 1999; Heemstra & Heemstra 2004). This is a benthopelagic species,

with a depth range from 15 to 200 m, occurring on sandy substrates, rocky reefs and wrecks (Griffiths & Hecht 1995). It feeds primarily at night on pilchard (*Sardinops sagax*) and horse mackerel (*Trachurus* spp. – Griffiths & Hecht 1995). *Atractoscion aequidens* exhibits a distributional break between western South Africa and southern Namibia due to the colder sea surface temperatures in the region (Griffiths & Hecht 1995). Therefore, it is considered that South African *A. aequidens* may be isolated from northern Benguela *A. aequidens* (Griffiths & Hecht 1995).

South African *A. aequidens* is a fast growing species, reaching up to 130 cm fork length (25 kg) in 9 years (Griffiths & Hecht 1995). Sexual maturity is reached at 90 cm (5 years), and spawning takes place in the austral spring (September-December) off the coast of KwaZulu-Natal. Adults exhibit an annual return migration, which appears to be connected with the annual migration of sardines (Griffiths & Hecht 1995). The South African population appears to be substructured according to age/size, with each subpopulation undertaking well defined migrations: 0-class and one-year-old fish occur mainly in the Eastern Cape, moving to the Western Cape between ages one and two, where they spend two to three years; sub-adults remain in the Western Cape for a further three to four years, moving inshore in summer and offshore in winter, until they reach sexual maturity. Once mature, they migrate annually north-eastwards to spawn off the KwaZulu-Natal coast. Eggs, larvae and possibly early juveniles may be transported southwards by the inshore peripheral waters of the Agulhas current (Griffiths & Hecht 1995).

No biological information is yet available for the northern Benguela population of *A. aequidens*, although it is an important fishery resource in the region where it is targeted by inshore subsistence- and line-fisheries.

The species is primarily a commercial and recreational line-fish species, and has been among the six most important species since the line-fishery industry was first established in the 1800s in South Africa (Hutton et al. 2001). Due to increased fishing pressures, the South African population was considered depleted by 2002 (FAO 2005b).

1.4.4. *Lichia amia* (L. 1758) - Leerfish

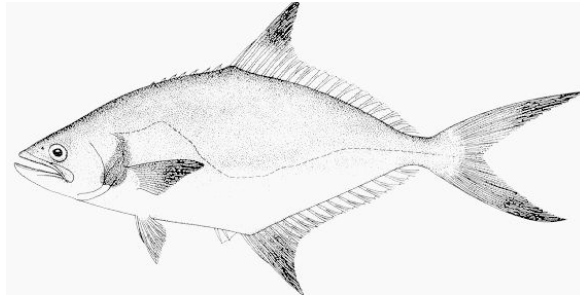


Figure 1.6: *Lichia amia* – adaptated from Heemstra & Heemstra (2004)

Lichia amia (L. 1758) is an inshore pelagic species of the Carangidae family, occurring in the surf zone and to 50 m depth (van der Elst et al. 1992). The species is distributed throughout the Mediterranean Sea, in the eastern Atlantic Ocean from the Gulf of Biscay to South Africa, and in the western Indian Ocean from South Africa to northern Mozambique (van der Elst et al 1992; Heemstra & Heemstra 2004). Maximum reported size is 200cm total length, and 50kg (Heemstra & Heemstra 2004).

As observed for *D. capensis*, a recent study on *L. amia* life history features revealed significant differentiation between samples from the northern (Angola) and southern (South Africa) Benguela regions (Potts et al. 2008). The Angolan *L. amia* populations appear to reach smaller sizes and weights (76.7 cm / 6.8 kg), and mature younger (62.3 cm / 2.4 years) than the South African population (180 cm / 50 kg; 80 cm / 3.5 years – van der Elst et al. 1992; Potts et al. 2008). Spawning seasons vary with location, taking place between June-November in Angola, and September-November in South Africa.

This is a highly prized angling fish species, being mainly targeted by recreational shore-, boat- and spearfishers (Heemstra & Heemstra 2004). In southern Angola the species is also an important resource for the inshore subsistence fishery (Potts et al. 2008), although there is no current information regarding the fishery status.

1.4.5. *Thunnus albacares* (Bonnaterre, 1890) – Yellowfin tuna

Thunnus albacares (Bonnaterre, 1890) is a meso/epipelagic oceanic and cosmopolitan tuna, occurring in offshore waters from the surface to 600m depth, with a global distribution confined to tropical and subtropical waters (FAO 2009). Although a worldwide species, tagging studies revealed that *T. albacares* migrates preferentially within ocean basins and exhibits limited dispersal between oceans (Ward et al. 1994a;

Appleyard et al. 2001). Four main stocks are traditionally considered to occur: Atlantic, Indian, West Pacific and East Pacific (Ward et al. 1994a), and thus in the Benguela Current region it is possible that two of these stocks co-exist, due to the confluence of Atlantic and Indian Oceans in the area. The species can grow to 220cm fork length and 190kg (Heemstra & Heemstra 2004). Sexual maturity is thought to occur at 90 – 100cm fork length, corresponding to 2 years old (Heemstra & Heemstra 2004).

Thunnus albacares represents a globally important fishery resource, and has recently been replacing more endangered tuna species in fisheries throughout the world (Wu et al. 2010). The largest catches occur in the equatorial region of the Pacific Ocean, but *T. albacares* supports a large fishery industry in both the Indian and Atlantic Oceans (Appleyard et al. 2001; Dammannagoda et al. 2008; FAO 2009). Despite a recent decrease in catches, the species is not considered endangered or overexploited (FAO 2009; IUCN 2010).

1.5. Aims and objectives

With fishing pressure increasing throughout the world's oceans, and climate change further threatening the survival of marine species, it is extremely important to assess current biodiversity levels, accurately identify population sub-structuring patterns and reconstruct evolutionary histories of commercially exploited fish species to understand the impact of fishing and provide a base for future sustainable harvesting plans.

In the present study, DNA sequencing and microsatellite genotyping were employed to investigate genetic diversity levels, gene flow / population connectivity, and evolutionary history of five fish species / species complex occurring across the Benguela Current region: *Diplodus capensis*; *Argyrosomus* spp.; *Atractoscion aequidens*; *Lichia amia* and *Thunnus albacares*. The study species were chosen on the basis of their common geographical distribution, contrasting life history characteristics, and because all are highly valuable fishery resources targeted by multiple fishery types across their distribution and are thus vulnerable to over-exploitation.

The overall aim of the present study was to investigate, and thus understand, the relationship between the geographical and historical features of the Benguela Current system and the genetic population connectivity and evolutionary histories of different fish species occurring throughout the region.

This thesis provides the first comprehensive study conducted within the Benguela Current system boundaries, comparing genetic diversity levels, population connectivity and evolutionary histories across a highly heterogeneous marine environment in a poorly studied geographical region. The present work is organized in eight chapters:

- Chapter 2 outlines common methodologies used for all studied species throughout this work, and includes in section 2.2.4 an explanation of the methodology used to isolate and develop microsatellite DNA markers for *A. aequidens*.
- Chapter 3 presents results and discussion of population sub-structuring and evolutionary history of *D. capensis*, based on mitochondrial and microsatellite markers.
- Chapter 4 is divided into three sections: *i*) mode and timing of speciation of the *Argyrosomus* genus in the eastern Atlantic, based on mtDNA and nDNA sequencing; *ii*) identification of *Argyrosomus* species composition in central

Namibia, based on a PCR-RFLP approach, in relation to a southwards distribution shift by *A. coronus*; and *iii*) population sub-structure and evolutionary history of *A. coronus* across its distribution range, based on mtDNA and microsatellite markers.

- Chapter 5 is divided into 2 sections: *i*) population sub-structure and evolutionary history of *A. aequidens* across the Benguela Current system, using mtDNA and newly developed microsatellite markers; and *ii*) evaluation of a cryptic speciation event in *A. aequidens*, based on phylogenetic data.
- Chapter 6 presents results and discussion of population sub-structure and evolutionary history of *L. amia* in the Benguela Current region, based on mtDNA markers.
- Chapter 7 investigates levels of genetic diversity and population connectivity of *T. albacares* around southern Africa, based on mtDNA and microsatellite markers.
- Chapter 8 is a general discussion based on previous chapters, comparing results obtained for the different study species in order to identify common patterns in evolutionary mechanisms shaping population sub-structuring of marine species occurring in heterogeneous environments, and also identify relevance for fishery management across the Benguela Current region.

METHODS

CHAPTER 2: General Methodology

2.1. Sampling

In order to assess the true genetic population sub-structure of a species it is necessary to obtain a representative sample of each population (Beebee & Rowe 2005; Heddrick 2005). Due to the geographical configuration of the Benguela Current and distributions of the studied species sampling took place in Angola, Namibia and South Africa, focusing on 11 main sampling areas distributed across the northern and southern Benguela sub-systems (Table 2.1).

To provide a species-wide scaling of population connectivity, phylogeographic patterns and phylogenetic relationships within each species, samples from outside of the Benguela region were collected by local collaborators in Portugal, Brazil, India and La Réunion (Table 2.1).

Three main sampling campaigns were conducted in Angola during June 2008, 2009 and 2010. Samples were collected from local markets, inshore subsistence fishers and recreational anglers. Namibian and South African samples were collected from recreational anglers during 2008 to 2010 by local collaborators.

One fin clip was removed from each sampled fish, and preserved in 95% ethanol immediately after capture whenever possible.

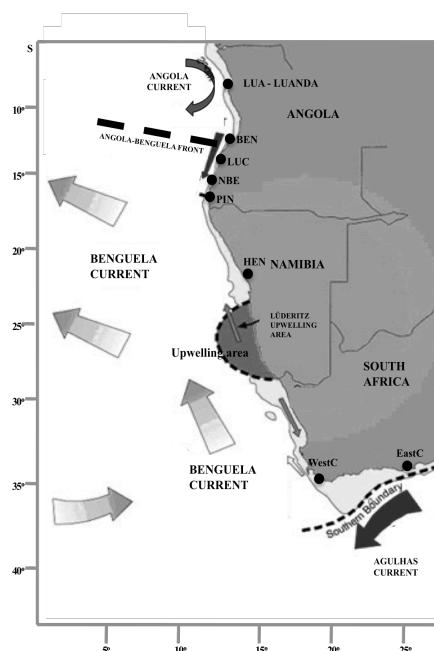


Figure 2.1: Main sampling locations around Southern Africa: Angola, Namibia, and South Africa (see Table 2.1 for details).

Table 2.1: Sampling locations around southern Africa for each of the study species: country, region and region code, sample size and latitude/longitude coordinates.

Species	Country	Region	Region code	Sample size	Coordinates
<i>Atractosion aequidens</i>	Angola	Luanda	LUA	59	8°47.263'S 13°14.32'E
		Baía Farta	BEN	24	12°35.516'S 13°13.595'E
		Lucira	LUC	109	13°50.635'S 12°27.166'E
		Namibe	NBE	79	15°10.374'S 12°04.863'E
		Pinda	PIN	99	15°43.414'S 11°53.658'E
	Namibia	offshore	NAM	9	-
	South Africa	Port Alfred	EastC	79	33°36.50'S 26°54.000'E
	Arniston	WestC	90	34°40.00'S 20°14.000'E	
Mauritanea	-	GM	2	-	
<i>Argyrosomus regius</i>	Portugal	Quarteira	KP	12	37°3.346'N 8°6.43'W
<i>Argyrosomus coronus</i>	Angola	Luanda	LUA	44	8°47.263'S 13°14.32'E
		Lucira	LUC	41	13°50.635'S 12°27.166'E
		Flamingo	FLA	178	15°10.374'S 12°04.863'E
		Cunene	CUN	26	17°15.207'S 11°45.13'E
Namibia	Henties Bay	HEN	86	22°7.404'S 14°16.139'E	
<i>Argyrosomus inodorus</i>	Namibia	Henties Bay	HEN	50	22°7.404'S 14°16.139'E
	South Africa	Port Alfred	EastC	50	33°36.500'S 26°54.000'E
<i>Argyrosomus japonicus</i>	South Africa	Algoa Bay	KSA	15	33°49.53'S 25°52.31'E
<i>Diplodus capensis</i>	Angola	Baía Farta	BEN	108	12°35.516'S 13°13.595'E
		Lucira	LUC	93	13°50.635'S 12°27.166'E
		Inamangando	INA	18	15°16.00'S 12°10.00'E
		Namibe	NBE	124	15°10.374'S 12°04.863'E
		Flamingo	FLA	275	15°10.374'S 12°04.863'E
	Namibia	Henties Bay	HEN	28	22°7.404'S 14°16.139'E
	South Africa	Cape Vidal	KZN	15	28°9.41'S 32°34.57'E
	St. Francis	EastC	80	33°36.500'S 26°54.000'E	
	Arniston	WestC	24	34°40.000'S 20°14.000'E	
<i>Diplodus sargus</i>	Portugal	Quarteira	DS	12	37°3.46'N 8°6.43'W
<i>Diplodus vulgaris</i>	Portugal	Alentejo	DV	20	37°27.20'N 8°49.36'W
<i>Lichia amia</i>	Angola	Flamingo	FLA	101	15°10.374'S 12°04.863'E
	South Africa	Port Alfred	EastC	81	33°36.50'S 26°54.000'E
		Arniston	WestC	17	34°40.00'S 20°14.000'E
<i>Thunnus albacares</i>	South Africa	KwaZulu-Natal	KZN	96	30°47.58'S 30° 25.12'E
		Eastern Cape	EastC	96	33°36.50'S 26°54.000'E
		Western Cape	WestC	96	34°40.000'S 20°14.000'E
	India	Kerala	KER	18	9°1.52'N 76°0.51'E
	La Réunion	Mozambique Channel/ La Réunion	LRE	47	20°34.20'S 52°36.91'E
	Sheychelles	-	SEY	6	4°32.36'S 55°23.35'E
	Brazil	Natal	BRA	96	5°47.218'S 35°10.56'W

2.2. Molecular techniques

2.2.1. DNA extraction

A total genomic DNA extraction was firstly conducted as described in Winnepeninckx et al. (1993), using the cetyltrimethyl ammonium bromide-chloroform / isoamyl alcohol (CTAB) technique. However, the method proved to be ineffective for many samples, whereas a standard phenol / chloroform:isoamyl alcohol extraction (Sambrook et al. 1989) proved to be much more effective. Precipitated DNA was resuspended in 50µl of Sigma Water[®]. Frozen samples, and those found to have less well preserved DNA, were extracted using the PeqLab Classic Line DNA[®] extraction kit.

Approximate concentration of extracted genomic DNA was assessed in a 2% ethidium bromide stained agarose gel, using Hyperladder IV (Bioline) as a size and concentration reference. In order to confirm DNA concentration, a random sample from each extraction batch was quantified in a spectrophotometer (Nanodrop).

2.2.2. PCR amplification and sequencing of mitochondrial and nuclear DNA loci

Assessment of population structure and phylogeographic patterns was conducted based on Polymerase Chain Reaction (PCR) amplification and sequencing of two mitochondrial DNA regions, the Control Region (CR) and the cytochrome c oxidase I (COI) gene region, for 12 to 20 individuals (where possible) per sampling site (Table 2.2).

Universal CR and COI primer pairs were used for *D. capensis*, *Argyrosomus* spp, *A. aequidens* and *L. amia* (Table 2.2). For *T. albacares*, the species-specific primers designed by Paine et al. (2008) were used. In all cases PCR mixtures and amplification protocols followed those described in the original reference, with the exception of annealing temperatures which were optimized here for each species (Table 2.2).

Success of PCR amplification of the target DNA region was assessed visually, for the presence of clean single products of the expected size against a known size standard (Hyperladder II, Bioline UK) in a 1% agarose gel stained with ethidium bromide.

Reconstruction of phylogenetic relationships within and between *A. aequidens* and *Argyrosomus* spp. combined sequences from mtDNA CR and COI (as above) with two further regions, mtDNA cytochrome b (cytb) and the 1st intron of the nuclear ribosomal gene S7. Amplification and sequencing of Cytb used the universal primer pair H16460 / GLUDLC following the original protocols (Palumbi et al. 2002), with annealing temperatures optimised for each species (Table 2.2).

Amplification of the S7 1st intron was first performed with the universal primers S7FRPEX1F and S7FRPEX2R (Chow & Hazama 1998), using the published protocol. However, it was not possible to obtain clear products, thus requiring the identification of species-specific primer pairs. PCR products of the correct expected size were separated and cut from ethidium bromide-stained agarose gels, and the DNA recovered using a Quiagen gel extraction kit[®] for multiple *A. aequidens* and *Argyrosomus* spp. individuals. Gel-extracted products were sequenced with the universal primers in both directions, and obtained sequences aligned using Sequencher 4.7 (GeneCode Corporation). Species-specific primer pairs were designed in Primer 3 (Rozen & Skalecky 1998) and used in subsequent amplification and sequencing:

Argyrosomus spp: S71FK (5' AATCTGCGCGTTTTTCACACCGT 3')

S72RK (5' GGCCTTTGTCTCTGTAGAGAGAAAC 3')

A. aequidens: S71Fga (5' CGCTTTAAAGTCGTTTAATCGGCGC 3')

S71Rga (5' GGCCTTTGTCTCTGTGGGGAGAAAC 3')

Table 2.2: Mitochondrial and nuclear DNA loci sequenced, primers utilised, total number of individuals per site sequenced and optimal annealing temperatures (T_a) for each species.

Amplified region	Primers used and authors	Species	Sample size	T _a (°C)
<u>MtDNA</u> Control Region	L16498/12SARH (Apte & Gardner 2002)	<i>A. aequidens</i>	184	48
		<i>A. coronus</i>	60	50
		<i>A. inodorus</i>	36	49
		<i>A. japonicus</i>	4	50
		<i>A. regius</i>	3	50
		<i>L. amia</i>	57	52
<u>MtDNA</u> Cytochrome oxidase I	FISHF1/FISHR2 (Ward et al. 2005)	<i>A. aequidens</i>	40	48
		<i>Argyrosomus</i> spp.	25	48
		<i>D. capensis</i>	165	48
		<i>D. sargus</i>	5	48
		<i>D. vulgaris</i>	1	48
<u>MtDNA</u> Cytochrome b	GLUDGL/H16460 (Palumbi et al. 2002)	<i>A. aequidens</i>	40	52
		<i>Argyrosomus</i> spp.	25	50
		<i>A. aequidens</i>	40	50
<u>Nuclear DNA</u> 1 st intron S7	S71Fga/S71Rga S71FK/S7R2K (this thesis)	<i>A. aequidens</i>	40	50
		<i>Argyrosomus</i> spp.	25	50

All obtained PCR products were cleaned using an enzymatic digesting protocol, consisting of 0.45U of Exo1 (New England Biolabs) and 0.9U of SAP (Fermentas) in 1x supplied buffer for 20µl of PCR product. PCR cleaning protocol was 37°C for 30 minutes, followed by 80°C for 15 minutes to deactivate enzymes, and 12°C for 5 minutes.

PCR products were sequenced in both directions, in an automated ABI-PRISM sequencer (Macrogen[®]), with the same primers used in the amplification protocols. In S7 the presence of a size-variable microsatellite insertion in the *A. aequidens* sequences made it difficult to sequence reliably through the entire product, so only forward sequences were obtained for this species. All mitochondrial sequences were visually aligned and inspected in BIOEDIT, and for each mtDNA region and species a multiple alignment was performed using CLUSTAL X (Thompson et al. 1997) with default gap opening options. In order to correctly identify and call all heterozygous positions, all S7 sequences were inspected and aligned in Sequencher 4.7 (GeneCode Corporation) using the default multiple alignment parameters.

2.2.3. Amplification and screening of microsatellite DNA markers

Investigation of genetic diversity levels, population sub-structure and recent demographic history was conducted using microsatellites DNA variation for *D. capensis*, *A. coronus*, *A. inodorus*, *A. aequidens* and *T. albacares* (Table 2.3). Standard procedures were used for microsatellite loci amplification, PCR product separation and genotyping, employing either previously published primer sets (*D. capensis*, *A. coronus*, *A. inodorus*, and *T. albacares*) or primer sets developed here (*A. aequidens*). Initially a PCR product screening system using primer labelling with a single fluorescent dye (Cy5), screened using the Pharmacia Biotech ALFExpressII automated slab gel DNA sequencer, was used to screen variation in *T. albacares*. Subsequent studies of *D. capensis*, *A. coronus*, *A. inodorus* and *A. aequidens* employed the Applied Biosystems (AB) 5-fluorescent dye system (6-FAM, NED, VIC and PET), screened on an AB3500 automated capillary DNA sequencer.

Diplodus capensis

Eight cross-specific microsatellite loci were amplified for 70 individuals per sampling site. After testing and optimisation of a range of previously published primers known to amplify in sparid fish the following gave consistent genotyping results: DSaM16,

DSaM27, DSaM34 and DSaM48 developed from the related European species *Diplodus sargus* (Perez et al. 2008); and Dvul4, Dvul33, Dvul61 and Dvul84 developed from another European species *Diplodus vulgaris* (Roques et al. 2007). Optimized PCR mixes included 1x NH₄Cl buffer, 2mM MgCl₂, 0.2mM dNTPs, 0.25pmol of each primer, 0.625U of Taq polymerase (Bioline UK) and 50-100ng of extracted DNA in a final volume of 10µl. Amplification protocols as in the original references were used, with modified annealing temperatures (Table 2.3). PCR products from multiple loci were combined and denatured in 10µl of Hi-Di formamide (AB) containing 0.2µl of 600-LIZ[®] size standard per sample, for 5 min at 95°C, and genotyped on an AB3500 Genetic Analyzer (Applied Biosystems). Genotype scores were generated using GENEMAPPER (ABIPrism).

Argyrosomus coronus / *A. inodorus*

Six cross-specific microsatellite loci (UBA5, UBA40, UBA50, UBA91, UBA853, and UBA854), developed from *Argyrosomus japonicus* (Archangi et al. 2009), were amplified for 40 individuals per sampling site. Optimized PCR mixes included 1x NH₄Cl buffer, 2mM of MgCl₂, 0.2mM of dNTPs, 0.5pmol of each primer, 0.2U of Taq polymerase (Bioline UK) and 50-100ng of extracted DNA in a final volume of 10µl. Published thermoprofile protocols were modified to ensure accurate amplification: changes were made in annealing temperatures and number of cycles (see Table 2.3), and the final extension step of 72°C for 10 min was removed. As for *D. capensis*, PCR products from multiple loci were combined and denatured in 10µl of Hi-Di formamide (AB) containing 0.2µl of 600-LIZ[®] size standard per sample, for 5 min at 95°C, and genotyped on an AB3500 Genetic Analyzer (Applied Biosystems). Genotype scores were generated using GENEMAPPER (ABIPrism).

Thunnus albacares

Four cross-specific microsatellite loci developed from bluefin tuna (*Thunnus thynnus thynnus*) and two *Thunnus albacares*-specific loci were amplified in up to 96 individuals per sampling site. The cross-specific loci were Tth178 and Tth7-16 from Clark et al. (2004) and Tth34 and Tth5 from McDowell et al. (2002), described to work across a wide range of *Thunnus* species, and the species-specific loci were cmrTa113 and cmrTa208 from Appleyard et al. (2001). Optimized PCR mixes included in 1x NH₄Cl buffer, 2.0mM MgCl₂, 0.8mM dNTPs, 1pmol of each primer, 0.4U Taq

polymerase (Bioline UK) and 50-100ng of extracted DNA in a final volume of 20 μ l. Published PCR protocols were modified to ensure optimal amplification rates (see Table 2.3).

PCR products were denatured with formamide plus size markers, and screened on a 6% denaturing polyacrylamide gel run on an ALFexpressII (Pharmacia Biotech) automated sequencer. Product sizes were determined against at least three Cy5-labelled internal size markers using Fragment Manager (Pharmacia Biotech). In order to ensure accurate allele size scoring between runs individuals with known allele sizes were used in each run as positive controls.

Table 2.3: Microsatellite loci used to screen genetic variation in *Diplodus capensis*, *Argyrosomus* spp. and *Thunnus albacares*: repeat type, optimised amplification conditions (annealing temperature and number of cycles) and dye labels used.

Species	Loci	Repetition pattern	T _a (°C)	Number of cycles	Dye label
<i>D. capensis</i>	DSaM16	(CA) ₃₄	58	30	6-FAM
	DSaM27	(CA) ₅ GA(CA) ₅ GA(CA) ₄ CGTGT(CA) ₁₀	58	30	VIC
	DSaM34	(GT) ₃₂	58	30	NED
	DSaM48	(CA) ₂₂	57	35	PET
	Dvul4	(CA) ₁₃	52	30	6-FAM
	Dvul33	(CA) ₁₁	52	30	VIC
	Dvul61	(GT) ₁₈ GA(GT) ₈	53	32	PET
	Dvul84	(GT) ₁₅	53	32	PET
<i>Argyrosomus spp.</i>	UBA5	(CT) ₁₆	48	35	6-FAM
	UBA40	(CA) ₁₇	48	35	PET
	UBA50	(GT) ₂₆	48	35	NED
	UBA91	(CT) ₁₃	52	35	VIC
	UBA853	(GA) ₂₄	48	35	6-FAM
	UBA854	(TG) ₂₃	48	35	VIC
<i>Thunnus albacares</i>	Tth178	(CCT) ₇ CTT(CCT) ₄ (CT) ₂	52	35	Cy5
	Tth7-16	(TATC) ₁₇	53	35	Cy5
	Tth5	(CTGT) ₄	48	35	Cy5
	Tth34	(CTGT) ₇	50	35	Cy5
	cmrTa-113	(CA) ₁₂	50	35	Cy5
	cmrTa-208	(CA) ₁₉	50	35	Cy5

Atractoscion aequidens

Due to the absence of published markers for this species, microsatellite sequences were isolated and locus primers developed for *A. aequidens* - see next section.

2.2.4. Isolation of 12 microsatellite markers for *Atractoscion aequidens* (Cuvier, 1830), Sciaenidae: an overexploited marine fish

Atractoscion aequidens microsatellites were isolated from an enriched partial genomic library created by methods outlined in Glenn & Schable (2005) and McKeown & Shaw (2008). Genomic DNA extracted from fin tissue from 4 individuals (sex unknown) was digested with *Rsa*I restriction enzyme (New England Biolabs), ligated to matching SNX linkers and amplified by PCR using a single primer (SuperSNX-24). PCR mixes contained 2 µl of linked fragments, 1x buffer, 25 µg/ml of BSA (bovine serum albumin), 0.5 µM of SuperSNX-24, 10 mM of dNTPs, 2 mM of MgCl₂, 1 U of *Taq* DNA polymerase (Bioline, UK), in a final volume of 25 µl. Thermocycling profiles consisted on an initial denaturation step of 95°C for 2 min, followed by 20 cycles of 95°C for 20 s, 60°C for 20 s, and a final extension step of 72°C for 1.5 min. Enrichment by selective hybridisation of biotin-labelled repeat motif oligonucleotide probes, (TG)₁₂, (GA)₁₂, (AAAT)₈, (AACT)₈, (AAGT)₈, (ACAT)₈ and (AGAT)₈, with the PCR products was performed in a reaction mix consisting of 2x hybridising solution (12x saline sodium citrate – SSC - plus 0.2% of sodium dodecyl sulfate - SDS), 1 µM of mix of biotin-labelled microsatellite probes and 10 µl of ligated DNA, in a final volume of 50 µl. The hybridisation mixture was incubated on a thermocycler at 95°C for 5 min, followed by 99 cycles of 70°C for 5 s and 0.2°C for 5 s, 20 cycles of 50°C for 10 min followed by a decrease of 0.5°C every 5 s until reaching 40°C. A final cooling step was performed at 15°C for 15 min.

Each enrichment reaction used 50 µl of streptavidin-coated magnetic beads (Dynabeads – DYNAL), which were washed with 250 µl of TE buffer (Tris-EDTA), and placed in a magnetic particle concentrator (MPC), which held the beads against the side of the tube while the free solution was removed by pipetting. This procedure was repeated twice with 1x hybridising solution (6x SSC, 0.1% SDS). Beads were finally resuspended in 150 µl of 1x hybridising solution. The DNA-probe mix was then added to the washed beads and incubated on an orbital shaker for 30 min, at room temperature. The obtained mix (DNA-probe plus cleaned Dynabeads) was then placed in the MPC and the supernatant was removed. A series of increasingly stringent washes of the supernatant were performed, consisting on 2 washes with 400 µl of 1x SSC plus 0.1% SDS, followed by 2 washes with 400 µl 1x SSC plus 0.1% SDS, while heating the solution to 5-10°C of the melting temperature for the oligo mix used (~50°C). After the final wash,

the beads were resuspended in 250 μ l of TE buffer, and the mix was incubated at 95°C for 5 min to separate DNA. The tube was quickly placed in the MPC and the supernatant, containing the enriched pool of fragments to be cloned, removed to a new tube. 22 μ l of sodium acetate/EDTA solution and 444 μ l of 95% ethanol were added to the DNA, and incubated at -20°C overnight. DNA was precipitated by centrifugation at 1300 rpm/min for 10 min. All ethanol was removed and DNA resuspended in 25 μ l of TLE buffer (Tris, Lithium chloride and EDTA). 2 μ l of microsatellite-enriched eluates were PCR amplified as described above and cloned using the TOPO-TA cloning kit, following the manufacturer guidelines (Invitrogen). Recombinant colonies were identified by inactivation of the B-galactosidase gene, individually transferred into 50 μ l of 10 mM Tris-HCL (pH 8.5) and incubated at 95°C for 10 min to promote plasmid DNA release. One μ l of each plasmid extract was submitted to PCR involving M13 forward and reverse primers. The amplification reaction contained 1x buffer, 1.5 mM MgCl₂, 0.2 mM dNTPs, 0.2 U of *Taq* DNA polymerase (Bioline, UK), 10 pmol of each primer and was performed through 30 cycles of 30 s at 95°C, 30 s at 52°C and 30 s at 72°C. PCR products were cleaned using the same enzymatic digestion protocol described in the previous section and sequenced using the internal T7 vector primer. Sequences were analysed using Tandem Repeats Finder (Benson 1999) and, where appropriate, primer pairs designed using Primer 3 (Rozen & Skalecky 1998).

From 32 primer pairs tested 12 polymorphic loci (Table 3.4) were selected for screening of genetic variation in 41 *A. aequidens* individuals collected at Namibe (NBE), Angola. For each locus the respective forward primer was labelled with a fluorescent dye at the 5' -end (Applied Biosystems). Each locus was individually amplified in a 10 μ l reaction mixture containing 100-200 ng of DNA, 1x buffer, 2.0 mM MgCl₂, 0.8 mM dNTPs, 0.2 pmol of each primer, 0.8 U of *Taq* DNA polymerase (Bioline UK). PCR thermoprofiles included an initial denaturation step of 94°C for 2 min, followed by 35 cycles of 94°C for 1 min, optimized annealing temperature (T_a - see Table 3.4) for each primer pair for 30 s, and 72°C for 1 min. PCR products were separated using an AB3500 (Applied Biosystems), and allelic calls performed using the GENEMAPPER 4.1 (Applied Biosystems).

All loci generated high quality products with allele sizes differing by expected multiples of their repeated motifs. Standard diversity indices for each locus, calculated in FSTAT (Goudet 1995), are presented in Table 2.4 along with primer sequences and allele size ranges. Tests for linkage disequilibrium (LD) and deviations of genotype proportions

from expectations of Hardy-Weinberg equilibrium (HWE) were performed for the 41 *A. aequidens* individuals caught in Namibe, using default parameters in GENEPOP 4.0 (Raymond & Rousset 1995). No significant linkage disequilibrium was detected between any locus pair. Genotype proportions conformed to HWE expectations for 10 of the 12 screened loci, with significant departures to HWE found in loci *Geelb28* and *Geelb31* due to an excess of homozygotes (Table 2.4).

Table 2.4: Primer sequences (GenBank accession numbers JF927900-JF927911) and characteristics of 12 microsatellite loci developed for *Atractoscion aequidens*: optimal annealing temperature (T_a); allele numbers (N_a) and size range, observed (H_o) / expected (H_E) heterozygosity. Values in bold were significant following Bonferroni correction.

Locus	Primer sequences (5'-3')	Repeat motif in cloned allele	T_a (°C)	N_a	Size range (bp)	H_o	H_E
Geelb5	F:GCAAGGGTGGGCTTTATT R:GCACACAGGTGTGAGCAT	(GA) ₁₄	56	18	142-196	0.872	0.907
Geelb7	F:TTGTCTTCTCCATCGCTGA R:CCTCTGCAAAATGTTTGTGTT	(CA) ₈ AA (CA) ₄	54	2	86-90	0.024	0.024
Geelb13	F:AACACTGCAGCTTCTGTCAA R:AGGGCTGACCGAGCTAAC	(CTAA) ₉	56	8	101-129	0.610	0.643
Geelb16	F:CGCCGTCACGTAAGTCTG R:CAGCAGACGCACCTTGTT	(CTAT) ₁₇	56	19	116-192	0.951	0.921
Geelb21	F:GCCATGAGCCTCACACAA R:CCGGATGGGACAGACAC	(CA) ₂₅	56	20	117-167	0.878	0.864
Geelb25	F:AATGTGCTTTGGCAATGG R:GGAAGAGATGTCTCTGAAGGAA	(GATA) ₃₀	56	19	146-234	0.925	0.914
Geelb27	F:TGGCCACCAGACTTTGTT R:GTTGGAGCTCTTTTTTCCT	(CTAT) ₂₇	54	19	175-255	0.902	0.926
Geelb28	F:CCTAATTCCTTGGGGTA R:GCACGTAATGAAAATGATGG	(CTAT) ₁₄	50	19	110-190	0.525	0.899
Geelb29	F:TGTGATGAAAATAGGCTGAA R:FGACGATTGCATGTTCTTG	(CTAT) ₁₅	56	19	106-182	0.854	0.911
Geelb30	F:GGTAAACATGTCCTGCCTA R:TTGGCAACAAGACTTTCCA	(GATA) ₁₇	54	17	174-258	0.927	0.911
Geelb31	F:GCTGTTACATAAACATAATATAGT R:TGCTGCTACTGGATCTTTG	(GATA) ₂₅	54	16	120-216	0.732	0.907
Geelb32	F:GGGGCTGAAGATGACCA R:TGGGCTCCTTTTTGTGTT	(GATA) ₂₄ (GATA) ₂₅ (GATA) ₉	54	37	179-313	0.875	0.962

2.3. Statistical analyses

2.3.1. Mitochondrial DNA

Population structure and phylogeographic patterns

Diversity levels were assessed as number of haplotypes, haplotype diversity and nucleotide diversity (H , h and π , respectively) in Arlequin 3.1.1 (Excoffier et al. 2005). Mitochondrial DNA is known to be subject to purifying selection over short timescales, which can influence haplotype frequencies and thus bias estimates of population structure and demographic history estimates (Avice 2000). To account for this potential influence Ewens-Waterson's F (Slatkin 1994), Tajima's D (Tajima 1989) and Fu's F_S (Fu 1997) summary statistics were computed to test whether the data conformed with expectations under neutral (i.e. non-selective) evolution. Statistical significance was assessed after 10000 permutations of the data, in Arlequin 3.1.1 (Excoffier et al. 2005). The most suitable nucleotide substitution model to account for observed patterns of sequence polymorphism was estimated in JModelTest (Posada 2008). Computation of likelihood scores for different models was performed for 5 substitution schemes, including estimation of proportion of invariable sites and gamma distribution, using an optimized Maximum Likelihood base tree. The most likely substitution model was chosen based on the Bayesian Information Criterion (BIC), and used in subsequent analyses.

Assessment of genetic population structure among samples was conducted using estimation of Wright's pairwise F_{ST} , analyses of hierarchical molecular variance (AMOVA), and through reconstructing haplotype relationships. Wright's F_{ST} is a measure of population subdivision, exhibiting values between 0 (no differentiation) and 1 (complete differentiation) between samples (Excoffier et al. 2005). Pairwise F_{ST} comparisons and AMOVA analyses were performed in Arlequin 3.1.1 (Excoffier et al. 2005), and statistical significance assessed after 10000 permutations. Different AMOVA were performed to test multiple hypotheses of differentiation between samples across the Benguela Current, depending on the species analyzed.

Reconstruction of phylogeographic patterns was visualised using a median-joining spanning network, implemented in NETWORK (Bandelt et al. 1999), in order to investigate the geographical distribution of haplotypes. Ambiguous connections between haplotypes, identified as loops, were resolved using the coalescent theory

approach: any given haplotype should be preferentially linked with the most abundant and/or geographically closest occurring haplotypes, as suggested by Grant & Bowen (2006).

Evolutionary history

Under normal demographic conditions coalescent processes ensure genealogical connections among genotypes within a species via vertical descent, even in the absence of interchange between lineages, due to mating and gene flow (Avice 2000). Therefore coalescent theory suggests that it is possible to follow a specific lineage back through time until reaching the most recent common ancestor. Based on the coalescent theory, demographic changes in population size will leave specific genetic signatures in the distribution of sequence types (haplotypes) within populations that can be detected using the appropriate methods. Reconstruction of evolutionary history may give useful insights into different evolutionary scenarios and past population genetic processes that influence a species' current genetic architecture.

In the present work, assessment of evolutionary history of populations was conducted by estimating measures of haplotype and nucleotide diversity, and calculating Tajima's D (Tajima 1989) and Fu's F_S (Fu 1997) statistics, which have been used to document past demographic events that may be related to historical climatic changes (Avice 2000; Grant & Bowen 2006; Hill et al. 2011; Lo Brutto et al. 2011). Grant & Bowen (1998) suggested a classification scheme for the relationship between haplotype and nucleotide diversity levels, which may give insight into a species demographic history. Marine fish species tend to exhibit high diversity levels, partially due to historically large effective population sizes, and Grant and Bowen (1998) suggested 4 different broad categories for the combination of diversity indices (h and π):

1. $h < 0.5$ and $\pi < 0.5\%$ - recent bottleneck or founder event; periodic region-wide bottlenecks or metapopulation structure within regions;
2. $h > 0.5$ and $\pi < 0.5\%$ - population expansion after a period of low effective population size; bottleneck followed by rapid population growth and accumulation of mutations;
3. $h < 0.5$ and $\pi > 0.5\%$ - strong historically recent bottleneck in a formerly large and stable population, or secondary contact between previously isolated populations: few, highly divergent haplotypes;

4. $h > 0.5$ and $\pi > 0.5\%$ - long evolutionary history of large and stable population size, or secondary contact between previously differentiated allopatric and diverse lineages.

Furthermore, fluctuations in effective population size due to expansions and contractions leave specific signatures in the distribution of nucleotide differences between individuals, that can be plotted in the form of sequence mismatch distribution histograms. The shape of such plots will depend on past demographic events, as populations that have undergone historically recent and / or sudden expansions are predicted to exhibit a characteristic unimodal distribution in individual pairwise sequence differences (Harpending 1994). Mismatch distribution analyses were conducted in Arlequin 3.1.1 (Excoffier et al. 2005), in order to investigate past demographic expansions in all study species. Significance of deviations from the hypothesis of a past demographic expansion was assessed using the “sum of squared differences” (SSD) test, after 10000 iterations, as implemented in Arlequin 3.1.1 (Excoffier et al. 2005). Parameters of a past population expansion were estimated based on the mean and variance of the observed mismatch distribution.

Time elapsed since expansion of populations was estimated using $\sigma = 2\mu t$, calculated in Arlequin 3.1.1 (Excoffier et al. 2005), where σ represents time since expansion in mutational units, $2\mu = umt$ where u = mutation rate and mt = sequence length, and t = number of generations elapsed since expansion. Using the isolation of the eastern Pacific Ocean and the Caribbean Sea by the uplift of the Isthmus of Panama, Donaldson & Wilson (1999) estimated a mutation rate of 3.6% per DNA base position per million years (MY) for the Control Region of a number of fish species. Although mutation rates may vary from species to species, due to differences in growth rate and generation time, the 3.6% substitution rate appears to be a fairly conservative approach (Avice 2000).

However, estimates of time since expansion based on mismatch distribution parameters have severe drawbacks as the only source of information about a species demographic history, since obtained histograms will be heavily influenced by early branching in the gene tree (Avice 2000). Therefore, evolutionary history and time since divergence were also assessed using the Bayesian approach implemented in BEAST 1.3.1 (Drummond & Rambaut 2007).

In order to accurately estimate past demographic changes it is necessary to have a measure of time, which can be obtained by using a calibrated molecular clock. There are several methods for calibration, the most common one being the use of a known

sequence mutation rate as suggested above for estimates of time since expansion based on mismatch distribution parameters. However, mutation rates can vary from species to species, depending on several factors such as metabolic rate and generation times (Avice 2000), which may render universal mutation rates difficult to apply. Other calibration methods include using sequences with known ages and applying an internal point calibrator, by either fixing the age of a node to a specific value based on independent evidence, or by placing a minimum distribution around an independent value (Drummond et al. 2006; Ho 2007). Calibration of internal nodes is commonly based on the fossil record or known biogeographical events, and requires previous knowledge of the relationship among samples being used. For monophyletic taxa, the timing of known biogeographical events such as the closure of the Isthmus of Panama can be used to inform calibrations (Ho & Phillips 2009).

Due to the absence of a fossil record for any of the studied species in the Benguela Current region, calibration of the molecular clock for the Bayesian approach in the present study was performed using two different approaches: i) fixing the mean sequence divergence rate per lineage at 1.5% per MY, considered the universal rate in marine fish COI and cytb regions (Bermingham et al. 1997); and ii) using the strengthening of the Benguela Current as a biogeographical event to calibrate key nodes in the separation of populations. The Benguela Current was established in the Miocene (12 MYA), but during the Pliocene-Pleistocene transition (~2 MYA) there was an intensification of the system's oceanographic features, which are thought to have influenced speciation processes in several marine taxa (Lessios et al. 1999; Bowen et al. 2001; Lessios et al. 2003; Waters & Roy 2003). Thus, the 2 MY date was used as the mean of a normal distribution to calibrate internal nodes, and a broad standard deviation (SD) was enforced to allow for uncertainty of time estimates (Drummond et al. 2006). Performance of each approach was compared based on the likelihood of the posterior probabilities of each model, as suggested by Drummond & Rambaut (2007). Convergence of run parameters for the most likely approach was estimated based on Effective Sample Size (ESS>200) in Tracer 1.6 (Rambaut & Drummond 2007). Divergence times were obtained from post burn-in results.

2.3.2. Microsatellites

Population structure

Genotype frequencies were tested for deviations from Hardy-Weinberg equilibrium assumptions (i.e. fits to expectations for single outcrossing populations) and for non-random association of alleles between loci (linkage disequilibrium), as implemented in Genepop 4.1 (Raymond & Rousset 1995). Statistical significance was assessed after 10000 iterations, and corrected for multiple tests using the Bonferroni method (Rice 1989). Obtained datasets were screened for amplification errors such as large allele drop out, stuttering and presence of null alleles using Microchecker (van Oosterhout et al. 2006), and FreeNA (Chapuis & Estoup 2007).

Intraspecific and within-population levels of genetic diversity were estimated as number of alleles (N_a), allelic richness (AR), observed and expected heterozygosity (H_o and H_e), and Wright's inbreeding coefficient (F_{IS}), as implemented in FSTAT (Goudet 1995). Statistical significance was assessed after 1000 permutations in FSTAT (Goudet 1995). Wright's inbreeding coefficient (F_{IS}) estimates the partitioning of genetic diversity within subpopulations and can be used to evaluate departures from Hardy-Weinberg equilibrium. This statistic varies between -1 (excess of heterozygotes) and 1 (excess of homozygotes), and subpopulations with high levels of inbreeding will exhibit significant positive F_{IS} values (Beebe & Rowe 2005).

Population structuring and genetic connectivity was investigated using multiple approaches. First Weir's (1986) F_{ST} was estimated between each pair of samples in each species using FreeNA (Chapuis & Estoup 2007). Statistical significance was assessed after 1000 bootstraps, using a jackknife approach (Chapuis & Estoup 2007). F_{ST} values can vary between 0 (no differentiation) and 1 (complete differentiation). Values above 0.2 are considered to represent high genetic differentiation, while values closer to 0 are commonly found in undifferentiated populations (Excoffier et al. 2005). Secondly, hierarchical analyses of molecular variance (AMOVA) were performed for different clustering hypotheses, in order to investigate the influence of particular oceanographic features of the Benguela Current in population sub-structuring for the study species. AMOVA test the partition of total genetic variation into sub-components based on genetic variability within populations, between populations within groups, and between groups (Excoffier et al. 2005). AMOVA tests were performed in Arlequin 3.1.1 (Excoffier et al. 2005), and statistical significance was assessed after 50000 permutations. Finally, a Bayesian approach was used to investigate population structure

without prior knowledge of geographical origin of samples, as implemented in STRUCTURE (Pritchard et al. 2000). The method aims to identify the most likely number of genetic clusters of individuals (K) in Hardy-Weinberg equilibrium represented within the dataset, without prior knowledge of the number of sampled populations. Cluster identification is based on model posterior probabilities, given the observed data. Simulations were conducted under the admixture model, that allows each individual to be assigned to multiple clusters based on its genotype frequency, with correlated allele frequencies, for a burn-in phase of 20000 Markov Chain Monte Carlo (MCMC) generations, followed by 80000 generations in the data collection phase. However, STRUCTURE appears to encounter problems when trying to estimate too many parameters at the same time (Pritchard et al. 2000). Consequently, the parameter that specifies the probability distribution from which allele frequencies are independently drawn (λ) was estimated in a previous run set to $K = 1$, and fixed in all subsequent runs in all species. In each analysis, five independent runs were performed for each value of K to ensure convergence of parameters during the runs. Estimation of the most likely K was performed based on the obtained posterior probabilities of the data (Evanno et al. 2005).

Demographic history

Determining effective population size (N_e) is of extreme importance for exploited marine species, since it represents a good estimator of recruitment levels (Hauser & Carvalho 2008). Two approaches can be used to calculate N_e : temporal and point estimates. Temporal approaches require at least two different samples from the same population set apart in time, while point estimates, such as LDN_e (Waples & Do 2008) can be applied within a single sample point. The LDN_e method evaluates linkage disequilibrium (LD), while correcting for sampling size bias (Waples 2006), and relies on the assumption that non-random mating within populations will have an impact on genotype frequencies, which can then be used to estimate N_e . Estimation of N_e was performed for each identified population in each species, after removing all alleles with frequencies below the critical thresholds of 5%, 2% and 1%, as suggest by Waples (2006). Confidence intervals for each estimate were assessed using a pairwise jackknife approach.

Changes in effective population size due to environmental events can have a profound effect in the genetic diversity of a species. Genetic methods, like the one implemented in BOTTLENECK (Piry et al. 1999), can detect signatures of recent population

contractions. Such events are commonly characterized by faster decrease in the number of alleles than in levels of heterozygosity, and thus populations that have undergone a recent bottleneck will exhibit higher levels of heterozygosity (relatively) than temporally stable populations. The hypothesis of recent bottleneck events was tested under the three commonly accepted potential mutation models for microsatellite evolution: Infinite Alleles model (IAM), Stepwise Mutation model (SPM) and Two-Phase Mutation model (TPM). The TPM was run with an assumption of 70% of stepwise mutations. Significant heterozygote excess was tested for using the Wilcoxon Rank test, after 10000 iterations.

RESULTS

CHAPTER 3: *Diplodus capensis*

3.1. Population structure and evolutionary history of *Diplodus capensis* (Smith 1844) in a heterogeneous environment: the Benguela Current

3.1.1. Introduction

Diplodus capensis (Smith, 1844) is a sparid fish, with a distribution range restricted to southern Africa, extending from central Angola to Mozambique (Heemstra & Heemstra 2004). A recent biological survey revealed significant life history and morphological differentiation between *D. capensis* from Angola and South Africa (Richardson 2010). While South African individuals reach a maximum size of 45 cm in 21 years and mature at 22 cm (4 years), Angolan *D. capensis* appear to grow slower (maximum age 31 years) and mature later (15 cm / 5 years) (Richardson 2010). The species exhibits differing spawning seasons throughout its distribution, which may be linked with optimal sea surface temperatures (17-20°C): from June to October in southern Angola; July to September in KwaZulu-Natal, South Africa, and October to December in Eastern Cape, South Africa (Mann & Buxton 1997; Mann & Buxton 1998; Richardson 2010). Observed life history and morphological differentiation between *D. capensis* samples may result from long-term population isolation, followed by local adaptation (Waples 1998). Therefore, these findings suggest that *D. capensis* in southern Africa may be composed of multiple, independent population units.

In the marine realm the mechanisms responsible for shaping population structure can be historical, such as large-scale climate-induced changes (e.g. Grant & Bowen 2006; Ruzzante et al. 2008; Pardinás et al. 2010), and/or contemporary (Hemmer-Hansen et al. 2007). Contemporary mechanisms shaping population evolution include: different spawning grounds and seasons; geographical distance; oceanographic features such as currents, fronts and upwelling cells; and environmental transitions promoting local adaptation (Hemmer-Hansen et al. 2007).

Diplodus capensis occurs in an unstable environment, the Benguela Current, which is considered a major biogeographical boundary, separating temperate and tropical fauna between Atlantic and Indian Oceans (Colborn et al. 2001; Lessios et al. 2001; Grant & Bowen 2006; Floeter et al. 2008). Previous studies have documented the influence of historical climatic fluctuations in the Benguela Current in shaping evolutionary history

of several marine species (e.g. Lessios et al. 1999; Bowen et al. 2001; Lessios et al. 2003; Matthee et al. 2007; von der Heyden et al. 2007; Neethling et al. 2008; von der Heyden et al. 2010). However, no studies have been conducted to investigate the influence of this oceanographic system on levels of gene flow and population differentiation.

Diplodus capensis represents a valuable fishery resource throughout its distribution, particularly in southern Angola where it is mainly targeted by the inshore subsistence fishery (Richardson 2010). Based on observed differences in spawner biomass-per-recruit for samples caught in protected and un-protected areas, Richardson (2010) revealed that exploitation appears to have reduced *D. capensis* biomass to 20% of its pristine values. Slow growing and late maturing species such as *D. capensis* are considered to be particularly vulnerable to over-exploitation (FAO 2001), thus the findings by Richardson (2010) highlight the species vulnerability to even low levels of exploitation. Therefore the present study aimed to: *i*) assess levels of genetic diversity among Angolan, Namibian and South African *D. capensis* populations; *ii*) investigate past and present levels of genetic population structuring, focusing mainly in southern Angola where the species appears to be under intense fishing pressure, and comparing local structuring with differentiation across the Benguela Current system; *iii*) document the species evolutionary history, in order to understand the influence of regional past climatic changes in population dynamics, to help inform future sustainable management plans that ensure the maintenance of the species genetic diversity and evolutionary potential; and to *iv*) investigate the systematic status of the species across southern Africa and in relation to European *Diplodus sargus*, as Heemstra & Heemstra (2004) changed the classification from *D. sargus capensis* to *D. capensis* without substantial evidence. Heemstra & Heemstra (2004) also suggested, based on external morphological characters, that populations of *D. capensis* from Cape Vidal (KwaZulu-Natal, South Africa) might be separated species from *D. capensis* found elsewhere in southern Africa, although a recent survey conducted in southern Angola did not reveal enough morphological differentiation for Angolan *D. capensis* to be considered a distinct species (Richardson 2010, but see Chapter 1.2.1).

3.1.2. Methods

Sampling and DNA extraction

Sampling was conducted in five locations in southern Angola and northern Namibia, in the winter months of 2008-2010 (Figure 3.1, Table 3.1). Samples were obtained from local markets, subsistence fishermen and recreational anglers. In addition, samples from 119 individuals were collected in three different sites in South Africa (Table 3.1), to compare genetic diversity levels and population connectivity across the Benguela Current region. In addition, *Diplodus sargus* (n=12) and *Diplodus vulgaris* (n=20) samples were collected in Europe (southern Portugal), in order to act as outgroups in phylogenetic analyses among *D. capensis* samples across the Benguela Current region, and also to investigate the genetic relationships between *D. capensis* and these closely related European species. A fin clip was removed from each fish and preserved in 95% ethanol immediately after capture.

Total genomic DNA was extracted following the phenol-chloroform method described by Sambrook et al. (1989).

Table 3.1: Sampling strategy for *D. capensis* across the Benguela Current region: sampling locations, sample code, sample size and latitude/longitude coordinates.

Country	Region	Code	Sample Size	Coordinates
Angola	Baia Farta	BEN	108	12°35.516'S 13°13.595'E
	Lucira	LUC	93	13°50.635'S 12°27.166'E
	Inamangando	INA	18	15°16.00'S 12°10.00'E
	Namibe	NBE	124	15°10.374'S 12°04.863'E
	Flamingo	FLA	275	15°10.374'S 12°04.863'E
Namibia	Henties Bay	HEN	28	22°7.404'S 14°16.139'E
South Africa	Cape Vidal	KZN	15	28°9.41'S 32°34.57'E
	Port Alfred	EastC	80	33°36.500'S 26°54.000'E
	Arniston	WestC	24	34°40.000'S 20°14.000'E

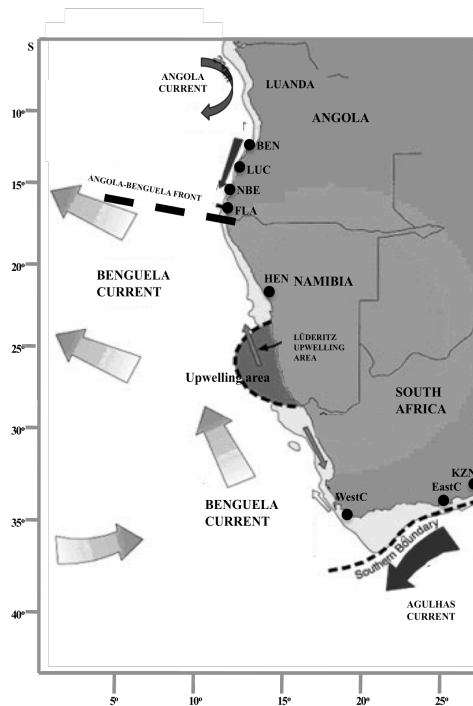


Figure 3.1: Sampling strategy for *D. capensis* across the Benguela Current, highlighting sampling sites, and their position relative to the major oceanographic features of the system: the Benguela, Angola and Agulhas Currents; position of the Angola-Benguela Front; central Namibia upwelling cell; continental shelf width.

Genetic screening

The DNA of 165 *D. capensis* individuals were PCR amplified and sequenced for a fragment of the COI gene, using the universal primer pair FishF1 and FishR1 (Ward et al. 2005) (see Chapter 2.2.2). Additional amplification and sequencing was performed for 5 *D. sargus* and 1 *D. vulgaris* for phylogenetic inference.

Eight cross-specific microsatellite loci (DSMa16, DSMa27, DSMa34, DSMa48, Dvul4, Dvul33, Dvul61 and Dvul84) were screened for genetic variation (see Chapter 2.2.2) in 70 individuals per sampling site, whenever possible, to investigate genetic diversity levels and population sub-structuring across the Benguela Current (Table 2.2).

MtDNA sequence analyses

Population structure and phylogeographic patterns

The complete COI sequence dataset was assessed for levels of haplotype (h) and nucleotide (π) diversity levels, fits to neutrality tests: Ewens-Watson's F , Tajima's D and Fu's F_S , and determination of the most suitable nucleotide substitution model was performed as previously described (Chapter 2.3.1).

Assessment of historical levels of *D. capensis* population connectivity was performed by estimating pairwise Wright's F_{ST} , testing different hypotheses of population

structuring through the analysis of hierarchical molecular variance (AMOVA), and reconstructing haplotype networks across the Benguela Current (Chapter 2.3.1).

AMOVA analyses were conducted for three different hierarchies of samples to investigate the influence of multiple oceanographic features within the Benguela system on the genetic sub-structuring of *D. capensis*: *i*) central Namibian perennial upwelling cell (northern vs. southern Benguela sub-system samples); *ii*) the position of the Angola-Benguela Front at time of sampling ($\sim 16^{\circ}\text{S}$ - Angola vs. Namibia plus South Africa), and *iii*) geographic clustering by country (Angola vs. Namibia vs. South Africa).

Evolutionary history

Investigation of *D. capensis* evolutionary history in the Benguela Current system was performed at both population and species levels. At the population level haplotype (h) and nucleotide (π) diversity measures, Tajima's D (Tajima 1989) and Fu's F_S (Fu 1997) statistics, and mismatch distributions of haplotype differences were estimated in samples across the Benguela system using Arlequin 3.1.1. (Excoffier et al. 2005) (see Chapter 2.3.1).

Assessment of *D. capensis* species status was conducted through reconstruction of phylogenetic relationships among sequences from individuals from the Benguela Current system and comparison to *D. sargus*, estimating time since most recent common ancestor (tmrca) in all identified clades. A total of 40 individual *D. capensis* (5 per sampling site), plus 5 *D. sargus* individuals were used to reconstruct phylogenetic relationships and compare genetic distances between *D. capensis* and *D. sargus*, and also within the Benguela samples, with *D. vulgaris* used as outgroup.

Average population differentiation, as suggested by Avise et al. (1998) was calculated as: (pairwise difference between groups A and B) $- 0.5 \times$ (pairwise difference within group A+B), using the most appropriate substitution model in MEGA 4.1. (Kumar et al. 2004).

Heterogeneity of base composition was evaluated with the χ^2 test, as implemented in PAUP (Swofford 1993). Assessment of gene trees was conducted using Bayesian analyses (BA), implemented in MrBayes and BEAST (Huelsenbeck & Ronquist 2001; Ronquist & Huelsenbeck 2003). In MrBayes, two independent analyses were run under the GTR model, for 1 million Markov Chain Monte Carlo (MCMC) generations, sampling every 1000th generation. Convergence of the model was based on log likelihood and split frequencies of standard deviations ($p < 0.01$). In BEAST, two

independent analyses were run for 10 million MCMC generations, with parameters recorded every 1000th generation. Convergence and stationarity of runs were estimated by examination of likelihood plots using Tracer 1.4 (Rambaut & Drummond 2007). A consensus tree was obtained after a burn-in period of 2500 generations, and reconstruction of both Bayesian trees was conducted in FigTree 1.3.1 (Rambaut 2009). Estimates of time since most recent common ancestor were conducted in BEAST 1.3.1 (Drummond & Rambaut 2007), under a strict molecular clock. The dataset was partitioned into coding (1st and 2nd codon positions) and non-coding regions (3rd codon position), with unlinked substitution rates. Runs were performed under a Yule speciation model for branching rates, and using the HKY model of nucleotide substitution. Two independent analyses were run for 10 million MCMC generations and logged every 1000th step. Independent runs were combined using LogCombiner 1.6.1 (Drummond & Rambaut 2007), and convergence was estimated based on Effective Sample Size (ESS>200) in Tracer 1.4 (Rambaut & Drummond 2007). Calibration of the molecular clock was performed using two different approaches: *i*) fixing the sequence divergence rate at 1.5% per million years, an accepted standard rate for COI in marine fish (Bermingham et al. 1997); and *ii*) using the establishment of the present features of the Benguela Current (~2 MYA) as a biogeographical calibrator for the separation of the northern and southern Benguela sub-system *D. capensis* populations (see Chapter 2.3.1).

Microsatellite analyses

Genetic diversity and population structure

Obtained genotype frequencies were tested for deviations from Hardy-Weinberg expectations of random mating within loci and samples, and for linkage disequilibrium (i.e. non-random association of alleles between loci within samples), using Genepop (Raymond & Rousset 1995). Occurrence of amplification errors such as large allele drop out and stuttering, and null alleles frequencies were assessed in Microchecker (van Oosterhout et al. 2006). Deviations of allele frequencies between samples from those expected under selectional neutrality were tested using the F_{ST} -outlier method of Beaumont and Nichols (1996), as implemented in LOSITAN (Antao et al. 2008): 2 independent runs were performed (100000 MCMC generations) using the “neutral” mean F_{ST} estimated under the stepwise mutation model (SMM).

Measures of genetic diversity such as allelic richness (AR), number of alleles (N_a), expected (H_E) and observed (H_O) heterozygosity and Wright’s inbreeding coefficient

(F_{IS}), were estimated as described in Chapter 2.3.2. As fishing can result in loss of genetic diversity in populations (Kenchington et al. 2003), a comparison was made between diversity levels in samples from over-exploited (BEN, LUC, NBE, HEN) and protected (FLA) areas, and between northern and southern Benguela sub-system samples, using FSTAT (Goudet 1995) with statistical significance assessed after 10000 permutations.

Assessment of population structure and gene flow within the Benguela Current region was investigated using three approaches: estimation of Weir's (1986) pairwise F_{ST} ; hierarchical analysis of molecular variance (AMOVA), computed to evaluate the same hypotheses tested with the mtDNA dataset; and employing the Bayesian approach implemented in STRUCTURE (Pritchard et al. 2000) (Chapter 2.3.2).

Demographic history

Estimates of effective population size (N_e) were conducted using three critical allele frequencies (0.05, 0.02, and 0.01) as implemented in LDN_e (Waples & Do 2008) for each population cluster identified according to observed genetic differentiation levels obtained with the methods described above. Confidence intervals for each estimate were assessed using a pairwise jackknife approach.

Estimates of gene flow were assessed using the Bayesian approach implemented in GENECLASS (Piry et al. 2004), where individuals are assigned to their most likely population of origin based on genotypic frequencies. As with N_e estimates, analyses were performed for identified population clusters, with significance assessed after performing 10000 simulations.

Changes in population effective size due to environmental events or over-exploitation were tested for each identified population cluster under three microsatellite mutation models, implemented in BOTTLENECK (Piry et al. 1999) (Chapter 2.3.2).

3.1.3. Results

MtDNA

Population structure and phylogeographic patterns

A total of 165 individuals, 20 per sampling site whenever possible, were sequenced for 615bp of mtDNA COI, resulting in 24 haplotypes described by 23 variable and 9 parsimony informative base positions. The HKY nucleotide substitution model was retrieved as the most suitable model of sequence evolution. Overall, significant

deviations from neutrality expectations were detected with Fu's F_S test, but not with either the Ewens-Watson's F or Tajima's D tests (Table 3.2). Fu's F_S neutrality test is known to be extremely sensitive to demographic changes, therefore observed deviations may be related with demographic events and not selective pressures (Excoffier et al. 2005). Overall haplotype and nucleotide diversity levels were moderately high ($h = 0.7073$, $\pi = 0.0037$, respectively), but varied substantially between samples for both h (0.125 to 0.700, WestC and BEN respectively) and π (0.0002 to 0.0016, WestC and BEN) (Table 6). Diversity levels were consistently higher in samples from southern Angola compared with samples from Namibia and South Africa (Table 3.2).

Table 3.2: Mitochondrial genetic diversity levels and neutrality tests for *D. capensis* COI region: **n** – number of individuals; **H** – number of haplotypes; **h** – haplotype diversity; **π** - nucleotide diversity; **F** – Ewens-Watson neutrality test; **D** – Tajima neutrality test; **F_S** – Fu neutrality test. Statistically significant results ($p < 0.05$) in bold.

	BEN	LUC	INA	NBE	FLA	HEN	WestC	EastC	KZN	Overall
n	20	20	16	20	20	20	17	20	12	165
H	8	6	3	4	7	3	2	4	3	24
h	0.7000	0.6737	0.4250	0.4895	0.6421	0.2789	0.1250	0.4316	0.3182	0.7073
π	0.0016	0.0016	0.0008	0.0010	0.0015	0.0005	0.0002	0.0008	0.0008	0.0037
F	0.974	0.840	0.743	0.868	0.960	0.899	1.000	0.875	1.000	1.000
D	-1.665	-0.866	-0.330	-1.260	-1.094	-1.141	-1.162	-1.191	-1.621	-1.208
F_S	-5.149	-2.229	-0.290	-1.024	-3.931	-1.206	-0.700	-1.713	-0.614	-11.087

Assessment of population structure using F_{ST} revealed two significantly differentiated groups of samples: Angola/Namibia and South Africa (Table 3.3). Pairwise F_{ST} comparisons between samples from the two groups ranged from 0.832 to 0.950 (LUC-KZN and HEN-WestC) and were significantly ($p < 0.001$) greater than zero. (Table 3.3). No significant values of F_{ST} were observed within each group, after Bonferroni correction for multiple tests (Rice 1989).

Table 3.3: Pairwise F_{ST} values based on mtDNA COI data, between *D. capensis* samples (see Table 3.1 for sample codes). Statistical significant results in bold ($p < 0.05$).

	BEN	LUC	INA	NBE	FLA	HEN	WestC	EastC	KZN
BEN	-								
LUC	0.073	-							
INA	0.013	0.070	-						
NBE	0.006	0.042	-0.034	-					
FLA	0.026	-0.024	0.026	-0.001	-				
HEN	-0.019	0.097	0.017	-0.007	0.036	-			
WestC	0.873	0.871	0.928	0.910	0.880	0.950	-		
EastC	0.838	0.834	0.884	0.872	0.844	0.909	0.004	-	
KZN	0.833	0.832	0.887	0.873	0.842	0.916	0.017	0.039	-

Of the three hierarchical population structures tested the northern-southern Benguela sub-system (i.e. upwelling cell) hypothesis explained the highest amount of variance among defined groups (86.13%), which was significantly different from zero ($p < 0.05$) (Table 3.4). The second hierarchy (structuring centred on the Angola-Benguela Front) produced lower and not significant ($p > 0.05$) levels of among-groups, and higher within groups, variance compared to the first hierarchy. The third hierarchy (geographical clustering by country) gave significant levels of among-groups variance, but lower than observed for the first hierarchy (Table 3.4).

Table 3.4: Analysis of molecular variance (AMOVA) results based on COI data, for the three population differentiation scenarios tested. Statistically significant results ($p < 0.005$) in bold.

	i) North - South Upwelling	ii) ABF	iii) Geographical clustering
Among groups	86.29	53.22	82.16
Within groups	0.31	27.49	0.47
Within populations	13.40	19.90	17.47

As observed for pairwise F_{ST} and hierarchical AMOVA tests, reconstruction of haplotype relationships using a network approach identified two main clusters, corresponding to individuals from Angolan/Namibian and South African sites (Figure 3.2). It was not possible to identify geographical patterns in the distribution of haplotypes within each cluster (Figure 3.2).

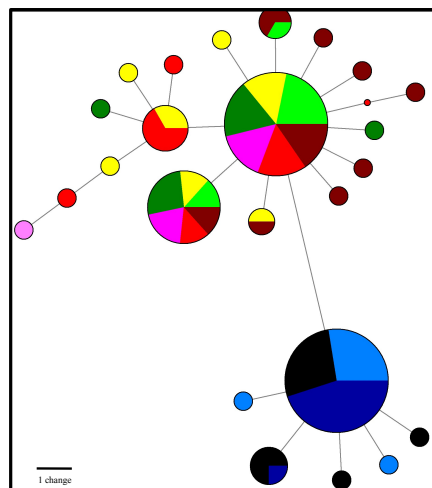


Figure 3.2: Reconstruction of haplotype network for *D. capensis* across the Benguela Current, based on 619bp of mtDNA COI: ●: HEN; ●: FLAM; ●: NAM; ●: INA; ●: LUC; ●: BEN; ●: EastC; ●: KZN; ●: WestC. Node sizes are proportional to the number of haplotypes. Red dots correspond to missing haplotypes.

In both haplotype clusters it was possible to identify a common (ancestral) haplotype, found in individuals from all sampling sites. The Angolan/Namibian cluster exhibited a higher number of private haplotypes and overall higher genetic diversity. The “ancestral” haplotypes in each of the two clusters differ by 4 mutational steps, while within each cluster most private haplotypes differ from the common haplotype by 1 to 3 mutational steps.

Evolutionary history

As significant life history and now genetic differentiation, has been observed between samples from the northern and southern Benguela sub-systems, reconstruction of *D. capensis* demographic history was conducted separately for the identified northern and southern haplotype clusters.

The northern *D. capensis* population exhibited higher genetic diversity, but lower nucleotide diversity, than the South African population (Table 3.5). Similar deviations from neutrality were observed in Tajima’s *D* and Fu’s *F_S* summary statistics, in both populations, suggesting a past demographic expansion (Table 3.5). Furthermore, it was not possible to reject the null hypothesis of a past demographic expansion (SSD=0.0003, SSD=0.0017, *p*>0.05, Table 3.5), and frequency histograms revealed a clear unimodal pattern in both populations (Figure 3.3). Using the obtained mismatch distribution parameters and different generation times for northern and southern *D. capensis* populations, time since expansion was estimated at 8.14 KY and 40.38 KY ago, respectively.

Table 3.5: *Diplodus capensis* genetic demographic history for northern and southern Benguela sub-system populations, based on mtDNA COI sequence variation: genetic diversity levels (*h* and π); neutrality tests (Tajima’s *D* and Fu’s *F_S*); mismatch distribution parameters: σ - time since expansion in mutation units, θ_0 - population size before expansion, θ_1 – population size after expansion; and time since expansion (*T* in KY).

	Northern	Southern
<i>h</i>	0.5313	0.3032
π	0.0012	0.006
<i>D</i>	-2.012	-1.875
<i>F_S</i>	-19.363	-4.473
Mean	0.729	0.364
Variance	0.675	0.367
SSD	0.0003	0.0017
σ	0.756	3.000
	(0.445-1.434)	(0-12.500)
θ_0	0.000	0.000
θ_1	99999.000	0.445
<i>T</i> (KY)	8.14	40.38
	(4.82-15.55)	(0-169.38)

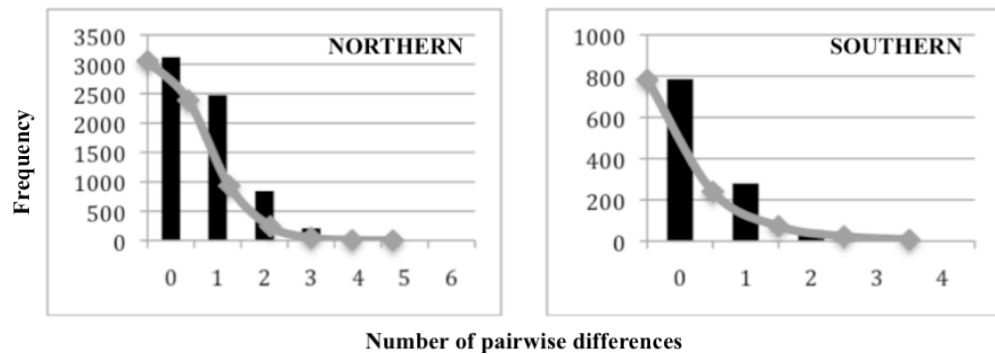


Figure 3.3: Mismatch distribution histograms for northern and southern Benguela sub-system *D. capensis* populations, based on mtDNA COI sequences. Filled bars indicate the observed frequency of pairwise differences and the grey line indicates the expected distribution under a model of rapid demographic expansion.

Assessment of nucleotide frequency heterogeneity did not retrieve statistically significant results ($\chi^2=1.975$, $p>0.05$), suggesting that the data could be used for phylogenetic inference. Estimates of population divergence, using the formula suggested by Avise et al. (1998), revealed lower values for differentiation between *D. capensis* from northern and southern Benguela (0.785%) compared with differentiation between *D. capensis* and *D. sargus* (~1.5%), and much lower than between *D. capensis* and *D. vulgaris* (~7.2%), and *D. sargus* and *D. vulgaris* (~5.6%).

Reconstruction of phylogenetic relationships among the different COI haplotypes revealed two divergent clades within *D. capensis*, corresponding to samples from northern (BA and BN individuals) and southern (BSA individuals) Benguela regions (Figure 3.4). The absence of shared haplotypes between regions, and the high statistical support for the two clades, indicates complete lineage sorting.

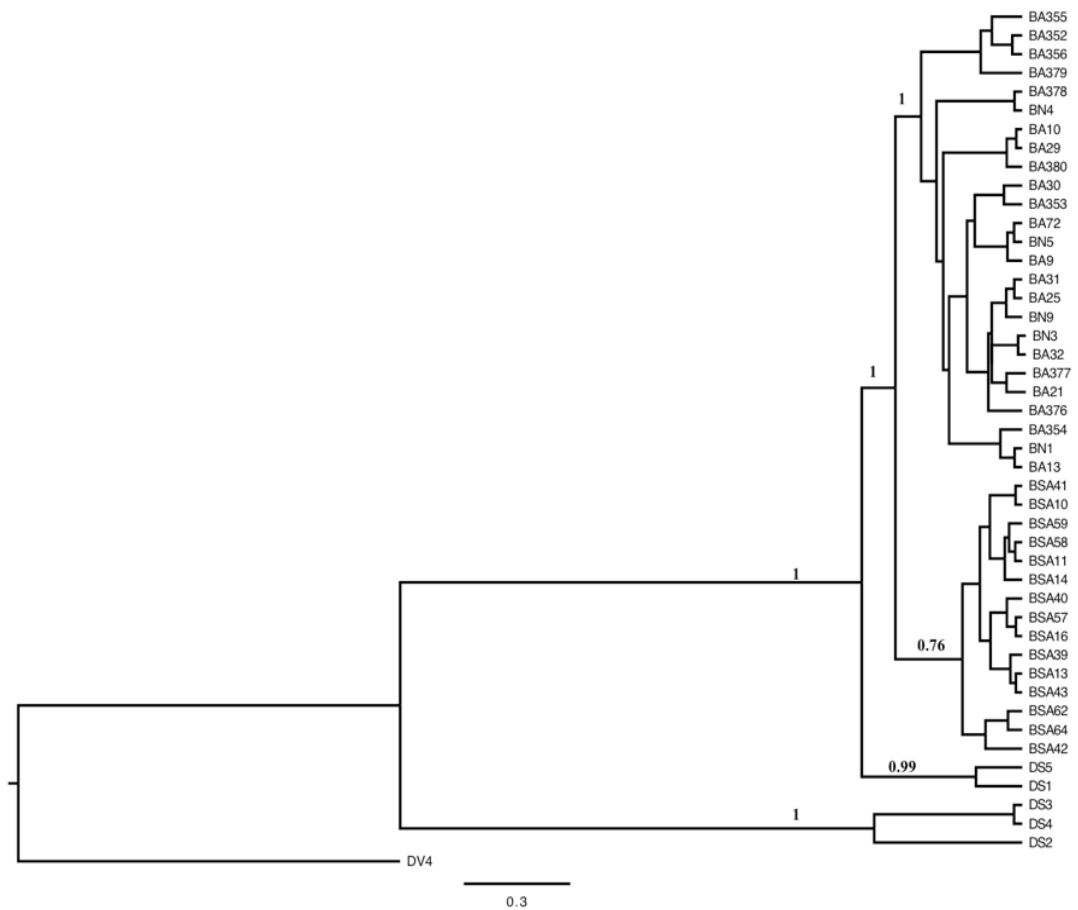


Figure 3.4: Reconstruction of phylogenetic relationships among COI haplotypes from northern (BA and BN) and southern (BSA) populations of *D. capensis*, plus *D. sargus* (DS) and *D. vulgaris* (DV); posterior probabilities above branches. Units in number of changes per year.

Observed branch lengths (evolutionary distance) between northern and southern clades of *D. capensis* were much shorter than observed between *D. capensis* and *D. sargus* (Figure 3.4), indicating much less divergence between these two populations than between the two distinct species. No obvious geographical differentiation was observed within either the Angolan/Namibian or the South African clades, indicating that *D. capensis* is composed of single historically panmictic populations throughout each regions, thus rejecting the hypothesis of differentiated populations / species within South Africa proposed by Heemstra & Heemstra (2004). The observed branch lengths and level of evolutionary differentiation (1.5%) between *D. sargus* and *D. capensis* confirms the conclusion of Heemstra & Heemstra (2004) that these are discrete species. Interestingly, two *D. sargus* individuals (DS1 and DS5, collected in Portugal) clustered much more closely with the *D. capensis* clade rather than the other *D. sargus* individuals, indicating that they may not be *D. sargus*, but rather be *D. capensis* occurring in the northern Atlantic.

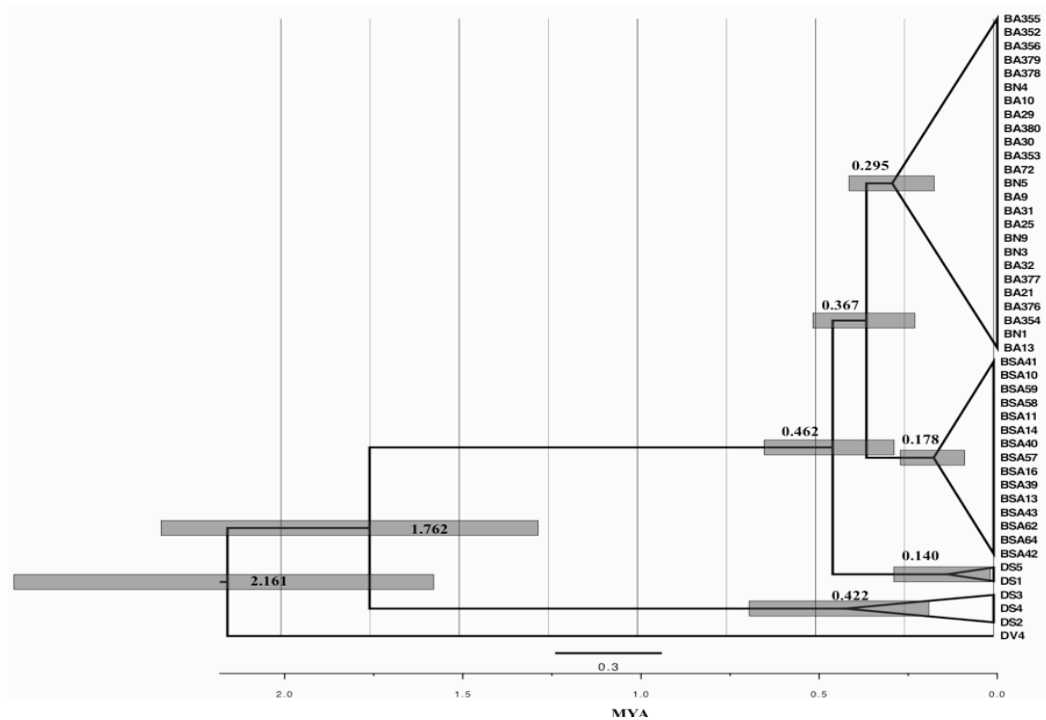


Figure 3.5: Chronograms of time since divergence (MYA, above nodes) among COI haplotype clades from *D. capensis*, *D. sargus* (DS) and *D. vulgaris* (DV) (grey bars = 95% highest posterior density intervals), using a sequence mutation rate of 1.5% per MY.

Estimates for time since most recent common ancestor, using the fixed sequence divergence rate, indicate that the separation of northern and southern *D. capensis* populations occurred 367.4 KYA, while divergence between *D. sargus* and *D. capensis* was estimated at 1.76 MYA (Figure 3.5). When tmrca was estimated using internal node calibration values were far greater: 1.67 MYA for northern/southern *D. capensis*, and 2.5 MYA for the *D. capensis* /*D. sargus* divergence. In this latter case sequence divergence rate was estimated at 0.6% per million years, which is very different from average COI divergence rates for fish species (Bermingham et al. 1997), suggesting that the used internal node calibration may not be an appropriate method to use in this situation.

Microsatellite analysis

Population structure and gene flow

A total of 389 individuals from 7 different localities were screened for 8 cross-specific microsatellite markers (Table 3.6). Large samples sizes are required in these markers, to take advantage of the higher statistical power present due to the larger allelic diversity exhibited. Therefore, screening was not possible for Inamangando (INA) and Cape Vidal (KZN) samples.

Obtained genotypes did not exhibit evidence of amplification errors such as null alleles or large allele drop-out, no loci exhibited significant linkage disequilibrium, and genotype frequencies conformed to Hardy-Weinberg expectations of random mating for the majority of loci and samples (Table 3.6). The EastC sample exhibited significant deviations from Hardy-Weinberg expectations, overall due to significant heterozygote deficit at locus DSMa16 (Table 3.6). Furthermore, sample NBE exhibited significant departures from linkage equilibrium between locus pairs DSMa27/Dvul4, DSMa34/Dvul4 and DSMa16/DSMa48. However, since there was no consistent pattern across samples or loci these deviations were considered to be a statistical artefact of multiple tests.

Estimates of departures from neutrality when the complete dataset was used identified two loci under directional selection (Dvul4 and Dvul33), under the SMM model. When the analysis was conducted for the northern and southern samples separately, evidence of balancing selection was detected in the southern population for locus Dvul84.

Multi-locus genetic diversity (observed heterozygosity) ranged from 0.773 (EastC) to 0.829 (LUC). Higher values of allelic richness, based on a minimum of 16 individuals were observed for the South African samples (WestC and EastC) than the northern region samples. Comparison of genetic diversity levels between sites with heavy exploitation (BEN, LUC, NBE and HEN) and a site with low exploitation (FLA) did not reveal significant differentiation ($p > 0.05$). A similar result was observed for comparisons between samples from the northern and southern Benguela regions ($p > 0.05$).

Table 3.6: Genetic diversity at 8 cross-specific microsatellite loci in *D. capensis* samples: **n** – number of individuals genotyped; **Na** – number of alleles; **AR** – allelic richness (minimum of 16 individuals); **H_E** – expected heterozygosity; **H_O** – observed heterozygosity; **F_{IS}** – inbreeding coefficient. Significant deviations to Hardy-Weinberg expectations in bold.

		BEN	LUC	NBE	FLA	HEN	WestC	EastC
DSMa16	n	70	70	68	70	21	28	60
	Na	13	13	12	16	6	21	25
	AR	8.955	8.223	8.269	9.549	5.699	15.909	16.779
	H_E	0.831	0.782	0.823	0.840	0.726	0.916	0.936
	H_O	0.871	0.874	0.779	0.800	0.762	0.964	0.833
	F_{IS}	-0.042	-0.107	0.061	0.055	-0.026	-0.034	0.118
DSMa27	n	70	70	68	70	21	29	60
	Na	11	13	16	14	8	13	18
	AR	6.407	8.119	8.774	7.652	6.995	10.553	10.597
	H_E	0.729	0.774	0.784	0.736	0.706	0.841	0.844
	H_O	0.729	0.757	0.735	0.743	0.809	0.862	0.800
	F_{IS}	0.008	0.029	0.070	-0.002	-0.122	-0.007	0.061
DSMa34	n	70	70	68	70	21	29	59
	Na	11	11	14	13	7	7	7
	AR	7.214	7.683	8.028	7.437	6.469	6.501	6.306
	H_E	0.722	0.716	0.709	0.694	0.732	0.789	0.780
	H_O	0.657	0.700	0.721	0.686	0.905	0.828	0.644
	F_{IS}	0.098	0.029	-0.009	0.019	-0.212	-0.031	0.183
DSMa48	n	70	70	62	70	16	29	60
	Na	29	26	29	30	18	23	25
	AR	17.844	17.363	17.207	17.115	18.000	16.538	15.922
	H_E	0.946	0.947	0.930	0.933	0.912	0.902	0.932
	H_O	0.914	0.900	0.919	0.886	0.941	0.897	0.900
	F_{IS}	0.041	0.057	0.019	0.058	0.004	0.023	0.034
Dvul4	n	70	70	67	70	21	29	60
	Na	14	13	14	14	10	20	21
	AR	8.505	8.843	8.357	8.815	8.933	16.037	13.604
	H_E	0.783	0.805	0.787	0.820	0.797	0.930	0.914
	H_O	0.729	0.743	0.809	0.700	0.714	0.847	0.846
	F_{IS}	0.076	0.085	-0.020	0.153	0.128	0.081	0.127
Dvul33	n	70	70	67	70	21	29	60
	Na	11	10	11	12	10	10	11
	AR	7.890	7.409	7.796	8.710	8.747	7.542	6.553
	H_E	0.749	0.764	0.780	0.797	0.746	0.669	0.632
	H_O	0.757	0.814	0.851	0.800	0.714	0.621	0.567
	F_{IS}	-0.004	-0.059	-0.083	0.003	0.067	0.090	0.119
Dvul61	n	70	70	66	70	21	28	54
	Na	31	31	28	31	21	22	24
	AR	17.956	18.428	17.901	19.209	18.322	17.353	16.674
	H_E	0.946	0.948	0.943	0.955	0.935	0.933	0.939
	H_O	0.900	0.943	0.942	0.914	0.905	0.929	0.890
	F_{IS}	0.063	0.013	0.027	0.050	0.057	0.023	0.063
Dvul84	n	70	70	65	70	21	28	54
	Na	11	12	13	10	11	11	11
	AR	8.922	8.568	9.019	8.352	9.994	8.308	7.163
	H_E	0.852	0.851	0.850	0.851	0.866	0.708	0.684
	H_O	0.871	0.900	0.815	0.886	0.904	0.643	0.704
	F_{IS}	-0.015	-0.051	0.049	-0.033	-0.020	-0.020	0.111
Average all loci	n	70	70	66	70	21	28	58
	Na	16	16	17	17	11	16	18
	AR	10.462	10.579	10.669	10.855	10.395	12.343	11.700
	H_E	0.820	0.823	0.826	0.828	0.803	0.836	0.832
	H_O	0.804	0.829	0.819	0.802	0.831	0.821	0.773
	F_{IS}	0.027	0.001	0.016	0.039	-0.010	0.036	0.080

The global multi-locus F_{ST} value across all samples was moderately high and significantly different from zero ($F_{ST} = 0.019$; $p < 0.01$), and pairwise comparisons

between samples ranged from -0.001 to 0.048 (BEN-NBE, BEN-WestC, respectively) (Table 3.7). As observed for the mtDNA dataset, estimates of genetic differentiation (F_{ST}) defined two groups of samples corresponding to the northern (BEN, LUC, NBE, FLA and HEN, i.e. Angolan and Namibian) and southern (WestC and EastC, i.e. South African) sub-system samples, where F_{ST} values between groups were all high and highly significant whereas values within groups were low and not significantly different from zero.

Table 3.7: Pairwise F_{ST} values between *D. capensis* samples based on 8 microsatellite loci. Values significantly greater than zero ($p < 0.05$) in bold.

	BEN	LUC	NBE	FLA	HEN	WestC	EastC
BEN	-						
LUC	0.0004	-					
NBE	-0.001	0.002	-				
FLA	0.001	0.001	-0.002	-			
HEN	0.005	0.005	0.003	0.005	-		
WestC	0.048	0.042	0.041	0.039	0.046	-	
EastC	0.048	0.041	0.042	0.041	0.048	-0.001	-

The hierarchical population structure analyses corroborated obtained F_{ST} comparisons, with the northern-southern Benguela division exhibiting the highest percentage of variance among groups (4.36%; $p < 0.05$) (Table 3.8). As with the mtDNA results the second hierarchy (structuring centred on the Angola-Benguela Front) produced lower and non significant ($p > 0.05$) levels of among-groups variance compared to the first hierarchy. The third hierarchy (geographical clustering by country) gave significant levels of among-groups variance, but lower than observed for the first hierarchy (Table 3.8).

Table 3.8: Analysis of molecular variance (AMOVA) results based on 8 microsatellite loci, for the three population differentiation scenarios tested. Statistically significant results ($p < 0.05$) in bold.

	i) North - South Upwelling	ii) ABF	iii) Geographical clustering
Among groups	4.21	2.924	3.51
Within groups	0.01	0.44	-0.01
Within populations	95.78	96.65	96.50

Bayesian analysis from cryptic population structure based on individual clustering (STRUCTURE) retrieved a similar differentiation pattern, identifying two genetic sub-populations as the most likely structure ($K = 2$, $\text{LnP}(D) = -14559.68$; Figure 3.6) corresponding to individuals from the northern and southern Benguela sub-system

samples, independently of the model used. High levels of admixture were indicated, suggesting shallow population differentiation.

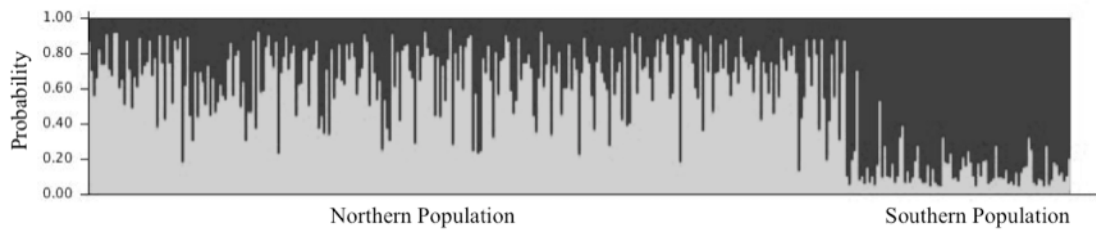


Figure 3.6: Bayesian analysis of individual multi-locus genotype clustering (STRUCTURE) hidden population structure, and admixture levels for *D. capensis* across the Benguela Current region.

When the loci indicated to be subject to selection (Dvul4 and Dvul33) were removed from the STRUCTURE analysis, no genetic sub-structure was observed between northern and southern populations ($K = 1$, $\text{LnP(D)} = -11323.4$). However, pairwise F_{ST} estimates, conducted without Dvul4 and Dvul33 still indicated differentiation between northern and southern *D. capensis* populations but with smaller values (Table 3.9), thus suggesting that these loci may be contributing to the observed differentiation levels.

Table 3.9: Pairwise F_{ST} values between *D. capensis* samples based on 6 microsatellite loci (potentially selected loci Dvul4 and Dvul33 removed). Values significantly greater than zero ($p < 0.05$) in bold.

	BEN	LUC	NBE	FLA	HEN	WestC	EastC
BEN	-						
LUC	-0.0009	-					
NBE	0.0001	0.0007	-				
FLA	0.0015	0.0003	-0.002	-			
HEN	0.0047	0.0035	0.0088	0.0065	-		
WestC	0.0275	0.0291	0.0222	0.0231	0.0324	-	
EastC	0.0308	0.0307	0.0240	0.0241	0.0340	0.0006	-

Therefore, the microsatellite results suggest that the *D. capensis* samples represent two differentiated populations occurring in the northern and southern Benguela sub-systems, and that the observed population differentiation may be related to local selection pressures. No significant differentiation was observed among southern Angola and Nambian samples, suggesting that these compose one single panmictic population.

Demographic history

Estimates of effective population size (N_e), migration and bottleneck events were conducted for the two identified populations: northern and southern Benguela. Despite large confidence intervals, values of N_e suggest that both *D. capensis* populations

exhibit relatively large long-term effective population sizes (Table 3.10). Furthermore, values appear to be consistently higher for the northern population than in the southern population.

Rejection of the null hypothesis of mutation-drift equilibrium (i.e. constant population size, no bottleneck) was only detected in the northern population under the IAM mutation model (Table 3.10). However, this result was not supported by results under both SMM or TPM mutation models. According to Piry et al. (1999), bottlenecks are more easy to detect if the loci evolve under the IAM model, than if they exhibit a strict SMM mutation model (Piry et al. 1999). Therefore, it is not possible, at the moment, to reject the possibility of a recent population crash in the northern population. No significant evidence of recent bottleneck events were detected in the southern population (Table 3.10).

Table 3.10: Demographic history of *D. capensis* populations in the northern and southern Benguela sub-systems: probability of significant departure from equilibrium population size (i.e. a bottleneck) and estimates of effective population size (N_e + 95% confidence intervals).

		Northern	Southern
Bottleneck	IAM	0.027	0.098
	SMM	0.996	0.996
	TPM	0.973	0.844
N_e	0.05	1928.5 (1529-∞)	966.0 (157.2-∞)
	0.02	5588.8 (1198.9-∞)	1617.8 (354.8-∞)
	0.01	142366.2 (2339.4-∞)	690.7 (252.1-∞)

Estimates of the extent and direction of migration, using the bayesian approach implemented in GENECLASS, indicated a low level of assymetric migration from the southern to the northern population. Of the 299 individuals analyzed from the northern Benguela region, 3 (~1%) were identified as more closely related to the southern population, suggesting that these may constitute migrants. These results support the shallow population differentiation indicated with STRUCTURE.

3.1.4. Discussion

Past and recent genetic diversity levels

Population assessment of genetic diversity for the mtDNA COI gene in *Diplodus capensis* revealed high haplotype diversity (overall $h = 0.7073$), but lower levels of nucleotide diversity (overall $\pi = 0.0037$). Nucleotide and haplotype diversity levels were consistently lower in the South African and Namibian samples, compared with the

southern Angolan samples. The observed mtDNA diversity values in *D. capensis* were slightly lower than those reported for the mtDNA control region sequences for European *D. sargus* (average $h = 0.925$, $\pi = 0.03$; Domingues et al. 2007). However, such disparities may be related with the nature of the marker used, as COI is known to accumulate mutation at a slower rate than the Control Region due to greater functional constraints (Brown & Simpson 1979).

Levels of genetic diversity revealed by microsatellite DNA screening were relatively high, across loci and samples, with observed heterozygosity (H_O) ranging from 0.773 to 0.836. These values are similar in range to nuclear diversity levels reported for other marine fish species, including sparids: e.g. *Acanthopagrus australis* $H_O = 0.783$ -0.812 (Roberts & Ayre 2010); *Pagellus bogaraveo* $H_E = 0.477$ -0.915 (Pinera et al. 2007). Long-term over-exploitation of populations may result in loss of genetic diversity (Kenchington et al. 2003; Hauser & Carvalho 2008). However, despite a reported decline in abundance in *D. capensis* (Richardson 2010) no significant differences in levels of genetic diversity were observed between samples collected in protected and un-protected zones in southern Angola, or between northern and southern Benguela populations. These results imply that the observed abundance decline in southern Angola has not yet influenced *D. capensis* diversity levels, which may be related to the existence of under-exploited areas in the region. Such areas may be acting as undesignated marine protected areas, which are known to contribute to restore and maintain local marine biodiversity (e.g. Perez-Ruzafa et al. 2006; Arrieta et al. 2010; Teske et al. 2010; Briggs 2011). On the other hand, marine fish are traditionally considered to have historically high effective population sizes, which will influence genetic diversity. Therefore, the present inability to detect a decrease in genetic diversity may result from high historical effective population sizes in *D. capensis*, as indicated by the bottleneck and N_e analyses.

Population differentiation and phylogeographic structure

Assessment of *D. capensis* population structure across the Benguela Current system identified two distinct and divergent genetic clusters, with no significant geographically-based differentiation detected within each cluster, a result confirmed using both mtDNA and nDNA markers.

Pairwise tests of genetic differentiation (F_{ST}) and phylogeographic reconstructions using the mtDNA COI sequence dataset revealed significant genetic divergence between samples from Angola to northern Namibia (northern Benguela) and South Africa

(southern Benguela). F_{ST} values were high, ranging from 0.832 to 0.950 for comparisons between the two clusters. Reconstruction of haplotype networks revealed an absence of shared haplotypes between the two regions, implying lack of gene flow and occurrence of complete lineage sorting (Avice 2000). These findings were further supported by AMOVA tests that identified the northern-southern sample groupings as representing the highest and most significant between-group component of genetic variance. Since mtDNA is maternally inherited, the observed complete lineage sorting combined with high levels of population differentiation, suggest the absence of (at least) female-mediated and larval gene flow across the Benguela region, resulting in isolation of populations.

Reconstruction of *D. capensis* population structure using nuclear markers identified exactly the same genetic clusters as those identified by the mtDNA analyses. Of the eight cross-specific microsatellite loci used, statistical tests identified two loci that may be subject to the action of positive selection (or linked to such DNA regions), and which were found to be contributing substantially to the observed population differentiation. These findings may suggest that observed genetic divergence in *D. capensis* might be a product of differential selection pressures across different regions of the Benguela Current system, which may have led to local adaptation (Waples 1998; Gaggiotti et al. 2009; Nielsen et al. 2009; Andre et al. 2011). Pairwise F_{ST} values for nDNA (0.039 to 0.048 between northern and southern samples) were smaller than those for mtDNA, an effect well described for microsatellite data due to much higher within-sample variance of these markers (Balloux & Lugon-Moulin 2002). Furthermore, although the Bayesian analyses identified two distinct genetic clusters, as observed for the F_{ST} comparisons, it also indicated a degree of admixture between clusters, suggesting the occurrence of relatively recent gene flow across the Benguela region.

Similar discrepancies between results obtained with nuclear and mitochondrial markers have been reported in several other marine species such as *Thunnus obesus* (Gonzalez et al. 2008), *Pomatoschistus minutus* (Larmuseau et al. 2010), *Xiphophorus helleri* (Tatarenkov et al. 2010), and the European sparid *Diplodus sargus* (Domingues et al. 2007). Such findings can be either interpreted as a product of male-biased dispersal, or statistical discrepancies due to the nature of the markers. As mtDNA is maternally inherited and no shared haplotypes were found between the two *D. capensis* populations this indicates no recent mtDNA gene flow, therefore the lower differentiation of nuclear markers would suggest male-biased dispersal (i.e. nuclear gene flow) across the Benguela region (Hutchings & Gerber 2002; Brunelli et al. 2010; Portnoy et al. 2010).

However, there is no evidence that *D. capensis* exhibits sex-biased dispersal (W. Potts, personal communication), and individuals are partially functional protandrous hermaphrodites (Mann & Buxton 1998; Richardson 2010) so that males may transform to females and thus contribute to the population mitochondrial gene pool. Therefore, it is unlikely that the observed differences between levels of mitochondrial and nuclear differentiation result from sex-biased dispersal. An alternative explanation may be linked to effective population sizes (N_e) and rates of marker frequency drift: mtDNA is haploid and maternally (clonally) inherited, which results in a fourfold lower effective population size than for nuclear DNA (Brown & Simpson 1979). This will result in slower mutation fixation rates and drift in allele frequencies in the nuclear genome, since high effective population sizes limit the action of genetic drift. Furthermore, microsatellites have a higher probability of exhibiting mutational homoplasy, which can further limit detection of genetic differentiation (Estoup & Cornuet 1999; Beebee & Rowe 2005). Traditionally, population differentiation in marine fishes by genetic drift is very weak, due to shallow (recent) population histories and historical high effective population sizes that do not allow accumulation of large genetic divergence (Galarza et al. 2009; Andre et al. 2011). If two closely related populations exhibit high allelic diversity and similar allelic frequencies, as observed for *D. capensis*, software like STRUCTURE may fail to distinguish between real admixture and no admixture at all, even when it detects significant sub-population structuring. Equally, because of high levels of within-population diversity such programmes will identify a few individuals that are, by chance, at the extremes of the genotype composition and so more similar to another population than to their population of origin. Therefore, apparent admixture in the microsatellite dataset can thus result from lack of statistical power to distinguish between populations. It has been considered that loci under divergent selection can help to detect accurate population structure in species with high effective population sizes (Nielsen et al. 2009; Andre et al. 2011). In the present study, two out of the eight neutral loci used were identified as statistical outliers, consistent with deviations from neutral expectations due to divergent selection. When these loci were removed from the analyses, STRUCTURE did not detect significant population differentiation. These findings highlight the potential of using selected markers to detect population structure in marine fishes. Thus, results obtained with microsatellite data cannot convincingly separate between complete isolation with no gene flow but absence of extensive drift due to historically high effective population sizes, and population differentiation with low levels of gene flow. Consequently, in view of the high and significant genetic

differentiation indicated by both mtDNA and microsatellite results, and the potential for statistical artefacts in the estimation of admixture using the microsatellite data, it is concluded that *D. capensis* population structure across the Benguela Current comprises two highly divergent populations with negligible (or zero) gene flow between them.

The observed *D. capensis* population structure appears to correlate geographically with the main oceanographic features of the Benguela Current system. The distinct genetic break point between samples from southern Angola / northern Namibia and South Africa coincides with the position of the perennial upwelling cell off central Namibia (Lüderitz) that is known to actively divide the system into two physically, chemically and biologically different sub-systems (Shannon 1985; Boyer et al. 2000; Lass & Mohrholz 2005; Hutchings et al. 2009). The Lüderitz perennial upwelling cell, consisting of strong offshore current flows of cold waters, is thought to block longshore transport of ichthyoplankton across the region, resulting in larval retention within both sub-systems to the north and south (Lett et al. 2007). This major oceanographic feature may, thus, be contributing to disruption of gene flow among *D. capensis* populations. However, although the upwelling cell could have a large influence in passive dispersion of pelagic phases, mobile adults could still be able to move through it. For example, absence of contemporary genetic differentiation across the Mediterranean sea in white seabream (*D. sargus*) was considered linked to adult dispersal abilities (Lenfant & Planes 1996; Bargelloni et al. 2005; Domingues et al. 2007), and major genetic differentiation was found to be temporal and not spatial (Gonzalez-Wanguemert et al. 2004; Gonzalez-Wanguemert et al. 2007; Gonzalez-Wanguemert et al. 2010; Kaouèche et al. 2011), suggesting that these sparids can disperse across vast geographical regions. However, *D. capensis* adults appear to be highly resident, with dispersal mainly occurring in the early phases of the life history (Richardson 2010). Limited adult dispersal combined with larvae retention in each sub-system can thus be contributing to the observed levels of genetic divergence across the Benguela Current. Likewise, observed absence of significant differentiation within each system, even though sampling sites were hundreds of km apart, could be related to larval dispersal capabilities. *Diplodus capensis* exhibits a protracted larval phase that can extend for up to 28 days (Patrick & Strydom 2009), and is considered to be a mechanism to enhance dispersal and survival. Extended larval phases will contribute to homogenize populations, as individuals can recruit hundreds of km away from their original spawning grounds (Bay et al. 2006; Galarza et al. 2009). Therefore, *D. capensis*

population structure in the Benguela Current system appears to have resulted from the combination between regional-scale oceanographic features and the species life history.

Evolutionary history

Inference of *D. capensis* evolutionary history revealed evidence of past population expansions in both regional populations, based on phylogeographic patterns, overall diversity levels, Tajima's D and Fu's F_S statistics, and mismatch distribution analyses. Both populations exhibited star-shaped phylogeographic patterns in mtDNA sequence diversity, which are commonly associated with a demographic exponential increase from a small female effective population size (Avice 2000). However, northern and southern populations exhibited different levels of haplotype and nucleotide diversity, suggesting two different demographic scenarios: the northern population exhibits evidence of a past bottleneck followed by rapid population growth, whilst the southern population appears to have undergone a more recent and/or severe bottleneck event, exhibiting few and highly divergent haplotypes (Grant & Bowen, 1998). However, these results contradict the time since expansion, estimated from mismatch distribution parameters: for the southern population an earlier expansion dating from the late Pleistocene (~40 KYA) is indicated, compared to the later time since expansion in the northern population, which dates from the early Holocene (~8 KYA). The confidence intervals on the estimates are much wider, however, for the southern population (in fact they overlap the present day) than the northern population, and so the apparently earlier time since expansion for the southern population may be a statistical artefact. Such estimates of divergence and expansion times agree with results obtained for population expansions in other marine species such as *Engraulis mordax* and *Sardinops sagax* in the eastern Pacific (Lecomte et al. 2004), and *Merluccius paradoxus* (23 KYA, von der Heyden et al. 2007) *Merluccius capensis* (6 KYA, von der Heyden et al. 2010) and *Caffrogobius caffer* (45 to 138 KYA, Neethling et al. 2008) in the Benguela Current region.

There may be several reasons to explain the disparity found between genetic diversity levels and estimates of time since expansion for the two *D. capensis* populations. For example, observed divergence may be linked to different paleo-oceanographic events in the Benguela Current region. The late-Pleistocene was characterized by cyclical glacial and inter-glacial periods that differentially influenced sea surface temperatures, sea levels and paleoproductivity in the northern and southern Benguela Current sub-systems (Marlow et al. 2000; Jahn et al. 2003). In particular, reported sea level regressions in

northern Benguela would limit availability of suitable habitat for inshore species due to a narrower continental shelf, while in South Africa sea level regressions may have had a smaller impact in the inshore environment due to the extensive and shallow Agulhas Bank (Ramsay & Cooper 2002). Nevertheless, the lower genetic diversity found in the southern population implies less genetic diversity recovery after the bottleneck event than that observed in the northern population. Whatever the cause and timing of the effect, the southern population appears to have suffered a more severe population size bottleneck during which it lost most of its mtDNA diversity.

Another consideration is that estimates of time since expansion using mismatch distribution parameters are point estimates, and may be biased by early branching events (Avice 2000). The assessment of *D. capensis* evolutionary history using the Bayesian approach implemented in BEAST suggests that the origin of haplotypes in the northern population lies deeper than those in the southern population, and the 95% highest posterior density interval (HPD) for both estimates overlap (see Figure 3.4), and thus differentiation between the two estimates is not statistically significant. As such, the most parsimonious explanation is that population expansion in both northern and southern Benguela populations may have occurred at roughly the same time.

Reconstruction of phylogenetic relationships in mtDNA COI sequence diversity among *D. capensis* samples revealed, as expected, two highly divergent clades composed by northern and southern populations. However, uncorrected pairwise distances were relatively small when compared with divergence between *D. sargus* and *D. vulgaris*, suggesting that although genetically distinct the two *D. capensis* populations may not yet be considered different species (Avice 2000; Ward et al. 2005), which supports the conclusion by Richardson (2010) based on morphological data. The mtDNA sequence data also did not support the separation as a distinct species of the KwaZulu-Natal population from other South African populations as proposed by Heemstra & Heemstra (2004). The COI sequence analysis did, however, support the previous separation by Heemstra & Heemstra (2004) of southern African *D. capensis* (previously *D. sargus capensis*) from European *D. sargus* (previously *D. sargus sargus*), estimated here to have occurred approximately 1.8 MYA. An interesting outcome of the phylogenetic analyses was the identification of two *D. sargus* individuals more closely associated with the southern African *D. capensis* clade than with other *D. sargus* individuals. This result may suggest that the *D. capensis* distribution range may extend further north than previously documented (Heemstra & Heemstra 2004), and that further studies regarding

the distribution and phylogenetic status within the genus are required, especially in the poorly documented waters of west Africa. Bayesian estimates of time since most recent common ancestor suggest that isolation between northern and southern *D. capensis* populations dates back ~350 KYA, during the late Pleistocene. This epoch was characterized by a steep drop in sea surface temperatures in advance of the onset of glacial periods (Marlow et al. 2000; Jahn et al. 2003). In particular, *D. capensis* population differentiation appears to coincide with the 3rd glacial age (455 – 380/300 KYA, Pisias et al. 1981). Marine species' response to glacial advances partially depends on species' cold tolerance and dispersal ability (Ruzzante et al. 2011). Thus, decreased sea surface temperatures could have been accompanied by a retreat of the warm-temperate *D. capensis* towards the areas influenced by the tropical Angola and Agulhas Currents in either sub-system. Therefore, *D. capensis* evolutionary history appears to be closely linked with past climatic changes in the Benguela Current.

Reconstruction of contemporary demographic changes for the microsatellite dataset did not produce conclusive results. Observed high levels of microsatellite genetic diversity may imply the absence of severe bottlenecks in the recent past (10s-1000s years). In addition, analyses of allele frequencies did not retrieve evidence of recent bottleneck events in the southern population, and results obtained for the northern population were highly dependent of the mutation model used. As suggested by Piry et al. (1999), evidence of recent bottlenecks is more easily detected if microsatellites evolve under a strict Infinite Alleles Model (IAM – Piry et al. 1999). Thus, observed significant deviations to predictions from migration-drift equilibrium detected in the northern population, under the IAM, may indicate the occurrence of a recent population decline, or at the very least cannot exclude its occurrence. Equally, the inability to detect a similar signal in the southern population cannot exclude the possibility of its occurrence, since methods employed to detect bottleneck signatures require severe losses of genetic diversity, which in populations with such high effective sizes would represent catastrophic crashes. Thus, these methods may fail to detect significant events at the genetic level that can still represent a disaster in terms of conservation biology (e.g. Riccioni et al. 2010)

As expected for a marine fish, estimates of *D. capensis* contemporary effective population sizes (N_e – the number of breeding individuals that contribute offspring to the next generation) were high. Overall values of N_e ranged from 1982 to 142366 in the northern population, and from 690 to 1617 in the southern population, depending on the

lowest allele frequency used. Although observed confidence intervals were extremely high, ranging from 690 to infinity, obtained estimates of N_e are within, or above, the typical range documented for several fish species (Hauser & Carvalho, 2008), and well above the considered minimum threshold for maintenance of a species' evolutionary potential ($N_e > 500$, Frankham et al. 2002). Such high effective population sizes can thus be contributing to observed high levels of polymorphism, and the inability to detect signals of over-exploitation in southern Angola. Analysis of the extent and direction of migration between populations suggested the existence of unidirectional gene flow from the southern to the northern population, which may be related to the northwards flow of the Benguela Current. However, *D. capensis* appears to be highly resident, and, as discussed above for the levels of admixture indicated, these findings may result from the combination of high effective population sizes and similar allelic frequencies in both populations, thus representing a statistical artefact.

Implications for fishery management and conservation efforts

The results here presented revealed two genetically divergent *D. capensis* populations in the northern and southern Benguela Current sub-systems. No significant differentiation was detected within each population, which may be related to the long-lived pelagic phase and possible larval retention within each Benguela sub-system (Lett et al. 2007; Patrick & Strydom 2009). Therefore, it is recommended that *D. capensis* populations of the northern and southern Benguela regions should be considered independent Evolutionary Significant Units (Moritz 1994). Based on the observed mitochondrial divergence levels, and complete lineage sorting, it is possible that these *D. capensis* populations are in the process of speciation. This hypothesis is further supported by the reported biological differentiation between populations (Richardson 2010), and the existence of loci displaying signals of selection, which may indicate the development of local adaptation.

The reported absence of significant differentiation within each population could be beneficial for future management and conservation plans, since any given site can be replenished by *D. capensis* from any location within that region. One effective way to ensure the maintenance of marine species diversity levels and evolutionary potential is through the establishment of marine protected areas (Lenfant 2003; Perez-Ruzafa et al. 2006; Arrieta et al. 2010; Briggs 2011). As suggested by Richardson (2010) this is possibly the best strategy to ensure conservation of *D. capensis* in southern Angola. In South Africa establishment of marine protected areas (MPAs) has been the strategy for

the last 20 years, with moderate success (von der Heyden et al. 2008; Sowman et al. 2011). At the moment in Angola there are regions that function as informal MPAs due to the difficulty of access, such as Baía dos Tigres (near the Cunene River Mouth), Flamingo river mouth, and the rocky region between Lucira and Benguela, making these ideal candidates for the establishment of formal MPAs. The establishment of MPAs should take into consideration larval dispersion routes, population connectivity and oceanographic processes (Briggs 2011; Dawson et al. 2011; Grantham et al. 2011). Thus, in order to ensure the establishment of suitable MPAs in southern Angola it is necessary to investigate *D. capensis* larval dispersion patterns and how they are influenced by the Benguela Current oceanographic features. Furthermore, reconstruction of *D. capensis* evolutionary history indicates that the species may be highly vulnerable to climatic fluctuations, suggesting that future climate-induced changes will possibly have a severe impact on *D. capensis* distribution range, population dynamics and biological features (van Hal et al. 2010; Lo Brutto et al. 2011).

CHAPTER 4: *Argyrosomus* spp.

4.1. Tempo and mode of evolution of *Argyrosomus* spp. (Perciformes, Sciaenidae) in the eastern Atlantic: evidence of Pleistocene origins

4.1.1. Introduction

Climatic fluctuations during the Pliocene and Pleistocene have influenced speciation events in several vertebrate species (Avice et al. 1998), including marine taxa such as sea urchin *Diadema* spp. (Lessios et al. 2001), anchovy *Engraulis* spp. (Grant & Bowen 2006), *Mugil cephalus* (Shen et al. 2011) and the shark family Orectolobidae (Corrigan & Beheregaray 2009). After the closure of the Isthmus of Panama (~3 MYA) potential contact between the Atlantic and Pacific Oceans for tropical, subtropical and warm temperate marine fauna was limited to the waters around southern Africa, as the northern and southern ocean passages around the Americas and northern Asia all lie in polar waters and so are assumed to be a complete barrier to migration / dispersal of warmer water fauna. However, even around southern Africa the cold sea surface temperatures of the Benguela Current may have limited migration/dispersal, thus being responsible for multiple allopatric speciation events suggested for taxa occurring between the eastern Atlantic and Indo-Pacific Oceans (e.g. Lessios et al. 1999; McCartney et al. 2000; Bowen et al. 2001; Colborn et al. 2001; Lessios et al. 2003).

The sciaenid fish genus *Argyrosomus* includes 10 species occurring in the eastern Atlantic and in the Indo-West Pacific (Sasaki 1989; Heemstra & Heemstra 2004). In the eastern Atlantic the genus exhibits an antitropical distribution with *A. regius* (Asso 1801) limited to the northeastern region, while *A. coronus* Griffiths and Heemstra (1995); *A. inodorus* Griffiths and Heemstra (1995); and *A. japonicus* (Temminck and Schlegel, 1844) occur in the southeastern Atlantic, in the Benguela Current region. The present distribution of *A. regius* ranges from France to Senegal in the eastern Atlantic (FAO 2005a), and is thought to be linked to the species temperature tolerance as feeding actively is greatly reduced in waters colder than 13-15°C and larval development requires temperatures between 20-21°C (FAO 2005a). In the southeastern Atlantic, the three *Argyrosomus* species exhibit partially overlapping distributions: *A. coronus* occurs from northern Angola to southern Namibia (Griffiths & Heemstra 1995; Potts et al. 2010); *A. inodorus* ranges from northern Namibia to the Kei River in eastern South

Africa, but exhibits a distributional break between central Namibia and Cape Point in South Africa (Griffiths & Heemstra 1995; Kirchner 1998); and *A. japonicus* is restricted to South African waters, from Cape of Good Hope to KwaZulu-Natal (Griffiths 1996). In all three Benguela region species, annual return migrations have been documented and appear to be linked to seasonal changes in sea surface temperatures (Griffiths 1996; Kirchner 1998; Potts et al. 2010). For example, the *A. coronus* annual return migration appears to be linked to the seasonal displacement of the Benguela-Angola Front that possess the suitable temperature for the species to occur (16°C-19°C, Potts et al. 2010), while *A. inodorus* appears to actively track water temperatures of 13-16°C (Kirchner 1998). Of the four *Argyrosomus* species occurring in the eastern Atlantic, *A. inodorus* exhibits the most divergent biological features: it is smaller, matures at smaller sizes, and occurs in deeper and colder waters than the other three species: *A. regius*, *A. coronus* and *A. japonicus* exhibit similar biological characteristics, such as maximum size and size at sexual maturity (Table 4.1 adapted from Potts et al. 2010).

Table 4.1: Comparison of life history features between *Argyrosomus* species in the eastern Atlantic (adapted from Potts et al. 2010).

	<i>A. regius</i>	<i>A. inodorus</i>	<i>A. coronus</i>	<i>A. japonicus</i>
Habitat	inshore, estuaries, coastal lagoons	inshore, nearshore	inshore, rocky reefs, nearshore, estuaries	inshore, rocky reefs, nearshore, estuaries
Maximum size (cm)	182	115	190	181
Size at sexual maturity (cm)	~80	31 / 34	82 / 90.4	95 / 110
Maximum age (yr)	-	25 / 28	13	42
Spawning	May-July (Europe) Jan-May (Africa)	September to December	September to December	August to January
Migration patterns	Adults and juveniles, Inshore/offshore and Longshore	Adults, Inshore/offshore (South Africa) and Longshore	Adults, Inshore/offshore and Longshore	Adults, Inshore/offshore and Longshore

The distribution ranges and biological features of these *Argyrosomus* species make them ideal candidates to investigate speciation in the marine environment. Therefore, the present study aims to assess timing and mode of evolution of the *Argyrosomus* genus in the eastern Atlantic, with a particular focus on speciation events across the Benguela Current region, using both mitochondrial and nuclear DNA markers. Contemporary levels and patterns of genetic diversity reflect historical population processes. Therefore, based on the *Argyrosomus* species current distribution ranges and biological features it is hypothesized that: *i)* *A. regius* shares a common ancestor with the

southeastern Atlantic *Argyrosomus* species; ii) *A. regius* and the southeastern species constitute sister taxa, as they appear to exhibit a typical antitropical distribution due to the vicariant effect of tropical waters in the equatorial region; iii) *A. inodorus* is the most genetically divergent species of the southeastern Atlantic group, due to colonization and adaptation to colder and deeper habitats in the Benguela Current region; iv) *A. coronus* and *A. japonicus* constitute sister taxa, isolated on either side of the Benguela Current due to the establishment of the system's oceanographic features; and v) speciation events in the eastern Atlantic, and particularly within the Benguela Current boundaries, will coincide with major climate-induced oceanographic changes in the region during the Pliocene-Pleistocene transition.

4.1.2. Methods

Sampling and DNA extraction

A total of 25 kob samples were collected throughout the eastern Atlantic. Due to the species distribution ranges *A. regius* samples were collected from the northeastern Atlantic, *A. coronus* samples were collected from northern and southern Angola, and from central Namibia; *A. inodorus* was sampled in central Namibia and in Eastern Cape, South Africa; and *A. japonicus* was caught in Eastern Cape, South Africa, which represents the southernmost limit of the influence of the Benguela Current (Figure 4.1, Table 4.2). All samples were collected either in fish markets or by local collaborators. Available sequences of *Cynoscion nebulosus*, a western Atlantic sciaenid, were used as an outgroup in all analyses to root phylogenetic reconstructions of relationships among the four *Argyrosomus* species. A fin clip was removed from each individual and fixed in 95% ethanol. DNA extraction was performed as previously described (Chapter 2.2.1.).

Table 4.2: Sampling strategy for *Argyrosomus* spp. in the eastern Atlantic, including country, region, sample size, and latitude/longitude coordinates.

Species	Country	Region	Sample size	Coordinates
<i>A. regius</i>	Portugal	Quarteira	3	37°3.346'N 8°6.43'W
	Angola	Luanda	2	8°47.263'S 13°14.32'E
Flamingo		4	15°10.374'S 12°04.863'E	
<i>A. coronus</i>	Namibia	Henties Bay	4	22°7.404'S 14°16.139'E
	Namibia	Henties Bay	4	22°7.404'S 14°16.139'E
<i>A. inodorus</i>	South Africa	Port Alfred	4	33°36.500'S 26°54.00'E
	South Africa	Algoa Bay	4	33°49.53'S 25°52.31'E

Genetic screening

All specimens were PCR amplified and sequenced for 3 mitochondrial DNA (mtDNA) loci (control region (CR), cytochrome c oxidase I (COI) and cytochrome b (cytb)), and one nuclear locus (1st intron of the S7 ribosomal gene), as described in Chapter 2.2.2.

Alignment of *Argyrosomus* spp. sequences was unambiguous for all mtDNA loci, but proved to be difficult for the S7 locus due to the presence of heterozygous positions. Heterozygous positions, defined as two clear and near equally sized peaks at the same position, were observed in all species. Therefore, S7 haplotypes were statistically resolved using PHASE 2.1.1 (Stephens et al. 2001). To decrease computational time only the most frequently occurring S7 haplotypes (frequency >1%) were used in phylogenetic reconstruction.

Evolutionary history

Reconstruction of phylogenetic relationships between *Argyrosomus* species in the eastern Atlantic were conducted combining all mtDNA loci into one concatenated dataset (mtDNA data), concatenating mtDNA and S7 (mtDNA-nDNA data), and on the S7 dataset (nDNA data) alone.

Heterogeneity of base composition was evaluated for all datasets with the χ^2 test, as implemented in PAUP 4.10 (Swofford 1993). To ensure that all loci could be concatenated, both mtDNA and mtDNA-nDNA datasets were tested for incongruent length differences (ILD), using the Tree-Branch-Recombination swapping method, as implemented in PAUP 4.10 (Swofford 1993). The ILD-test was performed for 1000 replicates, saving 2 trees in each step. The most appropriated nucleotide substitution model was estimated for each dataset in jModelTest (Posada 2008). Average uncorrected pairwise distances were estimated for each species pair, as implemented in MEGA 5.1 (Kumar et al. 2008)

Assessment of gene trees was conducted using two complementary inference methods: Maximum Likelihood (ML) and Bayesian analysis (BA). Maximum Likelihood analyses were conducted using a Neighbour-Joining starting tree (BIONJ), and ran under the aLRT method (Anisimova & Gascuel 2006) as implemented in PhyML (Guindon et al. 2009). Branch support was assessed with the χ^2 test, as recommended by Anisimova & Gascuel (2006), and branches with support above 0.5 (50% of retrieved trees) were retained. Bayesian analyses were performed in MrBayes 3.1 (Huelsenbeck & Ronquist 2001; Ronquist & Huelsenbeck 2003). In the BA analysis, all concatenated datasets were partitioned into individual loci, to allow evolutionary rates

and branch lengths to vary independently across partitions. Two independent sets of four chains were run for 1.5 million MCMC generations, and parameters were recorded every 100th generation. All branches with posterior probabilities above 0.5 were retained. Convergence and stationarity of runs were estimated by examination of likelihood plots, using Tracer 1.4 (Rambaut & Drummond 2007), and when variance of split frequencies was below 0.01 (Hall 2008). A consensus tree was obtained after a burn-in period of 2500 generations, using TreeAnnotator 1.6.1 (Drummond & Rambaut 2007). Reconstruction of ML and Bayesian trees were conducted in FigTree 1.3.1 (Rambaut 2009).

Tempo of evolution

In order to test whether datasets conformed to a strict molecular clock in the form of their evolutionary change, a likelihood test was conducted as implemented in MEGA 5.1 (Kumar et al. 2008). Obtained results confirmed that the data did fit to a clockwise mutation pattern, and substitution rates did not vary significantly between lineages, suggesting that a strict molecular clock could be enforced. Time since most common recent ancestor (tmrca) was estimated based on a species-level phylogeny, as implemented in BEAST 1.3.1 (Drummond & Rambaut 2007) under a strict molecular clock. The data were partitioned into coding and non-coding regions for the mtDNA dataset, and into coding / non-coding mtDNA / non-coding S7 regions for the mtDNA-nDNA dataset. Substitution rates were unlinked among partitions. Runs were performed under a Yule speciation process for branching rates, and using the HKY model of nucleotide substitution for the CR, cytb and S7 data sets, and a TRN model for the COI data set. Two independent analyses were run for 10 million generations and logged every 1000th step. Independent runs were combined using LogCombiner 1.6.1 (Drummond & Rambaut 2007), and convergence was estimated based on Effective Sample Size (ESS>200) in Tracer 1.4 (Rambaut & Drummond 2007). In order to check if posterior probabilities were influenced by the data, analyses were performed in which BEAST would only sample from the prior distribution (Drummond 2006).

Due to the absence of a fossil record for *Argyrosomus* spp. in the eastern Atlantic, calibration of the molecular clock was performed using two different approaches. Firstly, by fixing the mean sequence divergence rate per lineage at 1.5% per MY for the mtDNA dataset (considered the universal rate in marine fish COI and cytb regions - Bermingham et al. 1997), and at 0.23% per MY for the nDNA dataset (a value obtained from the divergence of *Anisotremus* spp. due to the closure of the Isthmus of Panama -

Bernardi & Lape, 2005). Secondly, using the timing of the strengthening of the Benguela Current (~ 2 MYA) as a biogeographical event to calibrate the separation of *A. coronus* and *A. japonicus*. The 2 MYA date was used as the mean of a normal distribution to calibrate the internal node, and a broad standard deviation (SD = 1 MY) was enforced to allow for uncertainty of time estimates (Drummond et al. 2006). Performance of each approach was compared based on the likelihood of the posterior probabilities of each model, as suggested by Drummond & Rambaut (2007). Convergence of run parameters for the most likely approach was estimated based on ESS>200 in Tracer 1.4 (Rambaut 2007). Divergence times were calculated from the post burn-in results, and TreeAnnotator 1.3.1 (Drummond & Rambaut 2007) was used to compose a maximum-clade-credibility tree, visualized in FigTree 1.3.1 (Rambaut 2009).

4.1.3. Results

Evolutionary history

Amplification and sequencing of mtDNA CR, mtDNA COI and mtDNA cytb, and nuclear S7 regions yielded fragments of 598bp, 654bp, 621bp and 463bp respectively. The full-concatenated mtDNA dataset (1873bp) exhibited 512 variable sites, from which 181 were parsimony informative; the concatenated mtDNA-nDNA dataset (2336bp) exhibited 585 variable sites, with 193 parsimony-informative sites.

Estimates of base heterogeneity composition were not significant for any of the datasets tested, suggesting that the sequences were suitable for phylogenetic inference. The ILD test did not detect significant differentiation between partitions in both mtDNA and mtDNA-nDNA datasets ($p>0.05$), which were thus utilized in subsequent phylogenetic analyses.

Estimates of uncorrected pairwise distances between species varied between the dataset used, being smaller for the nDNA data and higher for the mtDNA data (Table 4.3). However, despite the observed differences in degree of divergence, both datasets exhibited a similar pattern of genetic distances between species: highest values were observed for the comparisons *A. regius* / *A. japonicus* and *A. inodorus* / *A. japonicus*, and lowest for the comparisons *A. regius* / *A. inodorus* and *A. coronus* / *A. japonicus* (Table 4.3). Within the mtDNA dataset, the CR exhibited the highest genetic divergence values in all comparisons, while COI and cytb regions exhibited values with similar ranges. In particular, genetic divergence between the outgroup and the ingroup was significantly

higher for the CR sequence data than for the COI and cyb sequence data (Table 4.4). When all regions were concatenated, again genetic divergence was higher for the *A. regius* / *A. japonicus* and *A. inodorus* / *A. japonicus* comparisons, and lowest for the *A. regius* / *A. inodorus* and *A. coronus* / *A. japonicus* comparisons (Table 4.4).

Table 4.3: Uncorrected pairwise distances between *Argyrosomus* species: concatenated mtDNA-nDNA dataset above diagonal, separate mtDNA / nDNA datasets below diagonal.

	<i>A. regius</i>	<i>A. inodorus</i>	<i>A. coronus</i>	<i>A. japonicus</i>	<i>C. nebulosus</i>
<i>A. regius</i>	-	0.039	0.043	0.051	0.203
<i>A. inodorus</i>	0.047 / 0.009	-	0.045	0.052	0.214
<i>A. coronus</i>	0.050 / 0.015	0.052 / 0.014	-	0.035	0.207
<i>A. japonicus</i>	0.061 / 0.013	0.062 / 0.011	0.041 / 0.009	-	0.214
<i>C. nebulosus</i>	0.231 / 0.132	0.223 / 0.139	0.232 / 0.141	0.220 / 0.139	-

Table 4.4: Uncorrected pairwise distances between *Argyrosomus* species for individual mtDNA loci: cytb / COI sequence data above diagonal; CR sequence data below diagonal.

	<i>A. regius</i>	<i>A. inodorus</i>	<i>A. coronus</i>	<i>A. japonicus</i>	<i>C. nebulosus</i>
<i>A. regius</i>	-	0.049 / 0.039	0.048 / 0.036	0.059 / 0.051	0.122 / 0.132
<i>A. inodorus</i>	0.056	-	0.051 / 0.037	0.053 / 0.049	0.116 / 0.142
<i>A. coronus</i>	0.060	0.062	-	0.035 / 0.035	0.128 / 0.140
<i>A. japonicus</i>	0.070	0.079	0.054	-	0.131 / 0.135
<i>C. nebulosus</i>	0.424	0.430	0.443	0.424	-

Convergence of run parameters performed using Bayesian analyses was achieved for all datasets (Table 4.5), implying that retrieved phylogenetic relationships were the most robust.

Table 4.5: Estimates of convergence of run parameters for the three datasets used: split frequencies of standard deviations (StDev<0.01), effective sample size (ESS>200) and potential scale reduction factor (PSRF \approx 1).

	StDev	ESS	PSRF
mtDNA	0.009	301.296	~1.00
mtDNA-nDNA	0.008	216.97	~1.00
nDNA	0.004	819.031	~1.00

Reconstruction of *Argyrosomus* spp. phylogenetic relationships using both the Maximum Likelihood approach and Bayesian analyses retrieved identical topologies in all trees, and also independently of the dataset used (Figures 4.1 to 4.3). No significant differentiation was observed between the two inference methods, suggesting that retrieved relationships are the most probable ones. Nevertheless, the mtDNA dataset revealed a more clear separation of clades than that observed for the nDNA dataset (Figures 4.1 and 4.2). In particular, divergence between *A. regius* and the *Argyrosomus*

species occurring in the Benguela Current region was clearer for the mtDNA and mtDNA-nDNA datasets than for the nDNA dataset (Figures 4.1 - 4.3).

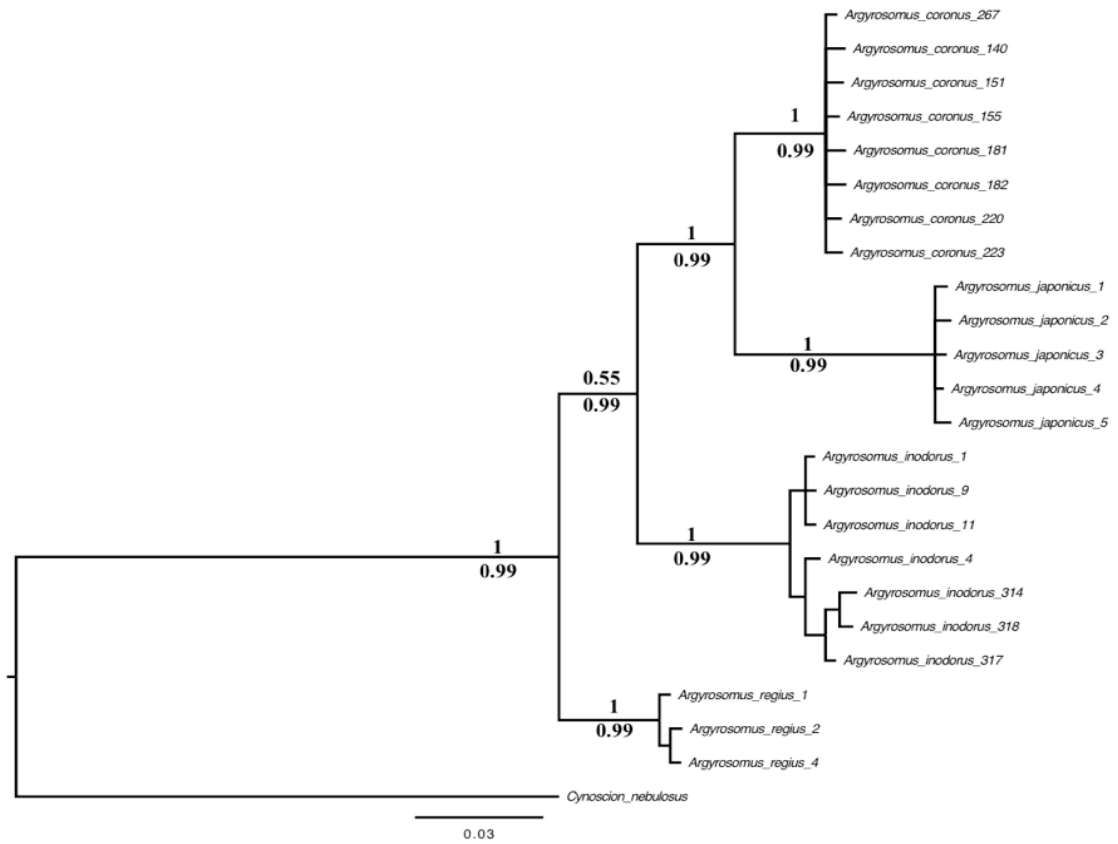


Figure 4.1: Reconstruction of phylogenetic relationships within *Argyrosomus* spp. using the concatenated mtDNA dataset. Statistical support for nodes is given for both Bayesian (posterior probabilities, above branches) and ML analyses (aRLT values, below branches). Outgroup = *C. nebulosus*.

Independently of the method and dataset used all recovered clades exhibited high statistical support (>0.9 probability), meaning that the same branching pattern was retrieved in over 90% of all simulated trees (Figures 4.1 to 4.3). However, the clade containing the Benguela Current *Argyrosomus* species (the Benguela clade) had a relatively low support for the mtDNA dataset in the Bayesian analyses (0.55 probability – Figure 4.1), suggesting that observed branching pattern was only retrieved in 55% of the trees analyzed. Nevertheless, as support obtained for the Maximum Likelihood method (0.99 probability), or for the nDNA and mtDNA-nDNA datasets (Figures 4.2 and 4.3, respectively) was significantly higher, this result may be a statistical artefact associated to the choice of outgroup.

Overall, regardless of the method and dataset employed, all trees exhibited four clear, reciprocally monophyletic and statistically well-supported clades, corresponding to the four identified kob species, even though *A. inodorus* was caught on both sides of the Benguela Current (see Table 4.2 for sample locations). Two major clades could be identified corresponding to the northeastern Atlantic (*A. regius*) and the southeastern Atlantic (Benguela Current species), suggesting that these taxa shared a common ancestor in the past. Within the Benguela clade, *A. inodorus* appears to have diverged earlier from a possible common ancestor, that later speciated into *A. coronus* and *A. japonicus*, which appear to be sister species (Figures 4.1 to 4.3).

Tempo of evolution

The chronograms for the speciation of *Argyrosomus* in the eastern Atlantic, applying both a fixed divergence rate and an internal node calibrator, can be seen in Figures 4.4 to 4.8. For both calibration methods, and in all datasets and analyses, mean posterior estimates of time since most recent common ancestor, sampling only from the prior distribution, were close to the prior node ages, indicating that both approaches were reasonably concordant (Sanders & Lee 2007).

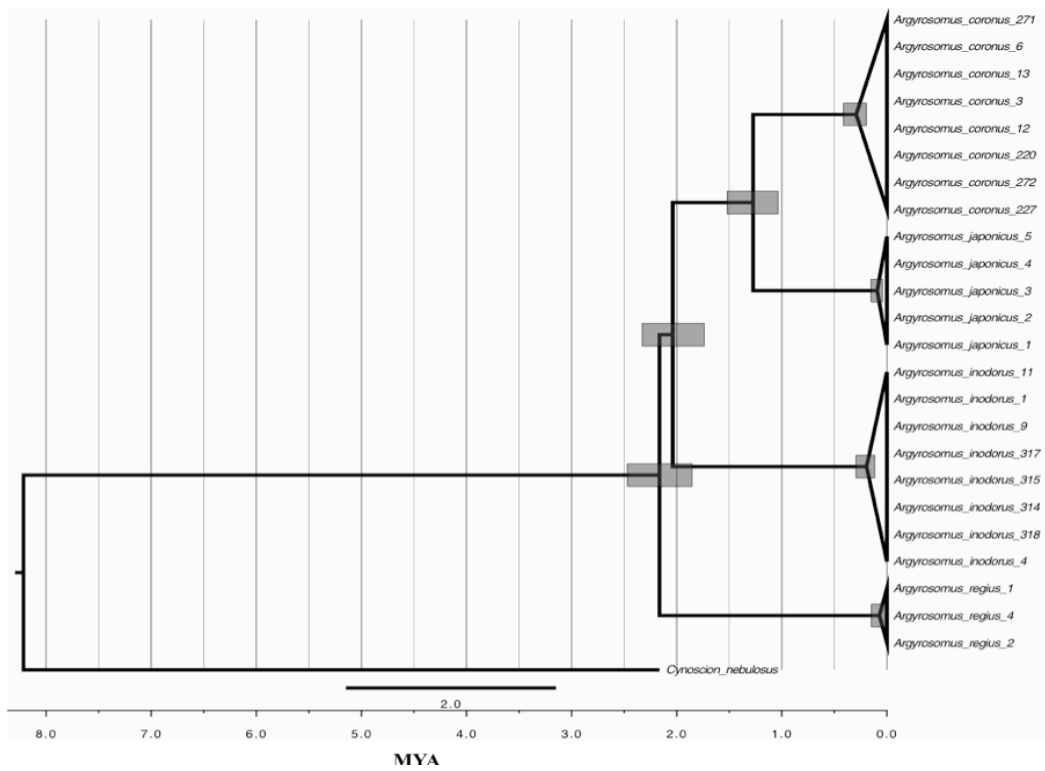


Figure 4.4: Chronogram of time since divergence estimated for *Argyrosomus* spp., for the mtDNA dataset, using a fixed mutation rate. Grey bars over branches represent 95% highest posterior density (HPD).

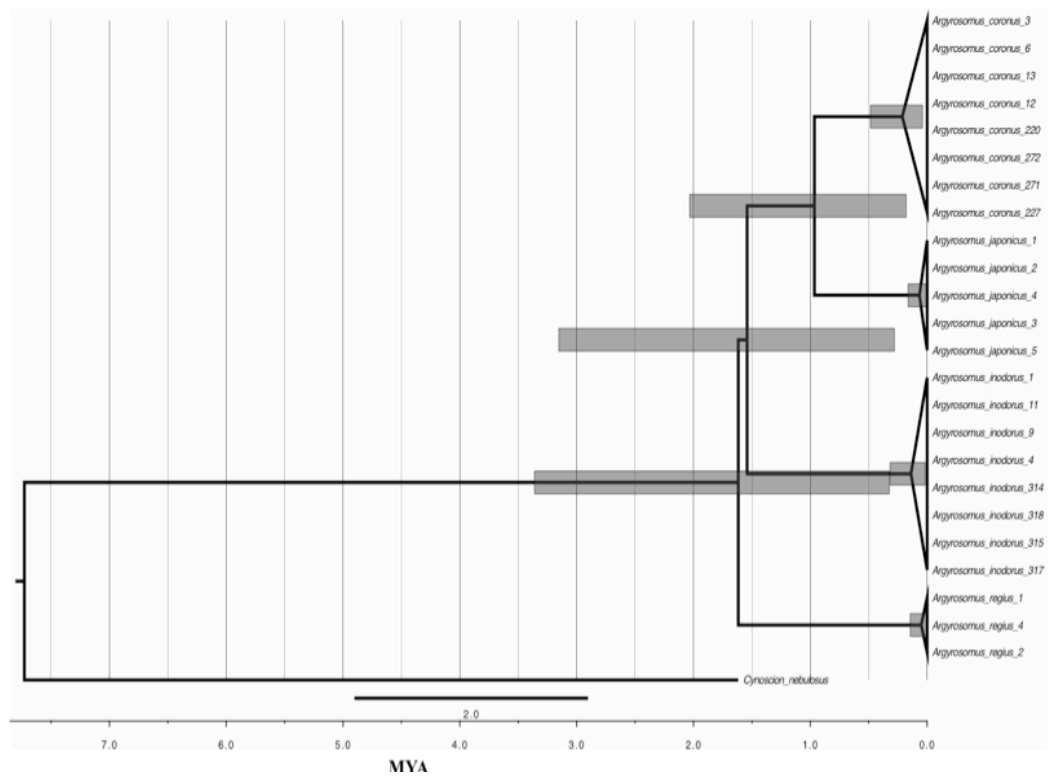


Figure 4.5: Chronogram of time since divergence estimated for *Argyrosomus* spp., for the mtDNA dataset, applying an internal node calibration point (~ 2 MYA). Grey bars over branches represent 95% highest posterior density (HPD).

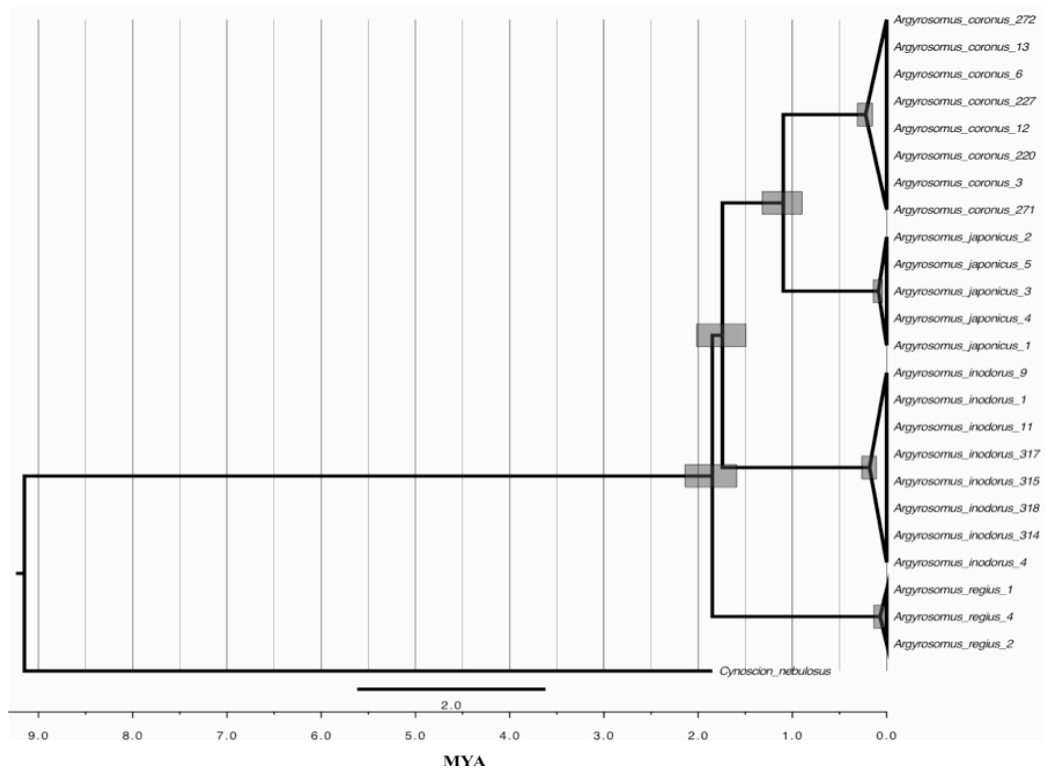


Figure 4.6: Chronogram of time since divergence estimated for *Argyrosomus* spp., for the mtDNA-nDNA dataset, using a fixed mutation rate. Grey bars over branches represent 95% highest posterior density (HPD).

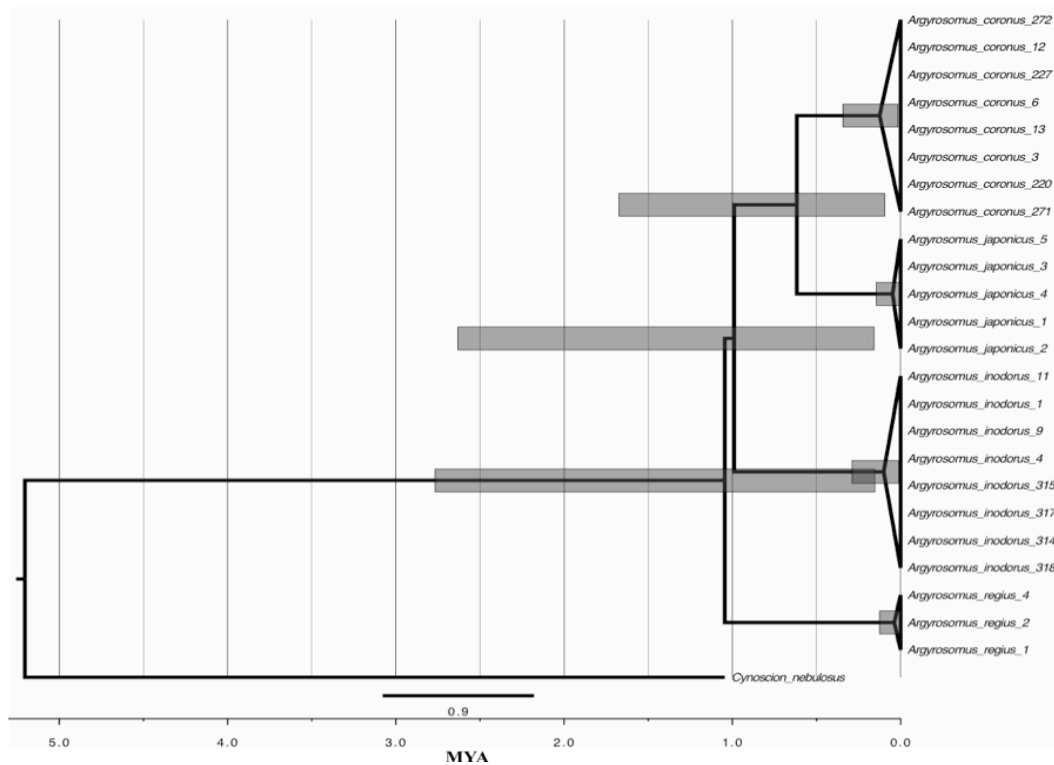


Figure 4.7: Chronogram of time since divergence estimated for *Argyrosomus* spp., for the mtDNA-nDNA dataset, applying an internal node calibration point (~ 2 MYA). Grey bars over branches represent 95% highest posterior density (HPD).

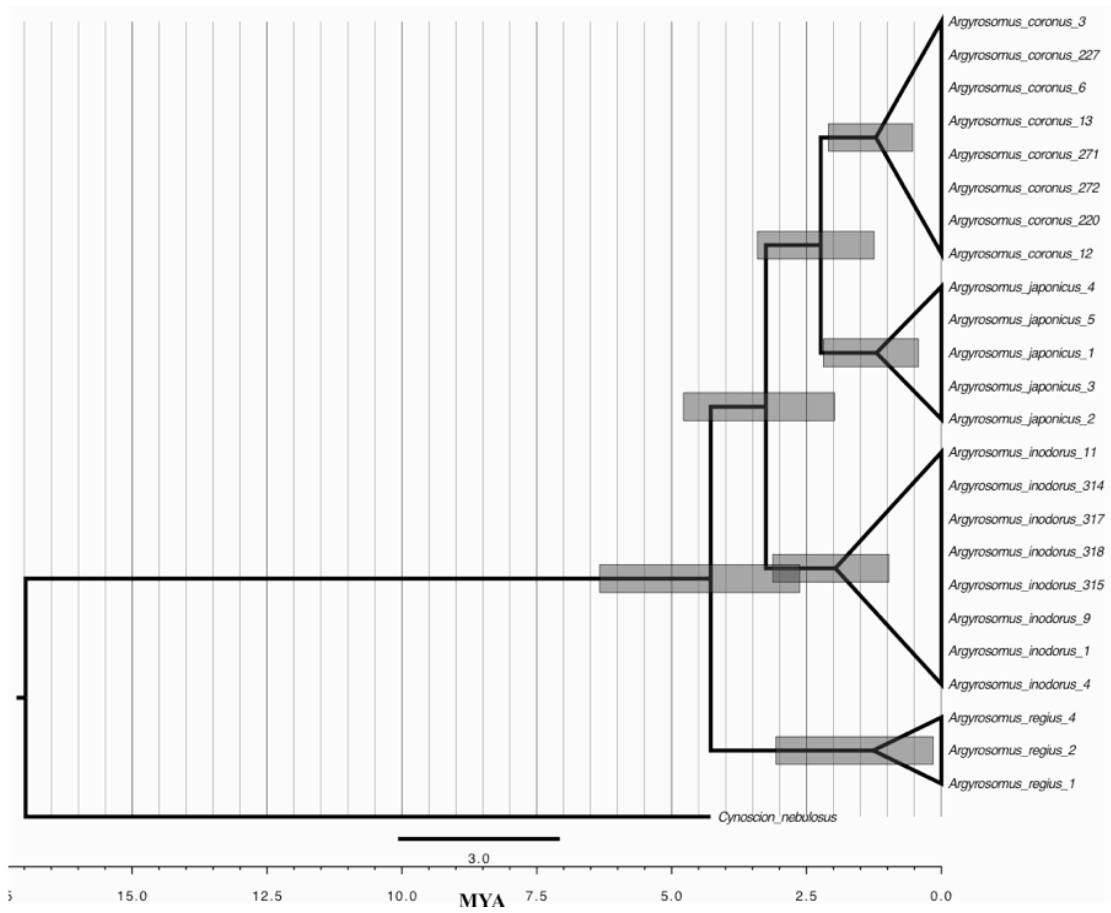


Figure 4.8: Chronogram of time since divergence estimated for *Argyrosomus* spp., for the nDNA dataset, using a fixed mutation rate. Grey bars over branches represent 95% highest posterior density (HPD).

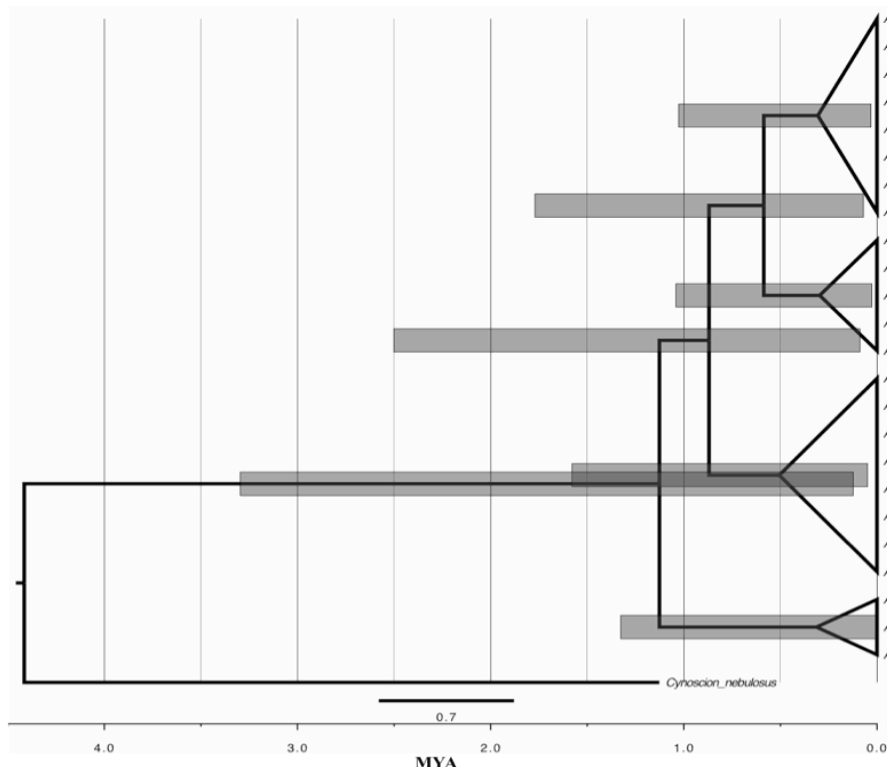


Figure 4.9: Chronogram of time since divergence estimated for *Argyrosomus* spp., for the nDNA dataset, applying an internal node calibration point (~ 2 MYA). Grey bars over branches represent 95% highest posterior density (HPD).

The obtained likelihood of posterior probabilities was similar for both calibration approaches in all datasets ($\ln(\text{likelihood})$ – Table 4.5), suggesting a similar fit of the models to the established prior distributions. However, observed confidence intervals (95% HPD) overlapped and were much larger for the biogeographical calibration approach than for the fixed divergence rate approach (Figures 4.4 – 4.8, Table 4.6). Substitution rates per partition were estimated at 1.9% substitutions per site per MY for *cytb* and 3.9% substitutions per site per MY for *CR*, for the mtDNA dataset, when the mean divergence rate per lineage was fixed at 1.5% per MY for *COI*. These divergence rate values were similar to those estimated for *CR* and *cytb* of other marine teleostes (Bermingham et al. 1997; Donaldson and Wilson 1999). When the 2 MY internal calibrator was applied sequence divergence rates were significantly lower for *COI* (0.7% per MY) and *CR* (1.6% per MY), similar for *cytb* (1.02% per MY) and higher for *S7* (0.45% per MY). Thus, it appears that the internal node calibration may not have been the most appropriate method to estimate time since most recent common ancestor (tmrca) for *Argyrosomus* spp.

Overall, estimates of tmrca were similar for the mtDNA and mtDNA-nDNA datasets, being consistently lower when the biogeographical approach was implemented (Table 4.6). Interestingly, when the 0.46% divergence rate (0.23% per lineage) was applied for the nDNA dataset tmrca estimates were significantly higher than those obtained for the same dataset using the biogeographical approach, or even for the mtDNA-nDNA combined dataset (Table 4.6). It appears that the 0.46% divergence rate may not be a suitable nucleotide substitution rate for the 1st intron of the *S7* ribosomal protein in these *Argyrosomus* species. When the mtDNA partitions were analyzed independently estimates of tmrca obtained with the fixed divergence rate approach were similar in range to those observed for the concatenated mtDNA and mtDNA-nDNA dataset, while the 2 MY internal calibration approach provided larger estimates of tmrca for *COI* and *cyt b* (Table 4.7), again suggesting that the biogeographical approach may not be the most suitable calibration method for estimates of tmrca based on mtDNA in this case.

However, despite broad and overlapping 95% HPD intervals, and independently of the observed differences between calibration method and dataset used, the obtained estimates of tmrca revealed a similar pattern of timing of speciation events in *Argyrosomus* in the eastern Atlantic: divergence of northeastern / southeastern *Argyrosomus* (*A. regius*) appears to have occurred between the late-Pliocene and early Pleistocene (4 – 1.12 MYA), being followed by two speciation events within the

Benguela Current region with divergence of *A. inodorus* in the early- to mid-Pleistocene (2.5 – 0.9 MYA), and divergence of *A. coronus* and *A. japonicus* in the mid- to late-Pleistocene (0.9 - 0.1 MYA) (Tables 4.6 - 4.7).

Table 4.6: Estimates of tempo of evolution of *Argyrosomus* spp. in the Benguela Current: *Ln(Likelihood)* - posterior probabilities of calibration method employed; *tmrca*- estimated time since most recent common ancestor (95% HPD in brackets).

	Calibration Method	Ln (Likelihood)	tmrca (MY)		
			Northeastern vs. Southeastern	<i>A.inodorus</i> vs. <i>A.coronus</i> / <i>A.japonicus</i>	<i>A.coronus</i> vs. <i>A.japonicus</i>
mtDNA	1.5%	-5119.442	2.165 (1.85-2.47)	2.038 (1.74-2.33)	1.277 (1.04-1.53)
	2 MY	-5122.410	1.617 (0.31-3.37)	1.542 (0.28-3.17)	0.965 (0.16-2.03)
nDNA	0.26%	-1029.184	4.365 (2.65-6.34)	3.326 (1.98-4.78)	2.298 (1.25-3.41)
	2 MY	-1029.219	1.127 (0.12-3.26)	0.869 (0.10-2.48)	0.586 (0.07-1.75)
mtDNA-nDNA	1.5%	-6181.583	1.849 (1.59-2.13)	1.743 (1.49-2.01)	1.097 (0.90-1.32)
	2 MY	-6181.433	1.045 (0.15-2.77)	0.989 (0.14-2.62)	0.617 (0.90-1.65)

Table 4.7: Estimates of tempo of evolution of *Argyrosomus* spp. in the Benguela Current for the three mtDNA regions sequenced (CR, COI and cytb): *Ln(Likelihood)* - posterior probabilities of calibration method employed; *tmrca*- estimated time since most recent common ancestor (95% HPD in brackets).

	Calibration Method	Ln (Likelihood)	tmrca (MY)		
			Northeastern vs. Southeastern	<i>A.inodorus</i> vs. <i>A.coronus</i> / <i>A.japonicus</i>	<i>A.coronus</i> vs. <i>A.japonicus</i>
CR	1.5%	-2182.68	2.857 (2.26-3.46)	2.331 (2.25-3.47)	1.834 (1.32-2.43)
	2 MY	-2183.52	2.881 (1.31-4.57)	2.706 (1.16-4.21)	1.751 (0.75-2.82)
COI	1.5%	-1484.54	1.681 (1.12-2.19)	1.333 (0.95-1.75)	0.927 (0.60-1.26)
	2 MY	-1489.58	3.781 (1.90-6.05)	2.998 (1.59-4.59)	2.185 (1.07-3.49)
Cytb	1.5%	-1412.93	2.157 (1.63-2.77)	1.639 (1.62-2.80)	1.252 (0.83-1.73)
	2 MY	-1406.86	3.182 (1.62-4.73)	2.410 (1.70-4.77)	1.903 (0.93-3.13)

4.1.4. Discussion

Evolutionary history of *Argyrosomus* spp. in the eastern Atlantic

Reconstruction of the evolutionary history of *Argyrosomus* species occurring in the eastern Atlantic, based on mitochondrial and nuclear DNA markers, revealed the

existence of multiple and independent speciation events. Based on observed tree topologies, northeastern Atlantic *Argyrosomus* (now *A. regius*) and southeastern Atlantic *Argyrosomus* appear to have diverged first, followed by the isolation of *A. inodorus* from the common ancestor of *A. coronus* / *A. japonicus*, and finally the divergence of *A. coronus* and *A. japonicus*, on either side of the Benguela Current system. Although it is not possible at this time to clearly infer the relationship between *A. regius* and the southeastern Atlantic *Argyrosomus* species, as no other species of this genus was analyzed, the retrieved phylogenetic relationship coupled with similar biological features suggest that *A. regius* may be a sister species of the southern Atlantic group.

The *Argyrosomus* species in the eastern Atlantic appear to exhibit a typical antitropical distribution (Hubbs 1952; Briggs 1987). Antitropical distributions are commonly found in temperate species that occur in both northern and southern hemispheres, but are absent from the warm equatorial regions between (Hubbs 1952; Briggs 1987). In many cases, due to high sea surface temperatures the tropical equatorial regions can act as insurmountable barriers contributing to gene flow disruption, genetic divergence and, eventually, reproductive isolation (Stepien & Rosenblatt 1996; Graves 1998; BurrIDGE 2002). Therefore, the tropical temperatures of the equatorial Atlantic can have played an important role in shaping the evolutionary history of *Argyrosomus* in the region, as all species exhibit specific temperature requirements throughout their life cycle. For example, *A. regius* requires temperatures between 14-23°C for growth and 20-21°C for larval development (Quero & Vayne 1985; FAO 2005a; Gonzalez-Quiros et al. 2011), while *A. coronus* prefers water temperatures of 16-19°C and *A. inodorus* appears to be adapted to colder temperatures (13-16°C) (Kirchner 1998; Potts et al. 2010). As average sea surface temperatures reported for the equatorial Atlantic range from 25°C to 35°C it is likely that this area represents unsuitable habitat, and may thus have contributed to the observed differentiation between northeastern and southeastern species. Similar antitropical distributions have been reported for other temperate marine species such as *Sardinops* spp. (Bowen & Grant 1997), *Pseudolabrus* spp. (Mabuchi et al. 2004) and *Squalus acanthias* (Verissimo et al. 2010).

How could the equatorial region of the Atlantic have influenced divergence between the northern and southern *Argyrosomus* species? There are two main biogeographical hypotheses to explain the observed antitropical distribution: long-distance colonization across unsuitable habitats by dispersal; or vicariant events (Briggs 1987). The dispersal hypothesis suggests that colonization from one temperate zone to the other may have

been accomplished either by transequatorial movements during periods of colder climate, such as glacial ages, or by island stepping-stone dispersal. The vicariant hypothesis implies that isolation between taxa previously distributed across the northern and southern hemispheres may have been related to the arising of barriers to dispersal that led to allopatric events (Briggs 1987). BurrIDGE (2002) suggested three different vicariant mechanisms that could lead to antitropical distributions: competition with better adapted species in equatorial regions; sea level rise and subsequent submergence of equatorial waters; and sea surface temperature increases during the mid-Miocene that would have rendered the equatorial regions unsuitable for temperate species to survive. Estimates of time since divergence between northern and southern hemisphere taxa could be used to inform which biogeographical hypothesis was responsible for the observed antitropical distribution (see Bowen & Grant 1997). The dispersal hypothesis implies that colonization between temperate regions could be a fairly recent event, dating from the glacial ages during the Pleistocene, while the vicariance hypothesis may imply older dates as divergence may be related to continental fragmentation and establishment of oceanographic features that could be 10s of millions of years old (Briggs 1987; Stepien & Rosenblatt 1996; BurrIDGE 2002). Approximate estimates of time since most recent common ancestor between *A. regius* and the southeastern species suggest that separation may have occurred during the Pliocene-Pleistocene transition (see next section), implying that dispersal across the equator due to colder sea surface temperatures may have been the most likely mechanism to influence the occurrence of *Argyrosomus* in both hemispheres. Transequatorial dispersal during recent glaciation events has been proposed as the main mechanism shaping antitropical distributions in temperate species, as a decrease of 1-2°C may have been sufficient to promote dispersion (Randall 1981). However, it is not possible to completely discard the vicariance hypothesis for the speciation of *A. regius*, as ancestral populations could have dispersed across the equatorial region during the Pliocene-Pleistocene transition, and becoming vicariantly isolated during warmer interglacial periods (Stepien & Rosenblatt 1996; BurrIDGE 2002). It is likely that divergence of *Argyrosomus* between the northeastern and southeastern Atlantic may have resulted from a combination of transequatorial dispersal during colder periods, followed by allopatric speciation on either side of the equator.

Another question regarding the antitropical distribution of *Argyrosomus* in the eastern Atlantic concerns the direction of dispersal. Could it have been a north to south dispersal, with *A. regius* being the present day representative of the common ancestor?

Or could it be a south to north dispersal, with the common ancestor migrating from the southern Atlantic? In order to answer these questions it would be necessary to sample other *Argyrosomus* species, occurring throughout the Indo-Pacific Ocean, to reconstruct the phylogenetic relationships within the genus, in order to understand if *A. regius* was more close related to the southeastern Atlantic species, or with western Indian Ocean species, which may indicate a possible Tethys Sea dispersion route. As it was not possible to obtain specimens of the remaining *Argyrosomus* species, it is not possible at this time to solve this question.

Within the southeastern Atlantic the suggested earlier and deeper divergence of *A. inodorus* is supported by its life history characteristics. When compared with the other *Argyrosomus* species, *A. inodorus* exhibits the most divergent biological features (Table 4.1, but see Griffiths 1997a; Kirchner 1998; Kirchner & Holtzhausen 2001), which may imply that the species evolved to occupy and exploit a different niche. Observed sister-species relationship between *A. coronus* and *A. japonicus* is also supported by similarity of their biological features (Table 4.1, but see Griffiths & Heemstra 1995; Griffiths 1996, 1997b; Cowley et al. 2008; Silberschneider & Gray 2008; Potts et al. 2010). Equally, *A. coronus* and *A. japonicus* life history characteristics closely resemble *A. regius* (Quero & Vayne 1985), which suggests that the common biological features may correspond to ancestral traits of the genus, and thus *A. inodorus* constitutes the most divergent species of the group. Similar biological features between the northeastern *A. regius* and the southeastern *A. coronus* and *A. japonicus* further support the hypothesis that these species share a common ancestor.

Argyrosomus inodorus is commonly found off the coasts of Namibia and the Eastern Cape in South Africa (Griffiths & Heemstra 1995). The Namibian shoreline is characterized by sandy bottoms with occasional rocky outcrops, colder sea surface temperatures, anoxic waters below a depth of 100m, and absence of freshwater inputs (Sakko 1998). The Eastern Cape coast however exhibits seasonal upwelling events, and includes both a region of extended continental platform (the Agulhas Bank) but also a narrow and shallow continental shelf from Port Elizabeth to East London (Heemstra & Heemstra 2004). In South Africa, *A. inodorus* distribution overlaps with *A. japonicus* between Cape Point and the Kei River. However, despite this overlap in distribution the two species occupy different habitats (Griffiths 1997a): *A. japonicus* can be found in estuaries and the nearshore environment (to 50 m depth), while *A. inodorus* rarely enters estuaries or the surf zone and is predominantly caught at depths of 10-100m in colder waters (Griffiths & Heemstra, 1995). Therefore, *A. inodorus* life history traits may have

resulted from adaptation to colder and deeper environmental conditions. Both *A. coronus* and *A. japonicus* have higher temperature requirements, and are commonly found associated with rocky reefs (Griffiths 1996; Potts et al. 2010), which may have impaired both species' ability to colonize the harsher Namibian coast and the colder habitats along the South African coast. For example, the present-day occurrence of *A. coronus* in Namibian waters is commonly associated with increased sea surface temperatures due to the seasonal displacement of the Angola-Benguela Front (Griffiths & Heesmtra 1995; Kirchner 1998; Potts et al. 2010).

The retrieved sister-species relationship between *A. coronus* and *A. japonicus* may have resulted from the action of the Benguela Current as a biogeographical barrier to dispersion. Allopatric speciation due to vicariant barriers is commonly characterized by the occurrence of sister-species on either side of the barrier (Palumbi 1992; Avise 2000), and is considered the most common form of evolution of coastal species in the Atlantic Ocean (Floeter et al. 2008). Multiple sister-species relationships have been documented occurring on either side of the Atlantic major biogeographical barriers: the mid-Atlantic Barrier (e.g. *Clepticus brasiliensis-africanus*, Heiser 2000); the Amazon freshwater input (e.g. *Diplodus argenteus-holbrooki*, Summerer et al. 2001; *Thalassoma bifasciatum-noronheum*, Costagliola et al. 2004); the emergence of the Isthmus of Panama (e.g. *Anisotremus virginicus-taenitus*, Bernardi & Lape 2005); and the Benguela Current (e.g. *Eucidera* spp., Lessios et al. 1999; *Aulostomus chinensis-strigosus*, Bowen et al. 2001). Therefore, the results suggest that evolution of the *Argyrosomus* genus in the southeastern Atlantic may be related to the oceanographic features of the Benguela Current.

The observed phylogenetic relationships, combined with the different life histories of the species, suggest that evolution in the eastern Atlantic, and particularly within the Benguela Current, may have resulted from isolation and/or local adaptation. The warm equatorial Atlantic waters may have contributed to the isolation of *Argyrosomus* in temperate zones in both the northern and southern hemispheres, leading to the isolation of *A. regius*, while within the Benguela Current region the inhospitable environment of the Namibian coast may have contributed to the isolation of *A. coronus* and *A. japonicus* on either side, while being colonized by the more adapted *A. inodorus*. The evolutionary history of *Argyrosomus* in the eastern Atlantic thus appears to have resulted from a case of allopatric speciation due to vicariance (*A. regius* / southeastern common ancestor; *A. coronus* / *A. japonicus*) and ecological speciation (*A. inodorus*). Ecological speciation is defined as “the process by which barriers to gene flow evolve

between populations as a result of ecologically based divergent selection” (Rundle & Nosil 2005), and results from the combination between ecological divergence, due to colonization of and adaptation to different habitats (Schluter 2009). Strong natural and/or sexual selection in different environments can lead to fast ecological differentiation, resulting in rapid speciation events (Rundell & Price 2009). Therefore, ecological speciation can occur in just thousands of years. Although this form is commonly found in species occurring in sympatry, and in adaptive radiation events, the process is thought to be initiated by geographical isolation of populations, followed by establishment of reproductive isolation mechanisms (Rundell & Price 2009). In the marine realm, ecological speciation has been reported in several species occurring in reefs, which tend to exhibit a high diversity of habitats (e.g. Taylor & Hellberg 2005; Ingram 2011; Mehner et al. 2011). In the case of *A. inodorus*, it is possible that a number of individuals from the common ancestor species, exhibiting higher tolerance to colder temperatures, occupied the Namibian coast adapting to the local environment. As such, genetic divergence may have occurred more rapidly due to isolation and adaptation, eventually followed by speciation of a small number of individuals in a harsh environment, possibly occurring in sympatry with the ancestral type, compared with *A. coronus* / *A. japonicus* that diverged by slow drift (and speciation) in large and stable populations occurring in allopatry. Estimates of time since most recent common ancestor (see next section) suggest a near simultaneous divergence of *A. regius* from the common southeastern Atlantic ancestor and *A. inodorus* from this same ancestor, thus supporting the hypothesis of an ecological speciation event. As suggested by Rundell & Price (2009), ecological speciation will occur at a much faster rate than allopatric speciation, since individuals that occupy similar niches will experience weaker divergent selection, as they do not ‘need’ to adapt. As a result, fixation of traits that could lead to reproductive isolation occurs over longer timescales in allopatric speciation (Schluter 2009), and estimates of divergence time for the *A. coronus* / *A. japonicus* split were far more recent than those obtained for the divergence of *A. inodorus* (see next section).

Tempo of evolution

Estimates of time since most recent common ancestor were conducted using two different calibration methods: enforcing a universal mutation rate, and using biogeographical events as a proxy for internal node calibration (Drummond 2006). Neither of these approaches is ideal, and thus obtained estimates should be regarded

with caution, particularly due to the observed broad and partially overlapping 95% HPD intervals. Nevertheless, not only were the mean posterior estimates close to the prior node ages, indicating that the calibration approaches were suitable (Sanders & Lee 2007), but the obtained mutation rates for the mtDNA dataset were similar to the ones described for marine fish in the literature (Bermingham et al. 1997; Donaldson & Wilson 1999), thus suggesting that obtained time estimates should be roughly accurate. Point estimates of time since most recent common ancestor suggested that divergence within the *Argyrosomus* genus in the eastern Atlantic occurred during the late Pliocene to late Pleistocene (3 - 0.1 MYA). The first speciation event separated the northeastern Atlantic *A. regius* from southeastern *Argyrosomus* spp. during the Pliocene-Pleistocene transition (3 - 2 MYA), followed by isolation of *A. inodorus* from the common southeastern Atlantic ancestor in the early to mid-Pleistocene (2 - 0.9 MYA), and the later divergence of *A. coronus* from *A. japonicus* in the mid- to late-Pleistocene (0.9 - 0.1 MYA).

The close association (in evolutionary timescales) observed between the divergence of northeastern (*A. regius*) and southeastern *Argyrosomus*, and of *A. inodorus* from the southeastern ancestor of *A. coronus* / *A. japonicus*, suggest that the paleoceanographic event that led to the observed antitropical distribution split may also have caused an environmental change in the Benguela Current region leading to the ecological isolation of *A. inodorus*.

The estimated divergence timescales here presented are in agreement with previous results obtained for speciation events between the Atlantic and Indo-Pacific marine fauna (e.g. 2 MYA – Lessios et al. 1999; 2.5 MYA – Bowen et al. 2001; ~0.8 MYA – Lessios et al. 2003; 2 MYA – Waters & Roy 2003; 2 MYA – Grant & Bowen 2006), coinciding with the Pliocene-Pleistocene transition (~2.5-2 MYA). During the Pliocene the oceans were characterized by warmer sea surface temperatures (3°C higher than the present day), reduced upwelling events and, in the North Atlantic, increased circulation and intensification of the Gulf Stream and the North Atlantic Current (Marlow et al. 2000; Etourneau et al. 2009; Filippelli & Flores 2009). However, around 3 MYA the final uplift of the Isthmus of Panama led to changes in the circulation patterns within the Atlantic Ocean, which resulted in a progressive reduction of sea surface temperatures and an increase of upwelling intensity in the eastern coastal regions. In the northern hemisphere, periodic increase and reduction of the ice sheets led to the establishment of glacial-interglacial cycles. The reduction in sea surface temperatures during the Pliocene-Pleistocene transition could have influenced dispersal of

Argyrosomus across the equatorial region, while warmer interglacial periods during the Pleistocene could have led to the isolation of *A. regius* in the northern hemisphere. For example, the observed distribution break in *Engraulis* spp. in the eastern Atlantic dates from the late Pleistocene and appears to be connected with the presence of warmer tropical waters in the equatorial region (Grant & Bowen 2006). In addition, climate-induced oceanographic changes during the Pliocene and Pleistocene have also been documented to have influenced antitropical distributions in several marine species in the Pacific: *Scomber japonicus* (0.34 - 1.34 MYA, Stepien & Rosenblatt 1996) and *S. australasius* (0.48 - 2.4 MYA, Scoles et al. 1998), *Sebastes* spp. (0.3 - 0.51 MYA, Rocha-Olivares et al. 1999), *Sardinops* spp. (1 - 2 MYA, Bowen & Grant 1997), *Pseudolabrus* spp. (5 - 3 MYA, Mabuchi et al. 2004), *Merluccius productus* and *M. gayi* (2.4-2.6 MYA, Stepien & Rosenblatt 1996; Quinteiro et al. 2000). It is likely that evolution of *A. regius* in the northeastern Atlantic may have been influenced by climatic fluctuations during the Pliocene-Pleistocene transition.

In the Benguela Current region the Pleiocene-Pleistocene transition was followed by a subsequent increase in upwelling intensity and paleoproductivity (Marlow et al. 2000; Jahn et al. 2003). During the Pliocene, sea surface temperatures (SSTs) were estimated at 26°C in the northern Benguela region, and by the mid-Pleistocene temperatures had dropped by up to 10°C (to 16°C) due to glacial advances in the northern hemisphere and Antarctic (Marlow et al. 2000). Marlow et al. (2000) identified five different phases of oceanographic changes in the northern Benguela Current sub-system during the Pliocene-Pleistocene transition. The speciation events here documented appear to have occurred during the final transition phases (three - five), characterized by a steep decrease in SSTs (Marlow et al. 2000). Marine species response to glacial periods partially depends on the species cold tolerance and dispersal ability (Ruzzante et al. 2011). Thus, decreased SSTs could have been accompanied by a retreat of the temperate southeastern *Argyrosomus* common ancestor towards the warmer Angola and Agulhas currents, in northern and southern Benguela respectively, leaving the Namibian coast available to colonization by individuals more tolerant to colder temperatures. An annual return migration, which is possibly connected with seasonal water temperature changes, can still be observed today in both *A. coronus* and *A. japonicus* (Griffiths 1996; Potts et al. 2010), suggesting that these species actively avoid colder waters. Therefore, observed temperature decreases in the Benguela region during the Pleistocene could have acted as an effective barrier to dispersion, and contributed to the observed speciation events.

4.2. First evidence of climate-induced shifts in dominant species in the Benguela Current: *Argyrosomus coronus* and *Argyrosomus inodorus*

4.2.1. Introduction

Argyrosomus inodorus Griffiths & Heemstra 1995 distribution ranges from northern Namibia to the Kei River in eastern South Africa, with a break between central Namibia and Cape Point, South Africa (Griffiths & Heemstra 1995). Migration between the Namibian and South African stocks was found to be restricted, and possibly absent, and so the two populations are thought to be isolated due to unsuitable sea surface temperatures between these areas (Kirchner & Holtzhausen 2001).

A. inodorus occurs in sympatry with two other kob species: *A. coronus* Griffiths and Heemstra, 1995 in northern and central Namibia (Kirchner 1998), and *A. japonicus* (Temminck and Schlegel, 1844) in South Africa (Griffiths 1997a). *A. coronus* is distributed from southern Namibia to northern Angola (Griffiths & Heemstra 1995; Griffiths 1997a; Kirchner & Holtzhausen 2001), although in the Namibian sector the population appears to be mainly composed by juveniles and sub-adults confined to the warmer surf-zone (Griffiths & Heemstra 1995; Kirchner 1998). *Argyrosomus coronus* is common north of Cape Frio (northern Namibia), but abundance is reported to decrease towards central Namibia (Kirchner 1998; Kirchner & Holtzhausen 2001; Potts et al. 2010). Overlap between the two species occurs off the Skeleton Coast Park, between 18°S-21°S, with a ratio of 9 *A. inodorus* to 1 *A. coronus* (Kirchner 1998). In South Africa, *A. inodorus* distribution overlaps with *A. japonicus* between Cape Point and Kei River. However, despite observed distribution overlap the two species occupy different habitats (Griffiths 1997a): *A. japonicus* can be found in turbid estuaries and in the nearshore environment (to 50 m depth), while *A. inodorus* rarely enters estuaries or the surf zone, and is predominantly caught at depths of 10-100m (Griffiths & Heemstra, 1995). Due to its larger size, *A. japonicus* is a prized angling species in the inshore environment, where it is mainly caught in estuaries and surf-zone throughout South Africa. The majority of *A. inodorus* catches are concentrated between Cape Point and East London, where it is mainly targeted by the line-fishery industry (Griffiths & Heemstra, 1995). Therefore, occurrence of the two species in South Africa is recognized, and management conducted according to each species' biological features (Griffiths 1997a).

Despite morphological similarities the three kob species exhibit distinctive biological features, namely size at maturity and growth rate (Kirchner 1998; Potts et al. 2010) (see Chapter 4.1). Potts et al. (2010) suggested that the *A. coronus* return migration may be linked with the seasonal displacement of the Angola-Benguela Front (ABF), which exhibits the species optimum temperatures (16-19°C). Sea temperature is one of the key factors influencing a species' distribution, and temperature-induced range shifts have been documented for multiple fish species (Nye et al. 2009; Fodrie et al. 2010; van Hal et al. 2010). In the Benguela Current region an increase of roughly 0.6°C in sea surface temperature has been reported in the last decade, accompanied by a southwards displacement of the ABF (Monteiro et al. 2008). Therefore, the observed sea surface temperature increase may have resulted in a southwards expansion of distribution range of *A. coronus*.

Argyrosomus inodorus is the most important linefish resource of Namibia, targeted by multiple fisheries and comprising up to 70% of total catches (Kirchner, 1998). Despite extensive distribution overlap between the two kob species in Namibia, it has been estimated that 90% of total kob catches are composed of *A. inodorus* (Kirchner 1998). Due to fishing limitations, inshore angling is mainly limited to the West Coast Recreational Area, where *A. inodorus* is thought to be the dominant species (Kirchner 1998). Therefore, to date kob fishery management within Namibia has been based on *A. inodorus* life history features alone, and the contribution of *A. coronus* is thought to be negligible (Kirchner & Holtzhausen 2001; Potts et al. 2010). However, if the observed increase in sea surface temperatures was followed by a southwards expansion of *A. coronus*, resulting in increased abundance of this species within the region of the west Coast Recreational Area, then the Namibian fishery may be increasingly composed of mixed kob species catches. In such cases of mixed-species fisheries it is vital to base management decisions on accurate species identification and estimates of relative abundance (Coyle 1997).

The main aims of the present study were to provide an accurate estimate of current relative abundance of *A. coronus* and *A. inodorus* in Namibian waters in order to identify the current species composition of the kob fishery, through development of a simple but reliable molecular genetic test for species identification. As it is difficult to routinely obtain fresh samples, the protein electrophoresis (allozyme) technique described by van der Bank & Kirchner (1997) was decided to be an unsuitable method for routine monitoring. Instead a Polymerase Chain Reaction-based Restriction Fragment Length Polymorphism (PCR-RFLP) approach, used successfully in other

fishery-related applications (Ward 2000), was developed and applied to kob species. Furthermore, a preliminary assessment of *A. inodorus* population connectivity and gene flow across the Benguela Current was conducted based on mtDNA and nuclear microsatellite markers, to investigate the species genetic structure and evolutionary history in the region.

4.2.2. Methods

Sampling and DNA extraction

Increased sea surface temperatures in the Benguela Current region may have led to a southwards expansion of *Argyrosomus coronus* distribution range, into central and southern Namibia, overlapping with the Namibian endemic *A. inodorus*. Therefore, in order to assess kob species composition and abundance in central Namibia, sampling of 146 kob individuals was conducted in the Namibian West Coast Recreational Area (Henties Bay – HEN), by a local collaborator during the austral summer months of 2008 and 2009 (Figure 4.10). As *A. coronus* adults reach larger sizes than *A. inodorus* adults, total length (in mm) was measured and recorded for each specimen caught to establish average size range of each species. Identification of *A. coronus* reference samples in southern Angola and *A. inodorus* reference samples in northern Namibia were based on external morphological features and otolith morphology. Otolith morphology is considered to be a good species diagnostic character in sciaenids.

Furthermore, to assess *A. inodorus* population connectivity and gene flow across the Benguela Current region an additional sample of 50 individuals was collected from Port Alfred (EastC), South Africa, by local collaborators (Figure 4.10).

In all cases, a fin clip was removed immediately after capture and fixed in 95% ethanol. Extraction of total genomic DNA was conducted according to the method of Sambrook et al. (1989) (see Chapter 2.2.1).

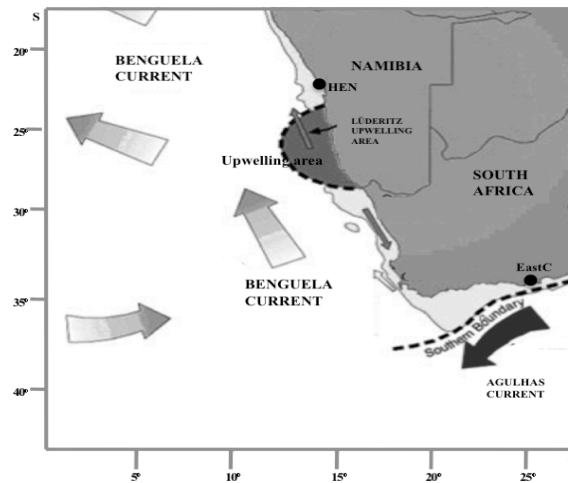


Figure 4.10: Sampling strategy for *A. inodorus* across the Benguela Current region, highlighting sampling sites, and their position relative to the major oceanographic features of the system: position of the Benguela and Agulhas Currents, central Namibia upwelling cell, and continental shelf width.

Development of a molecular test for species identification

Development of a molecular test for identification of kob species occurring in central Namibia was conducted using a PCR-RFLP approach. Two individuals from *A. coronus* (caught in southern Angola) and *A. inodorus* (caught at HEN), identified based on external morphological characters and otolith features, were PCR amplified and sequenced for a 700bp region of the mtDNA COI gene (see Chapter 2, section 2.2.2). Resulting sequences were aligned with BioEdit and identified individuals were used as reference samples from each kob species in the development of the PCR-RFLP species identification method. *Argyrosomus coronus* and *A. inodorus* reference sequences were introduced in the software NEBCutter (Vincze et al. 2003) to identify endonuclease restriction enzymes that would produce a species-specific digestion pattern of the COI PCR amplicon.

The enzyme HaeIII (New England BioLabs, UK) was predicted to cut the COI fragment at four restriction sites (at 232bp, 391bp, 436bp, and 671bp from the 5' end) in *A. coronus*, creating an expected pattern of five differently sized DNA fragments: 29bp, 45bp, 159bp, 232bp and 235bp; whilst in *A. inodorus* the same enzyme exhibited three restriction sites (at 232bp, 391bp, and 671bp) producing an expected pattern of four differently sized fragments: 29bp, 159bp, 232bp and 280bp. A 6µl volume of PCR product was digested for 1h at 37°C with 1U of HaeIII in 1x buffer (New England BioLabs, UK), and digestion was terminated with a final step of 80°C for 20min. Restricted products were run on EtBr stained (1%) agarose gels, and relative size of fragments was established against the Hypperladder II size marker (Bioline UK), and

using the reference samples as positive controls. Of the 146 individuals analyzed, COI PCR products from 20 random fish (but including all different restriction profiles observed) were sequenced in the forward direction to validate observed DNA profile.

After identification of specimens to species, the relationship between species and average total length was tested for 50 individuals from each species, using a Mann-Whitney non-parametric test in STATISTICA 10.

Genetic screening

Preliminary assessment of genetic diversity levels, population connectivity and evolutionary history of *A. inodorus* across the Benguela Current was conducted for samples from Namibia (HEN) and South Africa (EastC). The HEN sample was composed of individuals previously identified as *A. inodorus* based on observed RFLP profile.

A total of 36 *A. inodorus* individuals were PCR amplified and sequenced for a fragment of the mtDNA Control Region (CR), using the universal primer pair L16498/12SARH (Apte & Gardner 2002) (see Chapter 2.2.2).

Six cross-specific microsatellite loci (UBA5, UBA40, UBA50, UBA91, UBA853 and UBA854) isolated from *Argyrosomus japonicus* (Archangi et al. 2008) were screened in 40 individuals per sampling site to investigate genetic diversity levels, and population sub-structuring across the Benguela Current (Chapter 2.2, see Table 2.3).

Mitochondrial DNA sequence analyses

Population structure and phylogeographic patterns

The CR dataset was assessed for levels of haplotype diversity (h) and nucleotide (π) diversity, fits to neutrality tests: Ewens-Waterson's F , Tajima's D and Fu's F_S , and determination of the most suitable nucleotide substitution model was performed as previously described (Chapter 2.3.1). Inference of *Argyrosomus inodorus* population connectivity across the Benguela Current was performed by estimating pairwise Wright's F_{ST} and reconstructing haplotype networks (see Chapter 2.3.1).

Evolutionary history

Assessment of *A. inodorus* evolutionary history was performed using statistics such as haplotype (h) and nucleotide (π) diversity levels, Tajima's D and Fu's F_S neutrality tests, and by estimating mismatch distribution analyses for each identified population. Significance of deviations to the hypothesis of past demographic expansion was

assessed using the “sum of squared differences” (SSD) test, after 10000 iterations (Chapter 2.3.1). Time since expansion was estimated as $\sigma = 2\mu t$ (see Chapter 2.3.1), and a universal mutation rate of 3.6% per MY (Donaldson & Wilson 1999), was employed with generation time estimated at 2 years for females (Potts et al. 2010).

Microsatellite analyses

Population structure

Obtained genotypic frequencies were tested for deviations from Hardy-Weinberg expectations of random mating and from linkage equilibrium, as described in Chapter 2.4.2. Occurrence of amplification errors such as large allele drop out and stuttering, and estimation of null alleles frequencies were assessed in Microchecker (van Oosterhout et al. 2006). Levels of genetic diversity were estimated as number of alleles (N_a), allelic richness (AR), observed and expected heterozygosity (H_o and H_e), and Wright’s inbreeding coefficient (F_{IS}) (see Chapter 2.4.2).

Assessment of population sub-structuring was conducted based on Weir’s (1986) F_{ST} values. Preliminary analyses revealed that STRUCTURE was not able to discriminate between Namibian and South African *A. inodorus*, therefore an additional analysis was conducted to identify genetic discontinuities across the sampling area using GENELAND (Guillot et al. 2005). Inference of genetic discontinuities was performed for individual geo-referenced multi-locus genotypes, without prior knowledge of the number of populations (Guillot et al. 2005; Guillot et al. 2008; Guillot & Foll 2009; Guillot & Santos 2009). Three independent runs for $K = 1$ to 3 were performed to assess convergence of parameters. All analyses were conducted using the Dirichlet distribution as prior, with allele frequencies correlated, including spatial information, and estimating null allele frequencies (Guillot et al. 2008; Guillot & Santos 2009), and was performed for 100000 MCMC steps, sampling every 100th iteration. A final run was performed with a fixed K , given by the mode of the posterior distribution of the MCMC chain. A rough estimate of effective number of migrants (N_m) was conducted in Genepop 4.0.10 (Raymond & Rousset 1995). The effective number of migrants consists of the number of individuals that actively contribute to the gene pool of another population, and can be understood as effective gene flow. The method employed in Genepop generates a statistical distribution of private alleles frequency for each putative population, and can thus be used to estimate the number of individuals that are more likely to have originated in another population (Barton & Slatkin 1986).

4.2.3. Results

PCR-RFLP identification of kob species composition in the West Coast Recreational Area, Namibia

PCR amplification resulted in the expected product size (~700bp) in all individuals tested (see lane 2, Figure 4.11). Due to the small fragment size it was not possible to observe clearly the 29bp fragment, however HaeIII digestion provided very clear species-specific profiles, with four differently sized fragments in confirmed individuals of *A. coronus* (Profile A: 45bp; 159bp; 232bp; and 235bp – lanes 3 and 4 in Figure 4.11), and three fragments in *A. inodorus* reference individuals (Profile B: 159bp; 232bp and 280bp – lanes 5 and 6 in Figure 4.11).

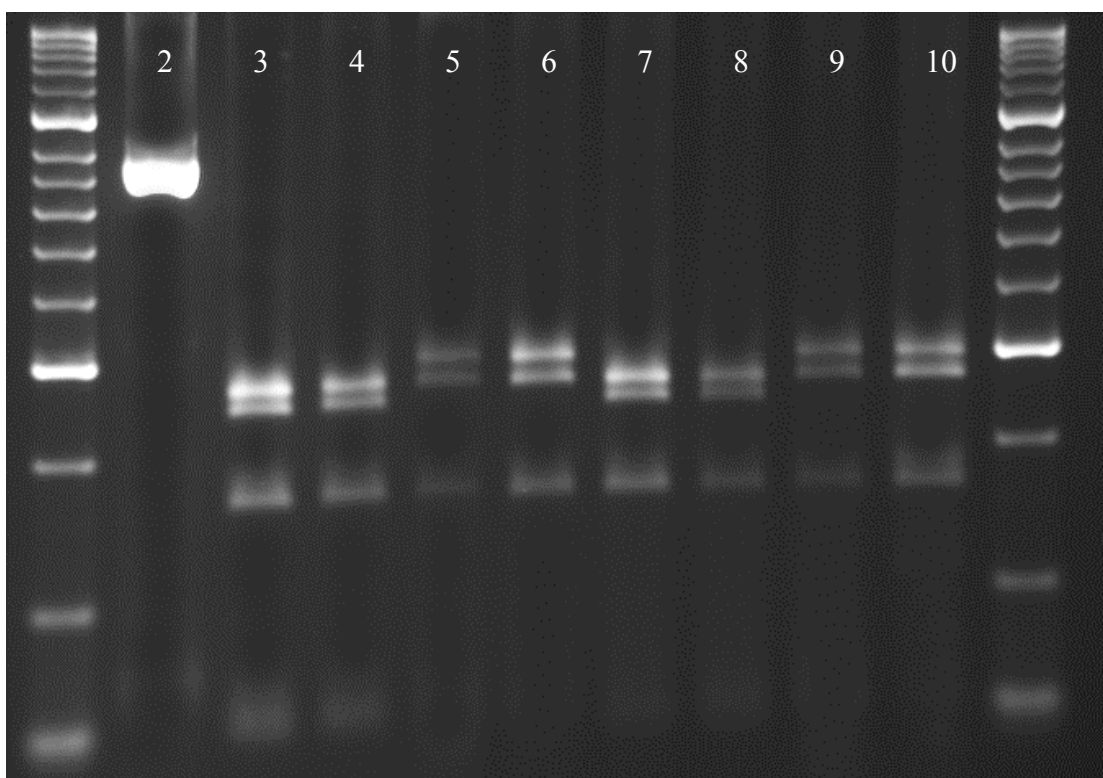


Figure 4.11: HaeIII restriction profiles from COI PCR products of *A. coronus* (lanes 3, 4, 7 and 8) and *A. inodorus* (lanes 5, 6, 9 and 10), plus the unrestrictied PCR product (lane 2) and DNA size ladder Hyperladder II (bright bands = 300bp and 1000bp).

Of the 146 kob specimens analyzed, 83 were identified as *A. coronus* (56.8%), while 63 were identified as *A. inodorus* (43.2%). All sequenced samples confirmed the species ID provided by the RFLP profile.

No significant differentiation between average total length of the identified *A. inodorus* and *A. coronus* was observed (Mann-Whitney U=1071.000, p>0.05).

Mitochondrial DNA sequence analyses

Population structure and phylogeographic patterns

Amplification and sequencing of mtDNA CR yielded a fragment of 704bp. A total of 36 individuals were analyzed, rendering 32 haplotypes, with 34 variable sites, from which 16 were parsimony informative. The Tamura-Nei nucleotide substitution model was retrieved as the most suitable for *A. inodorus* mtDNA dataset.

Overall haplotype diversity was high ($h = 0.991$), while nucleotide diversity was lower ($\pi = 0.006$), with HEN exhibiting higher values than EastC (Table 4.8). Deviations to the neutrality assumption were detected using Fu's F_S neutrality test for both samples, but not with either Ewens-Watson F test or Tajima's D test. Fu's F_S statistics are known to be particularly sensitive to demographic changes, and can retrieve significant results in populations that underwent past demographic expansions (Excoffier et al. 2005). Therefore, it is possible that observed neutrality deviations might be related to population changes, and not selective pressures.

Table 4.8: Mitochondrial genetic diversity levels and neutrality tests for *A. inodorus* CR: **n** – number of individuals; **H** – number of haplotypes; **h** – haplotype diversity; **π** - nucleotide diversity; **F** – Ewens-Watson neutrality test; **D** – Tajima neutrality test; **F_S** – Fu neutrality test. Statistically significant results ($p < 0.05$) in bold.

	HEN	EastC	Overall
n	18	18	36
H	18	14	32
h	1.000	0.968	0.991
π	0.008	0.004	0.006
F	-	0.862	0.966
D	-1.486	0.324	-1.554
F_S	-14.762	-10.099	-25.652

Although the F_{ST} value between the two samples was statistically significant ($F_{ST} = 0.092$, $p < 0.05$), reconstruction of haplotype relationships did not retrieve an obvious geographical pattern of haplotype distribution (Figure 4.12). Most individuals were represented by private haplotypes, and no obvious clustering was observed between Namibian and South African individuals/haplotypes. The majority of haplotype divergence was low, differing from one another by one to two mutational steps, with the exception of two HEN individuals, that diverged by 10 mutational steps (Figure 4.12).

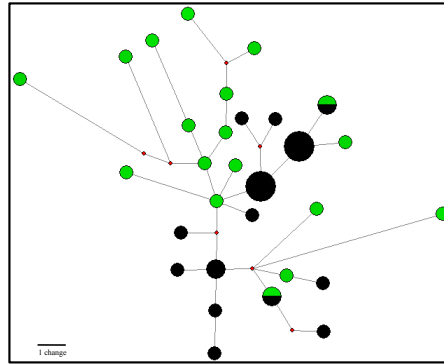


Figure 4.12: Reconstruction of haplotype network for *A. inodorus* across the Benguela Current, based on 794bp of mtDNA CR sequences: ●: HEN; ●: EastC. Node sizes are proportional to the number of haplotypes. Red dots correspond to missing haplotypes.

Inability to detect a common haplotype that could potentially represent the ancestral type, and observed high number of missing links (haplotypes - red dots in Figure 4.12) suggests that control region may be too variable to detect accurate population sub-structuring in *A. inodorus*.

Evolutionary history

As significant genetic differentiation was observed between samples from the northern and southern Benguela sub-systems, reconstruction of *A. inodorus* demographic history was conducted separately for each identified population.

The Namibian *A. inodorus* (HEN) population exhibited higher haplotype and nucleotide diversity levels than the South African population (EastC) (Table 4.9). However, similar deviations to neutrality were observed in both populations (Table 4.9). These findings, combined with mismatch distribution results, suggest the occurrence of past demographic expansion in both *A. inodorus* populations. Not only was it not possible to reject the null hypothesis of a past demographic expansion (SSD=0.043, SSD=0.011, $p > 0.05$, respectively - Table 4.9), but also frequency histograms revealed a clear unimodal pattern in both populations (Figure 4.13). Estimates of time since expansion, obtained based on mismatch distribution parameters (σ), point to a past population expansion at 30.97 KYA and 24.91 KYA, respectively.

Table 4.9: *Argyrosomus inodorus* genetic demographic history for northern and southern Benguela sub-system populations, based on mtDNA CR sequence variation: mismatch distribution parameters: σ - time since expansion in mutation units, θ_0 - population size before expansion, θ_1 - population size after expansion; and time since expansion (T in thousand years - KY). Statistical significant results ($p < 0.05$) in bold.

	HEN	EastC
Mean	5.876	2.856
Variance	7.801	1.769
SSD	0.043	0.011
σ	3.768	3.031
	(1.379-5.732)	(1.646-4.406)
θ_0	0.000	0.000
θ_1	99999.000	99999.000
Texp (KY)	30.97	24.91
	(13.60-56.54)	(16.24-43.46)

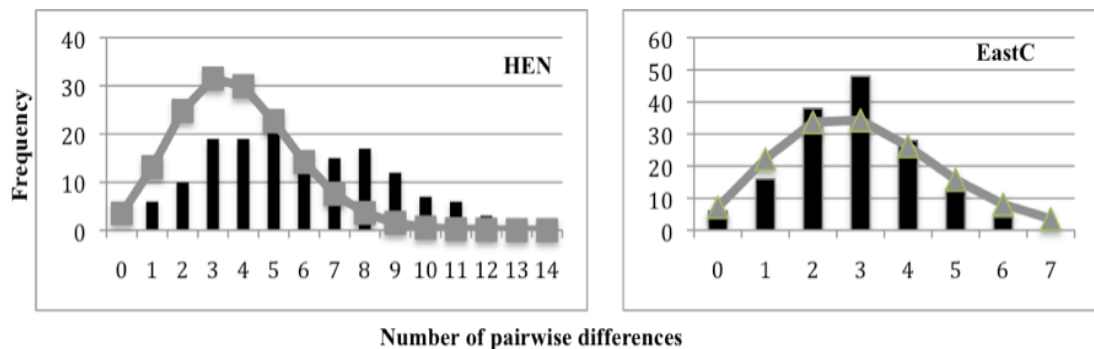


Figure 4.13: Mismatch distribution histograms for northern and southern Benguela sub-system *A. inodorus* populations, based on mtDNA CR sequences. Filled bars indicate the observed frequency of pairwise distribution, grey line indicates the expected distribution under a model of sudden demographic expansion.

Microsatellite analyses

A total of 80 individuals, 40 each from the Namibian and South African samples, were screened for 6 cross-specific microsatellite loci. No loci exhibited evidence of amplification errors, and all displayed genotype frequencies that conformed with Hardy-Weinberg (F_{IS} – see table 4.10) and Linkage Equilibrium expectations of random-mating across loci and samples. Levels of genetic diversity were quite high ($H_0 = 0.758$), although higher values of allelic richness and gene diversity were observed for EastC (Table 4.10).

Table 4.10: Genetic diversity at 6 cross-specific microsatellite loci in *A. inodorus* samples: **n** – number of individuals genotyped; **Na** – number of alleles; **AR** – allelic richness (minimum of 39 individuals); **H_E** – expected heterozygosity; **H_O** – observed heterozygosity; **F_{IS}** – inbreeding coefficient. Significant deviations to Hardy-Weinberg expectations in bold.

		HEN	EastC
UBA5	n	40	40
	Na	11	11
	AR	10.803	10.925
	H _E	0.819	0.825
	H _O	0.875	0.825
	F _{IS}	-0.047	0.003
UBA40	n	40	39
	Na	8	7
	AR	7.951	7.000
	H _E	0.765	0.807
	H _O	0.750	0.795
	F _{IS}	0.038	0.037
UBA50	N	39	40
	Na	14	15
	AR	13.974	14.899
	H _E	0.887	0.896
	H _O	0.821	0.800
	F _{IS}	0.066	0.038
UBA91	n	40	40
	Na	5	3
	AR	4.902	3.000
	H _E	0.361	0.387
	H _O	0.275	0.475
	F _{IS}	0.182	-0.207
UBA853	n	40	40
	Na	13	14
	AR	12.799	12.924
	H _E	0.831	0.872
	H _O	0.925	0.900
	F _{IS}	-0.100	-0.036
UBA854	n	40	40
	Na	9	7
	AR	7.604	11.899
	H _E	0.881	0.776
	H _O	0.975	0.675
	F _{IS}	-0.038	0.130
Average all loci	n	40	40
	Na	10	10
	AR	9.004	9.833
	H _E	0.757	0.760
	H _O	0.770	0.745
	F _{IS}	0.000	0.012

As observed for the mtDNA data, retrieved level of population differentiation was statistically significant ($F_{ST} = 0.036$, $p < 0.05$), suggesting significant genetic divergence between samples from Namibia and South Africa.

Although no significant genetic differentiation among *A. inodorus* populations was detected using STRUCTURE ($K = 1$, $\text{LnP}(D) = 1907.2$), inference of genetic discontinuities using Geneland converged to $K = 2$, revealing a clear separation between Namibian and South African *A. inodorus* populations, further supporting the hypothesis

of two isolated populations. Another run was performed with $K = 2$, revealing the probable geographical position of genetic clusters (Figure 4.14).

The estimated effective number of migrants (N_m), using the private allele method, was 6.98 individuals.

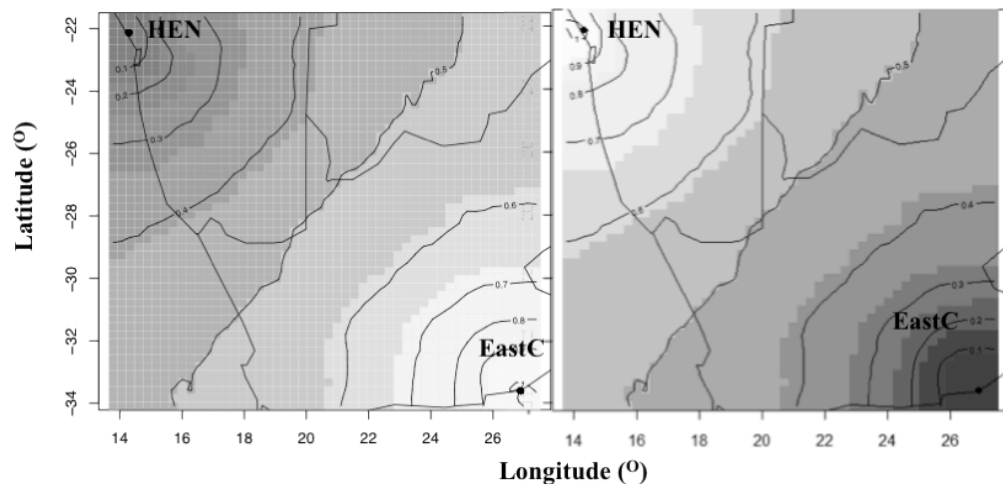


Figure 4.14: Map of posterior probability of population membership of geo-referenced *A. inodorus* samples, based on 6 microsatellite loci: HEN and EastC. Dark colors delineate areas of higher probability of population membership. Black isolines represent the level of genetic.

4.2.4. Discussion

PCR-RFLP identification of kob species composition in the West Coast Recreational Area, central Namibia

Molecular techniques, such as the ones employed in the present study, have increasingly been used in fishery-related studies, due to their usefulness in correctly identifying species, ability to detect hidden population structure and assess levels of gene flow (Ward 2000). In particular, the PCR-RFLP approach used in the present work appears to be an easy, reliable and inexpensive way to address such questions, when compared to DNA sequencing (e.g. Di Finizio et al. 2007; Triantafyllidis et al. 2007; Frontana-Uribe et al. 2008).

Genetic assessment of kob species composition off the coast of central Namibia indicated that, contrary to previous reports (Kirchner 1998), *A. coronus* is abundant and occurs at a ratio of approximately 3 : 2 (*A. coronus* : *A. inodorus*). If previous reports of kob species relative abundance were correct (1 : 9), then *A. coronus* appears to be replacing *A. inodorus* in the inshore angling catches of this area of central Namibia. This is a substantial change from the previous description of the distributional centres of abundance of these species, where *A. coronus* was thought to be common in southern

Angola and north of Cape Frio in Namibia, and that central and southern areas of Namibia were dominated by *A. inodorus* (Kirchner 1998). There was no significant difference between average sizes of individuals of the two species in the present sample, even though *A. coronus* are known to grow to larger sizes (Griffiths & Heemstra 1995). This size similarity may be related to the suggestion that the *A. coronus* Namibian population is composed mainly of juveniles, which have sizes similar to those of mature adult *A. inodorus* (Potts et al. 2010).

Argyrosomus coronus occurs only in the warmer surf-zone in Namibian waters, being mainly targeted by inshore anglers, while *A. inodorus* is also targeted by skiboat and line-fish boat fisheries. The lack of morphological characters that can easily identify the two species, and the absence of obvious size differences mean that it is difficult to distinguish (and so accurately record) the species, particularly in the recreational fishery. Current Namibian legislation allows keeping of up to 10 fish per day, as long as they are larger than 40 cm (Kirchner & Beyer 1999). According to the present study this would result in harvesting of juvenile *A. coronus* alongside adult *A. inodorus*. *Argyrosomus coronus* adults are common only in southern Angola, where they reproduce (Potts et al. 2010), and so the indiscriminate harvesting of juveniles in Namibian waters may have a severe impact on the Angolan stock. As obtained results indicate a situation significantly different from that upon which the fishery regulations were based (Kirchner & Holtzhausen 2001), it is suggested that a revision of the fisheries regulations in Namibia is needed, in order to account for increased *A. coronus* abundance in central Namibia. Additionally, further studies using the methods here developed should be conducted for individuals caught during the summer months, and in southern Namibia, to determine ratios of *A. inodorus* to *A. coronus* throughout the seasonal and geographical extent of the fishery.

Earlier estimates of kob species composition and abundance in Namibian waters relied mainly on morphological identification from otoliths (Kirchner 1998). Sciaenid otolith morphology is commonly used in species identification, due to their species-specific nature, thus decreasing the likelihood of misidentification (Sasaki 1989). Furthermore, van der Bank & Kirchner (1997) confirmed species identity in the fishery using a biochemical genetic approach. Therefore, it is unlikely that the previously described abundance values for both kob species were erroneous, and so the present observations of species abundance change are real. The observed abundance increase of *A. coronus* in Namibian waters combined with the recent reported decline in catch per unit effort in the recreational fishery in southern Angola (Potts et al. 2010) may thus

represent a first sign of climate-induced community changes in the Benguela Current region. As *A. coronus* avoids, or at least does not actively feed in, waters below 16°C or above 19°C (Potts et al. 2010) its increased presence may indicate a rise in sea surface temperatures in the region. A potentially more serious consequence of changing environmental conditions and associated species distribution is that migration patterns of the *A. coronus* appear to reflect the oscillation of the Angola-Benguela Front, and so changes in oceanographical features may have repercussions for the species' migration and reproductive patterns (Potts et al. 2010). Shifts in distribution range are thought to represent a species' first response to climate change (Grant & Bowen 2006; Ruzzante et al. 2008; Pardinas et al. 2010; Runge et al. 2010; Garroway et al. 2011; Hill et al. 2011; Lo Brutto et al. 2011). An increase of ~0.6°C in sea surface temperature has been reported for the northern Benguela region in the last decade (Monteiro et al. 2008), and it is possible that such change may have affected the seasonal displacement of the ABF, and consequently the distribution range of *A. coronus*. Such potentially serious implications for species biology indicate a need for further study of both oceanographic parameters and species distributions in Namibian waters.

Population structure of *A. inodorus* throughout the Benguela Current region

Traditionally, marine teleosts, including exploited species, present high levels of genetic diversity and low levels of population differentiation, both in mtDNA and nuclear genomes (Waples 1998; Ward 2000). Overall, levels of genetic diversity here reported for *Argyrosomus inodorus* for mtDNA ($h = 0.991$, $\pi = 0.006$) were similar to diversity levels documented for other marine fish species such as *Sciaenops ocellatus* ($h = 0.95$, $\pi = 0.057$ - Gold & Richardson 1998), *Pogonias cromis* ($h = 0.78$, $\pi = 0.0048$ - Gold & Richardson 1998), *Cynoscion nebulosus* ($h = 0.86$, $\pi = 0.0045$ - Gold & Richardson 1998), *Pannahia argentata* ($h = 0.998$, $\pi = 0.026$ - Han et al. 2008), and other teleosts occurring in the Benguela Current region: *Argyrosomus japonicus* ($h = 0.96$, $\pi = 0.009$ - Klopper 2005), *Rhabdosargus holubii* ($h = 0.91$, $\pi = 0.006$ - Oosthuizen 2007) and *Caffrogobius caffer* ($h = 0.96$, $\pi = 0.002$ - Neethling et al. 2008). Equally, genetic diversity levels obtained for 6 microsatellites across loci and samples were relatively high ($H_O = 0.771$, $H_E = 0.764$), and comparable to other teleost species such as *Thunnus obesus* ($H_O = 0.742$, Gonzalez et al. 2008) and *Scomberomorus cavalla* ($H_E = 0.311$ - 0.803, Gold et al. 2002).

Preliminary assessment of *A. inodorus* population genetic structure, using both mtDNA and nuclear datasets, revealed significant departures from the null hypothesis of

panmixia between Namibian and South African sites. Despite the absence of a clear geographical distribution of mtDNA haplotypes, the F_{ST} values here reported suggest a break in gene flow in *A. inodorus* between the northern and southern Benguela sub-systems, and were relatively higher (mtDNA $F_{ST} = 0.09$ and nDNA $F_{ST} = 0.036$) than those reported for other widespread marine teleosts such as *Thunnus thynnus* (mtDNA $F_{ST} = 0.023$; nDNA $F_{ST} = 0.002$ – Carlsson et al. 2004), *Thunnus obesus* (nDNA $F_{ST} = 0.000$ to 0.003 – Gonzalez et al. 2008), *Coryphaena hippurus* (mtDNA $F_{ST} = 0.000$ to 0.571 – Diaz-Jaimes et al. 2010), or even other sciaenid species such as *Micropogonias undulatus* (mtDNA $F_{ST} = 0.046$ – Lankford et al. 1999) and *Sciaenops ocellatus* (mtDNA $F_{ST} = 0.057$ – Gold & Richardson 1991).

High genetic diversity and low genetic differentiation, as here reported for *A. inodorus*, are considered to be related to historically high effective population sizes and/or high levels of gene flow between adjacent populations (Waples 1998). However, the preliminary estimate of effective number of migrants (N_{em}) for *A. inodorus* identified a small number of individuals (~ 7) as actively contributing to the gene pool, suggesting that effective gene flow between *A. inodorus* populations is relatively low. For example, the number of effective migrants detected between Atlantic and Indian Ocean populations of *Thunnus obesus* was higher ($N_{em} = 11.5$ and 27.9 individuals – Gonzalez et al. 2008) and significantly higher between *Coryphaena hippurus* populations ($N_{em} = 143$ to 846 individuals – Diaz-Jaime et al. 2010), agreeing with the lower levels of population divergence observed in this species when compared with *A. inodorus* (see above). In addition, tagging studies conducted in Namibia revealed that only 3 *A. inodorus* individuals were caught in South Africa (Kirchner 1998). Therefore, observed genetic differentiation between the two *A. inodorus* putative populations combined with the effective migration levels here reported and the known break in the species' distribution between Cape Point (South Africa) and Meob Bay (central Namibia), are possibly related to historically high levels of effective population size, combined with no significant gene flow due to limited dispersion across the Benguela Current region.

Despite the small number of sampling sites and samples per site, the genetic differentiation pattern here reported for *A. inodorus* appears to geographically coincide with the Benguela Current major oceanographic features, namely the presence of a perennial upwelling cell off the coast of central Namibia, colder sea surface temperatures between southern Namibia and western South Africa, and a narrower continental shelf in the region (Shannon 1985; Fennel 1999; Boyer et al. 2000). Perennial upwelling cells can disrupt longshore transport of pelagic eggs and larvae,

contributing to isolate populations on either side (Lett et al. 2007). Furthermore, *A. inodorus* exhibits a distribution break between southern Namibia and western South Africa, which is thought to be related to the colder sea surface temperatures in the area, that constitute unsuitable habitat for the species to occur (Griffiths & Heemstra 1995; Kirchner 1998). It is likely that the oceanographic features of the Benguela Current may be disrupting both adult and larval dispersal of *A. inodorus* across the region, thus contributing to shape the species' genetic population sub-structuring. Oceanographic features have been suggested to influence genetic population sub-structuring in many marine species as they may constitute barriers to gene flow, which can result in reproductive isolation and genetic divergence associated with the position of the barrier (Bernardi 2000; Knowlton 2000; Hemmer-Hansen et al. 2007; Floeter et al. 2008; Galarza et al. 2009; Gaither et al. 2010). For example, genetic sub-structuring patterns have been reported in multiple coastal species due to multiple oceanographic features such as the Almeria-Oran Front in the western Mediterranean (*Diplodus vulgaris*, *Symphodus tinca*, *Trypterigion delaisi*, *Serranus cabrilla*, *Mullus surmuletus* and *Apogon imberbis* – Galarza et al. 2009); the Antarctic Polar Front (*Dissostichus eleginoides* – Shaw et al. 2004); the Humboldt Current in the eastern Pacific (*Dosidicus gigas* and *Notochthamalus scabrosus* – Sandoval-Castellanos et al. 2007; Zakas et al. 2009); and coastal upwelling in New Zealand (*Patiriella regularis* – Waters & Roy 2004). In addition, similar findings were observed for *Diplodus capensis* using a higher number of sampling sites and samples (Chapter 3), thus suggesting that the Benguela Current oceanographic features may actively be contributing to isolate *A. inodorus* populations in either sub-system.

Nevertheless, due to the small number of sampling sites used in the present work, obtained results should be considered only a preliminary survey. As *A. inodorus* is considered overexploited in South African waters, the reported replacement by *A. coronus* in central Namibia may mean that the species is under threat throughout its distribution. New surveys of the species distribution, population dynamics and dispersion patterns across the Benguela Current region, using a higher number of sampling sites and samples per site, are thus required to ensure the maintenance of healthy populations, and the sustainability of this highly valuable fishery resource in a region with few natural food resources.

Evolutionary history

Assessment of *A. inodorus* evolutionary history was conducted for the two putative populations identified based on the levels of genetic differentiation: HEN and EastC. Although both populations revealed evidence of past demographic expansions based on Tajima's D and Fu's F_S summary statistics, and mismatch distribution analyses and histograms, observed differences between haplotype and nucleotide diversity levels suggest two different demographic scenarios for each population (Grant & Bowen 1998). Based on the relationship between genetic diversity levels, the HEN population appears to have a long evolutionary history, resulting from a large and stable effective population size, while the EastC population appears to have undergone a strong and historically recent bottleneck (Grant & Bowen 1998). The obtained estimates of time since divergence further support the hypothesis of two different demographic scenarios in each *A. inodorus* population, as time since expansion was calculated at ~31 KYA for HEN and ~25 KYA for EastC. As so, although preliminary, these results suggest that *A. inodorus* has undergone two different demographic expansions towards the end of the Last Glacial Maximum (in the late Pleistocene). Different time since expansion between populations, when the generation time is the same, may mean that genetic diversity levels will be higher in the older population than in the recently expanded, as the former will have more time to accumulate mutations (Avice 2000), and can thus account for the observed differences in genetic diversity levels.

In the Benguela Current system, the Pleistocene was characterized by multiple changes in sea surface temperature, sea levels and paleoproductivity, due to worldwide climate-induced changes (Jahn et al. 2003). It is likely that observed past demographic changes in *A. inodorus* were linked to paleo-oceanographic events in the Benguela Current region. In particular, both populations expansions appear to coincide with a reported productivity crash at ~ 41-25 KYA due to an intrusion of warmer water from the Angola Current (Sachs et al. 2001), which was followed by severe population crashes of small pelagic fish species such as *Engraulis* spp. (Grant & Bowen 2006). Although environmental changes are considered to have a greater impact in small pelagic fish species due to changes in productivity levels (Lo Brutto et al. 2011), they will also have an impact on piscivorous species such as *A. inodorus*, as availability of prey will decrease (Mueter et al. 2007).

Furthermore, the observed differences in estimates of time since expansion of the two putative *A. inodorus* population may be connected with different environmental conditions across the Benguela Current region. For example, during the last glacial

maximum there was a reported drop in sea levels of up to 120m in the southeastern Atlantic (Ramsay & Cooper 2002), which may have reduced availability of suitable habitats for coastal fish species, but the effects were not homogeneous throughout the Benguela Current region (Ramsay & Cooper 2002). For example, although in northern Namibia sea surface regressions of 120 m would greatly decrease the number of suitable habitats due to a narrower continental shelf, the southern Namibia region exhibits a larger continental shelf width, which may have served as refuge, maintaining patches of suitable habitats for local coastal species such as *A. inodorus*. In addition, *A. inodorus* exhibits specific temperature preferences of 13-16°C (Griffiths 1997a). Therefore, it is possible that during the reported warmer period in the last glacial maximum where the Angola Current was displaced further south, *A. inodorus* migrated towards southern Namibia where sea surface temperatures were colder, and availability of habitats and prey may have been higher, allowing the population to have a faster genetic recovery. In South Africa, although the broader continental shelf off the southwestern coast could have maintained suitable habitats for coastal species during sea level regressions in the late Pleistocene, sea surface temperatures in the region may have been higher than those off the Namibian coast due to direct influence of the Agulhas Current (Kirst et al. 1999; Chen et al. 2002), thus being unsuitable for *A. inodorus* populations to occur in the nearshore environment, and the population recovery only began towards the end of this warmer period (~25 KYA). In fact, presently the South African *A. inodorus* population exhibits an annual offshore migration that appears to be connected to specific temperature preferences of 13-16°C (Griffiths 1997a).

Pleistocene climate-induced changes have been reported as contributing to shape population demographic and genetic sub-structuring in several marine taxa. For example, climate fluctuations have been documented to have severely reduced *Engraulis mordax* and *Sardinops sagax* populations in the eastern Pacific (Lecomte et al. 2004), influence gene flow and population connectivity in *Mugil cephalus* in the northwestern Pacific (Shen et al. 2011) and in *Homarus americanus* in the northwestern Atlantic (Kenchington et al. 2009), reduce genetic diversity in *Engraulis capensis* (Grant & Bowen 2006) and *Merluccius capensis* (von der Heyden et al. 2010) also occurring in the Benguela Current region. Therefore, it is possible that past climatic events in the Benguela Current region have contributed to shape *A. inodorus* evolutionary history.

4.3. Evolutionary history of *Argyrosomus coronus* (Perciformes: Sciaenidae) in a highly unstable oceanographic system, the Angola-Benguela Front

4.3.1. Introduction

The Pleistocene glacial-interglacial cycles, characterized by changes in oceanographic circulation patterns, sea levels and sea surface temperatures, have been shown to have a particular and deep impact on distribution ranges and population connectivity for a number of marine species (Bowen & Grant 1997; Lecomte et al. 2004; Grant & Bowen 2006; Domingues et al. 2007; Janko et al. 2007; Gonzalez et al. 2008; Han et al. 2008; Ruzzante et al. 2008; Cardenas et al. 2009; Gante et al. 2009; Kenchington et al. 2009; Bester-van der Merwe et al. 2011). The effects of such drastic climate changes can be predicted to particularly affect species inhabiting unstable environments such as the Angola-Benguela Frontal system off southern Africa (von der Heyden et al. 2010).

The Angola-Benguela Front (ABF), off southwestern Africa, results from the interaction between the warm tropical Angola Current in the north and the cold Benguela upwelling system to the south (Fennel 1999; Lass et al. 2000; Mohrholz et al. 2004; Hutchings et al. 2009). The ABF is characterized by eddies with nutrient-rich upwelled water, and constitutes a biogeographical boundary between the sub-tropical ecosystem to the north and the cold-temperate ecosystem around the southern tip of Africa (Fennel 1999; Jahn et al. 2003; Floeter et al. 2008). The convergence zone occurs approximately off the coast of the Cunene River mouth in southern Angola (16°S), but can extend further south, reaching Walvis Bay, Namibia (23°S). Its position is linked with the South Atlantic Anticyclone (SAA), and exhibits a seasonal displacement. During the austral summer the SAA moves southwards and the Angola Current flow is at its maximum, resulting in the southwards movement of the ABF. In reverse, during austral winter and early spring the SAA moves northwards, the upwelling intensity off central Namibia increases, and the ABF is displaced further north as far as Benguela in central Angola (12°S) (Jahn et al. 2003; Shillington et al. 2004; Hutchings et al. 2009). The oscillatory nature of the ABF has been also documented to occur on much longer timescales (Gammelsrod et al. 1998; Fennel 1999; Kirst et al. 1999; Marlow et al. 2000; Chen et al. 2002; Jahn et al. 2003; Mohrholz et al. 2004; Shillington 2004; Farmer et al. 2005; Krammer et al. 2006; Leduc et al. 2010). During the Pleistocene the increase of

the northern hemisphere ice sheets resulted in a southwards displacement of the SAA, which led to a southern displacement of the ABF and a decrease in upwelling intensity in the northern Benguela region (Jahn et al. 2003), as documented by changes in calcareous nanoplankton assemblages, as these communities are known to respond quickly to climatic fluctuations (Krammer et al. 2006). In particular, during the mid-Pleistocene Revolution (0.9 - 0.4 MYA) the Benguela system entered an unstable mode, which was reflected in the ABF position (Jahn et al. 2003). Therefore, the documented cyclic oceanographic changes in the ABF may have influenced distribution ranges, population connectivity and demographic history of local marine species (e.g. Grant & Bowen 2006).

Argyrosomus coronus Griffiths and Hecht 1995, is a coastal sciaenid fish whose distribution range appears to be linked with the ABF (Potts et al. 2010). Juveniles and sub-adults occur throughout the year off the Cunene River mouth region, while adults undertake an annual return migration which appears to be linked to the ABF seasonal oscillation (Potts et al. 2010). Due to such annual return migration and life-history features *A. coronus* is regarded to comprise one panmitic population, and no population sub-structuring is thought to occur (Heemstra & Heemstra 2004; Potts et al. 2010). However, previous studies of other migratory fishes have demonstrated that they may still exhibit high levels of population structuring (Diaz-Jaimes & Uribe-Alcocer 2006; Puchnick-Legat & Levy 2006; Dammannagoda et al. 2008; Riccioni et al. 2010; Andre et al. 2011; Dammannagoda et al. 2011; Karl et al. 2011). Due to the geographical distribution of *A. coronus*, the ABF may play an important role in shaping any population structure. Furthermore, recorded cyclic climatic changes in the region could have influenced the species' demographic history and population evolution.

In the present work the influence of the ABF on genetic population structure and evolutionary history of *A. coronus* was investigated, to evaluate the species' response to past climatic changes and to establish a baseline assessment of genetic diversity for use in future planning for sustainable harvesting. Selectively neutral genetic markers, mitochondrial DNA (mtDNA) and nuclear microsatellite loci, were screened for variability in *A. coronus* to assess: *i*) levels of genetic diversity; *ii*) population sub-structuring patterns across the ABF region; and *iii*) evolutionary history.

4.3.2. Methods

Sampling and DNA extraction

Sampling of *A. coronus* was conducted in five localities spanning the species distribution range (Figure 4.15), during the austral winter months of 2005-2010 (Table 4.11).

Samples from Henties Bay (Namibia) were identified morphologically as *A. inodorus*, but 60% of individuals were subsequently identified genetically to be *A. coronus* (see previous section). Therefore, such individuals were considered to be *A. coronus* and used in the subsequent analyses.

Table 4.11: Sampling strategy for *A. coronus* across the northern Benguela sub-system: sampling locations, sample code, sample size and latitude/longitude coordinates

Country	Region	Code	Sample size	Coordinates
Angola	Luanda	LUA	44	8°47.263'S 13°14.32'E
	Lucira	LUC	41	13°50.635'S 12°27.166'E
	Flamingo	FLA	178	15°10.374'S 12°04.863'E
	Cunene	CUN	26	17°15.207'S 11°45.13'E
Namibia	Henties Bay	HEN	86	22°7.404'S 14°16.139'E

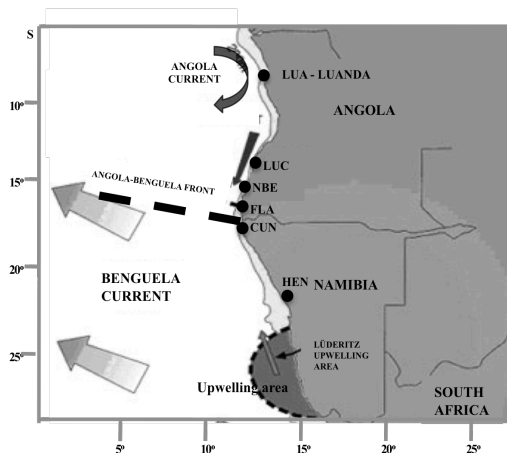


Figure 4.15: Sampling strategy for *A. coronus* across the northern Benguela sub-system, highlighting sampling sites and their position relative to the major oceanographic features of the system: the Benguela and Angola Currents; position of the Angola-Benguela Front; the major upwelling cell in central Namibia; continental shelf width.

Genetic screening

Amplification and sequencing of a fragment from the mtDNA Control Region (CR), using the universal primers L16498 / 12SARH (Apte & Gardner 2002), was performed for 12 individuals per sampling site, as described in Chapter 2.2.2.

Assessment of nuclear genetic diversity levels and population sub-structuring was performed using six cross-specific microsatellite loci, developed for *Argyrosomus japonicus* (Archangi et al. 2009), amplified for 40 individuals per sampling site (whenever possible) as described in Chapter 2.2.3.

Mitochondrial DNA analyses

Population structure and phylogeographic patterns

Estimates of haplotype (h) and nucleotide (π) diversity levels; Tajima's D , Fu's F_S and Ewens-Watersons F neutrality tests, and the most suitable nucleotide substitution model were conducted as described in Chapter 2.4.1.

Tests for significant differentiation between samples were conducted using Wright's pairwise F_{ST} estimates, analyses of molecular hierarchical variance (AMOVA), and reconstructing haplotype relationships (Chapter 2.4.1). The AMOVA was performed to investigate the hypothesis of significant population differentiation associated with the area only influenced by the warm Angola Current (LUA, LUC, FLA) and the area influenced by the Benguela Current (CUN and HEN) at the time of sampling ($\sim 16^\circ\text{S}$), thus investigating the impact of the ABF on the genetic structuring of *A. coronus*. Reconstruction of phylogeographic patterns was achieved using the median-joining spanning network, implemented in NETWORK (Bandelt et al. 1999), in order to investigate the geographical distribution of haplotypes. Ambiguous connections between haplotypes, identified as loops, were resolved using the coalescent theory approach: any given haplotype should be preferentially linked with the most abundant and geographically closest haplotype.

Evolutionary history

Reconstruction of *A. coronus* evolutionary history was performed based on haplotype (h) and nucleotide (π) diversity measures, and Tajima's D (Tajima 1989) and Fu's F_S (Fu 1997) statistics, for the complete dataset (Chapter 2.4.1). Mismatch distribution of haplotype differences was also used to infer past demographic changes, as populations that have undergone sudden expansions are expected to exhibit a characteristic unimodal distribution (Harpending 1994). Significance of deviations from the hypothesis of past demographic expansion was assessed using the "sum of squared differences" (SSD) test, after 10000 iterations (Chapter 2.4.1). Parameters of past demographic expansion were calculated based on the mismatch distribution mean and variance, while time since expansion was estimated as $\sigma = 2\mu t$ (see Chapter 2.4.1). A

universal mutation rate of 3.6% per MY, based on CR divergence rates in multiple fish in relation to the closure of the Isthmus of Panama (Donaldson & Wilson 1999), was used to calculate time since expansion, with generation time estimated at 4.3 years for females (Potts et al. 2010).

Microsatellite analyses

Genetic diversity and population structure

Obtained genotypic frequencies were tested for deviations to Hardy-Weinberg expectations of random mating, and for linkage equilibrium (i.e. non-random association of alleles between loci), in GENEPOP (Chapter 2.4.2). Occurrence of amplification errors such as large allele drop out and stuttering, and null allele frequencies, were assessed in Microchecker (van Oosterhout et al. 2006).

Levels of genetic diversity of *A. coronus* were estimated as number of alleles (N_a), allelic richness (AR), observed and expected heterozygosity (H_O and H_E), and Wright's inbreeding coefficient (F_{IS}) (Chapter 2.4.2). Different analyses were conducted in order to test if the *A. coronus* genetic population structure was composed by one panmitic stock, or by isolated population units. Genetic differentiation among samples was assessed using Weir's (1986) F_{ST} values computed between each pair of samples, and also through hierarchical analysis of molecular variance (AMOVA – see Chapter 2.4.2) to evaluate the hypothesis of population structure in *A. coronus* related to the position of the ABF. In addition, Bayesian approach implemented in STRUCTURE was used to investigate the possibility of cryptic population structure (Pritchard et al. 2000). All analyses were conducted as described in Chapter 2.4.2.

As a few individuals from the southern sampling sites, where the species has been described to co-occur with *A. inodorus* (see Chapter 4.2), exhibited slightly different allelic frequencies. As the occurrence of genetically divergent individuals within a sample may be due to the presence of cryptic taxa (i.e. species) or hybrids to related species (i.e. *A. inodorus*), investigation of genotype frequencies was conducted for both species, based on 40 *A. inodorus* individuals amplified for the same microsatellite loci. In addition, a spatial genetic clustering method for *A. coronus* individuals was evaluated using a factorial component analysis (FCA), as implemented in GENETIX (Belkhir et al. 1995). Contrary to other clustering methods, such as STRUCTURE (Pritchard et al. 2000) and GENELAND (Guindon et al. 2005), the FCA does not group individuals based on Hardy-Weinberg equilibrium assumptions, but on allelic frequencies and genetic relatedness.

Demographic history

Determining effective population size (N_e) can be of extreme importance for exploited marine species, such as *A. coronus*, since it represents a good estimator of relative recruitment levels (Hauser & Carvalho 2008). Based on obtained results for *A. coronus* population structure the dataset was treated as one panmictic population, and N_e was estimated at three critical allele frequencies (0.05, 0.02 and 0.01), as implemented in LDNe (Waples 2006), and confidence intervals for each estimate were assessed using a pairwise jackknife approach (see Chapter 2.4.2).

Changes in effective population size due to environmental events can have a profound effect in the genotypic diversity of a species, and genetic methods, such as that implemented in BOTTLENECK (Piry et al. 1999) can detect signatures of recent population contractions, based on heterozygosity levels (see Chapter 2.4.2). The hypothesis of a recent bottleneck event in *A. coronus* was tested under the three main accepted models of microsatellite mutation: Infinite Alleles Model (IAM), Stepwise Mutation Model (SMM) and Two-Phase Mutation Model (TPM). The TPM model was run with 70% SMM. Significant heterozygote excess was tested using the Wilcoxon Rank test, after 10000 iterations (Chapter 2.4.2).

Hybridization events

Preliminary investigation of genotype compositions of *A. coronus* identified individuals, mainly from the southern sampling sites HEN and CUN, that were genetically divergent from the majority of *A. coronus* individuals, exhibiting alleles common in *A. inodorus*. As in this region there is the possibility of misidentification of individuals between the two species (see Chapter 4.2), all individuals screened for microsatellite variation in the present study were checked using the genetic species ID method detailed in Chapter 4.2. The presence of genetically divergent individuals within a sample may be due to the presence of hybrids with related species (i.e. *A. inodorus*). To address the hypothesis of hybridization between *A. coronus* and *A. inodorus*, 40 *A. inodorus* individuals were amplified for the same microsatellite loci and genotypic frequencies estimated. Compliance with Hardy-Weinberg equilibrium assumptions and linkage equilibrium, and estimates of allelic range, number of alleles (N_a) and allelic richness (AR) were performed as described in Chapter 2.3.2. In order to investigate the suitability of the microsatellite dataset to detect multiple hybridization events five hybrid states were simulated using HybridLab (Nielsen et al. 2006): pure species, F1,

F2, backcross x pure *A. coronus*, and backcross x pure *A. inodorus*. For each state 60 hybrids were simulated, using as a starting dataset 30 genotypes confirmed as pure species from each of the putative parental kob species. Confirmed pure species genotypes and simulated genotypes were run in STRUCTURE (Pritchard et al. 2000) to test the accuracy of the software in detecting different levels of hybridization. Five independent iterations were run for $K = 2$ under the admixture model with independent allele frequencies, for 50000 MCMC steps after an equal initial burn-in period. Identification of putative hybrids was performed based on the posterior probability of assignment (q) of each individual analyzed. Vähä & Primmer (2006) suggest, based on a simulated dataset of microsatellite loci, that $q = 0.1$ is a highly efficient threshold to separate between parental individuals, F1s and hybrids resulting from backcrosses with the parental species. In all analyses thresholds were set to $q = 0.9$ for pure *A. coronus* and $q = 0.1$ for pure *A. inodorus*, while individuals with $0.1 < q < 0.9$ were considered hybrids. The Bayesian approach implemented in NewHybrids (Anderson & Thompson 2002) was used to corroborate the results obtained in STRUCTURE. Contrary to the method implemented in STRUCTURE, which aims to detect genetic clusters in Hardy-Weinberg and linkage equilibrium, the method implemented in NewHybrids uses genotypic frequencies to assess hybrid status of each individual, making it more sensitive to hybrid detection (Anderson & Thompson 2002). As suggested by Aboim et al. (2010), the hybrid assignment threshold of posterior probability (q_i) was lowered to 0.5. Analyses were conducted using the Jeffreys prior for mixing and allelic frequencies, for 50000 MCMC steps after an initial burn-in of 50000 MCMC steps (Anderson & Thompson 2002). Following the preliminary analyses, assessment of hybridization events and determination of hybrid status was performed on the original dataset with both STRUCTURE and NewHybrids using the same run parameters described above.

4.3.3. Results

Mitochondrial DNA

Population structure and phylogeographic patterns

A total of 60 *A. coronus* individuals, 12 per sampling site, were sequenced for 524bp of mtDNA CR, resulting in 47 haplotypes described by 46 variable sites of which 26 were parsimony informative. The Tamura-Nei (Tamura & Nei 1993) nucleotide substitution model, with variable rates among lineages ($\alpha=0.613$), was retrieved as the most suitable

model of sequence evolution. Significant deviations from neutrality expectations were detected with Fu's F_S test, but not with either Ewens-Watson's F , or Tajima's D . Fu's F_S neutrality test is known to be extremely sensitive to demographic changes, therefore observed deviations may be related with demographic events and not selection pressures. Overall haplotype and nucleotide diversity levels were high ($h = 0.990$, $\pi = 0.010$, respectively), and varied between $h = 0.970$ to 1.000 (LUC and CUN) and $\pi = 0.009$ to 0.014 (LUA and CUN) (Table 4.12).

Table 4.12: Mitochondrial genetic diversity levels and neutrality tests for *A. coronus* CR: **n** – number of individuals; **H** – number of haplotypes; **h** – haplotype diversity; **π** - nucleotide diversity; **F** – Ewens-Watson neutrality test; **D** – Tajima neutrality test; **F_S** – Fu neutrality test. Statistically significant results ($p < 0.05$) in bold.

	HEN	CUN	FLA	LUC	LUA	Overall
n	12	12	12	12	12	60
H	11	12	11	10	11	47
h	0.985	1.000	0.985	0.970	0.978	0.990
π	0.008	0.013	0.008	0.008	0.007	0.010
F	1.000	-	1.000	0.765	-	0.836
D	0.147	-1.040	-0.737	-0.111	-0.589	-1.501
F_S	-6.070	-6.064	-6.137	-4.037	-4.379	-25.445

Assessment of population structure could not reject the null hypothesis of a single panmictic population for *A. coronus* across its distribution range. All pairwise F_{ST} comparisons were small and not significantly different from zero, ranging from -0.039 to 0.035 (FLA-HEN and LUA-FLA) (Table 4.13). The hypothesis of divergence between samples north and south of the ABF was rejected, as the majority of genetic variance was found within samples (93.79%, $p < 0.05$), and only 4.44% explained by divergence between groups ($p > 0.05$).

Table 4.13: Pairwise F_{ST} values based on mtDNA CR data, between *A. coronus* samples (see Table 4.11 for sample codes). Values significantly greater than zero ($p < 0.05$) in bold.

	HEN	CUN	FLA	LUC	LUA
HEN	-				
CUN	0.017	-			
FLA	-0.039	0.018	-		
LUC	0.013	0.028	0.028	-	
LUA	0.032	0.015	-0.024	0.021	-

Reconstruction of haplotype relationships using a network approach did not identify obvious geographical patterns of haplotype distribution (Figure 4.16). The majority of individuals represented private haplotypes, and common (shared) haplotypes were equally distributed among sampling sites. Overall, haplotypes diverged from one

another by 1 to 2 mutational steps, with the exception of two LUA haplotypes that differed by 10 mutational steps (Figure 4.16).

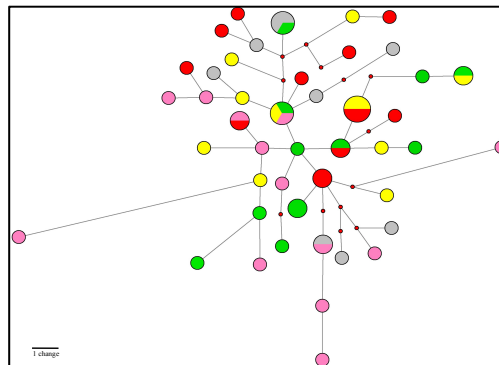


Figure 4.16: Reconstruction of haplotype network for *A. coronus* across the northern Benguela sub-system, based on 524bp of mtDNA CR sequences, in samples from 5 sites: ●: HEN; ●: FLAM; ●: CUN; ●: LUC; ●: LUA. Node sizes are proportional to the number of individuals possessing that haplotype. Red dots correspond to missing haplotypes.

Evolutionary history

Reconstruction of *A. coronus* demographic history was conducted for the complete dataset as no significant population differentiation was observed. Obtained negative and significant results for Tajima's D and Fu's F_S statistics suggested a past demographic expansion, as these tests are particularly sensitive to demographic changes. Furthermore, it was not possible to reject the null hypothesis of a past demographic expansion, based on the CR sequence mismatch distribution analysis (Table 4.14). A plot of the mismatch distribution (Figure 4.17) presented a close fit to expected variation under a hypothesis of recent population expansion (Harpending 1994). Based on a strict molecular clock with a mutation rate of 3.6% per MY, the estimate of time since divergence point to a past population expansion at 30.7 KYA.

Table 4.14: *A. coronus* genetic demographic history, based on mtDNA CR sequence variation: genetic diversity levels (h and π); neutrality tests (Tajima's D and Fu's F_S); mismatch distribution parameters: σ - time since expansion in mutation units, θ_0 - population size before expansion, θ_1 - population size after expansion; and time since expansion (T in KY). Statistical significant results ($p < 0.05$) in bold.

<i>A. coronus</i>	
h	0.990
π	0.010
D	-1.501
F_S	-25.445
Mean	5.352
Variance	5.907
SSD	0.001
σ	4.982
	(3.354-6.998)
θ_0	0.290
θ_1	99999.000
	30.70
Texp (KY)	(20.67-43.14)

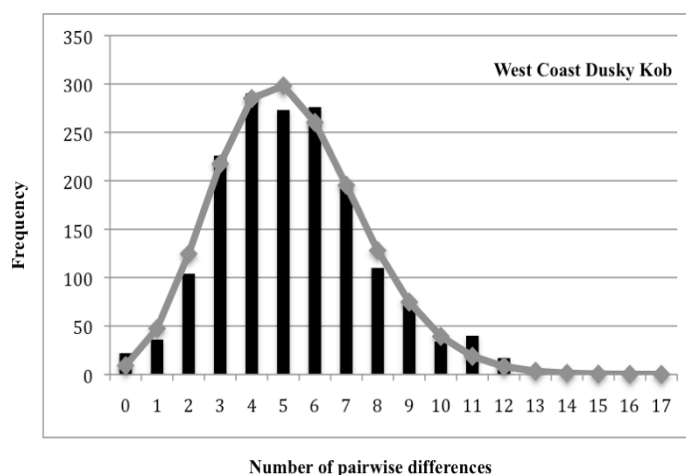


Figure 4.17: MtDNA CR sequence mismatch distribution histograms for the *A. coronus* population. Filled bars indicate the observed frequency of pairwise distribution, grey line indicates the expected distribution under a model of demographic expansion.

Microsatellite analyses

Genetic diversity and population structure

A total of 180 individuals were screened for 6 cross-specific microsatellite markers. Due to the small number of individuals sampled in the Cunene River Mouth (CUN, n=28), these individuals were only included in the factorial components analyses (FCA) and assignment tests (STRUCTURE), where samples sites were not defined. Due to difficulties during DNA extraction and amplification it was only possible to screen 34 individuals in the LUC sample.

The obtained microsatellite dataset did not exhibit evidence of amplification errors, and conformed with Hardy-Weinberg expectations of random-mating across loci and samples, and to linkage equilibrium between loci. Expected heterozygosity (H_E) levels ranged from 0.718 to 0.731 (FLA and CUN, respectively). Higher values of allelic richness were observed for samples CUN and LUC, which may be related with the smaller sample size in these sites. Comparison between sites with identical sample size, revealed LUA as the site with the lowest allelic richness (AR = 6.768), while HEN had the highest (AR = 9.004) (Table 4.15).

Table 4.15: Genetic diversity at 6 cross-specific microsatellite loci in *A. coronus* across 5 sites in the northern Benguela sub-system: **n** – number of individuals genotyped; **Na** – number of alleles; **AR** – allelic richness (minimum of 16 individuals); **H_E** – expected heterozygosity; **H_O** – observed heterozygosity; **F_{IS}** – inbreeding coefficient. Significant deviations to Hardy-Weinberg expectations in bold ($p < 0.05$).

		HEN	CUN	FLA	LUC	LUA
UBA5	n	40	26	40	34	40
	Na	6	6	7	6	5
	AR	5.610	6.000	6.529	5.945	4.999
	H_E	0.721	0.761	0.724	0.747	0.732
	H_O	0.775	0.615	0.700	0.853	0.925
	F_{IS}	-0.063	0.210	0.045	-0.127	-0.252
UBA40	n	40	26	40	34	40
	Na	15	16	14	15	14
	AR	13.457	16.000	12.433	14.030	12.264
	H_E	0.865	0.880	0.842	0.892	0.835
	H_O	0.825	0.808	0.825	0.971	0.950
	F_{IS}	0.059	0.102	0.033	-0.073	-0.125
UBA50	n	40	26	39	34	39
	Na	16	13	15	15	17
	AR	14.585	13.000	13.929	13.755	15.478
	H_E	0.884	0.875	0.882	0.888	0.894
	H_O	0.875	0.846	0.821	0.794	0.846
	F_{IS}	0.024	0.053	0.083	0.121	0.066
UBA91	n	40	26	40	33	34
	Na	5	4	4	3	3
	AR	4.260	4.000	3.530	2.958	2.650
	H_E	0.287	0.270	0.282	0.219	0.258
	H_O	0.275	0.308	0.325	0.182	0.226
	F_{IS}	0.054	-0.120	-0.139	0.183	0.142
UBA853	n	39	26	35	34	40
	Na	9	13	9	11	11
	AR	8.323	13.00	8.929	10.465	10.352
	H_E	0.870	0.878	0.849	0.848	0.830
	H_O	0.795	0.962	0.943	0.735	0.800
	F_{IS}	0.028	-0.076	-0.096	0.148	0.049
UBA854	n	40	26	40	34	40
	Na	9	7	8	8	6
	AR	7.790	7.000	7.167	7.516	5.867
	H_E	0.717	0.719	0.734	0.742	0.704
	H_O	0.700	0.654	0.625	0.706	0.900
	F_{IS}	0.039	0.146	0.161	0.064	-0.267
Average all loci	n	40	26	39	34	39
	Na	10	10	10	10	9
	AR	9.004	9.833	8.753	9.112	6.768
	H_E	0.724	0.731	0.718	0.728	0.709
	H_O	0.698	0.699	0.707	0.697	0.778
	F_{IS}	0.022	0.069	0.030	0.037	-0.080

Assessment of allelic frequencies for the six amplified microsatellite loci in both *A. coronus* and *A. inodorus* allowed identifying diagnostic alleles that would help to differentiate between the two kob species (Figure 4.18). In particular, alleles 133 in UBA5, 183 in UBA40, 183 in UBA50, 163 in UBA91, 184 and 188 in UBA853, and 181 in UBA854 appear to be common (even fixed) in *A. coronus*, but were only found in one to two *A. inodorus* individuals (allelic frequencies < 0.01), while alleles 153 in

UBA5, 167 in UBA40, 161 in UBA91, 174 in UBA853 and 185, 189 and 193 in UBA854 appear to be very common in *A. inodorus* but were found at low frequency (<0.01) in *A. coronus* (Figure 4.18).

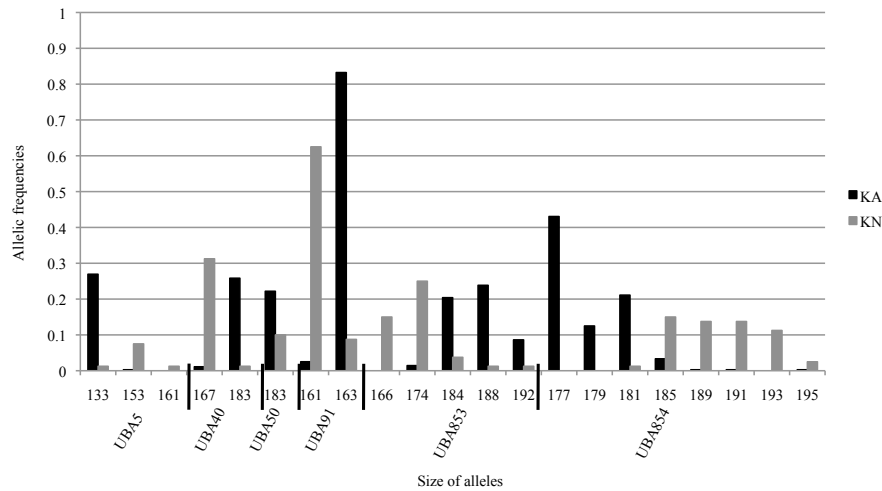


Figure 4.18: Allelic frequencies of diagnostic alleles at the six microsatellite loci used to genotype *A. coronus* and *A. inodorus*.

In the FCA the first two axes explained 11.28% of all variation and did not show distinct clustering of genotypes into more than one group (Figure 4.19). However, it was possible to observe a number of outlier individuals that did not group with the main cluster, due to divergent genotypic frequencies – individuals marked 1 to 4 on Figure 4.18: 1 = KA270 (CUN), 2 = KNA19 (HEN), 3 = KA190 (LUC) and 4 = KA258 (LUA).

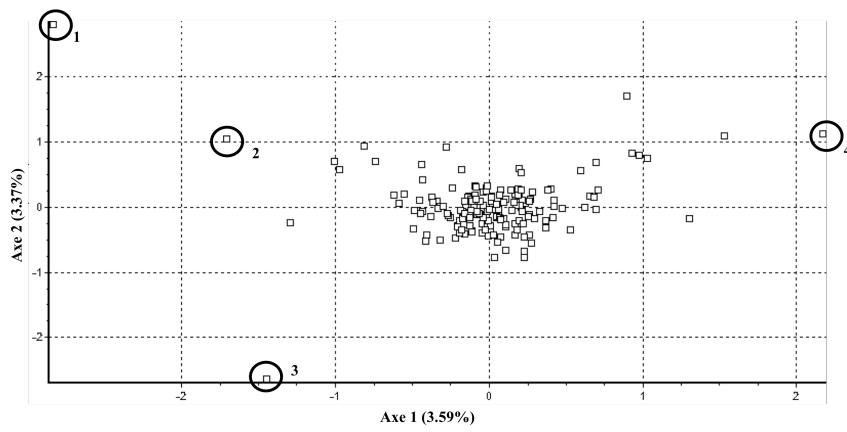


Figure 4.19: Factorial Components Analysis for *A. coronus* microsatellite genotypes. Marked circles correspond to outlier individuals: 1 = KA270 (CUN), 2 = KNA19 (HEN), 3 = KA190 (LUC) and 4 = KA258 (LUA).

Despite the presence of individuals with divergent genotypic frequencies, and as reported for the mtDNA marker, no significant genetic differentiation was observed among *A. coronus* sampling sites. The overall F_{ST} value was very low and not significantly different from zero ($F_{ST} = -0.001$; $p > 0.05$). Pairwise F_{ST} comparisons

ranged from -0.005 to 0.005 (FLA-CUN, LUC-HEN, respectively - Table 4.16), none of which were significantly different from zero. Equally, as observed for the mtDNA dataset, AMOVA did not indicate significant genetic variation partitioned between samples from areas influenced by the Angola and Benguela Currents, since the majority of variance was explained by polymorphism within populations (99.958%, $p < 0.05$) and not between groups (0.198%, $p > 0.05$).

Table 4.16: Pairwise F_{ST} values between *A. coronus* samples based on 6 microsatellite loci (see Table 4.11 for sample codes). Values significantly greater than zero ($p < 0.05$) in bold.

	HEN	CUN	FLA	LUC	LUA
HEN	-				
CUN	-0.004	-			
FLA	-0.003	-0.005	-		
LUC	0.005	-0.005	0.002	-	
LUA	-0.001	-0.002	-0.001	0.001	-

The Bayesian analysis conducted in STRUCTURE retrieved one cluster as the most likely number of populations in *A. coronus* ($K = 1$, $\text{Ln}(D) = -3910.7$). Therefore, the present findings suggest no evidence for more than one panmictic population across the species distribution.

Demographic history

As there was no evidence for a genetically substructured population, estimates of effective population size (N_e) and bottleneck events were conducted for the complete dataset. Despite large confidence intervals, assessment of N_e revealed high effective population size for *A. coronus*, ranging from 957 individuals, for the 1% allele frequencies threshold, to 3405 individuals for the 5% allele frequencies threshold (Table 4.17).

Assessment of recent bottleneck events did not reveal evidence of significant heterozygote excess for the *A. coronus* population, independently of the mutation model used (Table 4.17). Therefore, it was not possible to reject the null hypothesis of mutation-drift equilibrium, suggesting that the *A. coronus* population has not experienced severe bottleneck contractions in the recent past.

Table 4.17: Demographic history of the *A. coronus* population in the northern Benguela sub-system: probability of significant departure from equilibrium population size (i.e. a bottleneck) and estimates of effective population size (N_e + 95% confidence intervals).

<i>A. coronus</i>		
Bottleneck events	IAM	0.219
	SMM	1.000
	TPM	0.656
N_e	0.05	3405 (309.5 - ∞)
	0.02	1035 (348.4 - ∞)
	0.01	957.2 (374 - ∞)

Tests for hybridization

In order to investigate the origin of the highly divergent genotypes identified in a few *A. coronus* individuals, 40 *A. inodorus* individuals were amplified for the same microsatellite loci to provide a comparative allele frequency dataset to allow testing for hybridization events between *A. coronus* and *A. inodorus* (Figure 4.18). Obtained genotype frequencies for the *A. inodorus* sample conformed to Hardy-Weinberg and linkage equilibrium expectations, and no signal of inbreeding (F_{IS}) was detected.

Number of alleles (N_a) and allelic richness (AR) differed between the two species (Table 4.18), and diagnostic alleles were identified (Figure 4.18): allele 133 at locus UBA5, alleles 177 to 201 at locus UBA40, and alleles 199 and 201 at locus UBA50 were present in *A. coronus* but absent from *A. inodorus*, suggesting that these microsatellite loci could be used to differentiate between the two species.

Table 4.18: Comparison of genetic diversity at 6 microsatellite loci in obtained for *A. coronus* and Namibian *A. inodorus*: **n** – number of individuals; **Na** – number of alleles; **AR** – allelic richness (minimum of 40 individuals).

		<i>A. coronus</i>	<i>A. inodorus</i>
UBA5	n	180	40
	Na	9	11
	AR	8.933	10.803
UBA40	n	180	40
	Na	22	8
	AR	21.833	7.951
UBA50	n	178	40
	Na	22	14
	AR	21.887	13.974
UBA91	n	179	40
	Na	6	5
	AR	5.999	4.902
UBA853	n	174	40
	Na	16	13
	AR	16.000	12.799
UBA854	n	180	40
	Na	13	17
	AR	12.833	17.604

Analyses conducted using the simulated genotype dataset revealed that STRUCTURE could accurately detect F1 and F2 hybrids, but lost precision when detecting backcrosses with either parental species in 50% of cases. The number of incorrect assignments was reduced when the Bayesian approach implemented in NewHybrids was used, with only 13% of the backcrosses to pure *A. coronus* and 5% of backcrosses to pure *A. inodorus* not identified. These results suggest that the microsatellite dataset could be used to detect hybridization events between the two kob species, particularly if multiple methods are combined. However, some caution should be applied due to the relatively high levels of incorrect identification for hybrids resulting from backcrosses with pure *A. coronus*.

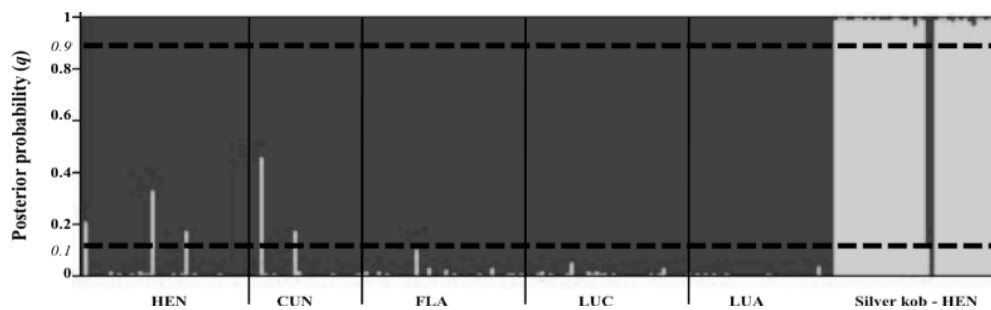


Figure 4.20: Multilocus assignment tests performed in STRUCTURE for hybrid identification based on 6 microsatellite loci: black bars indicate *A. coronus* genotypes, grey bars indicate *A. inodorus* genotypes (see Table 4.17 for individual identification). Dashed lines indicate probability of assignment to each species: $q > 0.9$ – pure *A. coronus*; $q < 0.1$ – pure *A. inodorus*; $0.1 < q < 0.9$ – putative hybrid.

When the original sample set was evaluated in STRUCTURE five *A. coronus* individuals (KNA19, KNA70 and KNA89 from HEN; KA270 and KA278 from CUN) and two *A. inodorus* individuals (KN109 and KN125) were identified as having admixed origins (Figure 4.19, and see Table 4.19). Analysis conducted in NewHybrids corroborated the majority of the identified putative hybrids, with the exception of individual KNA89 that was identified as pure *A. coronus*, and individual KA33 (FLA) that was indicated as a hybrid by NewHybrids, but not so by STRUCTURE (Table 4.19). Of the 40 *A. inodorus* screened for both mtDNA and nDNA microsatellite loci, 2 were identified as putative hybrids as they exhibited *A. inodorus* mtDNA haplotypes but *A. coronus* nuclear genotypes. Likewise, of the 40 *A. coronus* caught as *A. inodorus* in Henties Bays (HEN), 3 were identified as hybrids, exhibiting *A. coronus* mtDNA haplotypes but also a degree of admixture in their nuclear genotypes (Table 4.19). Of the 220 kob individuals screened for microsatellites (180 *A. coronus* and 40 *A. inodorus*) 8 were identified as putative hybrids based on multiple analyses (Table 4.17):

- individuals KNA19, KNA70 and KNA89 were caught at Henties Bay in Namibia (HEN) and identified morphologically as *A. inodorus*, but identified as *A. coronus* by mtDNA PCR-RFLP (Chapter 4.2), and indicated as hybrid backcrosses to *A. coronus* by the microsatellite analysis;
- individuals KA270, KA278 and KA33 were caught at sites CUN and FLA in Angola as *A. coronus*, identified as *A. coronus* by mtDNA CR sequencing, but were indicated as hybrid individuals, resulting from backcrosses to *A. coronus* by the microsatellite analysis;
- individuals KN109 and KN125 were caught at HEN as *A. inodorus* and were identified as *A. inodorus* by mtDNA PCR-RFLP (see Chapter 4.2), but were indicated as pure *A. coronus* individuals by their microsatellite genotypes (Table 4.19).

Table 4.19: *A. coronus* (KNA – Namibia, and KA – Angola) and *A. inodorus* (KN) individuals showing evidence of introgressive hybridization as diagnosed by morphology, mtDNA CR sequence data and microsatellite genotypic assignments using STRUCTURE and NewHybrids.

Individual	Sampling Site	Morphology	mtDNA	STRUCTURE (q)	NewHybrids
KNA19	HEN	<i>A. inodorus</i>	<i>A. coronus</i>	Admixed (0.21)	B x <i>A. coronus</i>
KNA70	HEN	<i>A. inodorus</i>	<i>A. coronus</i>	Admixed (0.33)	B x <i>A. coronus</i>
KNA89	HEN	<i>A. inodorus</i>	<i>A. coronus</i>	Admixed (0.17)	<i>A. coronus</i>
KA270	CUN	<i>A. coronus</i>	<i>A. coronus</i>	Admixed (0.46)	B x <i>A. coronus</i>
KA278	CUN	<i>A. coronus</i>	<i>A. coronus</i>	Admixed (0.18)	B x <i>A. coronus</i>
KA33	FLA	<i>A. coronus</i>	<i>A. coronus</i>	Not admixed (0.9 – <i>A. coronus</i>)	B x <i>A. coronus</i>
KN109	HEN	<i>A. inodorus</i>	<i>A. inodorus</i>	<i>A. coronus</i>	<i>A. coronus</i>
KN125	HEN	<i>A. inodorus</i>	<i>A. inodorus</i>	<i>A. coronus</i>	<i>A. coronus</i>

4.3.4. Discussion

Genetic diversity and population structure

Levels of genetic diversity documented for *Argyrosomus coronus* for mtDNA are similar in range to levels reported for other marine fish species, and in particular sciaenids: *Micropogonias undulatus* ($h = 0.47$, $\pi = 0.019$ – Lankford et al. 1999), *Sciaenops ocellatus* ($h = 0.95$, $\pi = 0.057$ - Gold & Richardson 1998), *Pogonias cromis* ($h = 0.95$, $\pi = 0.057$ – Gold & Richardson 1998), *Cynoscion nebulosus* ($h = 0.95$, $\pi = 0.057$ – Gold & Richardson 1998), *Pannahia argentata* ($h = 0.998$, $\pi = 0.026$ – Han et al. 2008), and *Larimichthys polyactis* ($h = 1.00$, $\pi = 0.0015$ – Kim et al. 2010). Compared to other fish species in the Benguela region, however, *A. coronus* exhibits the highest diversity levels documented for mtDNA (Teske et al. 2003; Grant & Bowen

2006; von der Heyden et al. 2007; von der Heyden et al. 2010), and only one other kob species (*Argyrosomus japonicus*) has similar values ($h = 0.96$, $\pi = 0.009$ – Klopper 2005). Equally, genetic diversity levels obtained for 6 microsatellites across loci and samples were relatively high ($H_O = 0.719$; $H_E = 0.731$), and comparable to other marine fish species such as *Cynoscion nebulosus* ($H_O = 0.21 - 0.39$ – Ward et al. 2007), *Thunnus obesus* ($H_O = 0.742$ – Gonzalez et al. 2008) and *Scomberomorus cavalla* ($H_E = 0.311 - 0.803$ – Gold et al. 2002).

The high genetic diversity levels here documented for *A. coronus* thus suggest that the species does not show evidence of recent population decline (10s – 100s years), which may be related to the low exploitation levels reported throughout its distribution (Potts et al. 2010), since long-term over-exploitation of populations may result in loss of genetic diversity (Kenchington et al. 2003; Hauser & Carvalho 2008). In fact, based on fisheries catches, Potts et al. (2010) suggests that *A. coronus* may still be in a relatively pristine state, as the species is not the main target of the southern Angola subsistence fisheries. Additionally, marine fish usually present historically high effective population sizes, which will influence genetic diversity. Therefore, present genetic diversity levels may also result from high historical effective population sizes in *A. coronus*, as it was confirmed by the estimates here of effective population size (N_e) and bottleneck analyses.

Oceanographic features such as the Angola-Benguela Front have been documented to influence the genetic sub-structuring of marine taxa by constituting barriers to gene flow by disrupting adult and/or larval dispersal, causing reproductive isolation and genetic divergence associated with the position of fronts and current boundaries (Bowen et al. 1994; Bowen & Grant 1997; Lessios et al. 2003; Waters & Roy 2004; Conover et al. 2006; Neethling et al. 2008; York et al. 2008; Diaz-Jaimes et al. 2010). However, assessment of *A. coronus* genetic population structure and phylogeographic patterns, for both mtDNA and microsatellite markers, revealed no evidence of anything other than a single panmictic population throughout the species distribution. Results for pairwise F_{ST} comparisons, hierarchical analysis of molecular variance between samples north and south of the ABF, and genetic clustering methods all failed to detect significant population differentiation, suggesting that the ABF does not greatly influence gene flow between *A. coronus* populations sampled on either side of this frontal system. The absence of barriers to gene flow and the subsequent panmictic population may be related with the species annual return migration. *A. coronus* is found only in the northern part of its distribution during the austral winter months (June-

September), which is thought to be linked with the northwards displacement of the ABF in the same period. Additionally, the large long-term effective population size (N_e) indicated may also contribute to genetic homogeneity in *A. coronus*, as large N_e can retard genetic drift and thus decrease the likelihood of population differentiation developing (Beebee & Rowe, 2005). Furthermore, *A. coronus* appears to have only a single spawning ground off southern Angola during the early austral summer (Potts et al. 2010). Thus, the combination of large N_e plus an annual return migration to one common spawning ground during a single season would be expected to maintain genetic homogeneity of the populations, and prevent sub-structuring in *A. coronus*.

The findings presented here, combined with the results obtained by Potts et al. (2010) on the biology of *A. coronus*, suggest that the species' evolutionary history is closely linked with the ABF. The apparent lack of influence on levels of genetic diversity and population sub-structuring by such a distinct oceanographic frontal system, when frontal systems elsewhere in the world typically subdivide species distributions (e.g. Shaw et al. 2004; Galarza et al. 2009), may be a product of this species' adaptation to living associated with the frontal system itself. The observed annual return migration is associated with seasonal displacements of the frontal zone, and thus climatic changes that affect the oscillatory pattern of the ABF will probably have a similar and direct impact on the distribution range and population dynamics of *A. coronus*. For example events such as the Benguela Niños can reduce or even halt the Benguela circulation, and consequently displace the ABF. An increase in frequency of these climatic anomalies has been reported in the region during the last few decades (Shillington et al. 2004), and has been accompanied by a 0.6°C increase in sea surface temperatures, followed by a poleward (south) expansion of surface warming at the ABF (Monteiro et al. 2008). Simultaneously, the distribution of *A. coronus* appears to be shifting southwards, with an increased abundance in central Namibia (see Chapter 4.2), and individuals caught as far south as St. Helena Bay in western South Africa (Lamberth et al. 2008). Thus, it appears that *A. coronus* is presently following the displacement of the ABF farther south, as it may have done in the past.

Evolutionary history

Assessment of *A. coronus* evolutionary history was conducted for the entire dataset, as no significant genetic sub-structuring was detected. Values for Tajima's D and Fu's F_S statistics, and sequence mismatch distribution analyses of the mtDNA data revealed evidence of a past population expansion. Estimates of female effective size at expansion

time in *A. coronus* was relatively small ($\theta_0 = 0.290$) suggesting the occurrence of a past demographic expansion from a reduced number of females (Excoffier et al. 2005). However, the haplotype network analyses, plus the observed high haplotype and nucleotide diversity, suggest a species exhibiting a long and stable evolutionary history according to the the assumption of Grant & Bowen (1998).

Although estimates of time since divergence should be regarded with caution due to the assumptions required to calibrate the molecular clock, the mtDNA data indicate that *A. coronus* underwent a population expansion around 30 KYA, towards the end of the Last Glacial Maximum (100-10 KYA). The present oceanographic features of the Benguela Current system were established by ~2 MYA during the Pliocene-Pleistocene transition (Fennel 1999; Marlow et al. 2000; Krammer et al. 2006), and so are too early to be responsible for the suggested population bottleneck and expansion. The Pleistocene, and especially the late Pleistocene, was characterized by cyclical glacial and inter-glacial periods during which the Benguela system experienced repeated changes in sea surface temperature, sea levels and primary productivity (Jahn et al. 2003). As changes in productivity will influence abundance levels of small pelagic species such as sardines and anchovies, it is considered that they will also have repercussions for piscivorous species such as *A. coronus* (Mueter et al. 2007). Pleistocene climate-induced changes have been suggested as contributing to population genetic signatures in several marine taxa (Lecomte et al. 2004; Domingues et al. 2007; Janko et al. 2007; Kenchington et al. 2009), including other southern African species. For example, low levels of haplotype and nucleotide diversity in anchovies (*Engraulius capensis*) and Cape Hake (*Merluccius capensis*) have been linked with warmer interglacial periods that reduced the availability of suitable habitat for the species in the Benguela Current region (Grant & Bowen 2006; von der Heyden et al. 2010). In particular, a productivity crash in the Benguela Current at ~41-25 KYA has been linked to a severe population crash in sardines and anchovies (Jahn et al. 2003; Grant & Bowen 2006). This event was thought to have greatly influenced demographic history of Cape Hake in the southern Benguela sub-system (von der Heyden et al. 2010). It is likely that the same climate-induced changes in the Benguela Current and local productivity could have similarly influenced *A. coronus* evolutionary history, in particular the indicated past demographic contraction.

Assessment of *A. coronus* population demography using microsatellite data did not reveal evidence of recent population contractions, as the population did not exhibit significant deviations from the null hypothesis of mutation-drift equilibrium,

independently of the mutation model employed. These results are in agreement with the findings of Potts et al. (2010) that *A. coronus* does not appear to be over-exploited at the moment, possibly due to the presence of an informal marine protected area in the southern Angola region. In addition, estimates of *A. coronus* effective population size were relatively high, ranging from 957 to 3405 individuals. In marine fish, N_e is estimated to vary between 100-1000s individuals, and is normally a good indicator of recruitment, since for most species the ratio N_e/N is very small (Hauser & Carvalho 2008). For conservation purposes Frankham et al. (2002) suggested a minimum threshold of $N_e = 500$, which is lower than the effective population size indicated for *A. coronus*, once again supporting Potts et al. (2010) hypothesis of a near-pristine population in Angola.

In summary, reconstruction of *A. coronus* evolutionary history suggests the occurrence of a historical bottleneck event, around 30 KYA, followed by demographic expansion and subsequent large and stable long-term effective population sizes.

Hybridization and climate change

Climate change-induced shifts in distribution ranges can bring into contact species that have evolved in allopatry (Hill et al. 2011; Lo Brutto et al. 2011). Such events could result in hybridization if species have not developed complete reproductive incompatibility, and thus the occurrence of hybrid zones is predicted to increase with climate change (Buggs 2007). The present study reports the first evidence of possible hybridization events between two kob species *A. coronus* and *A. inodorus* off the coast of Namibia. *Argyrosomus coronus* and *A. inodorus* are closely related species, and genetic data presented in section 4.1 indicate that they have diverged and have been evolving separately for the last ~2 MY. Until the last decade, overlap in the distributions of these two species was thought to be confined to a narrow zone off northern Namibia, where *A. coronus* was the numerically dominant species, with the population mainly composed by juveniles and sub-adults, and its abundance rapidly decreased further south off central and southern Namibia where it was replaced by *A. inodorus* (Kirchner & Beyer 1999; Kirchner & Holtzhausen 2001). However, a recent survey revealed a steep increase in *A. coronus* occurrence in central Namibia, and reported catches off western South Africa suggest that the species may be found throughout the Namibian distribution range of *A. inodorus* (Lamberth et al. 2008). Therefore, in recent years the distribution of *A. coronus* appears to have changed,

bringing it into greater contact with *A. inodorus*, thus increasing the chances of interbreeding between the two species.

Genetic clustering methods employed here revealed the presence of a number of *A. coronus* individuals with highly divergent microsatellite genotypes. All such individuals were collected at sites within the southernmost distribution of the species, namely the Cunene River mouth on the border between Angola and Namibia, and Henties Bay in central Namibia, the latter site being where a mtDNA analysis revealed that *A. coronus* is now highly abundant in the area where *A. inodorus* was previously dominant (see Chapter 4.2). Hybridization tests using *A. inodorus* individuals as a reference uncovered evidence of genetically admixed specimens, suggesting introgressive hybridization events between the two species. When hybrid status was classified the majority of admixed individuals were identified as backcrosses with the parental *A. coronus*. No F1 or F2 hybrids were observed in the dataset, despite preliminary tests showing that they could be accurately identified. Absence of F1 generation individuals has been described in multiple hybrid zones, and is commonly associated with selection against hybrids (Saavedra et al. 1996). Since the F1 generation is the most differentiated from both parental species, it tends to be more affected by fitness reduction linked to ecological, behavioural and genetic factors (Bridle et al. 2006). However, the presence of backcross individuals suggests that the F1 must at least be partially viable. Reproductive isolation between species can be achieved with either pre- or post-zygotic mechanisms. Pre-zygotic mechanisms are commonly established first, and tend to be related to colonization of different niches (Bierne et al. 2002), while post-zygotic barriers tend to evolve after species isolation and may involve inviability of hybrids or different gamete recognition mechanisms (Rogers & Bernatchez 2006; Palumbi 2009). The observed occurrence of backcrosses and introgressive hybridization between *A. coronus* and *A. inodorus* suggests that isolation between the two species has previously been maintained by pre-zygotic mechanisms such as the presence of different spawning grounds or spawning seasons (e.g. Aboim et al. 2010). *Argyrosomus inodorus* is known to spawn off southern Namibia, in the Meob Bay region, whereas *A. coronus* spawns off southern Angola, i.e. sites more than 2000 km apart (Kirchner & Holtzhausen 2001; Potts et al. 2010). However, recent *A. coronus* catches off St. Helena Bay in western South Africa (Lamberth et al. 2008) imply that the species is capable of at least crossing the Meob Bay *A. inodorus* spawning grounds, and so providing the potential for the hybridization events documented. Introgressive hybridization appears to be asymmetric, since all identified backcrosses were in the direction of *A. coronus*, which may be

related with biased assortative mating or sexual selection (Wirtz 1999; Meyer et al. 2006).

Two individuals identified as *A. inodorus*, by both morphological traits and mtDNA haplotype possessed nuclear genotypes which were more typical of *A. coronus* than *A. inodorus*. Such mitochondrial-nuclear incongruence can be generated by one-way introgressive hybridization where the clonal maternally-inherited mtDNA type of one parent species is retained down the female line but repeated backcrossing to the second parental species eventually dilutes out all detectable trace of the other parental species' nuclear genome (Aboim et al. 2010). In these cases it is considered that hybrid females may not experience strong fitness reduction, and in extreme situations mtDNA "capture" from one species to the other can occur (Wilson & Bernatchez 1998). Furthermore, two individuals morphologically identified as *A. inodorus* exhibited *A. coronus* mtDNA haplotypes, and were considered backcross (to *A. coronus*) hybrids according to their nuclear DNA. The apparent discordance between the three types of markers used to describe these species suggests that determining introgressive hybridization events should be done using multiple approaches, in order to secure the correct detection of hybrids (e.g. Aboim et al. 2010).

The small percentage of detected hybrids (3.64%) suggests that introgressive hybridization is a sporadic event, which may be connected with the recent and occasional presence of adult *A. coronus* in *A. inodorus* spawning grounds. Hybridization events can result in the establishment of hybrid zones, changes in genetic diversity, development of novel genetic combinations, extinction of some genetic forms, and ultimately speciation, thus actively changing a species' genetic architecture (Mallet 2005; Buggs 2007). The present study documented the possible establishment of an incipient hybrid zone between *A. coronus* and *A. inodorus* off the Namibian coast. This event may be related with the observed southwards shift in the distribution range of *A. coronus* due to increased sea surface temperatures in the northern Benguela region. In the past, similar climatic changes resulted in severe modification of global oceanographic features, such as disruption of current patterns, changes in sea levels and sea surface temperatures, which in turn influenced species distributions and connectivity. Ongoing climate change will, most likely, have similar repercussions for oceanographic systems, and the frequency of the observed hybridization events may increase, effectively compromising the genetic identity of both kob species.

CHAPTER 5: *Atractoscion aequidens*

5.1. Population structure and evolutionary history of *Atractoscion aequidens* (Cuvier, 1830) across the Benguela Current region

5.1.1. Introduction

Atractoscion aequidens (Cuvier, 1830) is a benthopelagic sciaenid fish occurring throughout the western coast of Africa, from Mauritania to South Africa, and in the eastern coast of Australia (Griffiths & Hecht 1995; Heemstra & Heemstra 2004). Due to unsuitably low sea temperatures, *A. aequidens* exhibits a distribution break between southern Namibia and western South Africa, and is thought to be composed of two isolated populations to the north and south of this break (Griffiths & Hecht 1995). South African *A. aequidens* is thought to be composed of one panmictic population, occurring as three distinct geographical stocks structured according to age and size, and exhibiting an annual spawning migration (Griffiths & Hecht 1995). *Atractoscion aequidens* has been one of the most important line-fishery resources in South Africa since the industry started in the 19th century (Hutton et al. 2001), and decades of over-exploitation led to the depletion of the stock by 2002 (FAO 2005b). Currently, there is no available information regarding the status of the *A. aequidens* population in Angola, although anecdotal evidence suggests a decline in captures throughout Angola (W. Potts, personal communication). Contrary to what is observed in the South African population (Griffiths & Hecht 1995), Angolan *A. aequidens* do not appear to undertake an annual return migration to a specific breeding site, since adults are captured year-round throughout Angola (W. Potts, personal communication).

In the last few decades increased fishing effort has led to a steep decline in a large number of marine fish species (e.g. Cochrane & Doullman 2005; Garcia & Grainger 2005). Even low levels of fishing effort may have a severe impact on species population dynamics by contributing to the constriction of geographical range, reduction of abundance, modifications in size and age structure, loss of highly fecund individuals, changes in life history features and loss of genetic diversity (Clark et al. 2000; Kenchington et al. 2003; Hutchings & Reynolds 2004; Palumbi 2004; Miete et al. 2010). Slow growing, late maturing and long-lived species such as *A. aequidens* are particularly vulnerable to over-exploitation (FAO 2001, 2005b). Determining accurate

population structure of commercially exploited species, such as *A. aequidens*, is essential to ensure the maintenance of high genetic diversity and evolutionary potential, and to achieve sustainable harvesting (Waples 1998; Conover & Munch 2002; Caddy & Seij 2005; Garcia & Grainger 2005; Hauser & Carvalho 2008). Although over-exploitation is one of the major threats to marine species, climate-induced changes are also of particular concern, especially in species occurring in unstable environments such as in the region of the Benguela Current (Briggs 2011; Dawson et al. 2011). It is, however, difficult to assess how a species will react to contemporary climate change, but understanding the evolutionary history of a species can give insight into the impact that past climatic fluctuations had on distribution, genetic diversity and population connectivity (Lo Brutto et al. 2011).

Therefore, the main aims of the present study were to: *i)* investigate the influence of regional oceanographic features on *A. aequidens* population connectivity and gene flow; *ii)* reconstruct the evolutionary history of *A. aequidens* across the Benguela Current region, since the present distribution range, level of diversity and connectivity patterns may reflect historical climate-induced changes in the Benguela region; and *iii)* establish a genetic baseline dataset to inform future management plans ensuring sustainable exploitation of this valuable fishery resource in a poverty-stricken area.

5.1.2. Methods

Sampling and DNA extraction

Sampling was conducted in five locations throughout Angola during the summer months of 2008-2010, in northern Namibia in 2009, and in the Eastern Cape and Western Cape provinces of South Africa in 2008 and 2009 respectively (Table 5.1, Figure 5.1). Samples were collected and DNA extracted as described in Chapter 2.2.1.

Table 5.1: Sampling strategy for *A. aequidens* across the Benguela Current region: sampling locations, sample code, sample size and latitude/longitude coordinates.

Country	Region	Code	Sample size	Coordinates
Angola	Luanda	LUA	59	8°47.263'S 13°14.32'E
	Baia Farta	BEN	24	12°35.516'S 13°13.595'E
	Lucira	LUC	109	13°50.635'S 12°27.166'E
	Namibe	NBE	79	15°10.374'S 12°04.863'E
	Pinda	PIN	99	15°43.414'S 11°53.658'E
Namibia	Henties Bay	HEN	9	-
South Africa	Port Alfred	EastC	79	33°36.50'S 26°54.000'E
	Arniston	WestC	90	34°40.00'S 20°14.000'E

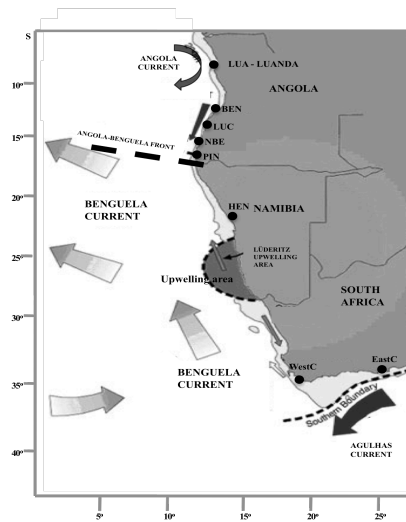


Figure 5.1: Sampling strategy for *A. aequidens* across the Benguela Current region, highlighting sampling sites, and their position relative to the major oceanographic features of the system: position of the Benguela and Agulhas Currents, central Namibia upwelling cell, and continental shelf width.

Genetic screening

A total of 144 *A. aequidens* individuals were amplified and sequenced for a fragment of mitochondrial DNA (mtDNA) Control Region (CR), using the universal primer pair L16498/12SARH (Apte & Gardner 2002), to investigate levels of mtDNA genetic diversity, phylogeographic patterns and to reconstruct evolutionary history, as described in Chapter 2.2.2

Eight species-specific microsatellite loci (Geelb5, Geelb13, Geelb16, Geelb21, Geelb27, Geelb29, Geelb30 and Geelb32), isolated from *A. aequidens* from southern Angola (see Chapter 2.2.4), were screened in up to 70 individuals per sampling site to investigate genetic diversity levels and population sub-structuring across the Benguela Current. As microsatellite analyses require larger samples sizes due to larger allelic diversity exhibited, the Baía Farta (BEN) and Namibian (HEN) samples were not used in the subsequent analyses.

Mitochondrial DNA sequence analyses

Population structure and phylogeographic patterns

Atractoscion aequidens individuals were assessed for levels of haplotype diversity (h) and nucleotide (π) diversity, fits to neutrality tests (Ewens-Waterson's F , Tajima's D and Fu's F_S), and determination of the most suitable nucleotide substitution model as previously described (Chapter 2.3.1). Assessment of population structure was performed through estimation of Wright's F_{ST} values between samples, analysis of hierarchical molecular variance (AMOVA), and by reconstructing haplotype

relationships across the region sampled (see Chapter 2.3.1. for details). AMOVA tests were conducted to investigate the influence of: *i*) the separation between the northern and southern Benguela *A. aequidens* populations; and *ii*) the Angola-Benguela Front (ABF) on the genetic structuring of the northern *A. aequidens* by evaluating the hypothesis of differentiation between samples from sites influenced by the Angola Current (LUA, BEN, LUC, NBE, PIN) and the Benguela Current (HEN, WestC, EastC).

Evolutionary history

Reconstruction of *A. aequidens* evolutionary history was performed using multiple approaches: estimates of haplotype (*h*) and nucleotide (π) diversity measures, Tajima's *D* (Tajima 1989) and Fu's F_S (Fu 1997) statistics, as well as mismatch distribution analyses were conducted for each identified genetic cluster (Chapter 2.3.1). Significance of deviations to the hypothesis of past demographic expansion was assessed using the "sum of squared differences" (SSD) test, after 10000 iterations (Chapter 2.3.1). Time since expansion was estimated as $\sigma = 2\mu t$ (see Chapter 2.3.1), using a universal molecular clock calibrated for fish species based on the closure of the Isthmus of Panama (3.6% per MY – Donaldson & Wilson 1999). Generation times were assumed to be 2.2 years for Angolan *A. aequidens* (W. Potts, personal communication), and 5 years for South African *A. aequidens* (Griffiths & Hecht 1995).

Microsatellite DNA analyses

Population structure and gene flow

Eight newly-isolated species-specific microsatellite loci (see Chapter 2.2.4) were amplified and screened for allelic variation in 268 individuals. The loci screened were Geelb5, Geelb13, Geelb16, Geelb21, Geelb27, Geelb29, Geelb30 and Geelb32, and PCR mixes and amplification protocols were performed as described in Chapter 2.2.4. Amplification products were screened on an AB3500 Genetic Analyzer (Applied Biosystems) with 600 LIZ as size standard. Individual genotypes at each locus were resolved with GENEMAPPER (Applied Biosystems).

Genotypic frequencies within samples were tested for deviations from Hardy-Weinberg outcrossing expectations within loci and for linkage equilibrium between loci (Chapter 2.4.2.). Amplification errors, such as large allele drop out and stuttering, were assessed in Microchecker (van Oosterhout et al. 2006). Null allele frequencies were estimated in FreeNA (Chapuis & Estoup 2007). Genetic diversity levels were estimated as number of

alleles (N_a), allelic richness (AR), observed and expected heterozygosity (H_O and H_E), and Wright's inbreeding coefficient (F_{IS}) (Chapter 2.4.2). Deviations of allele frequencies between samples from those expected under selectional neutrality were tested using the F_{ST} -outlier method of Beaumont and Nichols (1996), as implemented in LOSITAN (Antao et al. 2008): 2 independent runs were performed (100000 MCMC generations) using the "neutral" mean F_{ST} estimated under the infinite alleles mutation model (IAM) for the complete dataset, and for the Angolan and South African samples separately.

Investigation of current population structure and gene flow within the northern Benguela sub-system employed pairwise comparisons of Weir's (1986) F_{ST} between samples, hierarchical analysis of molecular variance (AMOVA) evaluating the hypothesis of a northern – southern Benguela differentiation, and determination of the number of sub-populations within the total dataset without *a priori* distribution of individuals using the Bayesian approach implemented in STRUCTURE (Pritchard et al. 2000) (Chapter 2.3.2.).

Demographic History

Estimates of effective population size (N_e) were conducted for three critical allele frequencies (0.05, 0.02, and 0.01) for the putative populations identified in the previous section, as implemented in LDN_e (Waples & Do 2008). Confidence intervals for each estimate were assessed using a pairwise jackknife approach.

Recent changes in population effective size, such as demographic contractions due to environmental events or over-exploitation were tested for each identified population under three microsatellite mutation models, as implemented in BOTTLENECK (Piry et al. 1999) (Chapter 2.3.2.).

5.1.3. Results

Mitochondrial DNA analyses

Population structure and phylogeographic patterns

A total of 104 northern (Angola plus Namibia) and 40 southern (South Africa) Benguela *A. aequidens* individuals were amplified for 578bp of mtDNA CR. Amplification and sequencing of northern *A. aequidens* CR retrieved 31 different haplotypes with 20 variable and 15 parsimony informative sites, and in southern *A. aequidens* 19 haplotypes with 20 variable and 14 parsimony informative sites were

observed. No haplotypes were shared between the Angolan and South African populations. The TrN (Tamura & Nei 1993) and HKY models were considered the most suitable nucleotide substitution models for the northern and southern Benguela *A. aequidens*, respectively. Overall for the northern population, significant deviations from sequence variation expectations under neutral evolution were detected with both Tajima's *D* and Fu's *F_S* test, but not with Ewens-Watterson *F* test (Table 5.2). Tajima's *D* and Fu's *F_S* neutrality tests are known to be sensitive to population changes, so observed deviations could be related to demographic events and not selective pressures, particularly since the same result was not observed for the Ewens-Watterson test. Deviations from neutrality were mainly due to the NBE and PIN samples, which exhibited significant results (Table 5.2). Equally, the southern population also exhibited significant deviations from neutral sequence evolution expectations, due to results obtained for the EastC sample. Overall, the northern *A. aequidens* population exhibited high levels of haplotype and nucleotide diversity ($h = 0.8527$ and $\pi = 0.0050$, respectively), with ranges of $h = 0.8053$ to 0.9211 (PIN and LUC) and $\pi = 0.0031$ to 0.0061 (NBE and LUA) (Table 5.2). Despite a smaller sample size, the southern *A. aequidens* population exhibited slightly higher genetic diversity values ($h = 0.900$; $\pi = 0.008$ – Table 5.2).

Table 5.2: Mitochondrial genetic diversity levels and neutrality tests for *A. aequidens* CR: **n** – number of individuals; **H** – number of haplotypes; **h** – haplotype diversity; **π** - nucleotide diversity; **F** – Ewens-Watterson neutrality test; **D** – Tajima neutrality test; **F_S** – Fu neutrality test. Statistically significant results ($p < 0.05$) in bold.

	LUA	BEN	LUC	NBE	PIN	HEN	Overall northern	WestC	EastC	Overall southern
n	20	17	20	20	20	7	104	20	20	40
H	9	9	8	8	11	4	31	10	13	19
h	0.8263	0.8603	0.8053	0.8053	0.9211	0.8095	0.8527	0.8368	0.9316	0.9000
π	0.0061	0.0055	0.0051	0.0031	0.0048	0.0046	0.0050	0.0073	0.0047	0.0080
F	0.880	0.883	0.782	0.782	0.356	0.705	0.997	0.916	0.866	0.969
D	-0.833	-0.643	-0.693	-0.288	-1.420	-0.963	-1.609	-0.463	-0.929	-0.563
F_S	-1.170	-2.118	-0.880	-2.579	-4.321	-0.426	-20.775	-1.401	-3.904	-6.106

Assessment of population structure revealed two deeply divergent populations, comprising samples from the northern (Angola / Namibia) and those from the southern Benguela sub-systems (South Africa) as shown by high, and highly significant, values of pairwise *F_{ST}* (Table 5.3). After Bonferroni correction for multiple tests (Rice 1989), pairwise *F_{ST}* values indicated no significant differentiation among Angolan and Namibian samples, suggesting that the species is composed by one panmictic population in the northern Benguela sub-system. Similarly there was no significant

differentiation indicated between the two South African samples, with F_{ST} (0.031) similar to the range observed between Angolan / Namibian samples (-0.031 to 0.095) (Table 5.3). Testing in AMOVA the hypothesis of a northern-southern Benguela population differentiation, influenced by the Benguela Current oceanographic features, indicated a strong genetic differentiation as the majority of sequence variability was contained between groups (Table 5.4). The hypothesis of a population divergence influenced by the position of the ABF, retrieve significant results for the differentiation among defined groups, however obtained values were smaller than for the northern-southern Benguela differentiation hypothesis (Table 5.4).

Table 5.3: Pairwise F_{ST} values based on mtDNA CR data, between *A. aequidens* samples (see Table 5.1 for sample codes). Values significantly greater than zero ($p < 0.05$) in bold.

	LUA	BEN	LUC	NBE	PIN	HEN	WestC	EastC
LUA	-							
BEN	-0.031	-						
LUC	0.004	-0.014	-					
NBE	0.023	0.003	-0.005	-				
PIN	0.095	0.071	-0.001	0.059	-			
HEN	-0.009	-0.036	0.012	0.025	0.088	-		
WestC	0.879	0.882	0.885	0.903	0.888	0.876	-	
EastC	0.888	0.891	0.894	0.911	0.896	0.889	0.031	-

Table 5.4: Analysis of molecular variance (AMOVA) results based on CR data, for the two population differentiation scenarios tested. Statistically significant results ($p < 0.05$) in bold.

	i) North / South of upwelling	ii) ABF
Among groups	89.945	75.53
Within groups	0.263	12.63
Within populations	9.789	17.54

No geographical association within regions was detected in the reconstructed haplotype networks. Among the northern Benguela cluster, two common haplotypes were observed, represented by individuals from all sampling sites (Figure 5.2). It was not possible to identify the most likely ancestral haplotype, as there were two similarly abundant haplotypes which were equally central in the network. Samples BEN and LUA exhibited the largest number of private haplotypes, supporting a picture of a single mixed population across the region. Haplotypes diverged from the central haplotype by one to seven mutational steps.

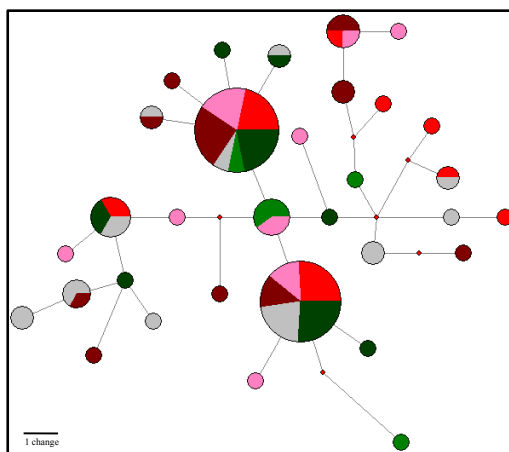


Figure 5.2: Reconstruction of haplotype network for *A. aequidens* across the northern Benguela sub-system, based on 578bp of mtDNA CR sequences: ●: HEN; ●: PIN; ●: NBE; ●: LUC; ●: BEN; ●: LUA. Node sizes are proportional to the number of haplotypes. Red dots correspond to missing haplotypes.

The haplotype network for the southern Benguela cluster (Figure 5.3) was similar to that observed for the northern Benguela cluster, with 3 centrally placed common haplotypes surrounded by a number of more rare haplotypes. There was no obvious geographical association among related haplotypes between the two sample sites.

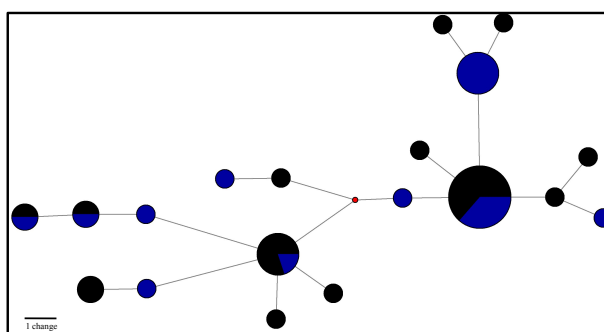


Figure 5.3: Reconstruction of haplotype network for *A. aequidens* across the southern Benguela sub-system, based on 578bp of mtDNA CR sequences: ●: WestC; ●: EastC. Node sizes are proportional to the number of haplotypes. Red dots correspond to missing haplotypes.

Evolutionary History

Reconstruction of the northern *A. aequidens* evolutionary history revealed evidence of past demographic expansion, despite observed high levels of genetic diversity (Table 5.5). The combination between haplotype and nucleotide diversity observed in both *A. aequidens* populations suggests a long and stable evolutionary history (Grant & Bowen 1998). However, both Tajima's D and Fu's F_S detected significant departures from neutrality expectations, and mismatch distribution analyses did not allow rejection of the null hypothesis of demographic expansion (Table 5.5), suggesting the occurrence of past population expansions in both *A. aequidens* populations. Also histograms of nucleotide differences exhibited a clear unimodal pattern (Figure 5.4), commonly

observed in species that have undergone demographic expansions (Harpending 1994). Estimates of time since population expansion gave values of 30.30 KYA and 24.53 KYA for the northern and southern *A. aequidens* populations, respectively (Table 5.5).

Table 5.5: *Atractoscion aequidens* genetic demographic history for northern and southern Benguela sub-system populations, based on mtDNA COI sequence variation: genetic diversity levels (h and π); neutrality tests (Tajima's D and Fu's F_S); mismatch distribution parameters: σ - time since expansion in mutation units, θ_0 - population size before expansion, θ_1 - population size after expansion; and time since expansion (T in KY). Statistical significant results ($p < 0.05$) in bold.

	Northern	Southern
h	0.853	0.900
π	0.005	0.008
D	-1.609	-0.565
F_S	-20.775	-6.106
Mean	2.868	4.653
Variance	4.425	9.082
SSD	0.006	0.008
σ	2.492	5.104
	(0.844-7.590)	(0.256-17.141)
θ_0	1.239	1.374
θ_1	7.317	10.160
T_{exp} (KY)	30.30	24.53
	(6.33-56.99)	(1.22-82.41)

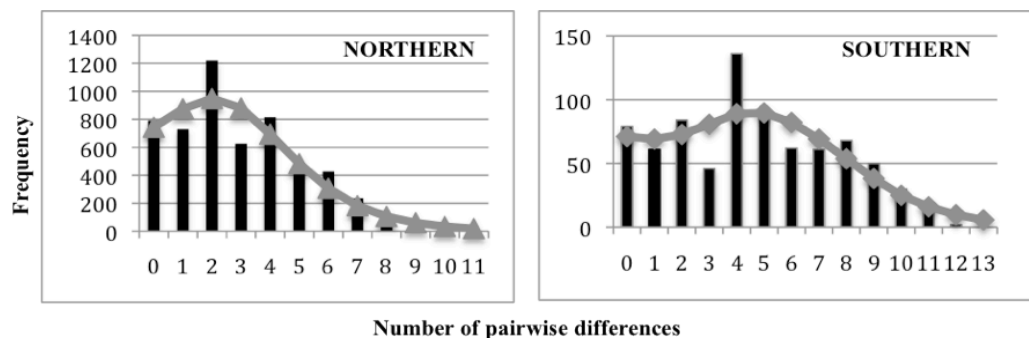


Figure 5.4: Mismatch distribution histograms for northern and southern Benguela sub-system *A. aequidens* populations, based on mtDNA CR sequences. Filled bars indicate the observed frequencies of pairwise mutational differences, grey line indicates the expected distribution under a model of sudden demographic expansion.

Microsatellite Analyses

Population structure and gene flow

A total of 395 individuals, from 6 different localities, were screened for 8 species-specific microsatellite loci (Table 5.6). Since larger sample sizes are required in these markers, to take advantage of their higher statistical power from the greater number of independent alleles present, screening was not possible for Baía Farta (BEN) and Namibia (HEN) samples.

Obtained genotypes did not exhibit evidence of amplification errors, and conformed to Hardy-Weinberg and linkage equilibrium expectations for the majority of loci and

samples (Table 5.6). However, significant deviations to Hardy-Weinberg expectations (F_{IS}) due to heterozygote deficits at particular loci were observed at LUC, NBE and PIN (Geelb32), and at EastC (Geelb29) (Table 5.6). Sample EastC also exhibited significant overall (multi-locus) F_{IS} . As heterozygote deficiency can be due to the presence of null alleles, estimates of null allele frequencies were conducted in FreeNA (Chapter 2.3.2). For LUC, NBE and PIN samples the occurrence of null alleles was estimated at a frequency lower than 5% in the locus reported to depart from Hardy-Weinberg equilibrium, whereas EastC exhibited a high frequency of null alleles in locus Geelb29 (16.02%). Two samples, NBE and PIN exhibited departures to linkage equilibrium between loci Geelb13/Geelb21/Geelb30 and Geelb13/27/5, respectively. However, since there was no consistent pattern across samples or loci, and no evidence of linkage disequilibrium when all Angolan samples were pooled together, such deviations were considered chance associations.

Estimates of departures from neutrality when the complete dataset was used identified two loci under directional selection (Geelb13 and Geelb21) and five loci under balancing selection (Geelb16, Geelb27, Geelb29, Geelb30, Geelb32), under the IAM model. When the analysis was conducted for the northern and southern samples separately, evidence of divergent selection was only detected in the northern group for locus Geelb21.

Levels of nuclear genetic diversity at single loci and across all loci, as assessed by number of alleles (N_a), allelic richness (AR) and expected heterozygosity (H_E), were similarly high across all samples, and were equally high in Angolan and South African populations (Table 5.6).

Table 5.6: Genetic diversity at 8 microsatellite loci in *A. aequidens* samples: **n** – number of individuals genotyped; **Na** – number of alleles; **AR** – allelic richness (minimum of 47 individuals); **H_E** – expected heterozygosity; **H_O** – observed heterozygosity; **F_{IS}** – inbreeding coefficient. Significant deviations to Hardy-Weinberg expectations in bold (corrected $p < 0.001$).

		LUA	LUC	NBE	PIN	WestC	EastC
Geelb5	n	48	70	66	70	70	69
	Na	22	23	26	25	24	25
	AR	21.916	21.684	23.967	22.749	21.839	23.206
	H_E	0.9282	0.9184	0.932	0.928	0.8980	0.9301
	H_O	0.9583	0.9714	0.8939	0.9286	0.9000	0.8551
	F_{IS}	-0.022	-0.051	0.039	0.007	0.005	0.090
Geelb13	n	47	70	68	70	70	70
	Na	7	10	9	8	4	6
	AR	7.000	9.001	8.260	7.626	4.00	5.562
	H_E	0.6747	0.6687	0.6448	0.6798	0.6406	0.6439
	H_O	0.6809	0.6174	0.6912	0.7286	0.6429	0.6143
	F_{IS}	0.002	0.003	-0.065	-0.065	0.004	0.022
Geelb16	n	48	70	67	70	70	70
	Na	20	20	21	20	21	23
	AR	19.937	18.846	19.800	18.722	19.401	20.958
	H_E	0.9271	0.9265	0.9247	0.9289	0.9271	0.9287
	H_O	0.8750	0.9571	0.9552	0.9714	0.8000	0.9429
	F_{IS}	0.067	-0.026	-0.025	-0.039	0.144	-0.007
Geelb21	n	47	70	68	70	70	70
	Na	20	24	21	22	19	21
	AR	20.000	21.960	20.010	19.746	16.887	18.436
	H_E	0.8938	0.8812	0.8824	0.8812	0.9019	0.9103
	H_O	0.8085	0.8429	0.8971	0.8714	0.9286	0.9429
	F_{IS}	0.106	0.051	-0.009	0.018	-0.022	-0.030
Geelb27	n	47	70	68	70	70	70
	Na	20	21	19	22	19	19
	AR	20.000	19.107	18.750	20.059	17.404	17.747
	H_E	0.9269	0.9266	0.9327	0.9279	0.9164	0.9179
	H_O	0.9574	0.9000	0.9118	0.9286	0.9714	0.9571
	F_{IS}	-0.022	0.036	0.030	0.006	-0.053	-0.035
Geelb29	n	48	70	68	70	70	70
	Na	17	18	20	22	39	32
	AR	16.937	16.867	19.006	19.590	34.618	29.066
	H_E	0.9164	0.9185	0.9220	0.9207	0.9601	0.9462
	H_O	0.8958	0.8571	0.8824	0.9143	0.9286	0.6286
	F_{IS}	0.033	0.074	0.050	0.014	0.040	0.339
Geelb30	n	48	69	68	70	70	70
	Na	19	17	20	22	19	21
	AR	18.916	15.921	18.508	19.630	18.038	19.134
	H_E	0.9167	0.9151	0.9199	0.9236	0.9252	0.9233
	H_O	0.8958	0.8986	0.9265	0.8857	0.9000	0.900
	F_{IS}	0.033	0.025	0.000	0.048	0.034	0.019
Geelb32	n	48	70	66	70	69	70
	Na	40	49	43	49	51	49
	AR	39.685	42.176	38.198	42.868	43.989	40.699
	H_E	0.9648	0.9677	0.9654	0.9710	0.9713	0.9649
	H_O	0.8958	0.8571	0.8788	0.8714	0.9710	0.8714
	F_{IS}	0.082	0.121	0.097	0.110	0.008	0.093
Average all loci	n	70	70	66	70	28	58
	Na	21	23	22	24	24	24
	AR	20.549	20.695	20.812	21.374	22.022	21.881
	H_E	0.8936	0.8903	0.8894	0.8951	0.8926	0.8956
	H_O	0.8710	0.8695	0.8796	0.8875	0.8803	0.8390
	F_{IS}	0.036	0.031	0.018	0.016	0.021	0.064

Overall F_{ST} among Angolan *A. aequidens* samples was low and not significantly different from zero ($F_{ST} = 0.0045$, $p < 0.001$). As observed for the mtDNA dataset, no

significant differentiation was observed between any of the Angolan samples, with pairwise comparisons ranging from -0.001 to 0.009 (LUA-LUC and LUA-PIN, respectively) (Table 5.7). Likewise, no significant differentiation was indicated between the two South African samples (Table 5.7). In contrast, as observed with the mtDNA data (Table 5.3), values of F_{ST} between Angolan and South African samples were high (for microsatellites) and significantly different from zero (Table 5.7), indicating substantial differences in allele frequencies between the two populations.

Table 5.7: Pairwise F_{ST} values between *A. aequidens* samples based on 8 microsatellite loci. Values significantly greater than zero (corrected $p < 0.001$) in bold.

	LUA	LUC	NBE	PIN	WestC	EastC
LUA	-					
LUC	-0.001	-				
NBE	0.001	0.000	-			
PIN	0.009	0.008	0.008	-		
WestC	0.056	0.058	0.060	0.052	-	
EastC	0.050	0.052	0.056	0.058	0.003	-

Hierarchical population structure analyses (AMOVA) corroborated the F_{ST} results, as the hypothesis of a northern-southern Benguela population differentiation was supported by a significant percentage of overall variability existing among groups (Table 5.8), whereas no significant degree among group variation existed between northern and southern Angolan samples (0.31%, $p > 0.05$). In both tests, as usually observed for microsatellite data, the majority of sequence variability was contained within rather than between populations (Table 5.8).

Table 5.8: Analysis of molecular variance (AMOVA) results based on 8 microsatellite loci, for the two population differentiation scenarios tested. Statistically significant results ($p < 0.05$) in bold.

	i) North - South Upwelling	ii) ABF
Among groups	5.291	0.31
Within groups	0.426	3.25
Within populations	94.282	96.45

Bayesian analysis of population structure corroborated the previous findings, identifying two distinct genetic clusters: northern population (Angolan individuals) and the southern population (South African individuals) (Figure 5.5). A single genetic cluster ($K = 1$, $\text{LnP(D)} = -14559.68$) was indicated for both the northern and the southern populations as the most likely population structure.

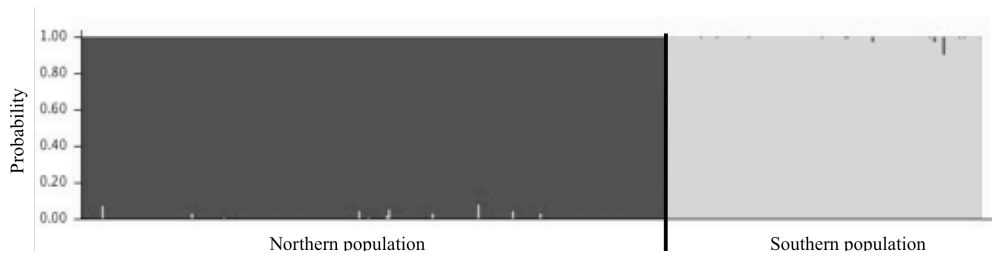


Figure 5.5: Bayesian analysis of individual multi-locus genotype clustering (STRUCTURE) cryptic population structure, and admixture levels for *A. aequidens* across the Benguela Current region.

Demographic history

Based on the retrieved population structure, estimates of effective size (N_e) and bottleneck events were conducted for the two populations identified: northern (Angola) and southern (South Africa) *A. aequidens*. Despite large confidence intervals, assessment of N_e suggests that *A. aequidens* in both regions exhibit large long-term effective population sizes (Table 5.9).

Rejection of the null hypothesis of mutation-drift equilibrium was detected in both *A. aequidens* populations (Table 5.9). In the northern population, evidence of past bottleneck events was only observed under IAM, while in South African *A. aequidens* bottleneck events were indicated under both IAM and TPM. Due to the nature of population bottlenecks, such events may be easier to detect under the IAM model than under a strict SMM mutation model (Piry et al. 1999). Therefore, it is likely that the northern *A. aequidens* population also experienced a recent population decline.

Table 5.9: Demographic history of *A. aequidens* populations in the northern and southern Benguela sub-systems: probability of departure from equilibrium population size (i.e. a bottleneck) and estimates of effective population size (N_e + 95% confidence intervals).

		Northern	Southern
Bottleneck events	IAM	0.004	0.004
	SMM	0.988	0.973
	TPM	0.187	0.008
N_e	0.05	1598.4 (602- ∞)	-189776.2 (544.5- ∞)
	0.02	754.6 (542.7- ∞)	1681.1 (662.8- ∞)
	0.01	1138.1 (797.3- ∞)	2863.7 (1059.3- ∞)

5.1.4. Discussion

Phylogeographic patterns and population structure

The results obtained in the present study revealed a distinct genetic differentiation between *Atractoscion aequidens* occurring in the northern and southern Benguela sub-

systems. In fact, observed levels of genetic differentiation suggest a possible cryptic speciation event (see section 5.2). Both *A. aequidens* populations exhibited high levels of mtDNA genetic diversity ($h = 0.8527$, $\pi = 0.0049$; and $h = 0.9000$, $\pi = 0.0080$, respectively), similar in range to that observed in other sciaenid species (Gold & Richardson 1998; Lankford et al. 1999; Han et al. 2008; Kim et al. 2010), and in particular to that observed in kob species (*Argyrosomus coronus*, *A. inodorus* and *A. japonicus*) occurring across the same geographical region (Klopper 2005; Chapter 4). Equally, genetic diversity revealed by microsatellite analyses was also high (mean $H_E = 0.9005$ in Angola; mean $H_E = 0.8976$ in South Africa), and comparable to other marine fish species (e.g. Gold & Richardson 1998; Gold et al. 2001; Riccioni et al. 2010), including species occurring in the same region such as *Diplodus capensis* (Chapter 3), *A. coronus* and *A. inodorus* (Chapter 4).

The observed significant values of multi-locus F_{IS} in EastC, due to heterozygote deficits, can have multiple causes that are not mutually exclusive: they can be a statistical artefact due to the presence of null alleles, or have a biological basis such as natural selection, non-random mating (inbreeding) or the Wahlund Effect (Beebee & Rowe 2005). Since the microsatellite loci employed in this study were specifically developed for *A. aequidens*, estimates of null allele frequencies were low (average 1.44% across loci and samples), and there was no evidence of significant population differentiation between samples within regions, it is not likely that the presence of null alleles was responsible for the observed deviations to Hardy-Weinberg equilibrium. Natural selection can influence estimates of outcrossing by decreasing the number of heterozygotes in a population, due to different survival success that can occur in early life stages (Andre et al. 2011). When all *A. aequidens* samples were tested for deviations from neutrality assumptions, only locus Geelb5 did not exhibit evidence of being under selection: loci Geelb13 and Geelb21 were identified as being under divergent selection, while remaining loci were identified as being under balancing selection. However, when samples were analyzed separately, only locus Geelb21 in the northern population exhibited significant departures from neutrality. Interestingly, locus Geelb21 was not one of the loci identified with deviations from Hardy-Weinberg equilibrium. Nevertheless, these results suggest that the *A. aequidens* may be under selection, which may have subsequently influenced estimates of heterozygotes. Conversely, the effects of non-random mating, either by inbreeding or by biased reproduction success between individuals, can also result in apparent heterozygote deficits. For example, family groups where only one or two families actively contribute

to the next generation can skew allelic frequencies, leading to inbreeding depression (Zarraonaindia et al. 2009). Another possible cause for inbreeding depression may be the presence of a small ratio between effective population size and census size (N_e / N). Although most marine species are thought to exhibit large populations, the effective population size can be three to four times smaller than the census size (Hauser et al. 2002). Low effective population sizes, combined with overexploitation can make some marine species more vulnerable to inbreeding depression (Hoarau et al. 2005). Although the N_e / N ratio for the two *A. aequidens* populations is not known, the southern population is considered to be depleted due to intense commercial fishing over the last few decades (FAO, 2005b). As such, at the moment it is not possible to discard the possibility that observed heterozygote deficits may be linked to inbreeding depression in *A. aequidens*. Finally, the Wahlund Effect (Sinnock 1975) consists of an apparent departure from indications of panmixia, either by significant deviations from Hardy-Weinberg equilibrium or linkage equilibrium, due to the presence of a mixed sample of individuals from two separate and genetically differentiated populations (e.g. Ward et al. 2007). The Wahlund Effect is thought to be fairly common in marine species, particularly in those who exhibit local recruitment and high dispersal potential (Ward et al. 2007; Gonzalez et al. 2008), such as the western Atlantic sciaenid *Cynoscion nebulosus* (Ward et al. 2007), and the European white seabream *Diplodus sargus* (Lenfant 2002; Gonzalez-Wanguemert et al. 2007; Gonzalez-Wanguemert et al. 2010). However, as there is no evidence for genetically differentiated sub-populations within the northern or southern populations of *A. aequidens* it is unlikely that the Wahlund Effect is responsible for the departures to Hardy-Weinberg or linkage equilibrium observed in just one or two samples within each regional population.

Another possible explanation, and probably the most parsimonious one, is related to statistical significance of multiple tests. In any given statistical test there is a probability of 5 in 100 to reject the null hypothesis merely due to chance. These results are considered to be false positives (type I error), and it is likely that observed deviations from Hardy-Weinberg equilibrium were a statistical artefact due to multiple tests.

Significant genetic differentiation was observed between samples of *A. aequidens* from the northern and southern Benguela sub-systems, when assessed using both mtDNA and nuclear DNA markers. Haplotype networks did not reveal any shared haplotypes between the two populations, and F_{ST} values for both mtDNA and nDNA were high and significantly greater than zero, rejecting the null hypothesis of panmixia throughout the Benguela Current region. Observed F_{ST} values for pairwise comparisons between

northern and southern *A. aequidens* samples (average mtDNA $F_{ST} = 0.890$, average nDNA $F_{ST} = 0.055$) were much higher than those reported for other widespread marine fish species such as *Thunnus thynnus* (mtDNA $F_{ST} = 0.023$; nDNA $F_{ST} = 0.002$ - Carlsson et al. 2004), *Thunnus obesus* (nDNA $F_{ST} = 0.000$ to 0.003 - Gonzalez et al. 2008), *Coryphaena hippurus* (mtDNA $F_{ST} = 0.000$ to 0.571 - Diaz-Jaimes et al. 2010), and other sciaenid species such as *Micropogonias undulatus* (mtDNA $F_{ST} = 0.046$ - Lankford et al. 1999) and *Sciaenops ocellatus* (mtDNA $F_{ST} = 0.057$ - Gold & Richardson 1991).

No significant genetic differentiation was observed between sampling sites within either the northern or southern Benguela *A. aequidens* populations, when assessed using mtDNA or nuclear microsatellite DNA markers. These results suggest that populations of *A. aequidens* in the northern (Angola / Namibia) and southern (South Africa) Benguela sub-systems each consist of single panmictic populations over large geographical areas. Although the number of sampling sites was limited within South Africa, the genetic results presented here support the previous description of South African *A. aequidens* as consisting of one migratory stock throughout the distribution (Griffiths & Hecht 1995).

Oceanographic features such as currents, fronts and eddies can influence gene flow and connectivity among adjacent populations by disrupting larval and/or adult dispersal (Grant & Bowen 1998; Riginos & Nachman 2001; Evans et al. 2004; Hemmer-Hansen et al. 2007; Galarza et al. 2009; Gonzalez-Wanguemert et al. 2010; White et al. 2010). The observed genetic differentiation between northern and southern *A. aequidens* populations appears to coincide with the major oceanographic features of the Benguela Current system, such as the perennial upwelling cell off central Namibia, low sea surface temperatures off southern Namibia and western South Africa, and a narrow continental shelf throughout Namibia (Hutchings et al. 2009). Upwelling cells can induce local larval retention on either side by disrupting longshore transport (Lett et al. 2007) and driving pelagic eggs and larvae offshore where the environment is unsuitable for survival and/ or recruitment, thus allowing population divergence. The perennial upwelling cell off central Namibia can be disrupting gene flow between *A. aequidens* populations. Similar findings have been documented in other marine species occurring in upwelling regions (*Patiriella regularis* - Waters & Roy 2004). In addition, the genetic differentiation observed in *A. aequidens* coincides with the described distribution break that appears to be linked with the colder water temperatures observed off southern Namibia and western South Africa (Griffiths & Hecht 1995). Although

genetic divergence between northern and southern *A. aequidens* populations was substantial, no differentiation was observed within either population despite the presence of spatially heterogeneous environmental conditions in both the northern and southern Benguela sub-systems. The influence of oceanographic features in shaping population sub-structuring will depend on the species life history features (Galarza et al. 2009). Despite being genetically divergent, both *A. aequidens* populations exhibit similar life history features such as protracted spawning seasons and the production of pelagic eggs and larvae (W. Potts personal communication), which may encourage dispersal and survival in temporally and spatially unstable environments. Furthermore, the northern population of *A. aequidens* appears to be continuously distributed throughout Angola (W. Potts, personal communication), and the southern population has only one known spawning site located off the coast of KwaZulu-Natal (Griffiths & Hecht 1995). These reproductive strategies can be predicted to homogenize genetic population sub-structuring of both *A. aequidens* in the northern and in the southern Benguela regions.

Evolutionary history

A number of analyses of the mtDNA dataset all revealed evidence of historical population demographic expansions: star-shaped haplotype networks (Avice 2000); departures from neutral expectations in Tajima's D (Tajima 1989) and Fu's F_S (Fu 1997) statistics; and sequence mismatch distributions (Harpending 1994). Although high haplotype and nucleotide diversity in both *A. aequidens* populations suggest a long and stable evolutionary history (Grant & Bowen 1998), estimates of female effective population size at the time of the last expansion (θ_0) were relatively small, suggesting that demographic expansion occurred from a reduced number of females (Excoffier et al. 2005). The microsatellite dataset also revealed evidence for recent bottlenecks in population size in both the northern and southern Benguela populations.

Estimates of time since expansion should always be regarded with caution, especially when a universal molecular clock is used for calibration, since divergence rates may vary from species to species due to different growth rates and generation times (Avice 2000). However, the use of an inferred divergence rate of 3.6% sequence divergence per MY for the marine fish mtDNA Control Region appears to be a fairly conservative approach (Donaldson & Wilson 1999; but see von der Heyden et al. 2010). Using a molecular clock calibrated at 3.6% per MY, and estimating generation time at 2.2 and 5 years for the Angolan and South African populations respectively, expansions in both

Angolan and South African *A. aequidens* populations appear to date to around 30-25 KYA, towards the end of the Pleistocene.

The Benguela Cold Current is one of the oldest upwelling systems in the world (Shannon 1985): based on paleoproductivity peaks the system is thought to have originated in the mid-Miocene (10 MYA, Krammer et al. 2006), and evolved to its present day features during the Pliocene-Pleistocene transition (2 MYA, Marlow et al. 2000). The Pliocene-Pleistocene transition was characterized by a generalized cooling, followed by strengthening of upwelling intensity (Marlow et al. 2000). During the second half of the Pleistocene, the Benguela system entered a highly unstable mode, with multiple changes in sea surface temperature, sea levels and paleoproductivity due to worldwide climate-induced changes (Jahn et al. 2003). Changes in productivity affect recruitment levels of small pelagics such as sardines and anchovies, which in turn would have had a severe impact on piscivorous species such as *A. aequidens* (Mueter et al. 2007). A severe population crash was reported for sardines and anchovies in the Benguela Current region between 41-25 KYA, coincident with a productivity crash in the region (Jahn et al. 2003; Grant & Bowen 2006). This reduction in small pelagic fish populations is thought to have greatly influenced demographic history of Cape Hake, another demersal piscivore species in the southern Benguela sub-system (von der Heyden et al. 2010). Additionally, cyclic glacial events during the late-Pleistocene resulted in changes in sea level in the Benguela region. Such regressions reached up to 120m below present sea levels (Ramsay & Cooper 2002), which combined with the narrow continental shelf in the Benguela region could have severely reduced the number and size of suitable local habitats (von der Heyden et al. 2010), in particular for benthopelagic species such as *A. aequidens*. A number of marine species across the Benguela Current region show evidence of past population expansions dating from the end of the Pleistocene (Gopal et al. 2006; Matthee et al. 2007; von der Heyden et al. 2007; von der Heyden et al. 2010). Therefore, climate-induced changes in productivity in lower trophic levels, and in size and distributions of habitats may have had a synergistic effect, leading to severe population crashes in *A. aequidens* populations across the Benguela region in the (geologically) recent past.

Despite the evidence for past population size bottlenecks and subsequent expansions, estimates of present day (and recent historical) effective population size from the microsatellite data were relatively high, ranging from 754 to 1598 individuals in northern *A. aequidens* and >1681 individuals in the southern *A. aequidens* populations.

These values of N_e are very similar to the ones observed for *Argyrosomus coronus* (Chapter 4.3.), and are within the documented range for marine species (100s-1000s Hauser & Carvalho 2008). For conservation purposes Frankham et al. (2002) suggested a minimum threshold of $N_e = 500$, which is far below the retrieved northern and southern *A. aequidens* effective population sizes, suggesting that despite the possibility of a recent population contraction the species may still be in a healthy state at least in terms of genetic diversity.

Implications for fisheries and conservation

Results in the present study suggest that *A. aequidens* exhibits two genetically divergent populations occupying the northern and southern sub-systems of the Benguela Current region, and indicate no effective gene flow between the two areas. The absence of shared haplotypes suggests complete lineage sorting and reciprocal monophyly, and consequently both *A. aequidens* populations should be managed independently as Evolutionary Significant Units (ESU *sensu* Moritz 1994).

The northern and southern Benguela *A. aequidens* populations exhibit high genetic diversity levels, although it is not possible at the moment to discard the hypothesis of a recent population contraction, which may represent the first signs of over-exploitation. The retrieved population structure may account for the observed diversity levels, as both populations appear to be composed of single panmictic demes across their respective distributions. However, there are no limitations to captures of *A. aequidens* by inshore artisanal and subsistence fisheries throughout Angola at the moment, which may lead to over-exploitation of the resource, as has happened for the South African population (FAO 2005b). In order to ensure the maintenance of Angolan *A. aequidens* genetic diversity levels and evolutionary potential it is necessary that future harvesting plans should limit the daily amount of captured fish, while establishing a no-take season corresponding to the species spawning season.

Implications of climate change

Climate change is possibly one of the major threats for marine species today (Briggs 2011; Dawson et al. 2011), especially if occurring in highly unstable environments such as the Benguela Current. How a species will react to climate-induced changes will depend on factors such as growth rate, generation time and dispersal abilities (Briggs 2011; Dawson et al. 2011; Lo Brutto et al. 2011). Consequently, it is not easy to make predictions. Nevertheless, the distribution and level of present-day genetic diversity

levels often reflect historical processes, knowledge of which can be used as valuable clues to the likely course of future environmentally-driven population genetic changes (Lo Brutto et al. 2011). In both the northern and the southern *A. aequidens* populations, the present work uncovered evidence of past population contractions that appear to coincide with climate-induced fluctuations in the Benguela Current. Although *A. aequidens* should not be considered a cold-water species, it is also not a tropical species (Griffiths & Hecht 1995; Heemstra & Heemstra 2004). Therefore, the warmer currents occurring along the northern and southern boundaries of the Benguela Current could limit dispersion across and out of the region, in the case of abrupt sea temperature changes, as observed in the past for other fish species (Grant & Bowen 2006). Such a scenario could lead to severe population crashes and, eventually, local extinctions. Furthermore, climate-induced changes have the potential to affect productivity levels, which will have repercussions throughout the trophic web, as appears to have happened in the past in this region (Marlow et al. 2000; Jahn et al. 2003). Therefore, although large-bodied fish species such as *A. aequidens* are thought to be more resilient to climate change when compared with small pelagics such as sardines (Lo Brutto et al. 2011), the present study suggests that *A. aequidens* can still be severely affected, and that the impact of climate change will greatly depend on a species' life history features.

5.2. Marine population evolution across the Benguela Current system: molecular evidence for allopatric speciation in a Sciaenid fish, *Atractoscion aequidens* (Cuvier 1830)

5.2.1. Introduction

Allopatry is considered to be the most common speciation process in marine organisms, particularly within the Atlantic Ocean basin (Palumbi 1992; Floeter et al. 2008). The isolation of populations by the closure of the Isthmus of Panama, the output of freshwater from the Orinoco and Amazon rivers, and the establishment of the Benguela Current are considered to be major vicariant events responsible for the formation of numerous new species in the Atlantic (Floeter et al. 2008). In particular, the establishment of the Benguela Current system off southwestern Africa is postulated to have led to the isolation of a number of marine taxa between the Atlantic and Indo-Pacific Oceans (Lessios et al. 1999; McCartney et al. 2000; Bowen et al. 2001; Colborn et al. 2001; Lessios et al. 2001; Grant & Bowen 2006; Floeter et al. 2008).

The Benguela Current is one of the oldest and most productive upwelling systems in the world (Shannon 1985; Diester-Haass et al. 1988; Krammer et al. 2006). With its present day features fully established by 2 MYA, the Benguela Current is characterized by several coastal upwelling cells throughout its range, the largest located off Lüderitz in central Namibia (Shannon 1985; Fennel 1999; Marlow et al. 2000; Shillington et al. 2004; Hutchings et al. 2009). This cell is maintained throughout the year and marks an oceanographic break-point in the system, dividing it into the northern and southern Benguela sub-systems (Shillington et al. 2004). Oceanographic features such as the Lüderitz upwelling cell limit the dispersal of coastal species (Hemmer-Hansen et al. 2007; Lett et al. 2007; Galarza et al. 2009), potentially constraining gene flow, inducing population differentiation and speciation (Waters & Roy 2004; Zardi et al. 2007). For example, two large Sciaenid fish (*Argyrosomus japonicus* and *Argyrosomus coronus*) have disjunct distributions associated with the southern and northern Benguela sub-systems, respectively, but have similar life history (Griffiths & Hecht 1995, Potts et al. 2010) and molecular genetic characteristics (see Chapter 4.1.). These characteristics suggest that in the past these two species were a single species distributed across the whole region, but subsequently became split into two allopatric populations by the coastal cold water intrusion during the formation of the Benguela Current. Therefore the

oceanographic features of the Benguela Current may represent strong vicariant barriers to population connectivity of local fish species. It is important to understand how and why oceanographic barriers to population connectivity affect evolution and speciation (i.e. distribution of genetic biodiversity) as future climate change may have a severe impact on the strength or persistence of these barriers.

Atractoscion aequidens (Cuvier, 1830) is a coastal species belonging to the Sciaenidae family (Sasaki 1989). It has a widespread but disjunct distribution, with populations occurring on the east coast of Australia and on the south and west coast of Africa (Sasaki 1989; Heemstra & Heemstra 2004). Within the African distribution, the species is commonly found on the south and east coast of South Africa (Benguela southern frontal zone), uncommon on the west coast of South Africa and Namibia, common in Angola (Benguela northern frontal zone), and occasionally found along northwestern African coast (Griffiths & Hecht 1995; Heemstra & Heemstra 2004). The reduced abundance on the coasts of western South Africa and Namibia is thought to be related to the oceanographic features of the Benguela Current such as low sea surface temperatures and deep anoxic waters, and physical features of the region, namely a narrow continental shelf (Griffiths & Hecht 1995). In South Africa, *A. aequidens* undertakes seasonal longshore reproductive migrations and inshore-offshore feeding migrations, both thought to be related to availability of prey (*Sardinops sagax*) and sea surface temperature (Griffiths & Hecht 1995). Such life history features are characteristic of migratory fish species, with large size and late age at maturity (Roff 1988). In contrast, there is no published information on the biology or life history of this species in the northern Benguela sub-system.

Results obtained in the previous section suggest that in the Benguela Current region *A. aequidens* comprises two highly divergent populations, with no apparent gene flow between the two (see section 5.1). Therefore, the present section aims to: *i*) reconstruct phylogenetic relationships of *A. aequidens* within the Benguela Current region; *ii*) compare obtained results with levels of genetic divergence among other Sciaenid fish species distributed across the same geographical area; and *iii*) investigate the repercussions of the physical distribution break in the species population structure, relating them with historical changes in oceanographic features of the Benguela Current.

5.2.2. Methods

Sampling and DNA extraction

Phylogenetic analyses were conducted for a total of 35 *A. aequidens* individuals, collected from 5 coastal localities in Angola and 2 in South Africa (Table 5.8). Four individuals were also collected from a commercial vessel off the Namibian coast. In order to compare genetic divergence levels within and between *A. aequidens* from the northern and southern Benguela sub-systems with other similar taxa across the region, four other sciaenid species were sampled: *Argyrosomus coronus* Griffiths and Heemstra 1995 that occurs in southern Angola, *A. inodorus* Griffiths and Heemstra 1995 that occurs in South Africa and northern Namibia, *A. japonicus* (Temminck and Schlegel 1843) that occurs in South Africa (and Australia), and the European *A. regius* (Asso 1801) that was used as an outgroup comparison for the Benguela region kob species (Table 5.10). Phylogenetic relationships were reconstructed using three individuals from each species, as described in Chapter 4.1. Additionally, DNA sequences from the more distantly related (western Atlantic) sciaenid *Cynoscion nebulosus* available on GenBank were used for outgroup rooting in all phylogenetic analyses, in order to understand the direction of evolution in these species.

Table 5.10: Sampling strategy for *A. aequidens* phylogenetic study: sampling locations, sample code, sample size and latitude/longitude coordinates.

Species	Country	Region	Code	Sample size	Coordinates
<i>A. aequidens</i>	Angola	Luanda	GA	5	8°47.263'S 13°14.32'E
		Baia Farta		5	12°35.516'S 13°13.59'E
		Lucira		5	13°50.635'S 12°27.16'E
		Namibe		5	15°10.374'S 12°04.86'E
		Pinda		5	15°43.414'S 11°53.65'E
	Namibia	offshore	GN	4	-
South Africa	Port Alfred	GSA	5	33°36.50'S 26° 54.00'E	
	Arniston		5	34°40.00'S 20° 14.00'E	
<i>A. regius</i>	Portugal	Quarteira	KP	3	37°3.346'N 8°6.43'W
<i>A. coronus</i>	Angola	Flamingo	KA	2	15°10.374'S 12°04.86'E
		Cunene		1	17°15.207'S 11°45.13'E
<i>A. inodorus</i>	Namibia	Henties Bay	KN	2	22°7.404'S 14°16.139'E
	South Africa	Port Alfred		1	33°36.500'S 26° 54.00'E
<i>A. japonicus</i>	South Africa	Algoa Bay	KSA	3	33° 49.53'S 25°52.31'E

Genetic screening

All specimens were Polymerase Chain Reaction (PCR) amplified and sequenced for 3 mtDNA regions (Control Region, cytochrome c oxidase I and cytochrome b) and one nuclear DNA region (1st intron of the S7 ribosomal gene), as described in Chapter 2.2.2.

Sequencing was performed for both forward and reverse directions using an ABI 3730 sequencer (Macrogen, Korea), with the same primers used in PCR amplification. Obtained sequences were aligned and manually inspected using Sequencher (GeneCode Corporation).

Alignment of *A. aequidens* and *Argyrosomus* spp. sequences was unambiguous for all mtDNA loci. However, alignment of S7 1st intron sequences proved to be difficult due to the presence of a variable length microsatellite region around 280bp into the sequence in all *A. aequidens* samples. Due to the presence of the microsatellite insertion, it was not possible to sequence the complete S7 fragment for the *A. aequidens* individuals, making it difficult to obtain an accurate sequence alignment between the two genera for this region. Therefore, *A. aequidens* and *Argyrosomus* spp. were analyzed separately for the nDNA and concatenated mtDNA-nDNA datasets. Heterozygous base positions (defined as two clear, nearly equal sized peaks at the same position) were observed in S7 sequences at a frequency of 5.65% for the northern Benguela *A. aequidens*, but at a lower frequency for both the southern Benguela *A. aequidens* (0.33%) and *Argyrosomus* samples (average 1%). Haplotypes were statistically resolved using PHASE 2.1.1 (Stephens et al. 2001), and to decrease computational time only the most common ones (at frequencies > 1%) were used in phylogenetic reconstructions.

Phylogenetic analyses of evolutionary history

Phylogenetic analyses of *A. aequidens* and *Argyrosomus* spp. datasets were conducted on concatenated mtDNA data, the full concatenated mtDNA plus nDNA data and on nDNA data alone (for each genus separately where nDNA involved – see above). All alignments were tested for heterogeneity of base composition using the χ^2 test, as implemented in PAUP (Swofford 1993). To ensure that all loci could be grouped together, both datasets were tested for incongruent length differences (ILD), as implemented in PAUP (Swofford 1993). The ILD-test was performed using a Tree-Branch-Recombination swapping method, for 1000 replicates, and saving 2 trees in each step. Retrieval of the most appropriate nucleotide substitution model was performed in jModelTest (Posada 2008). The most probable substitution model was chosen based on the Bayesian Information Criterion (BIC), and used in further analyses. Two different approaches were employed in the reconstruction of phylogenetic relationships. First, for the Maximum Likelihood (ML) method implemented in PhyML (Guindon et al. 2009), all analyses were conducted using a variant of the Neighbour-

Joining starting tree (BIONJ), run using the aLRT method, with branch support assessed with a χ^2 test as recommended by the authors (Anisimova & Gascuel 2006). Second, a Bayesian approach was used as implemented in MrBayes (Huelsenbeck & Ronquist 2001; Ronquist & Huelsenbeck 2003), with the mtDNA dataset partitioned into the three amplified mtDNA regions, and evolutionary rate and branch lengths allowed to vary independently across partitions. Two independent sets of four chains were run for 2 million MCMC generations, with parameters recorded every 100th generations. Convergence and stationarity of runs were estimated by examination of likelihood plots using Tracer 1.4. (Rambaut & Drummond 2007), and the standard deviation of split frequencies (Stdev<0.01 – Hall 2008). A consensus tree was obtained after a burn-in period of 2500 generations, using TreeAnnotator 1.6.1 (Drummond & Rambaut 2007). Reconstruction of ML and Bayesian trees were conducted in FigTree 1.3.1 (Rambaut 2009).

Genetic population differentiation and gene flow

Allopatric speciation events are characterized by disruption of gene flow between adjacent populations, which results in population isolation and subsequent differentiation. As suggested by Avise et al. (1998) population differentiation was calculated as:

(pairwise sequence differences between groups A and B) – 0.5 x (pairwise sequence differences within group A + group B).

Pairwise differences were calculated using the most appropriate substitution model, in MEGA 4.1 (Kumar et al. 2008). Wright's pairwise F_{ST} between samples was used as a proxy for genetic differentiation to detect gene flow between samples from the northern and southern Benguela sub-systems. Under an island model of gene flow, F_{ST} values are directly proportional to the number of migrants exchanged between populations, and can be expressed as $F_{ST} = 1/2 \times (N_{em} + 1)$, where N_e = effective population size and m = number of migrants (Excoffier et al. 2005). However, the assumptions underlying the island model (e.g. an infinite number of populations, of equal size, each giving and receiving the same fractions of migrants each generation), might not be met in natural populations, and the estimation of gene flow according to Wright's F_{ST} should not be taken as an exact value. Thus, this estimate was used as a proxy for the magnitude of differences between species, and not considered a precise measure of genetic migration (Kelly & Eernisse 2007).

Time since divergence

Testing using Mega 4.1 (Kumar et al. 2008) indicated that the mtDNA sequence data were consistent with expectations for consistency of evolutionary rates under a maximum likelihood molecular clock, so a strict molecular clock was enforced for estimation of time since divergence between sequences and taxa. Time since most recent common ancestor (t_{mrca}) was estimated using BEAST 1.6.1 (Drummond & Rambaut 2007), with data partitioned into the three mtDNA regions, with substitution and clock models unlinked among partitions. Runs were performed under a Yule speciation process for branching rates, using the HKY + gamma model of nucleotide substitution for the CR and cytb data sets, and TRN + gamma model for the COI data set. Two independent analyses were run for 10 million generations and logged every 1000 steps. Independent runs were combined using LogCombiner 1.6.1 (Drummond & Rambaut 2007), and convergence was estimated in Tracer 1.6 (Rambaut & Drummond 2007). Due to the absence of a fossil record for *A. aequidens* and *Argyrosomus* spp. in the Benguela Current region, calibration of the molecular clock for estimating t_{mrca} was performed using two different approaches: i) fixing the substitution rate for the COI dataset (1.5% per MY – Bermingham et al. 1997), with remaining substitution rates estimated based on the COI rate; and ii) employing the timing of intensification of the upwelling system in the Benguela Current (~2 MYA) as an internal node calibrator for the divergence of *Argyrosomus coronus* and *A. japonicus* in the region, as described in Chapter 4.1. A normal distribution was applied around the point calibration with broad standard deviations (SD) to allow for uncertainty in the estimates (Drummond et al. 2006). Performance of each approach was compared based on the likelihood of the posterior probabilities of each model (Drummond & Rambaut 2007). Convergence of run parameters for the most likely approach was estimated based on ESS>200, in Tracer 1.4 (Rambaut 2007). Divergence times were calculated from the post burn-in results, and TreeAnnotator 1.3.1 (Drummond & Rambaut 2007) was used to compose a maximum-clade-credibility tree, visualized in FigTree 1.3.1 (Rambaut 2009).

5.2.3. Results

Phylogenetic analyses of evolutionary history

Concatenation of the three mtDNA regions sequenced for *A. aequidens* and *Argyrosomus* spp. samples resulted in a dataset consisting of 1878 aligned base pairs (bp), displaying 348 variable sites and 327 parsimony informative sites (excluding *C.*

nebulosus). Of the 327 parsimony informative sites, 71 represented fixed differences between two distinct *A. aequidens* clades. Due to an insertion consisting of a repetitive stretch of DNA in the S7 1st intron in *A. aequidens* (see above), reliable sequencing was only possible for the first 302bp of this region. Of these 302bp, 157 were variable and 118 parsimony informative. Although sequencing of the S7 1st intron in all *Argyrosomus* species was straightforward, yielding a 463bp fragment, with 73 variable and 14 parsimony informative sites, the region sequenced overlapped that sequenced in *A. aequidens* sequence by only 40bp. Therefore, due to the inability to obtain an accurate alignment, nDNA datasets were analyzed independently for the two genera.

No departure from homogeneity of base frequencies was detected for any dataset ($\chi^2=17.263$ $p>0.05$ for mtDNA; $\chi^2=1.677$ $p>0.05$ for mtDNA-nDNA; $\chi^2=10.652$ $p>0.05$ for nDNA), suggesting equal nucleotide frequencies among samples. The ILD test indicated that the three mtDNA regions could be concatenated into a single sequence ($p>0.05$), whereas the mtDNA-nDNA dataset could not be concatenated ($p<0.05$). Consequently, in subsequent analyses the mtDNA-nDNA dataset was partitioned, allowing estimation of different rates and branch lengths in each run. The most suitable model of nucleotide substitution retrieved for both mtDNA and mtDNA-nDNA datasets was Tamura-Nei, with heterogeneous rates among lineages ($\gamma = 0.121$ and 0.111 , respectively). For the nDNA data alone, the nucleotide substitution model varied with the dataset analyzed: for *A. aequidens* the best model was Jukes-Cantor, with heterogeneous rates among lineages ($\gamma = 0.210$), while for the *Argyrosomus* spp dataset the best model was Felsenstein81.

Both Maximum Likelihood and Bayesian phylogenetic analyses of the three datasets produced highly resolved phylogenies with identical topologies and robust branch support (Figures 5.6 - 5.9). Concatenated mtDNA and mtDNA-nDNA datasets, as well as nDNA alone, supported a reciprocally monophyletic division between two clades of *A. aequidens* samples corresponding to northern and southern Benguela (i.e. Angolan / Namibian and South African) populations, and reciprocally monophyletic divergence between all of the *Argyrosomus* spp. (as detailed in Chapter 4.1).

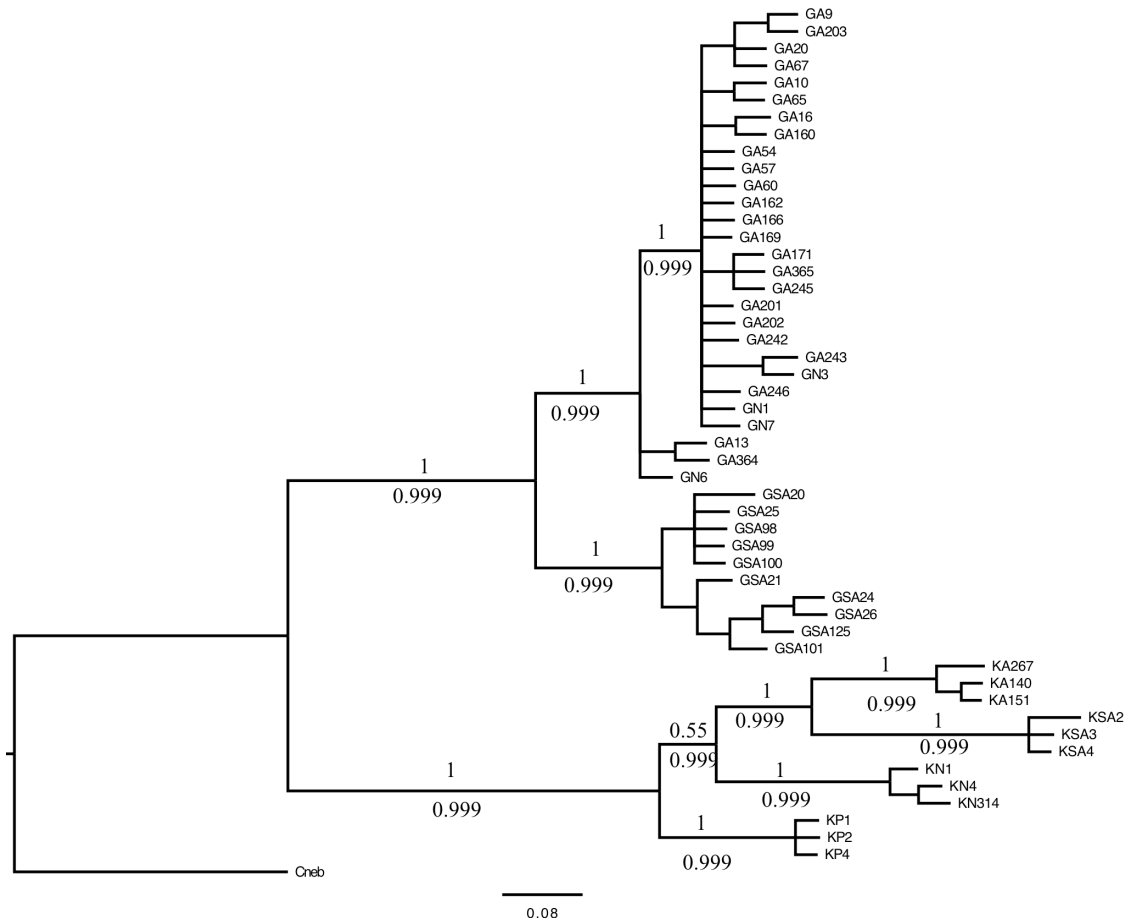


Figure 5.6: Reconstruction of phylogenetic relationships within *A. aequidens* (GA + GN – northern; GSA – southern Benguela sub-systems) and among *Argyrosomus* species (see Table 5.10 for species codes) from the Benguela region and *Argyrosomus regius* (KP) from Europe, using concatenated mtDNA (CR+COI=cytb) data. Statistical support for nodes is given for both Bayesian (posterior probabilities above branches) and ML analyses (aRLT values below branches). Outgroup: *Cneb* (*C. nebulosus*).

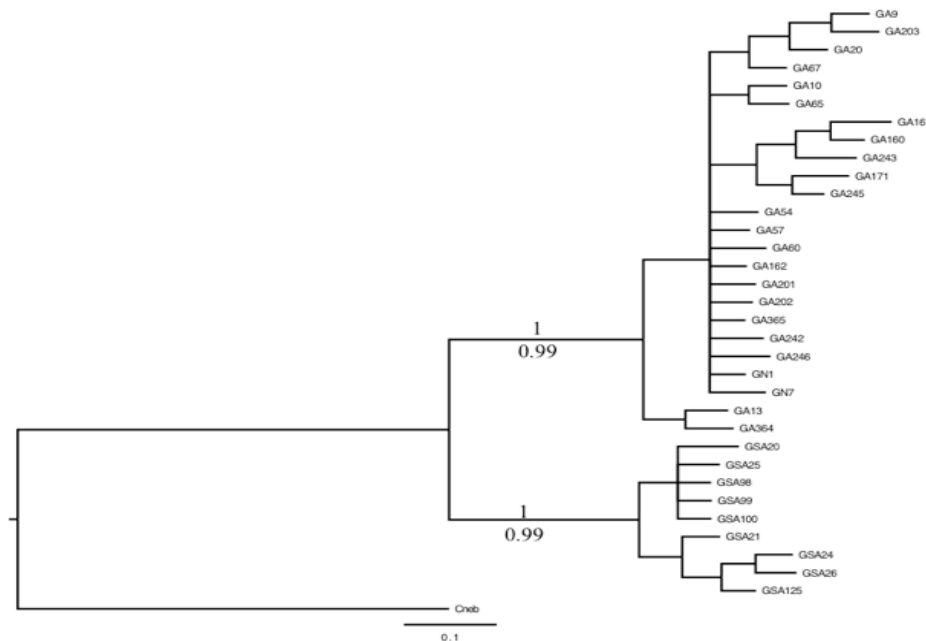


Figure 5.7: Reconstruction of phylogenetic relationships within *A. aequidens* (GA + GN – northern; GSA – southern Benguela sub-systems), using mtDNA-nDNA dataset. Statistical support for nodes is given for both Bayesian (posterior probabilities above branches) and ML analyses (aRLT values below branches). Outgroup: *Cneb* (*C. nebulosus*).

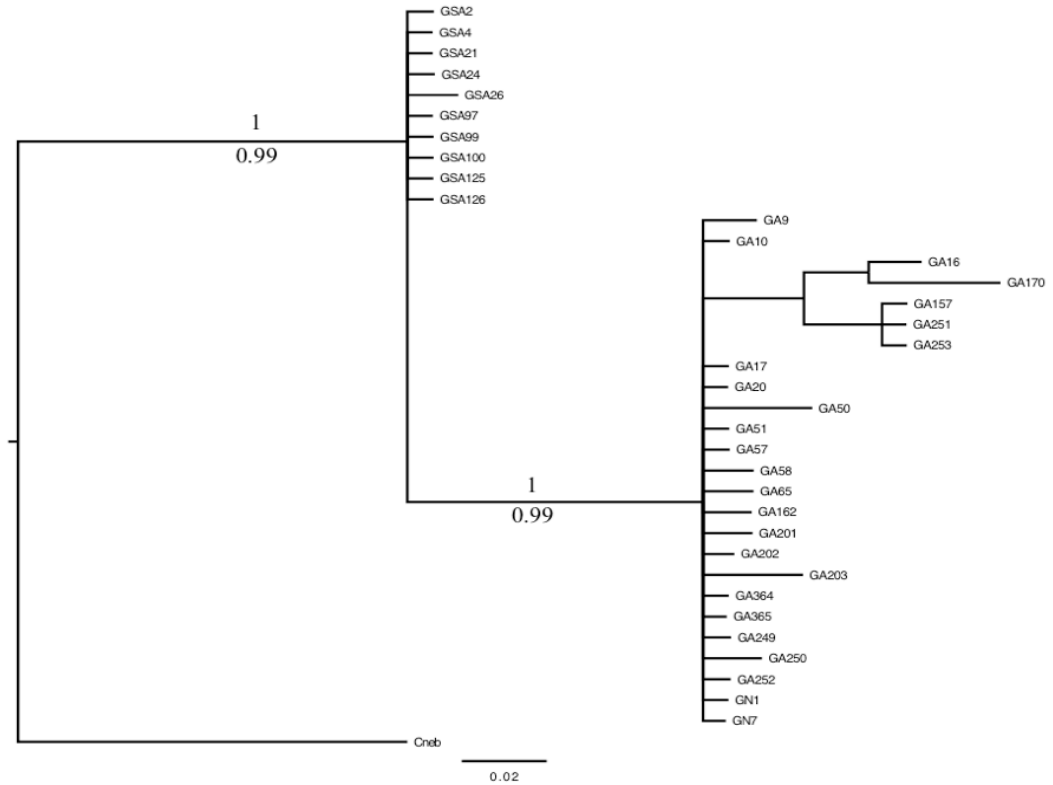


Figure 5.8: Reconstruction of phylogenetic relationships within *A. aequidens* (GA + GN – northern; GSA – southern Benguela sub-systems) using nDNA. Statistical support for nodes is given for both Bayesian (posterior probabilities above branches) and ML analyses (aRtL values below branches). Outgroup: Cneb (*C. nebulosus*).

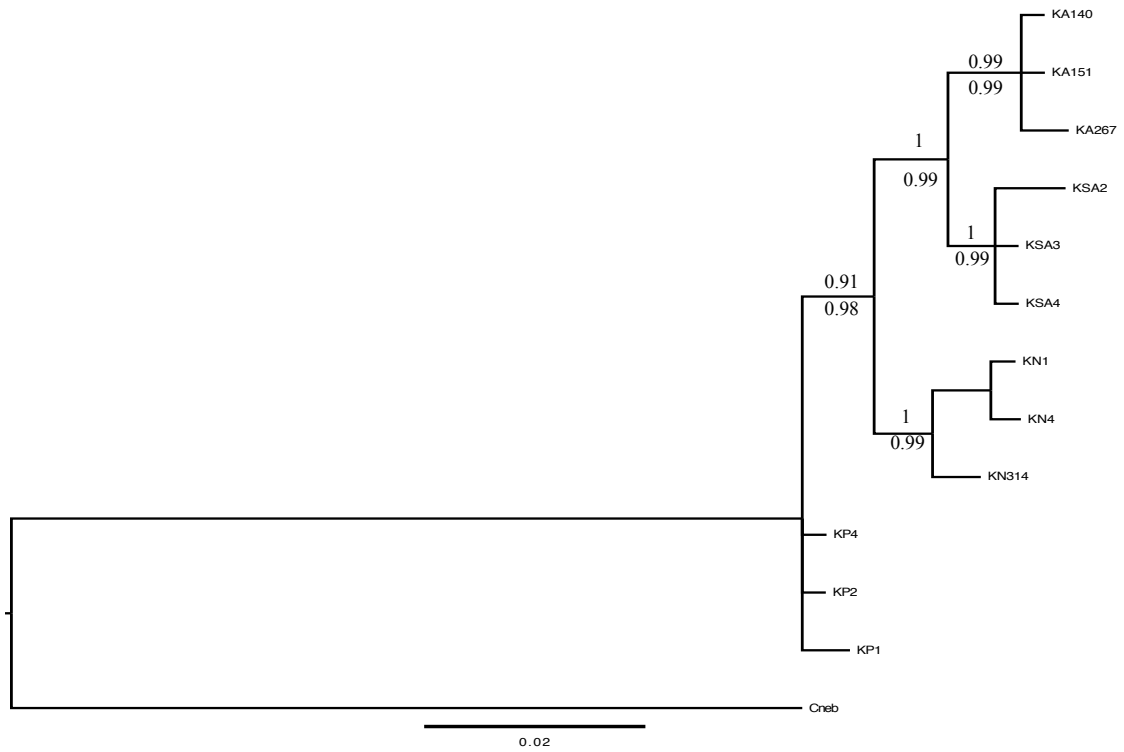


Figure 5.9: Reconstruction of phylogenetic relationships among *Argyrosomus* species from the Benguela region, and *Argyrosomus regius* (KP) from Europe (see Table 5.10 for species codes), using nDNA data. Statistical support for nodes is given for both Bayesian (posterior probabilities above branches) and ML analyses (aRtL values below branches). Outgroup: Cneb (*C. nebulosus*).

Although the datasets containing nDNA sequences had to be analyzed separately, it is possible to observe that retrieved branch lengths between the two *A. aequidens* clades and between *A. coronus* and *A. japonicus* are very similar, suggesting a similar level of evolutionary divergence (Figures 5.8 – 5.9).

Population differentiation and gene flow

Estimates of pairwise distances were very similar for mtDNA, mtDNA-nDNA and nDNA datasets for *A. aequidens* comparisons (Tables 5.11-5.12). There was, however, some difference in values between mtDNA and nDNA datasets for comparisons involving *Argyrosomus* species. Pairwise distances between northern and southern *A. aequidens* clades varied from 0.042 to 0.049 (Table 5.11), and were similar in range to distances (around 5%) between known *Argyrosomus* species (Table 5.11).

In both *A. aequidens* and *Argyrosomus* cases, divergence between populations/species was roughly 10 times higher than observed differentiation within populations/species (Table 5.12). Therefore, observed genetic differentiation between northern and southern Benguela *A. aequidens* was very similar to described divergence between different *Argyrosomus* species, occurring in the Benguela Current.

Table 5.11: Uncorrected pairwise distances calculated for concatenated mtDN, mtDNA-nDNA and nDNA datasets, between northern (GA) and southern (GSA) clades of *A. aequidens* and different *Argyrosomus* species (see Table 5.10 for species codes).

	Between Populations						
	GA-GSA	KA-KN	KA-KSA	KA-KP	KN-KSA	KN-KP	KSA-KP
mtDNA	0.049	0.054	0.041	0.052	0.065	0.048	0.064
mtDNA-nDNA	0.046	0.042	0.034	0.042	0.050	0.038	0.051
nDNA	0.042	0.015	0.010	0.016	0.011	0.090	0.013

Table 5.12: Uncorrected pairwise distances calculated for concatenated mtDNA, mtDNA-nDNA and nDNA datasets, within northern (GA) and southern (GSA) clades of *A. aequidens* and different *Argyrosomus* species (see Table 5.10 for species codes).

	Within Populations					
	GA	GSA	KA	KN	KSA	KP
mtDNA	0.004	0.004	0.003	0.004	0.001	0.001
mtDNA-nDNA	0.005	0.004	0.004	0.003	0.002	0.001
nDNA	0.002	0.012	0.002	0.001	0.003	0.002

Genetic differentiation between samples calculated as F_{ST} (Table 5.13) between *A. aequidens* clades and among *Argyrosomus* species, for both concatenated mtDNA and

nDNA datasets, were similarly high and all significantly greater than zero. In particular, obtained F_{ST} values for the mtDNA dataset were close to 1 for all *A. aequidens* and *Argyrosomus* comparisons (Table 5.13). Although nDNA F_{ST} values were slightly lower than mtDNA, once again observed levels of divergence within *A. aequidens* were similar in range to those among different species of *Argyrosomus* (Table 5.13). Estimates of gene flow between groups ($N_e m$, effective migration – Table 5.13) derived from F_{ST} were effectively zero both between clades within *A. aequidens* and between *Argyrosomus* species.

Table 5.13: Genetic differentiation (pairwise F_{ST}) and gene flow (effective migration, N_{em}), calculated for concatenated mtDNA and nDNA datasets, between northern (GA) and southern (GSA) clades of *A. aequidens* and different *Argyrosomus* species (see Table 5.10 for species codes). Values significantly greater than zero ($p < 0.05$) in bold.

		GA- GSA	KA- KN	KA- KSA	KA- KP	KN- KSA	KN- KP	KSA- KP
F_{ST}	mtDNA	0.905	0.905	0.895	0.906	0.947	0.928	0.976
	nDNA	0.551	0.911	0.720	0.899	0.933	0.749	0.943
N_{em}	mtDNA	0	0	0	0	0	0	0
	nDNA	0	0	0	0	0	0	0

Time since divergence

Using sequence divergence in the 3 mtDNA regions and a strict molecular clock approach both methods of calibration produced similar estimates of time to the most common recent ancestor (tmrca), i.e. time since divergence, between taxa (Table 5.14). The main difference between the two methods regarded the 95% highest posterior density (HPD) confidence interval that was much broader for the internal node estimation than for the strict mutation rate. However, the obtained divergence rate for the internal calibration was of 2% per MY for the mtDNA dataset, which is within the estimated divergence rates for mitochondrial DNA of fish species.

Table 5.14: Estimates of time since divergence for the northern (GA) and southern (GSA) *A. aequidens* clades and *Argyrosomus* spp. (see Table 5.10 for species codes) in the Benguela Current region: **Ln(Likelihood)** = posterior likelihood of calibration method employed, and estimated time since most recent common ancestor (MY).

Calibration Method	Ln (Likelihood)	Estimated time since most recent common ancestor (MY)			
		GA vs. GSA	KP vs. Southern Kob	KN vs. Southern Kob	KA vs. KSA
1.5%	-5593.11	1.85 (1.46-2.26)	2.11 (1.76-2.47)	1.98 (1.64-2.34)	1.31 (1.02-1.61)
2MY	-5717.56	1.65 (0.46-3.01)	1.89 (0.58-3.35)	1.73 (0.55-3.11)	1.15 (0.36-2.10)

The tmrca between northern and southern *A. aequidens* clades appears to have occurred at approximately 1.85 MYA (1.46 - 2.26 MYA), which overlaps with the values estimated for the divergence of the Benguela Current *Argyrosomus* species from the European *A. regius* (KP – southern KOB: 1.76-2.47 MYA), the divergence of *A. coronus* and *A. japonicus* (KA – KSA: 1.02-1.61 MYA), and the isolation of *A. inodorus* (KN – southern KOB: 1.64-2.34 MYA) (Table 5.15, Figure 5.10).

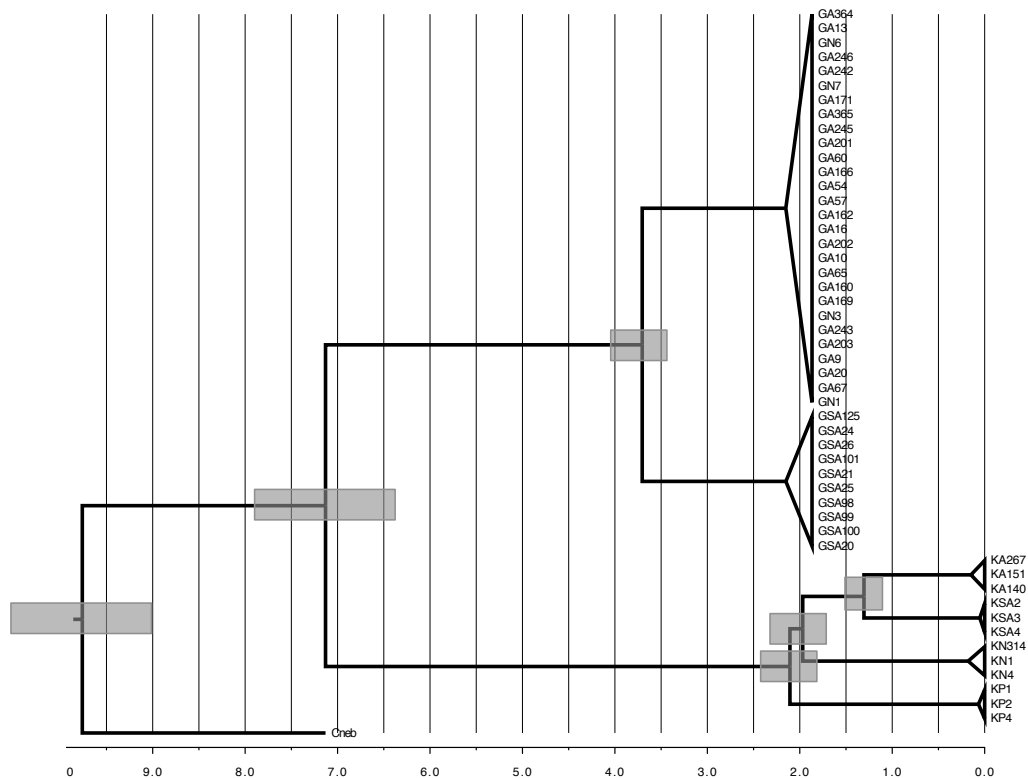


Figure 5.10: Estimated chronogram of time since divergence for *A. aequidens* clades and *Argyrosomus* species across the Benguela Current region, based on the concatenated mtDNA dataset. Grey bars correspond to the 95% highest posterior probabilities for each estimate (see Table 5.10 for clade and species codes).

5.2.4. Discussion

Genetic evidence for cryptic speciation

Reconstruction of phylogenetic relationships for both mitochondrial and nuclear DNA markers revealed a deep and reciprocally monophyletic bifurcation between two highly divergent clades comprising *A. aequidens* samples from the northern (i.e. Angola / Namibia) and southern (i.e. South Africa) Benguela sub-systems. Inter-lineage sequence divergence was ten times higher than intra-lineage divergence (4.9% vs. 0.4% for concatenated mtDNA sequences), and similar to levels of genetic divergence (around

5%) observed between distinct *Argyrosomus* species distributed across the same geographical region. Similar mtDNA sequence divergence levels have been documented among other described sciaenid species (Lakra et al. 2007; Alves-Costa et al. 2008; Han et al. 2008; Lakra et al. 2009). Such distinct differences between levels of intra- and inter-lineage divergence can be considered an indicator of cryptic speciation, as suggested by the “10x rule” for the mitochondrial cytochrome c oxidase I gene (Hebert et al. 2003; Zemplak et al. 2009).

Reproductive isolation is considered to be a fundamental criterion in species status recognition. In allopatry, the assessment of reproductive isolation is difficult since absence of gene flow might be due to the barrier alone and not intrinsic to the biology of the population (Palumbi 1992; Bernardi & Lape 2005). However, if enough time has passed allopatric populations can accumulate enough genetic divergence to become reproductively isolated (Knowlton 2000), as studies on allopatric speciation resulting from the closure of the Isthmus of Panama suggest that 3 MY is sufficient time for reproductive barriers to develop (Knowlton & Weigt 1998; Donaldson & Wilson 1999; Lessios et al. 1999; McCartney et al. 2000; Bowen et al. 2001). The level of genetic differentiation between populations, measured as Wright’s F_{ST} , can be used as a proxy for estimating gene flow and, consequently, reproductive isolation between populations (Excoffier et al. 2005). The F_{ST} values between the two clades of *A. aequidens* for both mitochondrial and nuclear markers were high (0.91 and 0.55 respectively), and similar to the levels observed between *Argyrosomus* species. These results, coupled with the observed reciprocal monophyly and the presence of multiple diagnostic nucleotide sites, suggest an absence of gene flow between the northern and southern populations (Colborn et al. 2001). Furthermore, the congruence between mitochondrial and nuclear lineages suggests the occurrence of complete lineage sorting of ancestral polymorphism (Avice 2000; Shen et al. 2011). Therefore, all these results point to the effective reproductive isolation of the two *A. aequidens* clades, and thus support the hypothesis of an allopatric speciation event having occurred for this species within the Benguela Current region.

An on-going study on *A. aequidens* biological and morphological features has revealed that individuals sampled in the northern and southern Benguela sub-systems exhibited significant differences in biological characteristics: Angolan fish exhibited smaller sizes (70cm vs. 1300cm), slower growth rates and matured earlier (2.2 years vs. 5 years) than individuals sampled in South African (W. Potts, personal communication). The

evolution of alternative life history strategies by the two clades provides strong supporting evidence for allopatric speciation, but what could be driving differential life history evolution? Although there is a general consensus that larger and faster growing marine species generally occur in higher latitudes, life history differences in *A. aequidens* may be related to seasonal migrations linked to food availability (Roff 1988), with either the development or the cessation of a spawning migration in the southern or northern Benguela clades respectively. The southern Benguela (South African) clade of *A. aequidens* undertakes extensive annual migrations, presumed to be related to feeding on migratory pelagic prey species, particularly *Sardinops sagax* (Griffiths & Hecht 1995). With an extended spawning season and consistent catches throughout the year at the spawning grounds, probably resulting from a year-round abundance of small pelagic species, there is no information to suggest that a similar migration occurs in the northern Benguela (Angolan) clade (W. Potts, personal communication). Furthermore, as abundance of small pelagics is directly linked to high primary productivity (Cole & McGlade 1998), and as primary productivity is greater in northern Benguela (Boyer et al. 2000), it is likely that prey availability was less of a constraint in the northern than in the southern sub-system.

However, contrary to the observed genetic and biological differentiation, morphological analyses does not allow differentiation of northern and southern *A. aequidens* clades (W. Potts, personal communication). This is not an unexpected result, since the same pattern has been found in multiple fish species (Colborn et al. 2001; Worheide et al. 2008; Griffiths et al. 2010; Watanabe et al. 2010), and particularly in sciaenids (Vinson et al. 2004; Santos et al. 2006; Lakra et al. 2007; Accioly & Molina 2008; Lakra et al. 2009), suggesting that for many fish species morphological change occurs at a slower pace when compared with genetic or life history variation (Colborn et al. 2001; Worheide et al. 2008; Griffiths et al. 2010; Watanabe et al. 2010). For example Santos et al. (2006) reported deep phylogenetic divergence based on mitochondrial cytochrome *b* between populations of the sciaenid *Macrodon ancylodon* in South America, without equivalent morphological differentiation. The existence of cryptic species can be attributed to the relative stability of the marine environment on evolutionary time scales: despite the short-term location of particular habitats changing due to climatic and sea-level fluctuations, these habitats will still exist on a broad geographic scale for millions of years (Jackson 1995). The Benguela Current represents a heterogeneous environment with seasonal changes in sea surface temperature and productivity, but the present day features of the whole system have remained stable for the last 2 MY. The

populations of *A. aequidens* occupy similar physical habitats to either side of the upwelling cell, which may explain why they have retained ancestral morphological characters.

In conclusion, observed biological differentiation between the two *A. aequidens* clades and the absence of corresponding morphological variation supports the hypothesis of a cryptic speciation event within the Benguela Current region.

Allopatric speciation and the Benguela Current

The present study has established that breakdown of gene flow and subsequent genetic divergence, and probably cryptic speciation, in *A. aequidens* corresponds with the geographical position of the Benguela Current. But which features of the system might cause isolation, and is it likely that this oceanographic feature initiated the divergence as well as maintaining present day isolation?

The Benguela Current system is thought to have developed in the Miocene, around 12 MYA, and was fully formed by the late Miocene/upper Pliocene at 6 MYA (Diester-Haass et al. 1988; Diester-Haass 1990; Diester-Haass et al. 2002; Krammer et al. 2006). The present-day pattern of oceanographic features was established in the beginning of the Pleistocene, around 2 MYA (Marlow et al. 2000), and since that time the system has experienced cyclical changes in sea level, water temperatures and upwelling intensity, especially during glacial periods (Marlow et al. 2000; Jahn et al. 2003). For example, sea levels are estimated to have dropped around 300m and upwelling intensity increased during the Last Glacial Maximum in the late Pleistocene (Siesser & Dingle 1981). Changes in sea levels during this time are thought to be responsible for population differentiation and speciation events in several marine species, and changes in water temperature would also greatly affect the distribution of marine fishes (Ruzzante et al. 2011). The colder water off southern Namibia and western South Africa, the narrow continental shelf off southern Namibia, and the perennial upwelling cell off central Namibia, might all constitute unsuitable habitat for *A. aequidens* and so fragment the distribution of adults while presenting a barrier to dispersal of eggs and larvae (Lett et al. 2007).

To understand if the oceanographic features of the Benguela Current influenced the geographical isolation of the two *A. aequidens* clades it is necessary to estimate time since divergence. Estimating divergence times based on molecular data should be regarded with caution, since several assumptions are required to calibrate the molecular clock (Drummond et al. 2006; Ho et al. 2007). In this case, due to the lack of a fossil

record the clock calibration was conducted with two different approaches, but independently of the method used the time since divergence of the clades was estimated at circa 1.8 MYA. This estimate suggests that the divergence between the two *A. aequidens* clades occurred soon after the establishment of the present Benguela Current system (Marlow et al. 2000), and that subsequent multiple glacial cycles during the mid-to late-Pleistocene have not interrupted the isolation. It can be concluded therefore that the major long-term oceanographic features (the cold water upwelling) are most likely responsible for isolation of the two clades in their respective regional populations, as observed for the divergence of the kob sister species *A. coronus* and *A. japonicus* across the same area (see Chapter 4.1). The absence of shared haplotypes between the two clades, in both mitochondrial and nuclear markers, suggests a complete absence of present and historical gene flow (Avice 2000).

Describing a new species

Despite the existence of a unifying theory underlying the importance of selection in the speciation process, there is no equivalent unity regarding which criteria should be used to describe a new species (Carcraft 2000). This ambiguity has led to multiple species concepts being proposed (Mallet 2007), the most commonly used being: the Biological Species Concept, which relies on reproductive isolation (Mayr 1942); the Phylogenetic Concept, which requires the existence of diagnostic characters (Carcraft 1983); the Evolutionary Concept, based on the existence of independently evolving lineages (Simpson 1951); and the Ecological Concept, which requires different species to occupy different niches (van Valen 1976). Independently of the concept used, there is a general agreement on the fundamental nature of a species: species are separately evolving metapopulation lineages (de Queiroz 1998, 2007). Based on the premise that species are lineages, and that multiple criteria can be used in their identification, a new theory has emerged: the General Lineage Concept (de Queiroz 1998, 2007), which proposes that the greater the number of species criteria satisfied by a group, the more likely it becomes that the group is a distinct lineage (de Queiroz 1998; Reeves & Richards 2011). Reeves & Richards (2011) suggested that if a lineage supports criteria such as reciprocal monophyly, presence of diagnostic characters, absence of genetic intermediates, intrinsic reproductive isolation and local adaptation, it should be considered an independent evolving lineage, and consequently a new species.

Phylogenetic reconstruction for *A. aequidens* evolutionary history reveals the existence of two reciprocally monophyletic clades, with the presence of fixed diagnostic

characters. Levels of population differentiation indicate an absence of gene flow, and congruence between mitochondrial and nuclear lineages implies the occurrence of complete lineage sorting. The genetic analyses support the existence of two independently evolving lineages in *A. aequidens*. In addition, reported significant differences in life history features may be related to local adaptation, further supporting the hypothesis of speciation in *A. aequidens*. Thus, these results conform to the requirements of the General Lineage Species Concept (de Queiroz 1998), and *A. aequidens* in the Benguela Current region should be considered two distinct species, corresponding to the northern and southern Benguela sub-system distributions.

CHAPTER 6: *Lichia amia*

6.1. Population structure and evolutionary history of a coastal pelagic fish in the Benguela Current: *Lichia amia* (L.1758)

6.1.1. Introduction

Marine species are considered to have fewer constraints to dispersal when compared to terrestrial species, as biogeographical barriers are not as evident, and many species exhibit pelagic phases in their early life cycle (Palumbi 1992; Avise 2000). Nevertheless, several studies have reported strong population structuring and barriers to gene flow in marine species (Bremer et al. 1998; Gold et al. 2002; Durand et al. 2005; Bester-van der Merwe et al. 2011).

The Benguela Current has been considered a major biogeographical barrier, separating Atlantic and Indo-Pacific tropical marine taxa (Bowen et al. 1994; McCartney et al. 2000; Colborn et al. 2001; Lessios et al. 2003). Cases of population differentiation have been observed in regions with intense upwelling systems mainly due to the offshore transport of pelagic eggs and larvae, where the environment is unsuitable for survival and / or recruitment, leading to disruption of gene flow among geographically close populations, with subsequent accumulation of genetic divergence (Apte & Gardner 2002; Waters & Roy 2004; Ravago-Gotanco et al. 2007).

Lichia amia (L. 1758) is a cosmopolitan pelagic carangid fish distributed throughout the Mediterranean, along the western coast of Africa, and around the southern and eastern coasts of South Africa (Heemstra & Heemstra, 2004). In the Benguela Current region, the species is most abundant from southern Angola to the eastern coast of South Africa, with a reported break of abundance in southern Namibia (Potts et al. 2008). A recent life-history study of the species in Angolan waters revealed that Angolan individuals appear to grow faster, mature younger and exhibit a longer spawning season than South African individuals (Potts et al. 2008). These results, allied with descriptions of distinct spawning grounds, may imply some form of isolation and local adaptation to the northern and southern Benguela environments. Due to the transboundary nature of this valuable fishery resource, it is necessary to assess genetic population structure and evolutionary history, in order to ensure that *L. amia* is sustainably harvested. Therefore, the main aims of the present study are to: *i*) investigate population connectivity and

levels of gene flow in *L. amia* across the Benguela Current region, using a mitochondrial DNA (mtDNA) marker; *ii*) reconstruct evolutionary history of the species in the area, in order to understand the influence of the Benguela Current system in *L. amia* population dynamics; and *iii*) provide basic information for future management plans in the region, in order to ensure sustainable harvesting, and the maintenance of the species' evolutionary potential.

6.1.2. Methods

Sampling and DNA extraction

Sampling was conducted in three sites within the *L. amia* distribution range in the Benguela Current (Table 6.1, Figure 6.1). Samples were collected during the austral summers of 2008-2009, from local collaborators. Due to the difficulty of sampling this species (all individuals have to be caught by rod and line), and low availability of *L. amia* during sampling seasons, the present sampling strategy was quite limited in scope, but represents populations to either side of the Benguela upwelling area. DNA extraction was conducted as described in Chapter 2.2.1.

Table 6.1: Sampling strategy for *L.amia* across the Benguela Current: sampling sites, sample codes, sample size and geographical coordinates.

Country	Region	Code	Number of Samples	Coordinates
Angola	Flamingo	FLA	101	15°10.374'S 12°04.863'E
South Africa	Port Alfred	EastC	81	33°36.500'S 26°54.000 E
	Arniston	WestC	17	34°40.000'S 20°14.000'E

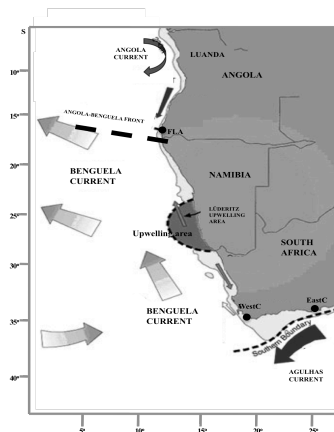


Figure 6.1: Sampling strategy for *L. amia* across the Benguela Current, highlighting sampling sites, and their position relative to the major oceanographic features of the system: the Benguela, Angola and Agulhas Currents; position of the Angola-Benguela Front; central Namibia upwelling cell; continental shelf width.

Genetic screening

A fragment of mtDNA Control Region (CR) was PCR amplified and sequenced with the universal primer pair L16498/12SARH (Apte & Gardner 2002) for 20 individuals per sampling site whenever possible, as described in Chapter 2.2.2.

Mitochondrial DNA analyses

Population structure and phylogeographic patterns

Haplotype (h) and nucleotide (π) diversity levels, and Tajima's D , Fu's F_S and Ewens-Watson F neutrality tests were estimated in Arlequin 3.1.1 (Excoffier et al. 2005), with statistical significance assessed after 10000 permutations (Chapter 2.4.1). The most suitable nucleotide substitution model was estimated in jModelTest (Posada 2008), as described in Chapter 2.3.1.

Investigation of *L. amia* genetic sub-structuring patterns across the Benguela Current was conducted by estimating Wright's pairwise F_{ST} values; performing hierarchical analysis of molecular variance (AMOVA) to test the hypothesis of genetic differentiation of populations to the north and south of the perennial upwelling cell in central Namibia; and reconstructing genetic relationships among haplotypes, as described in Chapter 2.3.1. Furthermore, using a geographical based analysis, the relationship between population genetic sub-structuring and geographical distance was assessed using GENELAND (Guillot et al. 2005): 5 independent runs were conducted to estimate the most likely number of genetic clusters ($K = 1$ to 3). Each run was performed for 100000 MCMC iterations, saving every 1000th step. Estimate of true K was achieved after an initial burn-in period of 2500 MCMC steps. Posterior distributions of most likely K were mapped in order to identify the geographical position of genetic discontinuities.

Evolutionary history

Reconstruction of *L. amia* evolutionary history was performed based on diversity levels (h and π), deviations from neutrality (Tajima's D and Fu's F_S statistics) and mismatch distribution analyses for each population identified (Chapter 2.3.1). In order to estimate time since expansion generation time was set to 2.4 years for the Angolan population (Potts et al. 2008) and 4 years for the South African population (Heemstra & Heemstra 2004). Calibration of the molecular clock was based on a universal mutation rate of 3.6% per MY for the CR of marine fish (Donaldson & Wilson 1999).

In addition, estimation of time since most recent common ancestor (tmrca) for the northern-southern Benguela population divergence was performed in BEAST 1.6.1 (Drummond & Rambaut 2007). Two independent runs were conducted under a strict molecular clock, using the HKY nucleotide substitution model, and establishing a coalescent tree prior with constant size. Each run was analyzed for 10 million MCMC generations, sampling every 1000th generation. Convergence of run parameters was assessed in Tracer 1.5 (Rambaut & Drummond 2007), based on Effective Sample Size (ESS>200). Obtained trees were combined using TreeAnnotator 1.6.1 (Drummond & Rambaut 2007), and visualized in FigTree 1.3.1 (Rambaut 2009). As previously described (see Chapters 2, 3, 4 and 5), calibration of the molecular clock was performed using two different approaches: *i*) fixing the mean divergence rate at 3.6% per MY (1.8% per lineage), considered the universal rate in marine fish CR (Donaldson & Wilson 1999); and *ii*) using the strengthening of the Benguela Current (~2 MYA) as a node calibrator for the separation of northern and southern *L.amia* populations. Convergence of run parameters for the most likely approach was estimated based on ESS>200, in Tracer 1.4 (Rambaut 2007). Divergence times were calculated from the post burn-in results.

6.1.3. Results

Mitochondrial DNA analyses

Population structure and phylogeographic patterns

Amplification and sequencing of mtDNA CR for 57 *L. amia* individuals yielded fragments of 581bp, containing 14 polymorphic sites representing 13 different haplotypes. Within samples haplotype diversity (h) ranged from 0.658 to 0.765, and nucleotide diversity (π) ranged from 0.002 to 0.003, with the FLA and EastC samples exhibiting highest number of haplotypes and haplotype diversity (Table 6.2). Mean values across the whole dataset were: $h = 0.867$, and $\pi = 0.007$. No significant departures from the assumption of neutrality were observed, for any of the tests employed (Table 6.2). The HKY model was considered to be the most suitable nucleotide substitution model for the *L. amia* CR dataset.

Table 6.2: Mitochondrial genetic diversity levels and neutrality tests for *L. amia* CR sequences: **n** – number of individuals; **H** – number of haplotypes; **h** – haplotype diversity; π - nucleotide diversity; **F** – Ewens-Watson neutrality test; **D** – Tajima neutrality test; **F_S** – Fu neutrality test. Statistically significant results ($p < 0.05$) in bold.

	FLA	WestC	EastC	Overall
n	20	20	17	57
H	6	4	6	13
h	0.765	0.658	0.765	0.867
π	0.002	0.002	0.003	0.007
F	0.485	0.718	0.468	0.781
D	-0.311	0.727	0.790	0.841
F_S	-1.024	0.822	-1.418	-0.834

Reconstruction of *L. amia* haplotype networks revealed a clear separation into two clusters representing samples from the northern and southern Benguela sub-systems (Figure 6.2). The majority of haplotypes within either population diverged from each other by one or two mutational steps, while divergence between the haplotype clusters from different populations was by 6 mutational steps (Figure 6.2). No shared haplotypes were observed between the two sub-system populations. No significant geographical association was observed within each cluster, suggesting that South African *L. amia* may be composed by one mixed population.

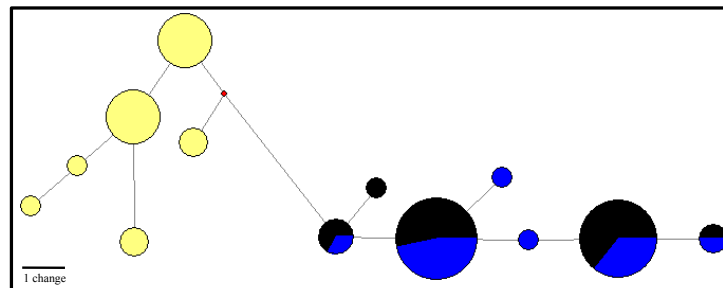


Figure 6.2: Reconstruction of haplotype network for *L. amia* across the Benguela Current, based on 581bp of mtDNA CR sequences: ●: FLAM; ●: EastC; ●: WestC. Node sizes are proportional to the number of haplotypes. Red dots correspond to missing haplotypes.

As observed in the phylogeographic analysis, genetic differentiation tests rejected the null hypothesis of panmixia in *L. amia* throughout the Benguela Current region, revealing 2 genetically divergent populations corresponding to the northern (FLA) and southern (WestC and EastC) Benguela Current sub-systems. Pairwise F_{ST} values were high and significantly different from zero between samples from the northern and southern Benguela sub-systems, but low and non-significant between the two samples from within the southern sub-system (Table 6.3). The hypothesis of genetic differentiation between *L. amia* from the northern and southern Benguela sub-systems was further corroborated by the AMOVA test, as 79.25% of genetic variance was

distributed between groups ($p < 0.05$), and only 21.81% ($p < 0.05$) was found within populations.

Table 6.3: Pairwise F_{ST} values based on mtDNA CR data, between *L. amia* samples (see Table 6.1 for sample codes). Values significantly different from zero ($p < 0.005$) in bold.

	FLA	WestC	EastC
FLA	-		
WestC	0.783	-	
EastC	0.776	-0.051	-

A similar outcome was obtained when the geographical component of genetic differentiation was considered in GENELAND. Maps of posterior probability of assignment revealed two geographically-based genetic groups, corresponding to northern and southern Benguela Current sub-systems (Figure 6.3).

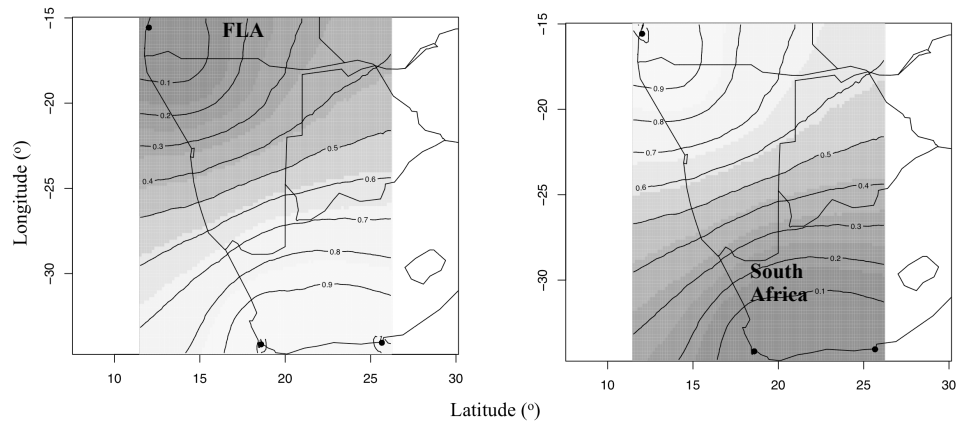


Figure 6.3: Map of posterior probability of population membership of geo-referenced *L. amia* samples, based on mtDNA CR data: FLA (left) and South Africa (right). Dark colors delineate areas of higher probability of population membership. Black isolines represent the level of genetic divergence.

Evolutionary history

Assessment of *L. amia* evolutionary history in the Benguela Current was conducted for the two distinct sample clusters (Angola – FLA – and South Africa – WestC + EastC) separately. The Angolan *L. amia* population exhibited higher values of haplotype diversity (h) than the South African population, although nucleotide (π) diversity levels were similar in both populations (Table 6.4). Although Tajima's D and Fu's F_S did not exhibit significant deviations to neutrality assumptions in both samples, which can be observed in populations with past demographic changes, mismatch distribution analyses did not allow rejection of the null hypothesis of rapid demographic expansions in both populations (Table 6.4). In addition, reconstruction of frequency histograms revealed a clear unimodal distribution in both cases, further supporting the hypothesis of past

demographic expansions in both *L. amia* populations (Figure 6.4). Time since expansion, based on a universal CR calibrated molecular clock and observed mismatch distribution parameters, was estimated to have occurred at 17.76 KYA and 12.69 KYA for the northern and southern populations respectively (Table 6.4).

Table 6.4: *Lichia amia* genetic demographic history for northern and southern Benguela sub-system populations, based on mtDNA CR sequence variation: genetic diversity levels (h and π); neutrality tests (Tajima's D and Fu's F_S); mismatch distribution parameters: σ - time since expansion, in mutation units; θ_0 - population size before expansion; θ_1 - population size after expansion; and time since expansion (T in KY). Statistical significant results ($p < 0.05$) in bold.

	Angola	South Africa
h	0.765	0.700
π	0.002	0.002
D	-0.311	0.443
F_S	-1.024	-1.255
Mean	1.526	1.402
Variance	1.446	1.257
SSD	0.007	0.031
σ	1.783	2.123
	(0-4.512)	(0-5.342)
θ_0	0.026	0.000
θ_1	8.384	3.970
Texp (KY)	17.76	12.69
	(0-44.94)	(0-31.92)

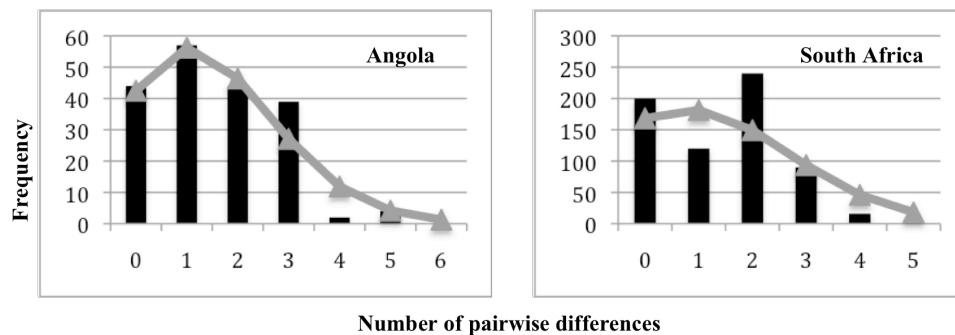


Figure 6.4: Mismatch distribution histograms for northern and southern Benguela sub-system *L. amia* populations, based on mtDNA CR sequences. Filled bars indicate the observed frequency of pairwise distribution, grey line indicates the expected distribution under a model of sudden demographic expansion.

Estimates for time since most recent common ancestor (t_{mrca}), based on a fixed sequence divergence rate, indicated that the separation of northern and southern *L. amia* populations occurred ~202 KYA (Table 6.5). When t_{mrca} was estimated using internal node calibration, values were far greater: 969 KYA (Table 6.5). However, as observed for *D. capensis* (see Chapter 3), in this case sequence divergence rate per lineage was estimated at 0.4% per MY, which is very different from the average CR divergence

rates for fish species (Donaldson & Wilson 1999), suggesting that the used internal node calibration may not be an appropriate method in this situation.

Table 6.5: Estimates of time since most recent common ancestor for *L. amia* in the Benguela Current based on CR sequences, including 95% highest posterior probabilities (HPD in brackets).

Calibration Method	Ln (Likelihood)	Estimated time since most recent common ancestor (KY)
1.5%	-959.724	202 (96.6-287)
2 MY	-959.179	969 (309-1833)

6.1.4. Discussion

Population structure and phylogeographic patterns

Despite the limited sample coverage, the results obtained presented a clear picture of significant genetic differences between two divergent *L. amia* populations in the Benguela Current region: one in southern Angola and the other in South Africa. Values of genetic differentiation (F_{ST}) between the two populations were higher than those commonly observed in marine species with cosmopolitan distributions (Bremer et al. 1998; Grant & Bowen 1998; Colborn et al. 2001; Ely et al. 2005; Grant & Bowen 2006; Diaz-Jaimes et al. 2010; Dammannagoda et al. 2011). Combined with the observed absence of shared haplotypes between populations, such high values of differentiation imply the presence of a substantial barrier to gene flow between the two populations (Avice 2000). Although it is not possible at the moment to completely discard an Isolation-By-Distance model of connectivity and genetic divergence, due to the small number of samples used and the large geographical distances between them, the absence of significant differentiation between the two South African samples suggests that gene flow between areas within regions may be high and that within regions populations are genetically undifferentiated. When compared to the patterns of genetic differentiation observed for other coastal fish species across the same area (*D. capensis*, *A. inodorus* and *A. aequidens* – see Chapters 3, 4.2 and 5.1), this suggests that the oceanographic features of the Benguela Current play an important role in shaping genetic population structure of *L. amia* around southern Africa. Population structuring due to oceanographic features has been documented for multiple marine species (Bremer et al. 1998; Graves 1998; Fullard et al. 2000; Carlsson et al. 2004; Evans et al. 2004; Bargelloni et al. 2005; Dammannagoda et al. 2008; Cardenas et al. 2009; Galarza et al. 2009; Kenchington et al. 2009; Diaz-Jaimes et al. 2010; Bester-van der Merwe et al.

2011). In particular, strong upwelling cells such as the one present in the Benguela Current region have been linked to gene flow interruption between adjacent populations, due to disruption of longshore transport of pelagic eggs and larvae (Bowen & Grant 1997; Waters & Roy 2004). The perennial nature of the Benguela Current major upwelling cell may, thus, be contributing for gene flow disruption between *L. amia* populations, by inducing local larval retention (Lett et al. 2007). Nevertheless, the cosmopolitan distribution of the species suggests large dispersal potential, and the large and highly mobile pelagic adults could have the ability to disperse/migrate across distances encompassing the perennial upwelling cell. Thus, other oceanographic features are likely to contribute to the observed high levels of genetic divergence. Evidence indicates that *L. amia* do not occur off the coast of a large region of southern Namibia due to unsuitably cold sea surface temperatures (Potts et al. 2008). Furthermore, for reproduction the species requires estuarine environments, habitats that along the Namibian coast are confined to the northern and the southern border at the outflows of the Cunene and the Orange rivers, respectively (Heemstra & Heemstra 2004). Additionally, only two breeding grounds have been reported in the region: one off the coast of southern Angola (northern Benguela), the other off the coast of KwaZulu-Natal in eastern South Africa (Heemstra & Heemstra 2004; Potts et al. 2008). The use of distinct geographical spawning areas is considered to be an important contemporary mechanism influencing a species' population structure (Hemmer-Hansen et al. 2007). Therefore, the existence of two reproductively isolated *L. amia* populations in the Benguela Current region may be a product of the interaction of multiple oceanographic and environmental features, such as colder sea surface temperatures and offshore currents associated with the perennial upwelling cell respectively disrupting larval and adult dispersal and a patchy distribution of suitable breeding habitats entraining reproductive migrations to either end of the geographical distribution in southern Africa. These environmental features would act to restrict both larval and adult dispersal, decreasing gene flow across the region and allowing local adaptation to the different environments, as reflected by the observed differences in biological features of fish in the northern and southern Benguela sub-systems (Potts et al. 2008).

Evolutionary history

Reconstruction of *L. amia* evolutionary history revealed evidence of past population expansions. Low haplotype and nucleotide diversity within populations, combined with the observed star-shaped haplotype network, imply the occurrence of evolutionarily

recent demographic expansions from small populations sizes (Grant & Bowen 1998; Avise 2000). Mismatch distribution analyses further supported the hypothesis of past demographic expansion, generating estimated times since expansion of ~17 KYA, and ~14 KYA for northern (Angola) and southern (South Africa) populations respectively. These time estimates suggest that both *L. amia* populations underwent a population expansion roughly at the same time during the end of the last glacial age in the Pleistocene (Marlow et al. 2000). Cyclic climatic changes in the Benguela Current during the Pleistocene have been reported as contributing to shape population genetic signatures in several southern African marine taxa, with multiple species showing evidence of population expansion during the end of the Last Glacial Maximum (~18 KYA) (Gopal et al. 2006; Matthee et al. 2006; Matthee et al. 2007; von der Heyden et al. 2007; von der Heyden et al. 2010). Also as observed for *D. capensis*, time since divergence for the two *L. amia* populations was estimated at ~202 KYA. The second half of the late Pleistocene (0.5 - 0.01 MYA) was characterized by the establishment of 40 KY and 100 KY glacial cycles – the Milankovitch cycles (Pisias & Moore 1981; Schmieder et al. 2000). In particular in the Benguela Current region the late Pleistocene was characterized by abrupt changes in circulation patterns, decreased sea surface temperatures and lower sea levels, which greatly influenced upwelling intensity and paleoproductivity (Kirst et al. 1999; Marlow et al. 2000; Jahn et al. 2003). In a backwards scale, the second glacial age (the Santa Maria period in South America or the Riss period in the Alps) is considered to have lasted from ~200 KYA to 130 KYA (Pisias & Moore 1981), thus observed estimate of time since most recent common ancestor for *L. amia* appears to coincide with the onset of this glacial cycle. The decrease in sea surface temperatures, followed by a fall in sea level, could have influenced *L. amia* population connectivity between the northern and southern Benguela sub-systems, contributing to the observed divergence. Changes in sea surface temperatures and sea levels are considered to be key factors influencing dispersion and population connectivity in marine species (Grant & Bowen 1998; Knowlton 2000; Kenchington et al. 2009), as present-day dispersion ranges and population structure patterns in most cases appear to be related with climatic fluctuations during the Pleistocene (Avise et al. 1998; Grant & Bowen 1998; Graves 1998; McCartney et al. 2000; Ruzzante et al. 2008; Kenchington et al. 2009; Bester-van der Merwe et al. 2011). If the northern and southern *L. amia* populations became isolated during the last but one glacial age, then it suggests that they remained isolated during the short interglacial period around 130-120 KYA. Obtained results for *L. amia* suggest that past climatic

changes in the Benguela Current may have contributed to shape the species' evolutionary history, with population expansions within the northern and southern sub-systems occurring during the present warmer period after the Last Glacial Maximum, whilst isolation of the two populations appears to be connected with a cold period during an earlier glacial maximum.

Implications for fishery management

Despite the small number of sampling sites, results in the present study revealed strong genetic divergence between samples of *L. amia* collected from the northern and southern Benguela sub-systems. The absence of shared haplotypes between populations (i.e. complete lineage sorting) suggests the existence of effective barriers to gene flow in the region. Therefore, based on observed reciprocal monophyly the establishment of two Evolutionary Significant Units (ESU *sensu* Moritz 1994) is suggested. Although the small number of sampling sites does not allow the identification of the physical boundaries of each ESU, based on the low differentiation observed between South African samples (i.e. presence of single panmictic populations within regions), and comparable results obtained for other local coastal fish species such as *D. capensis* (Chapter 3) it is suggested that biogeographical boundaries in the region are used as proxies for the ESU delineation. Consequently, the northern Benguela sub-system should represent an independent ESU from the southern Benguela sub-system and management should be conducted accordingly for each population. However, in the marine environment the mechanisms responsible for shaping population structure may be not only historical processes, but also contemporary ones (Hemmer-Hansen et al. 2007). Therefore, it is suggested that further studies should be conducted, using microsatellite markers to investigate levels of *L. amia* population connectivity and gene flow, in order to establish sustainable harvesting plans, that can ensure the maintenance of the species evolutionary potential.

CHAPTER 7: *Thunnus albacares*

7.1. Population and phylogeographic structuring of *Thunnus albacares* (Bonnaterre, 1788) around southern Africa: implications for fisheries management and conservation

7.1.1. Introduction

Thunnus albacares (Bonnaterre, 1788) is an oceanic tuna, with a global distribution confined to tropical and subtropical waters (FAO 2009). The species represents an important fishery resource, and has in recent years replaced the more endangered tuna species as the target of capture fisheries throughout the world (Wu et al. 2010). The largest catches are documented for the equatorial region of the Pacific Ocean, but *T. albacares* also supports a large fishery industry both in the Indian and Atlantic Oceans (Appleyard et al. 2001; Dammannagoda et al. 2008; FAO 2009). Despite a recent decrease in captures, *T. albacares* is not considered endangered or overexploited (FAO 2009; IUCN 2010).

Although a worldwide species, tagging studies have revealed that *T. albacares* migrate preferentially within ocean basins, and exhibit limited dispersion between oceans (Ward et al. 1994a; Appleyard et al. 2001). For tropical pelagic fishes such as bigeye tuna, albacore, striped marlin and white marlin, cold currents like the Benguela Current in southern Africa have been documented to limit migration. Thus, it has been proposed that after the closure of the Isthmus of Panama dispersion between the Atlantic and Indo-Pacific Oceans became limited and population differentiation ensued in these species (Chow & Ushiyama 1995; Bremer et al. 1998; Graves & McDowell 2003). The observed dispersion constraints in *T. albacares* may thus be related with the cold water temperatures off southern Africa and southern America (Bremer et al. 1998; Graves & McDowell 2003). The existence of such ecological dispersal limitations was supported by Ward et al. (1997) who identified four discrete *T. albacares* stocks based on allozymes and mitochondrial DNA: Atlantic Ocean, Indian Ocean, and Eastern and Western Pacific Ocean. However Appleyard et al. (2001) and Diaz-Jaimes & Uribe-Alcocer (2006) found only weak population differentiation between the two Pacific *T. albacares* stocks. Using mitochondrial markers, Ely et al. (2005) observed a similar pattern of shallow divergence between the *T. albacares* stocks of the Atlantic and

Indian Oceans. All of these authors suggested that the observed results were possibly related with the large historical effective populations sizes in *T. albacares* retarding genetic differentiation even in the absence of current gene flow. However, absence of inter-oceanic differentiation in such tropical marine fish may also be connected with historical periods of increased gene flow between populations during warmer interglacial periods in the Pleistocene. During the interglacial periods the influence of cold water biogeographical barriers would decrease, and thus connectivity between populations could be restored (Graves 1998; Diaz-Jaimes et al. 2010). Therefore, it is necessary to distinguish between past and present processes shaping population structure in highly migratory fish species like *T. albacares*. For example, a study of skipjack tuna (*Katsuommus pelamis*) using mitochondrial markers did not detect population differentiation between the Atlantic and Indo-Pacific Ocean stocks (Ely et al. 2005), but a recent study using nuclear markers revealed evidence of population substructuring in the western Indian Ocean, suggesting that recent processes play an important role in shaping the species genetic structure (Dammannagoda et al. 2011).

Previous studies using mitochondrial DNA markers revealed the presence of 4 discrete *T. albacares* stocks, and a recent study employing microsatellites revealed weak, but significant, differentiation in the western Indian Ocean, suggesting that *T. albacares* exhibits a more complex population structure than previously thought (Dammannagoda et al. 2008). Therefore, it is necessary to conduct surveys at a finer geographical scale to investigate the population dynamics of the species. In South Africa, due to the confluence of the Atlantic and Indian Oceans, two *T. albacares* stocks are thought to occur (Ward et al. 1994a; Ely et al. 2005), making this area an ideal place to assess population differentiation both in terms of past and present processes. Furthermore, the South African *T. albacares* fishery is managed differently according to catch location: captures in the Atlantic waters off South Africa are regulated by the International Commission for the Conservation of Atlantic Tunas (ICCAT), whilst the Indian Ocean Tuna Commission (IOTC) regulates catches on the Indian Ocean coast. Thus, it is necessary to understand if *T. albacares* off the coast of South Africa is composed by one or two discrete stocks, in order to establish a sustainable harvesting plan for the species in the region.

In the present work the aim was to assess: *i*) levels of population differentiation and gene flow in *T. albacares* off the coast of South Africa, using mtDNA and microsatellite markers; *ii*) the evolutionary history of the species in the region, to understand the influence of the Benguela Current in isolating Atlantic Ocean from

Indian Ocean populations; and *iii*) the phylogeographic patterns between the Atlantic and Indo-Pacific Oceans, in order to set the basis for the establishment of an accurate fisheries management plan for *T. albacares* off the South African coast.

7.1.2. Methods

Sampling and DNA extraction

A total of 235 individuals were collected by local collaborators during 2008-2009 from three sites in the South African provinces of Eastern Cape, Western Cape and KwaZulu-Natal, either from commercial vessels or regional fishing competitions (Table 7.1). In order to better understand the wider geographical relevance of genetic differentiation of *T. albacares* off South Africa, additional sampling took place in the Indian Ocean (La Réunion; Seychelles and Kerala, SW India) and Atlantic Ocean (Brazil) by local collaborators. In particular, 18 out of 47 individuals from the La Réunion site were sampled in the northern Mozambique Channel, with remaining samples caught off the coast of La Réunion (Table 7.1). A fin clip of each individual was removed immediately after capture, and fixed in 95% ethanol. Genomic DNA was extracted as described in Chapter 2.1.1.

Table 7.1: Sampling strategy for *T. albacares*: sampling locations, sample code, sample size and latitude/longitude coordinates.

Country	Region	Code	Sample size	Coordinates
South Africa	KwaZulu-Natal	KZN	96	30°47.58'S 30°25.12'E
	Eastern Cape	EastC	96	33°36.500'S 26° 54.00'E
	Western Cape	WestC	96	34°40.000'S 20° 14.00'E
India	Kerala	KER	18	9°1.52'N 76°0.51'E
La Réunion	La Réunion	LRE	29	21°06.00'S 55°36.00'E
	North Mozambique Channel		18	20°34.20'S 52°36.91'E
Seychelles	-	SEY	6	4°32.36'S 55°23.35'E
Brazil	Natal	BRA	96	5°47.218'S 35°10.56'W

Genetic screening

A fragment of the COI gene was PCR amplified and sequenced using the primers of Paine et al. (2008) for 15 individuals per sampling site (whenever possible), as described in Chapter 2.2.2.

Four cross-specific microsatellite loci from bluefin tuna (*Thunnus thynnus thynnus*) and two *T. albacares* species-specific loci were used to investigate genetic structuring between the Atlantic and Indian Oceans (Chapter 2.2.3). Large sample sizes are required in these markers to take advantage of the higher statistical power present due to

the larger allelic diversity exhibited. Therefore, screening was not possible for the SEY sample, and samples from LRE and KER were grouped together to constitute a combined Indian Ocean sample (IO), after testing for genic and genotypic variation between them to provide a more accurate estimate of allele frequencies.

Mitochondrial DNA analyses

Population structure and phylogeographic patterns

Mitochondrial DNA haplotype (h) and nucleotide (π) diversity levels, Tajima's D , Fu's F_S and Ewens-Watson's F neutrality tests, and the most suitable nucleotide substitution models, were assessed as described in Chapter 2.3.1.

Population structure was inferred through Wright's F_{ST} statistic, analysis of molecular variance (AMOVA) and the reconstruction of a median-spanning haplotype network (see Chapter 2.3.1). The AMOVA was performed to test the hypothesis of an Atlantic (BRA + WestC) – Indian Ocean (EastC + KZN + KER + SEY + LRE) partitioning of genetic variation. In addition, as Ely et al. (2005) suggested that *T. albacares* off the western coast of South Africa originated from the Indian Ocean, F_{ST} comparisons and the AMOVA test were also performed for the isolated BRA sample vs. all the remaining samples grouped together to form an Indian Ocean cluster (WestC + EastC + KZN + KER + SEY + LRE).

Evolutionary history

Historical demographic changes in *T. albacares*, such as population contraction and expansion were investigated using haplotype and nucleotide diversity measures, and Tajima's D (Tajima 1989) and Fu's F_S (Fu 1997) statistics, as these tests are sensitive to changes in population dynamics. In addition, the hypothesis of a rapid demographic expansion was tested through the analysis of sequence mismatch distributions, for each population previously identified. Significance of the hypothesis was tested using the “sum of squared differences” (SSD) test, implemented in Arlequin v3.1.1 (Excoffier et al.). An approximate estimate of time since expansion was calculated based on $\sigma = 2\mu t$ (Harpending 1994) (see Chapter 2.3.1 for details). In order to calibrate the molecular clock a universal COI divergence rate of 1.5% per MY, determined for other fish species (Bermingham et al. 1997), was used. Generation time was estimated at two years (Heemstra & Heemstra 2004).

Microsatellite analyses

Genetic diversity and population structure

Genotype frequencies within individual samples and loci were tested for conformity to Hardy-Weinberg equilibrium expectations of outcrossing and to linkage equilibrium, as described in Chapter 2.3.2. MICROCHECKER (van Oosterhout et al. 2006) was used to identify technical problems in microsatellite amplification, such as large allele dropout or stuttering. FreeNA (Chapuis & Estoup 2007) was used to investigate occurrence and frequency of null alleles for each locus and sample.

Measures of genetic diversity were assessed as allelic richness (AR), number of alleles (Na), expected (H_E) and observed (H_O) heterozygosity, and inbreeding coefficient (F_{IS}) across loci (see Chapter 2.3.2).

Assessment of population structure of *T. albacares* off South Africa was investigated using two different approaches. First, estimation of genic and genotypic differentiation per locus and sample was conducted using exact tests as implemented in GENEPOP 1.2 (Raymond & Rousset 1995) with statistical significance tested using default permutation parameters. Genic differentiation was also estimated using Weir's (1996) F_{ST} , globally and pairwise between samples, as implemented in FreeNA (Chapuis & Estoup 2007) with significance from zero assessed after 1000 permutations. As the presence of null alleles can decrease apparent differentiation within populations, and conversely increase apparent differentiation between populations (Chapuis & Estoup, 2007), the ENA method implemented in FreeNA was used to estimate genetic differentiation levels among *T. albacares* samples. In addition, as mentioned above for the mtDNA dataset, Weir's (1986) F_{ST} comparisons were also performed between the sample BRA and remaining samples grouped together (WestC + EastC + KZN + LRE). Secondly, a Bayesian approach was used to investigate cryptic population structure, as implemented in STRUCTURE (Pritchard et al. 2000). Simulations were conducted under the admixture model, that allows each individual to be assigned to multiple clusters based on its genotype frequencies; with correlated allele frequencies, for 20000 Markov Chain Monte Carlo (MCMC) generations in the burn-in phase, followed by 80000 generations in the data collection phase for K between 1 and 7 (K = number of postulated populations). Five independent runs were performed for each K to ensure convergence of parameters during the runs. Estimation of the most likely K was performed based on the obtained posterior probabilities of the data (Evanno et al. 2005) (see Chapter 2.4.2). In addition, identification of possible genetic discontinuities along the sampling area was determined by using the R package GENELAND (Guillot et al.

2005). In this approach the inference of such discontinuities is carried out without previous knowledge on the number of populations, as in STRUCTURE, but is performed from individual geo-referenced multi-locus genotypes (Guillot et al. 2008; Guillot & Foll 2009; Guillot & Santos 2009). The entire data set of sampled individuals is perceived as belonging to one of many possible populations in Hardy-Weinberg equilibrium. The model assumes that individuals within populations are randomly located, and the loci display linkage equilibrium. Inference of the number of genetic discontinuities is performed via simulation of the posterior distribution of parameters by MCMC (Guillot et al. 2005). Due to constraints in sampling marine organisms (e.g. multiple fish caught in long trawls), individuals sampled within the same site were assigned the same geographical coordinate. Five sites with different geographical coordinates were identified (Table 7.1). The inference algorithm was launched using the Dirichlet distribution as prior for allele frequencies, with allele frequencies correlated, using spatial information, and estimating null allele frequencies. Due to the highly migratory nature of *T. albacares*, a coordinate error of 1° was implemented. Five preliminary runs were performed for K between 1 and 7, K being the number of populations, to assess convergence of the model. A final run was performed with a fixed K , identified as the most likely number of populations, based on the mode of the posterior distribution of the model. Each analysis was run for 1 million iterations, sampling every 100th iteration (Guillot et al. 2008; Guillot & Foll 2009; Guillot & Santos 2009).

Futhermore, assessment of recent levels of gene flow was conducted using a Bayesian approach to assign individuals to their most likely population of origin, as implemented in GENECLASS (Piry et al. 2004), with statistical significance assessed after performing 10000 simulations. As this analysis requires postulation of an exact number of population units, two approaches were conducted: using sampling sites as proxies for populations; and dividing the dataset into Atlantic (BRA) and Indian Ocean (WestC + EastC + KZN + LRE + KER) populations, with all South African samples assigned to the Indian Ocean based on the results obtained by Ely et al. (2005).

Demographic history

Changes in effective population sizes due to natural causes or over-exploitation can leave signatures in a species genetic diversity levels. Such events are characterized by the disappearance of rare alleles, and can thus be detected using genetic methods. Demographic changes in *T. albacares* were assessed using BOTTLENECK (Piry et al.

1999). Significant deviations from the null hypothesis of population stasis were assessed with the Wilcoxon Sign Rank test. Distribution of H_E values was obtained performing 10000 coalescent simulations. Since there is no consensus about the accuracy of microsatellite mutation models, the analysis was repeated for the three models available: Infinite Allele Model (I.A.M.), Stepwise Mutation Model (S.M.M), and Two-Phase Mutation Model (T.P.M.) where 30% of mutations were allowed to occur in a multi-step manner (see Chapter 2.3.2).

Effective population size (N_e) can be a good estimator of recruitment in marine fishes and its estimation is of great value for exploited fish species (Hauser & Carvalho 2008). Estimates of effective population size for *T. albacares* were conducted with LDNe (Waples & Do), for three different critical levels of rare allele frequencies: 0.05, 0.02 and 0.01. 95% Confidence intervals were calculated using a jackknife approach (Chapter 2.3.2). One caveat when assessing N_e estimates is that it is necessary to know the number of population units a priori. As such, N_e was estimated for the number of populations previously identified.

7.1.3. Results

Mitochondrial DNA analyses

Population structure and phylogeographic patterns

Amplification and sequencing of a 700bp fragment of the COI gene for 91 individuals found 17 different haplotypes characterized by 19 variable sites, of which 8 were parsimony informative. Overall, haplotype diversity (h) varied between 0.2571 (WestC) and 0.8190 (BRA), with average $h = 0.5465$ across all samples combined (Table 7.2). Nucleotide diversity (π) varied between 0.0006 (WestC) and 0.0018 (BRA), averaging $\pi = 0.0011$ across samples (Table 7.2).

Results obtained for estimates of deviation to the hypothesis of COI neutrality varied with the method used (Table 7.2). While most samples exhibited significant departures from neutrality in Fu's F_S and Tajima's D summary statistics, the same was not observed for the Ewens-Waterson's F test (Table 7.2). As both Fu's F_S and Tajima's D are known to show evidence of departures to neutrality due to demographic changes (Excoffier et al. 2005), and obtained results were not consistent through samples and tests, it is likely that observed deviations to neutrality are not due to selective pressures acting upon *T. albacares* COI region. The Tamura-Nei evolution model (with

homogeneous rates among lineages), was determined to be the most suitable nucleotide substitution model for *T. albacares* COI dataset.

Table 7.2: Mitochondrial genetic diversity and neutrality tests for *T. albacares* COI region: **n** – number of individuals; **H** – number of haplotypes; **h** – haplotype diversity; **π** - nucleotide diversity; **F** – Ewens-Watson neutrality test; **D** – Tajima neutrality test; **F_S** – Fu neutrality test. Statistically significant results ($p < 0.05$) in bold.

	BRA	WestC	EastC	KZN	LRE	SEY	KER	Overall
n	15	15	15	15	15	4	12	91
H	7	3	3	6	6	2	3	17
h	0.8190	0.2571	0.5143	0.5714	0.5714	0.5000	0.3182	0.5465
π	0.0018	0.0006	0.0008	0.0008	0.0011	0.0014	0.0007	0.0011
F	0.451	1.000	0.629	1.000	1.000	1.000	1.000	0.999
D	-1.116	-1.685	-0.268	-1.816	-1.983	-0.710	-1.629	-2.290
F_S	-3.434	-0.831	-0.248	-4.982	-3.537	1.097	-0.614	-17.335

Reconstruction of *T. albacares* haplotype network revealed a star-shaped pattern (Figure 7.1), with one very common haplotype found in individuals from all sampling sites, which can be interpreted as an “ancestral” haplotype for *T. albacares*. A second widespread haplotype was observed in individuals from BRA, LRE, EastC and WestC suggesting the retention of ancestral variation across both oceans. It was not possible to identify a clear geographical pattern in *T. albacares* haplotype distribution. Overall, haplotypes differed from the central common type by one to three mutational steps, with the BRA sample exhibiting the highest number of private haplotypes and highest genetic diversity (Figure 7.1).

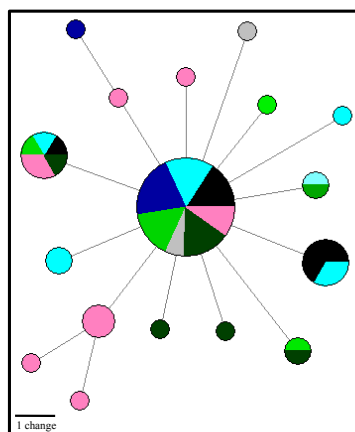


Figure 7.1: Reconstruction of haplotype network for *T. albacares*, based on 700bp of mtDNA COI sequences: ●: KER; ●: SEY; ●: BRA; ●: LRE; ●: EastC; ●: KZN; ●: WestC. Branch lengths are proportional to the number of differences, and node sizes are proportional to the number of haplotypes.

Despite the absence of identifiable geographical patterns among *T. albacares* samples, assessment of population structure using F_{ST} revealed low, but significant, genetic

differentiation between BRA and the remaining samples (Table 7.3). Pairwise F_{ST} values between samples with similar sample size ranged from -0.022 to 0.138 (LRE-KZN and BRA-EastC) (Table 7.3). All comparisons involving BRA were significantly ($p < 0.001$) greater than zero, with the exception of the BRA-SEY comparison, which may represent a statistical artefact due to the SEY small sample size (Table 7.3). No significant values of F_{ST} were observed among remaining samples, after Bonferroni correction for multiple tests (Rice 1989). When the genetic differentiation was calculated based on two putative populations: Atlantic (BRA) and Indian Ocean (WestC + EastC + KZN + LRE + SEY + KER), obtained F_{ST} value was higher ($F_{ST} = 0.142$) and significantly different from zero ($p < 0.001$).

Table 7.3: Pairwise F_{ST} values based on mtDNA COI data, between *T. albacares* samples (see Table 7.1 for sample codes). Values significantly greater than zero ($p < 0.001$) in bold.

	BRA	WestC	EastC	KZN	LRE	SEY	KER
BRA	-						
WestC	0.098	-					
EastC	0.138	0.107	-				
KZN	0.082	-0.015	0.018	-			
LRE	0.082	0.000	0.066	-0.022	-		
SEY	0.057	0.103	0.138	0.023	0.023	-	
KER	0.098	0.002	0.097	-0.004	-0.038	0.069	-

Despite the significant F_{ST} values found between BRA and the remaining samples, no significant differentiation between the Atlantic and Indian Ocean regions was detected using AMOVA: the majority of variance was detected within populations and not among groups (Table 7.4). However, when the Atlantic – Indian Ocean differentiation hypothesis was tested using only the BRA sample as a representative of the Atlantic stock and grouping the WestC sample in the Indian Ocean cluster there was a steep increase in the genetic variance detected among groups, and a decrease in the genetic variance detected within populations (Table 7.4).

Table 7.4: Analysis of molecular variance (AMOVA) results based on COI data, for the two population differentiation scenarios tested. Statistically significant results ($p < 0.005$) in bold.

	BRA + WestC	BRA
	vs.	vs.
	EastC + KZN + LRE + SEY +	WestC + EastC + KZN + LRE
	KER	+ SEY + KER
Among groups	2.49	13.73
Within groups	0.01	1.07
Within populations	92.77	85.19

Evolutionary history

Reconstruction of *T. albacares* evolutionary history was conducted for two putative populations: one consisting solely of BRA (representing the Atlantic Ocean) and one consisting of the remaining samples pooled together (representing the Indian Ocean). The Atlantic Ocean population exhibited higher haplotype (h) and nucleotide (π) diversity levels than the Indian Ocean population (Table 7.5). Tajima's D and Fu's F_S neutrality tests exhibited similar significant deviations to neutrality in both populations (Table 7.5), suggesting the occurrence of past demographic expansions. These results were further corroborated by mismatch distribution analyses, as the SSD tests did not allow rejection of the null hypothesis of past demographic expansion (Table 7.5), and plotting of mismatch distributions exhibited a clear unimodal pattern characteristic of populations that have undergone a demographic expansion in the past (Figure 7.2), in either *T. albacares* population.

Table 7.5: *Thunnus albacares* genetic demographic history for Atlantic Ocean and Indian Ocean populations, based on mtDNA COI sequence variation: genetic diversity levels (h and π); neutrality tests (Tajima's D and Fu's F_S); mismatch distribution parameters: σ - time since expansion in mutation units, θ_0 - population size before expansion, θ_1 - population size after expansion; and time since expansion (T in KY). Statistical significant results ($p < 0.05$) in bold.

	Atlantic Ocean	Indian Ocean
h	0.8190	0.457
π	0.0018	0.0009
D	-1.116	-2.268
F_S	-3.434	-23.391
Mean	1.257	0.646
Variance	0.712	0.614
SSD	0.020	0.0003
σ	1.438 (0.00-3.23)	0.748 (0.00-4.02)
θ_0	0.000	0.142
θ_1	99999.000	1.231
Texp (KY)	34.21 (0.00-76.7)	19.80 (0-95.7)

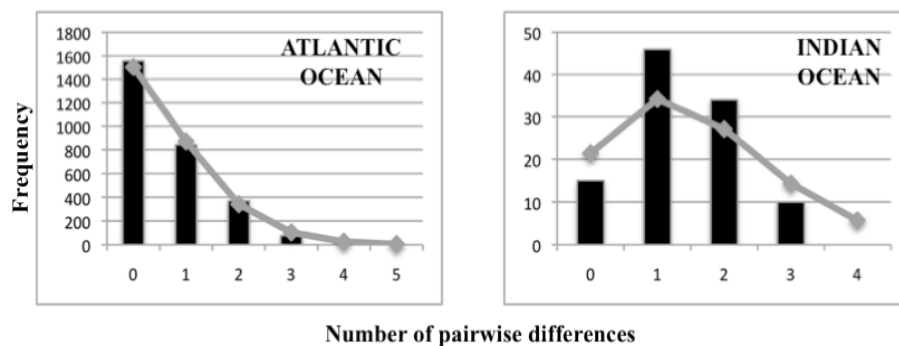


Figure 7.2: Mismatch distribution histograms for Atlantic Ocean and Indian Ocean *T. albacares* populations, based on mtDNA COI sequences. Filled bars indicate the observed frequency of sequence differences, grey line indicates the expected distribution under a model of rapid demographic expansion.

Estimates of time since population expansion were calculated using obtained mismatch distribution parameters (σ), the universal divergence rate for COI derived for fish species (1.5% per MY – Bermingham et al. 1997) and estimating generation time as 2 years (Heemstra & Heemstra 2004). Overall estimates point to population expansion at ~34 KYA and ~20 KYA for the Atlantic and Indian Ocean populations, respectively (Table 7.5).

Microsatellite analyses

Genetic diversity and population structure

As mentioned above, microsatellite analyses require larger samples sizes due to the larger allelic diversity exhibited. Therefore, samples from LRE and KER were grouped together into sample IO as no significant differentiation was detected between them using genic and genotypic variation tests (genic: $\chi^2 = 29.623$, $p > 0.05$; genotypic: $\chi^2 = 20.616$, $p > 0.05$).

Microchecker and GENEPOP analyses did not reveal evidence of amplifications errors such as stuttering or loss of larger alleles, or of linkage disequilibrium for any of the loci tested. However, analyses of Hardy-Weinberg equilibrium showed that loci Tth7-16 and cmrTa113 had significantly positive F_{IS} values across all samples, while loci Tth178 and cmrTa208 showed significant F_{IS} values in samples BRA, EastC, KZN, IO, and BRA, WestC, KZN, respectively (Table 7.6). Analyses conducted in FreeNA suggested that the observed excess of homozygotes for the identified loci with departures to Hardy-Weinberg equilibrium was due to the presence of null alleles. Estimated frequencies ranged from 0.000 (loci Tth34, Tth5 and cmrTa208) to 0.251 (locus Tth7-16), with an average of 0.068 across loci and samples.

Overall expected heterozygosity (H_E) was 0.753, while observed heterozygosity (H_O) was 0.628. Between samples, the WestC presented higher values of expected heterozygosity, while EastC exhibited higher levels of number of alleles and allelic richness (Table 7.6).

Table 7.6: Genetic diversity at 6 cross-specific microsatellite loci in *T. albacares* samples: **n** – number of individuals genotyped; **Na** – number of alleles; **AR** – allelic richness for a minimum of 57 individuals; **H_E** – expected heterozygosity; **H_O** – observed heterozygosity; **F_{IS}** – inbreeding coefficient. Significant deviations to Hardy-Weinberg expectations in bold.

		BRA	WestC	EastC	KZN	IO
Tth178	n	70	63	68	70	59
	Na	11	10	14	12	11
	AR	10.409	9.705	13.589	11.522	10.897
	H_E	0.844	0.799	0.810	0.811	0.806
	H_O	0.771	0.778	0.618	0.629	0.644
	F_{IS}	0.093	0.036	0.245	0.231	0.209
Tth34	n	70	68	67	66	58
	Na	13	15	14	13	14
	AR	15.409	14.384	13.501	12.707	15.000
	H_E	0.804	0.824	0.813	0.829	0.831
	H_O	0.729	0.826	0.821	0.788	0.810
	F_{IS}	0.101	0.005	-0.002	0.057	0.033
Tth7-16	n	70	67	69	70	57
	Na	16	18	19	18	15
	AR	15.409	17.653	18.038	17.407	15.000
	H_E	0.910	0.910	0.907	0.913	0.9.00
	H_O	0.643	0.716	0.681	0.714	0.474
	F_{IS}	0.300	0.220	0.256	0.224	0.481
Tth5	n	70	69	67	68	59
	Na	6	6	6	6	7
	AR	5.998	5.999	5.997	5.999	6.998
	H_E	0.623	0.643	0.617	0.555	0.614
	H_O	0.586	0.667	0.612	0.544	0.644
	F_{IS}	0.260	-0.029	0.015	0.027	-0.006
cmrTa113	n	70	70	70	70	58
	Na	15	16	14	13	15
	AR	14.398	15.206	13.740	12.442	14.931
	H_E	0.866	0.881	0.824	0.857	0.846
	H_O	0.671	0.629	0.600	0.514	0.603
	F_{IS}	0.232	0.293	0.279	0.406	0.295
cmrTa208	n	70	70	70	69	59
	Na	7	7	6	5	3
	AR	6.802	6.746	5.808	4.995	3.000
	H_E	0.459	0.488	0.531	0.475	0.418
	H_O	0.343	0.443	0.500	0.420	0.424
	F_{IS}	0.260	0.100	0.065	0.121	-0.006
Average (all loci)	n	70	68	69	69	58
	Na	11	12	12	11	11
	AR	11.404	11.616	11.779	10.845	10.971
	H_E	0.762	0.773	0.744	0.761	0.741
	H_O	0.631	0.669	0.605	0.641	0.606
	F_{IS}	0.176	0.115	0.156	0.194	0.193

Exact tests of genic and genotypic differentiation, based on allele and genotypic frequencies, revealed evidence of population differentiation between samples. In both cases, the BRA sample was significantly different from all other samples, but there were no significant differences among the remaining samples (Table 7.7). Significant exact tests results between BRA and other samples were predominantly due to variation at loci Tth178, Ta113 and Ta208 (Table 7.7).

Table 7.7: Genic and genotypic χ^2 tests, above and below diagonal respectively, between *T. albacares* samples based on 6 microsatellite loci. Statistically significant comparisons after Bonferroni corrections in bold ($p < 0.005$).

	BRA	WestC	EastC	KZN	IO
BRA	-	44.011	42.881	45.994	∞
WestC	28.424	-	29.566	20.054	20.418
EastC	31.611	20.682	-	25.158	15.321
KZN	29.296	14.195	15.464	-	24.201
IO	32.173	14.164	10.393	15.906	-

Despite the significant differentiation of BRA detected by the exact tests, pairwise F_{ST} values were quite low and ranged from -0.0017 (EastC - IO) to 0.0053 (BRA – EastC) (Table 7.8). Likewise, global estimates of genetic variation were quite low (less than 1% of total variation - $F_{ST} = 0.002$).

Estimates of pairwise F_{ST} did not vary substantially between corrected and uncorrected datasets (Table 7.8), suggesting that the presence of low frequencies of null alleles did not influence the estimates of differentiation. Significant pairwise differences were found between the KZN-BRA samples, after Bonferroni correction (Table 7.8). When genetic differentiation was calculated between the BRA sample and the remaining samples pooled together, obtained F_{ST} value was small and non significant ($F_{ST} = 0.0029$, $p > 0.05$).

Table 7.8: Pairwise F_{ST} values for *T. albacares* obtained with FreeNA, based on 6 microsatellite loci. Uncorrected values are displayed above the diagonal, values corrected by the ENA method are displayed below the diagonal. Significant results in bold ($\alpha = 0.005$).

	BRA	WestC	EastC	KZN	IO
BRA	-	0.0003	0.0053	0.0026	0.0010
WestC	0.0009	-	0.0047	0.0012	0.0003
EastC	0.0059	0.0048	-	0.0033	-0.0017
KZN	0.0037	0.0014	0.0020	-	0.0004
IO	0.0005	0.0010	-0.0002	0.0009	-

Although the STRUCTURE analyses did not detect significant genetic differentiation among *T. albacares* samples ($K = 1$), assessment of genetic discontinuities using Geneland converged to $K = 2$, suggesting the presence of 2 different populations (Figure 7.3). Another run was performed for $K = 2$, revealing the probable geographical position of genetic discontinuities in the dataset (Figure 7.3).

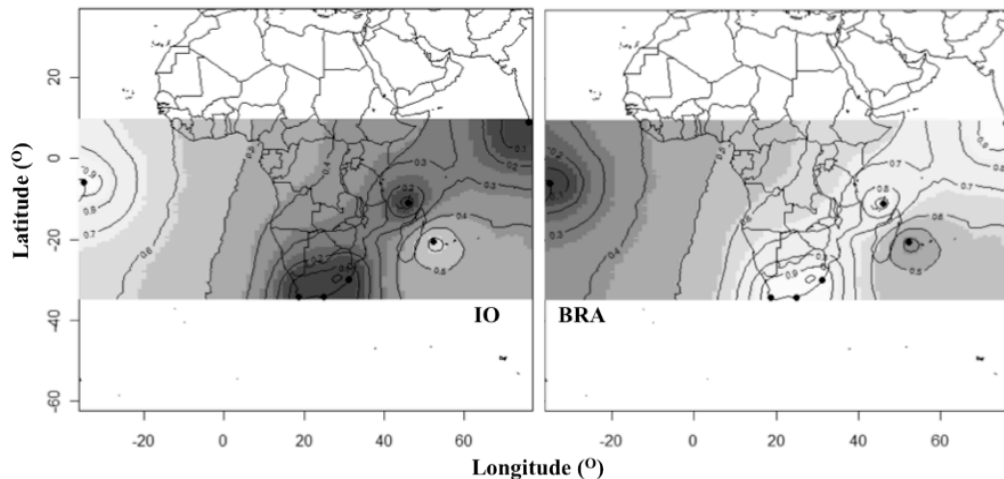


Figure 7.3: Map of posterior probability of population membership of geo-referenced *T. albacares* samples, based on 6 microsatellite loci: Indian Ocean (IO - left) and Atlantic Ocean (BRA - right). Dark colors delineate areas of higher probability of population membership. Black isolines represent the level of genetic differentiation.

As observed for the exact tests of differentiation, the Geneland analysis indicated BRA to be differentiated from the sampling sites in South Africa (WestC, EastC, KZN) and the Indian Ocean. Although no genic or genotypic differentiation was observed between Indian Ocean samples (LRE and KER), which allowed them to be grouped together into the IO sample (see above), it is possible to observe a grouping of South Africa (WestC, EastC, KZN), India (KER) and the 18 samples caught in the north Mozambique Channel (see Table 7.1), separate from the 29 samples collected off the coast of La Réunion island, suggesting a possible sub-structuring within the Indian Ocean.

Assignment tests, based on the Bayesian approach implemented in GeneClass, conducted for sample sites as independent population units, and with an Atlantic-Indian Ocean break enforced, did not retrieve significant results: each individual had equal probability of assignment to any given sample ($p > 0.05$).

Demographic history

Tests for bottleneck events and effective population size (N_e) were conducted for the two putative *T. albacares* populations: Atlantic Ocean (BRA) and Indian Ocean (IO). No significant evidence of heterozygote excess was detected in the bottleneck tests

independently of the test used, and as so the null hypothesis of mutation-drift equilibrium could not be discarded in either population (Table 7.9).

Overall, obtained values of N_e suggest that *T. albacares* populations exhibit relatively large long-term effective population sizes, with N_e estimated at 175.4 and 646.6 individuals, for a critic allelic frequency of 5% (Table 7.9). However, some estimates were negative (* in Table 7.9), which implies an infinite N_e due to the absence of evidence of any disequilibrium caused by genetic drift due to a finite number of parents (Waples 2006). Such a result is commonly related with sampling size bias, where the sample size is smaller than the true N_e , nevertheless N_e can still be manually calculated based on the parameters provided by the LDNe software (harmonic mean and r^2 - linkage disequilibrium measure) (Waples 2006).

Table 7.9: Demographic history of *T. albacares* populations in the northern and southern Benguela sub-systems: probability of significant departure from equilibrium population size (i.e. a bottleneck) and estimates of effective population size (N_e + 95% confidence intervals).

		BRA	IND
Bottleneck events	I.A.M	0.055	0.055
	S.M.M	0.984	1.000
	T.P.M.	0.500	0.945
N_e	N_e (1%)	267.9 (123.9-∞)	11111* (1111.9-∞)
	N_e (2%)	311 (125.3-∞)	8772* (1238.3-∞)
	N_e (5%)	175.4 (77.3-∞)	905.8 (306.3-∞)

7.1.4. Discussion

Genetic diversity levels

Assessment of mitochondrial DNA genetic diversity for the COI gene in *Thunnus albacares* revealed moderate levels of haplotype diversity (overall $h = 0.5465$), and relatively low levels of nucleotide diversity (overall $\pi = 0.0011$). Haplotype diversity within samples ranged from 0.257 to 0.819, while nucleotide diversity varied between 0.0006 and 0.0018. For both parameters, the lowest values were observed in the South African Western Cape province sample (WestC), and the highest in the western Atlantic sample (BRA). These values are very similar in range to those described for other *T. albacares* populations in previous studies (Ely et al. 2005; Dammannagoda et al. 2008; Wu et al. 2010), and for other tuna species such as *Thunnus obesus* (Durand et al. 2005).

Although the presence of null alleles in the nuclear dataset may have some influence in the estimation of allelic frequencies (Chapuis & Estoup 2007), diversity measures such as allelic richness and expected heterozygosity are quite resilient to mean null allele frequencies below 0.15 (Chapuis 2006). As null allele frequencies reported here (except for locus Tth7-16 for sample IO) had means below this threshold, it is considered that nuclear genetic diversity levels can be calculated with confidence. Population genetic assessment of allele frequencies across all sampling sites revealed high levels of genetic diversity within samples. The diversity measures here documented (overall $H_E = 0.753$; range 0.741 - 0.762) are similar to or higher than those obtained in previous studies of *T. albacares*: $H_E = 0.619$ in the western Pacific (Appleyard et al. 2001); $H_E = 0.523 - 0.604$ in northern and southern Pacific (Diaz-Jaimes & Uribe-Alcocer 2006); and $H_E = 0.542 - 0.941$ in Sri Lanka (Dammannagoda et al. 2008). Obtained *T. albacares* gene diversity levels are also similar to those reported for other tuna species, such as *T. obesus* in the Atlantic ($H_E = 0.64 - 0.73$, Durand et al. 2006), and *T. thynnus* ($H_E = 0.64 - 0.70$, Carlsson et al. 2004). Observed differences between nuclear genetic diversity values obtained in this study and the ones previously reported in Appleyard et al. (2001) and Diaz-Jaimes & Uribe-Alcocer (2006) may be related with different fishing impact on the relevant populations, as large fishing effort can have a direct impact on genetic diversity levels in fishes (Kenchington et al. 2003; Hauser & Carvalho 2008). For *T. albacares* the highest catches are reported to occur in the Pacific Ocean, which may be responsible for the observed differences.

Population differentiation and phylogeographic structure

Analysis of population differentiation using the mtDNA dataset revealed a small, but consistent and significant difference between the western Atlantic (BRA) and remaining samples ($p < 0.005$). The Seychelles (SEY) was not indicated as significantly different from BRA, but this may represent a statistical artefact given the small sample size of the SEY sample. Other pairwise F_{ST} comparisons were not significant, ranging from -0.027 (among Indian Ocean samples KZN, LRE and KER), to 0.138 (between Eastern Cape province – EastC – and SEY). The hierarchical analysis of variance did not indicate significant mtDNA differentiation between *T. albacares* populations of the Atlantic and Indian Oceans. However, when the hypothesis of a western Atlantic (BRA) – Indian Ocean (WestC + EastC + KZN + LRE + SEY + KER) differentiation was tested the genetic variance distributed among groups increased, while the genetic variance distributed within populations decreased. Furthermore, when F_{ST} comparisons were

performed between the western Atlantic and the Indian Ocean samples, the observed value was higher and significantly different from zero ($F_{ST} = 0.142$, $p < 0.001$). As so, these results suggest that *T. albacares* in the western Atlantic (BRA) may represent the Atlantic population, while *T. albacares* in the Western Cape province in South Africa (WestC) appear to be genetically closer to the Indian Ocean population, as previously suggested by Ely et al. (2005). The phylogeographic reconstruction of haplotype relationships did not reveal a clear pattern of geographical structuring, as the pattern of one very common (i.e. ancestral) haplotype present in all sampling sites plus many private haplotypes shared only by one to three individuals, does not refute a hypothesis of a single population with high levels of gene flow across the area sampled (Avice 2000). However, a greater degree of grouping of the western Atlantic (BRA) haplotypes may suggest some degree of isolation of this area: of the 7 BRA haplotypes 5 are private (8 individuals), 1 is the ancestral (5 individuals) and only 1 haplotype (2 individuals) is shared with individuals from the remaining sampling sites. Ely et al. (2005) also documented low levels of differentiation between Atlantic and Indo-Pacific samples, based on mtDNA ATCO region. These authors suggested that the observed shallow divergence between what was concluded to be isolated populations possibly resulted from historically large effective population sizes in *T. albacares* preventing substantial differentiation due to genetic drift over the limited time since population isolation. The findings here presented are also consistent with this hypothesis.

After taking account of the presence of null alleles in the dataset, using the ENA option in FreeNA (Chapuis & Estoup 2007) and the null allele option implemented in GENELAND (Guillot & Foll 2009), levels of genetic differentiation (pairwise F_{ST}) for the microsatellite dataset were low and in most comparisons not significant. However, exact tests of allele frequencies indicated small, but significant, differences between BRA and KZN (average $F_{ST} = 0.0027$), a result supported by the GENELAND analysis of genetic discontinuities associated with geographical location. Similar F_{ST} values were reported for other widespread pelagic fish species as *T. thynnus* ($F_{ST} = 0.002$ – Carlsson et al. 2004) and *T. obesus* ($F_{ST} = 0.000$ to 0.003 – Gonzalez et al. 2008) that exhibited significant inter-oceanic genetic differentiation. In addition, no substantial or significant differentiation was detected among South African samples, suggesting that they represent a single population, and that these samples are consistent with being part of the Indian Ocean population grouping rather than the Atlantic grouping. Therefore, and although observed low genetic differentiation could not truly dismiss some level of gene flow, the microsatellite data suggest that population differentiation in *T. albacares* is

mainly found between the Atlantic and Indian Oceans, rather than within each ocean, as observed for mtDNA in this study and previously reported by Ward et al. (1995) and Ely et al. (2005). The results obtained with microsatellite data suggest that observed shallow divergence among *T. albacares* populations might be linked to long term high effective population sizes, which may contribute to decrease genetic differentiation due to drift over the limited time since population isolation.

The observed break between *T. albacares* Atlantic Ocean and Indo-Pacific Ocean populations has also been reported for several other tropical and temperate fishes, such as the pelagic species *T. alalunga* and *T. obesus* (Chow & Ushiyama 1995; Bremer et al. 1998) and the coastal benthopelagic species such as *Diplodus capensis* (see Chapter 3), *Argyrosomus inodorus* (see Chapter 4.2), *Atractoscion aequidens* (see Chapter 5.1) and *Lichia amia* (see Chapter 6), and has traditionally been linked to the presence of the Benguela Current off southern Africa acting as a barrier to gene flow (e.g. Bowen et al. 2001; Lessios et al. 2003; Floeter et al. 2008). In the case of *T. albacares*, the colder sea surface temperatures in the region may be playing an important role in disrupting gene flow between the Atlantic Ocean and Indian Ocean populations. Interestingly, genetic variation observed between the two major clades to either side of this proposed barrier was deeper in the coastal species (nDNA: *D. capensis* $F_{ST} = \sim 0.043$; *A. inodorus* $F_{ST} = \sim 0.036$; *A. aequidens* $F_{ST} = \sim 0.055$) than in the oceanic pelagic *T. albacares* (nDNA $F_{ST} = 0.002$), suggesting that the oceanographic features of the Benguela Current, namely colder sea surface temperatures and the perennial upwelling cell, appear to have a deeper influence in disrupting gene flow in coastal species than in oceanic species such as *T. albacares*. For example, no significant differentiation was observed between dolphinfish individuals from the Atlantic and Indo-Pacific Oceans (Diaz-Jaimes et al. 2010), reinforcing the hypothesis that the colder waters of the Benguela Current have a lesser impact in isolating populations in oceanic pelagic species.

Evolutionary and recent demographic history

Inference of demographic history and population dynamics revealed evidence of a past population expansion in *T. albacares*. The observed star-shaped COI haplotype pattern is commonly found in populations that have undergone an exponential population increase, starting from a small effective size (Avise 2000). The mtDNA genetic diversity levels, Tajima's D and Fu's F_S statistics and mismatch distribution analyses further support this hypothesis. Haplotype and nucleotide diversity levels are useful tools in demographic history inference. Haplotype diversity condenses information on

the number and frequency of haplotypes in a population, regardless of their relationship, while nucleotide diversity measures sequence divergence between individuals, independently of the number of haplotypes (Grant & Bowen 1998; Avise 2000). Grant and Bowen (1998) suggested a specific relationship between these two measures. For example, low haplotype and nucleotide diversity levels are commonly found in populations that have suffered either a severe recent bottleneck or a selective sweep. The observed high haplotype but low nucleotide diversity in *T. albacares* suggests rapid population growth from a small effective population size (Grant and Bowen, 1998). The significantly negative results obtained for Tajima's D and Fu's F_S , combined with the unimodal sequence mismatch distributions do not contradict such a hypothesis of a demographic expansion in *T. albacares*. Similar results were also described for *T. albacares* by Ely et al. (2005) and Dammannagoda et al. (2008).

Reconstruction of demographic changes for the microsatellite dataset is congruent with the reported mtDNA demographic history. Observed high levels of microsatellite genetic diversity imply an absence of severe population bottlenecks in the recent past (10s-100s years). In addition, mutation-drift equilibrium analyses of allele frequencies did not reveal evidence of recent bottleneck events.

Estimates of *T. albacares* effective population sizes (N_e) from the microsatellite data were relatively high. Overall values varied between 656 to 10613 individuals, depending on the lowest allele frequency used. Such values are within the range documented for other fish species: from 100s-1000s (Hauser & Carvalho, 2008), and are well above the considered minimum threshold for maintenance of a species evolutionary potential ($N_e > 500$ Frankham et al.). Ely et al. (2005) reported an historical female N_e of 535 individuals. Thus, *T. albacares* appears to have maintained high effective population sizes at least through recent historical timescales.

Given the suggested demographic history for *T. albacares* (past bottleneck plus population expansion, but not in the recent past, and large effective population size), the shallow genetic divergence between Atlantic Ocean and Indian Ocean populations could be consistent with recent historical isolation (i.e. limited or absent gene flow) where genetic drift is restricted by large population sizes.

Implications for fishing and conservation efforts

Cosmopolitan distributions, migratory nature and high effective population sizes have a synergistic effect in increasing the difficulty of assessing population structure in large pelagic fishes (Riccioni et al. 2010). The findings here presented for *T. albacares*

support previous studies (Ward et al. 1997; Ely et al. 2005) in suggesting the existence of a shallow population structure, which separates Atlantic Ocean and Indian Ocean stocks. No differentiation was detected within the South African population, despite these stocks being distributed across the confluence of the two oceans. In fact, both mtDNA and microsatellite markers suggest that *T. albacares* captured off the Atlantic coast of South Africa are more closely related to Indian Ocean populations. However, one caveat of the present study is the absence of *T. albacares* samples from the eastern Atlantic. The observed shallow differentiation between individuals from western Atlantic (BRA) and southeastern Atlantic (WestC) may be a result of population substructuring within the Atlantic Ocean. Bard & Scott (1991) suggested that *T. albacares* in the Atlantic are composed of only one stock, with seasonal migration from eastern to western areas. Scoles & Graves (1993) likewise did not detect population structuring within *T. albacares* across the Atlantic basin. The combination of the obtained results in the present study and previous findings support the hypothesis that *T. albacares* in South African waters are an extension of the Indian Ocean population.

In South Africa, the Western Cape province tuna fishery is regulated by the ICCAT, while the Eastern Cape and KwaZulu-Natal fisheries are regulated by the IOTC. Based on the present findings it is suggested that the stocks should be managed only by the IOTC, and should be considered part of the Indian Ocean stock. On a more global scale, *T. albacares* appears to be composed of ocean-scale populations with very high effective population sizes, and if there is genetic subdivision of the global population in the Atlantic and Indo-Pacific Oceans these populations are very similar genetically. These characteristics may make the species more resilient to fishing than other tuna species. However, if the species is harvested at the same levels as *T. thynnus* a subsequent crash will ensue. Therefore, future management plans should restrict the volume of catches to ensure the maintenance of the species evolutionary potential.

DISCUSSION

CHAPTER 8: General Discussion and Conclusions

8.1. Limitations of the present work

Before starting any work intended to investigate distribution and organization of genetic diversity within and among populations it is necessary to define accurate sampling and which markers to use.

In order to guarantee a representative and comprehensive sampling strategy, it is required to sample evenly throughout a species distribution range, while collecting sufficient number of replicates to ensure statistical significance (Chakraborty 1992). In theory, each sample should represent a single sub-population or deme (Balloux & Lugon-Moulin 2002), and a single generation, as genetic diversity can vary not only in space but also in time (Waples 1998). However, it may be difficult to accurately know in advance sub-population structure, which leads one to consider each sample as one deme. Furthermore, some species such as fish may exhibit long-lived individuals and overlapping generations that make accurate temporal sampling difficult (Waples 1998; Balloux & Lugon-Moulin 2002). In addition, biological and environmental information should also be collected, if possible, to help interpretation of observed patterns of genetic variability.

Genetic population sub-structuring can result either from genome-wide processes such as reduced gene flow and genetic drift, or locus-specific processes such as recombination, selection and mutation (Whitlock & McCauley 1999). Genetic markers neutral to the effects of selection are used in molecular ecology studies to assess evolutionary history, phylogeographic patterns, genetic diversity, variation within and among populations, and gene flow (Avice 2000; Sunnucks 2000; Balloux & Lugon-Moulin 2002; Beebee & Rowe 2005; Selkoe & Toonen 2006), as locus-specific selection effects can bias estimation of these parameters.

Although these considerations were taken into account when preparing the present work, there were some limitations that could not be overcome, and so should be accounted for.

8.1.1. Sampling

As with many studies of marine species, sampling was the most limiting step in the present work due to difficulties in physical access to sites and samples, and to obtain the required number of replicates for each marker used.

Based on the Benguela Current configuration, extensive sampling was to be conducted throughout three different countries: Angola, Namibia and South Africa. However, time and financial constrictions severely limited the original sampling strategy and led to a larger effort being conducted in Angola, where the Angola and Benguela Currents meet. Although in limited numbers, it was still possible to obtain samples from the three countries, due to the establishment of local collaborations. One major limitation of the present work is the absence of sampling sites from southern Namibia and western South Africa that would be necessary to identify the specific position of the boundaries of each reported population. Nevertheless, most of the study species show a distribution break in this area, or exhibit very low abundance (W. Potts, personal communication), and the sampling distribution may indeed reflect the species distribution, or at least the areas where it is abundant enough to sample effectively.

Special attention was given to obtain a sufficient number of individuals for each marker used. In all cases, individuals were obtained from local markets, inshore subsistence fisheries and recreational anglers either personally, in three main sampling campaigns conducted in southern Angola during June of 2008, 2009 and 2010, or by local collaborators in Angola, Namibia and South Africa. The number of individuals collected for each studied species in each site was highly dependent on composition of daily catches and the good will of the fishermen. In some cases, such as *Lichia amia*, it was not possible to obtain the required number of individuals at all since local fishermen did not commercially target the species and it is very difficult to personally catch large numbers of this species by rod-and-line, so this species was not included in some statistical analyses.

8.1.2. Markers and statistical analyses

In the present work three different types of neutral markers (mitochondrial DNA regions, nuclear gene locus, and nuclear microsatellite markers) were employed to address questions of evolutionary history, species composition, distribution of genetic diversity, gene flow and population sub-structuring. The combination between these

types of neutral markers has been extensively used in molecular ecology studies since they provide a deeper insight into the evolution of species population structure and genetic diversity through time, due to their different nature, variability and sensitivity (Beebee & Rowe 2005). In particular, in marine species microsatellites have helped to detect population sub-structuring even at small spatial scales (e.g. Galarza et al. 2009). In the present study, some species exhibited evidence that could indicate a possible cryptic population structure within sites, due to significant deviations from Hardy-Weinberg equilibrium in loci that did not exhibit significant frequencies of null alleles. These findings may suggest the existence of sub-structuring by mixing of different genetic pools or due to differential selective pressures. However, such initial evidence was not confirmed in further analyses. As marine species commonly exhibit high effective population sizes and dispersal potential, larger numbers of loci and individuals are required in population analyses (Chakraborty 1992). Thus, it is possible that the inability to detect sub-structuring and accurately assign individuals to the original population, in some of the studied species, could be related to insufficient statistical power. However, given the presence of distinct genetic differentiation between populations in some parts of the range of each of the species studied (i.e. that where present differentiation was detected by the markers used), it would appear that the marker combinations used did have sufficient power to detect major patterns of genetic differences, which was the main aim of the present study. An emergent field in the study of population sub-structuring in marine species suggests that loci under selection should be used, as they require a smaller number of replicates and can detect local adaptation, thus recovering a species “true” genetic structure (Tobler et al. 2009; Andre et al. 2011; Ingram 2011; Ruzzante et al. 2011). However, at the present time markers known to be under selection were not available for the studied species, but would be an important area to investigate in future given the substantial environmental and habitat variation present across the area and species studied.

8.2. Contributions to the knowledge of genetic population sub-structuring of marine species

8.2.1. Genetic diversity and population structure of the study species

Traditionally, marine species are assumed to exhibit panmictic (or at most shallow) population sub-structuring throughout their distribution due to high dispersal potential, shallow (i.e. recent) evolutionary histories, and historically large effective population sizes (Palumbi 1992). An increasing number of studies have, however, revealed significant genetic differentiation in some species, even at small spatial scales (Clark et al. 2004; Evans et al. 2004; Dammannagoda et al. 2008; Galarza et al. 2009). Commonly, such genetic discontinuities are associated with barriers to gene flow such as biogeographical boundaries, oceanographic currents, upwelling cells and physical gradients (Gaggiotti et al. 2009; Galarza et al. 2009; White et al. 2010).

The Benguela Current is considered an important biogeographical barrier within the Atlantic (Floeter et al. 2008), being responsible for isolating members of the temperate and tropical marine fauna between the Atlantic and Indo-Pacific Oceans (e.g. Bowen et al. 2001; Lessios et al. 2003; Floeter et al. 2008). In the present work, one of the main aims was to assess the influence of the Benguela Current oceanographic features in genetic sub-structuring and gene flow of local fish species. Five different inshore (*Diplodus capensis*, *Argyrosomus inodorus*, *Argyrosomus coronus*, *Atractoscion aequidens* and *Lichia amia*) and one offshore species (*Thunnus albacares*) were studied, as it is easier to identify the influence of external factors in genetic differentiation in multiple species by a comparative approach (Hemmer-Hansen et al. 2007). Using evidence from mitochondrial and nuclear markers, a common pattern emerged in all inshore fish species: substantial genetic differentiation between samples collected in the northern and southern regions of the Benguela Current system, but no significant divergence among samples within each region. Furthermore, mitochondrial DNA (mtDNA) results revealed historical absence of gene flow between these genetic clusters, with the exception of *A. inodorus*. Even for *T. albacares*, the pelagic species, small but significant genetic differentiation was observed across the Benguela region, between the western Atlantic Ocean and Indian Ocean populations.

In the marine realm, average levels of genetic divergence for fish species are commonly small ($F_{ST} = 0.020$ for nuclear microsatellites), and lower than observed in freshwater ($F_{ST} = 0.144$) or anadromous ($F_{ST} = 0.081$) species (Ward et al. 1994b; but see Waples 1998). In the present work, population differentiation levels varied between markers, species and sampling sites, but the majority were consistently higher than often observed for marine fauna. Overall, *A. aequidens* exhibited the highest pairwise F_{ST} values, in particular for mtDNA, for the comparison between Angolan and South African samples (Chapter 5.1). In fact, observed genetic divergence was so high that it led to an additional study into the species level status of the two populations. Reconstruction of phylogenetic relationships using both mitochondrial and nuclear markers revealed evidence of cryptic speciation, with the northern samples proposed as constituting a distinct independent species from the southern samples (Chapter 5.2). In addition, microsatellites were isolated and primers developed for what is now known to be the northern Benguela *Atractoscion* species to help address questions of genetic sub-structuring in each species (Chapter 2.2.3). Developed markers proved to be highly polymorphic in both *A. aequidens* populations, and observed diversity levels were similar in range to those described for other teleost species (e.g. Gold & Richardson 1998; Gold et al. 2001; Riccioni et al. 2010), and in the other study species – *D. capensis* (Chapter 3), *A. inodorus* (Chapter 4.2), *A. coronus* (Chapter 4.3), and *T. albacares* (Chapter 7). As observed with mtDNA, assessment of population sub-structuring in the northern Benguela population with microsatellite markers revealed one panmictic population, despite sampling sites being thousands of km apart across an area where the environment is unstable due to the confluence of the Angola and Benguela Currents (Chapter 5.1).

As observed for *A. aequidens*, analyses of population structure of *D. capensis* and *L. amia* also revealed strong genetic divergence (mtDNA mean $F_{ST} = 0.77$ and $F_{ST} = 0.90$, respectively – $p < 0.001$) between northern and southern Benguela samples (Chapters 3 and 6), allowing rejection of the null hypothesis of panmixia across the whole region in these species. However, due to limited number of samples and replicates per site, it was not possible to investigate *L. amia* genetic sub-structuring using microsatellites.

In *D. capensis*, amplification of 8 cross-specific microsatellite markers, developed for the European sparids *Diplodus sargus* (Perez et al. 2008) and *Diplodus vulgaris* (Roques et al. 2007), revealed a pattern of genetic sub-structuring across the Benguela Current identical to what was obtained with mtDNA analyses, and observed for both *A. aequidens* and *L. amia*. Interestingly, significant deviations from Hardy-Weinberg

equilibrium due to an excess of homozygotes were reported for one South African sample, at loci that did not exhibit significant frequencies of null alleles (Chapter 3). Deviations from Hardy-Weinberg can result from null alleles, different selective pressures or the mixing of different genetic pools in the site – the Wahlund Effect (Sinnock 1975; Lenfant 2002; Gonzalez et al. 2008). Similar results were documented for *D. sargus*, where no genetic differentiation was observed across the Mediterranean Sea (Lenfant & Planes 1996; Bargelloni et al. 2005; Domingues et al. 2007) but was found within localities, suggesting that population sub-structuring was temporal and not spatial (Gonzalez-Wanguemert et al. 2004; Gonzalez-Wanguemert et al. 2007; Gonzalez-Wanguemert et al. 2010; Kaouèche et al. 2011). In addition, assignment tests detected high levels of nuclear admixture between the two genetic clusters, despite the observed historical absence of female (mtDNA) gene flow. Such disparity between mitochondrial and nuclear markers has also been observed for other marine species (e.g. Lemaire et al. 2005; Gonzalez et al. 2008; Larmuseau et al. 2010; Tatarenkov et al. 2010) including *D. sargus* (Domingues et al. 2007), and may be related to male-biased dispersion, as observed in sandbar sharks (Portnoy et al. 2010). However, there is no evidence of sex-biased dispersion in *D. capensis*, and individuals are functional protandric hermaphrodites (Mann & Buxton 1998; Richardson 2010), developing from males into females. All individuals can contribute to the mitochondrial gene pool, and thus if contemporary gene flow was male-biased it would still be detected in mtDNA analyses. In this case, apparent differences between *D. capensis* mtDNA and microsatellite DNA may have resulted from the different nature of each marker, as suggested by Domingues et al. (2007) in *D. sargus* (see Chapter 3).

Assessment of *A. inodorus* population structure was limited due to a small number of sampling sites, and thus obtained results should be considered preliminary. Even so, it was possible to observe a genetic break across the Benguela Current identical to that observed in *D. capensis*, *A. aequidens* and *L. amia*, although divergence levels were considerably lower in *A. inodorus* (Chapter 4.2). These findings may imply that isolation between northern Namibia and eastern South Africa populations may be more recent than observed in the other study species, and possibly related to large long term effective population sizes in *A. inodorus* that would limit the accumulation of genetic differentiation due to drift. In addition, these results may also indicate the occurrence of occasional gene flow across the Benguela Current region, as the system experiences years of complete circulation disruption due to climate induced changes (the Benguela Niños), with increased sea surface temperatures and breakdown of the perennial

upwelling cell off central Namibia (Shillington et al. 2004). If recurrent gene flow does occur in *A. inodorus*, then it would be interesting to investigate what it is about the biology of this species that allows it to migrate across the upwelling region when the other study species cannot.

Investigation of genetic sub-structuring of *A. coronus* was possible only in Angola and central Namibia, as this area constitutes the main distribution range of the species (Griffiths & Heemstra 1995). *A. coronus* was not examined to compare divergence levels across the Benguela Current, but rather within Angola, where the Angola and Benguela Currents meet and form the Angola-Benguela Front (Chapter 4.3). As observed in *D. capensis* and *A. aequidens*, no significant genetic differentiation of populations was detected across this region when screened at 6 cross-specific microsatellite loci, even though sampling sites spanned thousands of km and were distributed across the areas of influence of both the Angola Current and Benguela Current. Such results support the hypothesis proposed by Potts et al. (2010) that *A. coronus* is composed of one panmictic population, that exhibits a seasonal return migration linked to the displacement of the Angola-Benguela Front.

As observed in the other study species, no significant genetic differentiation was detected in *T. albacares* across South Africa (Chapter 7). In this case, the sampling strategy was different as the main aim was to investigate population genetic sub-structuring between the Atlantic and Indian Oceans, with particular focus on the coast of South Africa. However, by including samples from Western Cape in South Africa and northern Brazil, it was possible to indirectly assess the influence of the Benguela Current as a barrier to dispersal by *T. albacares*. Overall, levels of genetic differentiation in *T. albacares* were the lowest observed for any species in this study, and agree with what is expected for a globally distributed pelagic fish species with potential for extensive dispersal by both adult and early life history stages (Waples 1998; Ward 2000; Andre et al. 2011). Very low, but statistically significant, levels of genetic differentiation were observed between the Brazilian samples and samples from the western Indian Ocean (including all South African sites), suggesting the breakdown of gene flow among *T. albacares* populations. The inclusion of the South African west coast sample (technically in the Atlantic Ocean) within the Indian Ocean genetic cluster provides further evidence that it is the Benguela Current system (rather than the Atlantic Ocean-Indian Ocean boundary) that acts as a barrier to gene flow in this region. Although the results obtained were not completely conclusive, lower levels of genetic divergence observed for *T. albacares* compared to other (coastal) fish species across the

region suggest either that *T. albacares* populations in the Atlantic and Indian Oceans are more recently isolated than for other species, or that there is some level of recurrent gene flow across the Benguela Current region. In addition, historically high levels of effective population size in an abundant pelagic species such as *T. albacares* can also have contributed to the observed small genetic differentiation, as it would limit divergence due to drift.

The observed genetic discontinuities in *D. capensis*, *A. inodorus*, *A. aequidens*, *L. amia*, and to a smaller extent in *T. albacares*, all coincide with two major oceanographic features of the Benguela Current region: the perennial upwelling cell off Lüderitz in central Namibia; and the region of colder waters off southern Namibia (Shannon 1985; Hutchings et al. 2009). The Lüderitz upwelling cell divides the Benguela Current into two environmentally different sub-systems, the northern and southern Benguela (Shannon 1985; Hutchings et al. 2009). A recent study by Lett et al. (2007) revealed that the upwelling cell acts as an impermeable barrier to the longshore transport of pelagic eggs and larvae, contributing to larval retention, and thus disrupting gene flow between northern and southern Benguela (Lett et al. 2007). Similar findings of population genetic differentiation have been observed in other species distributed across areas with local upwelling elsewhere in the world, for example in the New Zealand starfish *Patiriella regularis* (Waters & Roy 2004), the pantropical sea urchin *Tripneustes* spp. (Lessios et al. 2003) and the southern African mussel *Perna perna* (Zardi et al. 2007). However, contrary to what is observed in the species in the present study, dispersion in the examples cited above was mainly restricted to the early stages of the life cycle as in each case the adults are non-vagile life stages. *Diplodus capensis*, *A. inodorus*, *A. aequidens*, *L. amia* and *T. albacares* all have the ability to migrate as juveniles, sub-adults and adults and so the observed levels of genetic differentiation, and suggested absence of gene flow, must also be related to mechanisms other than simply physical movement effects of the perennial upwelling cell.

Most marine species exhibit specific temperature requirements throughout their life cycle, with sea surface temperatures being particularly important cues for larval development, reproduction and feeding. In the Benguela Current system distinct seasonal and geographical patterns of variation in sea surface temperatures appear to influence the seasonal migrations of *A. coronus* (Potts et al. 2010) and *A. inodorus* (Kirchner & Holtzhausen 2001), induce reproduction in *D. capensis* (Richardson 2010), and are associated with distribution breaks in *A. aequidens* (Griffiths & Hecht 1995), *L.*

amia (Potts et al. 2008) and *A. inodorus* (Griffiths & Heemstra 1995). Therefore, the colder sea surface temperatures off the coast of southern Namibia and western South Africa may act as an environmental barrier to dispersion by adults as well as larvae in these species, contributing to the observed levels of genetic differentiation. As *A. inodorus* appears to be more cold tolerant, occurring at greater depths than other kob species (Griffiths & Heemstra 1995), it is possible that adults of this species could still be able to disperse across southern Namibia, where low sea surface temperatures are considered unsuitable for the occurrence of study species such as *L. amia* and *A. aequidens* (Griffiths & Hecht 1995; Potts et al. 2008). Likewise, the observed shallow divergence in populations of *T. albacares* may be linked to the species life history features, namely its offshore migration abilities. While the inshore species in this study are limited to coastal areas where the influence of the Benguela Current oceanographic features is felt with higher intensity, *T. albacares* adults may be able to avoid the potential barrier of cold and turbulent waters in the shallow coastal areas due to its offshore migration abilities, indicated by the facility of individuals to migrate across the Pacific Ocean (5000 km of open ocean - Appleyard et al. 2001).

As the high levels of genetic divergence observed between *D. capensis* and *A. aequidens* populations in the northern and southern Benguela sub-systems were accompanied by significant biological and morphological differentiation (W. Potts, personal communication; Richardson 2010), it is likely that isolation in these species may have been followed by local adaptation (Waples 1998; Schulte 2001). The detection of loci under divergent selection in *D. capensis* and *A. aequidens* (Chapters 3 and 5.1) may further support this hypothesis.

Despite the environmental heterogeneity present within the northern Benguela sub-system, no significant subpopulation genetic differentiation was observed within Angolan *D. capensis*, *A. aequidens* and *A. coronus*. As suggested by Galarza et al. (2009), the influence on genetic structuring of oceanographic features such as the Lüderitz upwelling cell and the Angola-Benguela Front will depend on a species' life history, particularly adult migration abilities and temperature tolerance, and duration of early life stages.

As mentioned above, the colder sea surface temperatures off southern Namibia are thought to constitute unsuitable habitat for the occurrence of *A. aequidens* contributing to the isolation of populations across the Benguela Current region. However, Angolan *A. aequidens* adults are found along the Angolan coast throughout the year (W. Potts,

personal communication), suggesting that the regional oceanographic features of the northern Benguela sub-system do not have a major impact in the species distribution range and, subsequently, in genetic sub-structuring. *A. coronus* exhibits an annual return migration that appears to be linked to the seasonal displacement of the Angola-Benguela Front (Potts et al. 2010), and exhibits one specific spawning ground in southern Angola, which may have contributed to the observed genetic homogeneity. On the contrary, in the case of *D. capensis*, tagging studies by Richardson (2010) suggested that adults were highly resident, remaining within a 10 km radius of their capture-release site. It would be expected to find some level of genetic sub-structuring across the Angolan coast, if the movements of adults were the main form of dispersal in *D. capensis*. However, independently of the degree of mobility and residency of adults, all species exhibit protracted spawning seasons plus pelagic eggs and larvae, all features that are thought to potentially increase dispersion and survival (Griffiths & Hecht 1995; Griffiths & Heemstra 1995; Silberschneider & Gray 2008; Potts et al. 2010; Richardson 2010). Although no information is available on larval ecology of Angolan *A. aequidens* and *A. coronus*, studies conducted on Australian *A. japonicus* revealed that settlement occurs on average one month after spawning and larvae are able to disperse up to 22.4 km at velocities of up to 16.6 cm.s^{-1} (Clark et al. 2005). As *A. japonicus* and *A. coronus* exhibit very similar life history features (Griffiths 1996; Potts et al. 2010) it is likely that the larval characteristics of the two species are also similar. Likewise, South African *D. capensis* larvae settle at 12 mm (~28 days), appear to be able to disperse long distances without feeding (up to 32.4 km) and at speeds of up to 35.2 cm.s^{-1} , a value greater than any previously obtained for other temperate Sparidae larvae (Patrick & Strydom 2009). Prolonged larval stages are known for contributing to homogenize populations, as they can settle many km from their point of origin (Neethling et al. 2008; Galarza et al. 2009), and so it is likely that they may be contributing to the observed panmictic population structures within the Angolan population. Therefore, observed population structure of *D. capensis*, *A. coronus* and *A. aequidens* in the northern Benguela sub-system appears to have resulted from a combination between adult dispersal abilities, and early life stages features.

8.2.2. Comparison of patterns of genetic diversity between the Benguela Current and other oceanographic systems of the world

In the marine realm, average levels of genetic divergence for widespread marine teleosts are commonly small (average $F_{ST} = 0.020$ for nuclear microsatellites – Ward et al. 1994b; but see Waples 1998). Low genetic differentiation of marine species is thought to be related to high dispersal potential (as adults or larvae), recent (“shallow”) evolutionary histories (i.e. not enough time has elapsed to accumulate large genetic divergence) and historically high effective population sizes (which slow divergence under genetic drift). In particular, large pelagic species such as *Thunnus thynnus* (mtDNA $F_{ST} = 0.023$; nDNA $F_{ST} = 0.002$ - Carlsson et al. 2004), *Thunnus obesus* (nDNA $F_{ST} = 0.000$ to 0.003 - Gonzalez et al. 2008), and *Coryphaena hippurus* (mtDNA $F_{ST} = 0.000$ to 0.571 - Diaz-Jaimes et al. 2010) are typical cases of shallow genetic differentiation of marine species. However, recent studies have revealed that inshore / coastal species, such as *Diplodus sargus* (nDNA $F_{ST} = 0.000$ – 0.118, Domingues et al. 2007), *Diplodus vulgaris* (nDNA $F_{ST} = 0.018$, Galarza et al. 2009) and *Mullus surmuletus* (nDNA $F_{ST} = 0.071$, Galarza et al. 2009), may exhibit slightly higher levels of genetic differentiation, which are thought to be linked to regional oceanographic features.

Traditionally, the disruption of gene flow and subsequent genetic differentiation in marine species has been associated either with substantial biogeographical barriers such as the mid-Atlantic Barrier (e.g. *Clepticus brasiliensis-africanus*, Heiser 2000) and the freshwater input of the Amazon and the Orinoco Rivers, or with oceanographic features such as the frontal systems off southern Australia (e.g. *Tursiops* sp., Bilgmann et al. 2007), the Humboldt Current and its associated upwelling areas (e.g. *Jehlius cirratus* and *Notochantalmus scabrosus*, Zakas et al. 2009), the Antarctic Polar Front (e.g. *Dissostichus eleginoides*, Shaw et al. 2004) and the Atlantic-Mediterranean transition (*Diplodus sargus*, Domingues et al. 2007). In most cases observed genetic differentiation was higher in species isolated by biogeographical barriers than in species isolated by oceanographic features, as the latter can be more permeable to gene flow than the former.

It is interesting to note that levels of population genetic differentiation reported in the present study for most inshore species tested were higher than those observed in species distributed across other oceanographic systems such as the Humboldt Current region (*Cancer setosus*: $F_{ST} = 0.026$, Gomez-Uchida et al. 2003; *Dosidicus gigas*: $F_{ST} = 0.076$

– 0.151, but no significant differentiation within the Humboldt Current, Sandoval-Castellano et al. 2007), the Atlantic-Mediterranean transition (*Diplodus sargus*: $F_{ST} = 0.00 - 0.328$, Domingues et al. 2007) or the western Mediterranean frontal system (Galarza et al. 2009). In fact, levels of genetic divergence obtained in the present study were more similar to those reported for species separated by the Isthmus of Panama (e.g. *Anisotremus virginicus-taenitus* Bernardi & Lape 2005), an obviously impermeable barrier to marine species genetic exchange. Therefore, although Floeter et al. (2008) considered the Benguela Current as a ‘soft’ biogeographical barrier in the Atlantic Ocean, as the Humboldt Current appears to be in the eastern Pacific Ocean, the present work revealed that the oceanographic features of the Benguela system may be a major barrier that actively disrupts gene flow in inshore species within its boundaries, and the level of its influence in shaping genetic sub-structuring appears to depend on the species life histories. Furthermore, combination of results obtained with mitochondrial DNA and nuclear microsatellites suggest that disruption of gene flow and population genetic divergence in species across the Benguela Current region it is not only historical but remains an ongoing process.

8.3. Contributions to the knowledge of evolutionary and demographic history in marine species

8.3.1. Evolutionary history of the study species

Present distribution ranges, patterns of genetic variability and population connectivity in many cases result from the interaction of both contemporary and historical processes (e.g. Avise et al. 1998; Lo Brutto et al. 2011). In the marine realm, climate-induced environmental changes during the Pleistocene have influenced the evolutionary history of many species through cyclical changes in sea surface temperatures, sea levels, paleoproductivity and circulation patterns (e.g. Grant & Bowen 1998; Graves 1998; Grant & Bowen 2006; Hemmer-Hansen et al. 2007; Janko et al. 2007; Worheide et al. 2008; Kenchington et al. 2009; Bester-van der Merwe et al. 2011). With particular reference to the present project, the strengthening of the upwelling component of the Benguela Current during the Pleistocene has been suggested as a major factor underlying the isolation of multiple taxa between the Atlantic and Indian Oceans (Lessios et al. 1999; McCartney et al. 2000; Bowen et al. 2001; Colborn et al. 2001). Furthermore, many other species occurring in the Benguela Current region exhibit evidence of past population expansions during the end of the last glacial period and beginning of the warmer Holocene period, such as Cape Hake (von der Heyden et al. 2010), rock lobster (Matthee et al. 2007) and gobies (Neethling et al. 2008).

In the present work, reconstruction of evolutionary histories of all study species revealed evidence of past demographic changes that appear to coincide with periods of major climate-induced oceanographic changes in the Benguela Current during the Pleistocene. Based on reconstruction of phylogenetic relationships using mitochondrial and nuclear markers, mitochondrial diversity indices, mismatch distribution analyses and phylogeographic networks, three key events or periods were indicated:

1 – Allopatric isolation of populations in northern and southern Benguela sub-systems, and subsequent speciation of *Argyrosomus* spp. and *A. aequidens* dating from the Pleiocene-Pleistocene transition (~2 MYA);

- 2 – Allopatric isolation and sub-specific genetic divergence of populations in the northern and southern Benguela sub-systems of *D. capensis* and *L. amia*, dating from the mid- to late Pleistocene major glacial periods (0.5 – 0.1 MYA);
- 3 – Population crashes followed by demographic expansions in all study species, dating from the most recent glacial period (120 – 10 KYA).

The evolutionary histories of *Argyrosomus* spp. and *A. aequidens* populations in the Benguela Current region were very similar. In both cases intensification of the upwelling system, with subsequent decrease of sea surface temperatures and lowered sea levels, appear to be connected with genetic isolation of populations either side of the perennial upwelling cell. In *A. aequidens* this process led to a cryptic speciation event, resulting in the formation of a new species (Chapter 5.2). *A. aequidens* genetic divergence can be considered a classic case of allopatric speciation associated with the formation of a vicariant barrier (Mayr 1942). Evolution of *Argyrosomus* spp. in the eastern Atlantic, with a particular focus in the Benguela Current system, appears to have been a more complex process, with multiple independent speciation events (Chapter 4.1). The observed antitropical distribution of *Argyrosomus* in the eastern Atlantic may have resulted from transequatorial expansions or colonizations during colder glacial periods, followed by allopatric speciation of *A. regius* from a southeastern Atlantic *Argyrosomus* species (that was the common ancestor of *A. inodorus*, *A. coronus* and *A. japonicus*) during warmer interglacial periods, where the tropical waters would constitute a vicariant barrier to dispersion (Brigg 1987; Burrige 2002). As observed for *A. aequidens*, the sister-species relationship found between *A. coronus* and *A. japonicus*, occurring in Angola and South Africa respectively, also implies isolation and speciation due to a vicariant barrier (Mayr 1942; Floeter et al. 2008). However, the earlier and more pronounced divergence of *A. inodorus* appears to have resulted from ecological speciation, which tends to be faster and derives from colonization of a new habitat, followed by local adaptation and speciation (Rundle & Nosil 2005). The hypothesis of two different types of speciation events in kob is further supported by observed differences in the biological and life history features of the four species. While *A. regius*, *A. coronus* and *A. japonicus* exhibit similar features, consistent with allopatric speciation (not driven by selective differences that would then alter morphological or life history characteristics), *A. inodorus* is the most differentiated species in terms of habitat occupancy, maximum size, growth rate, reproductive biology, and cold- and depth-tolerances (Griffiths & Hecht 1995; Griffiths 1996, 1997a; Kirchner 1998;

Cowley et al. 2008; Potts et al. 2010), suggesting that the latter species evolved in a different environment. Likewise, *T. albacares* exhibited evidences of past population contraction and expansion around 20 KYA (Chapter 7).

Argyrosomus coronus, *A. inodorus*, *A. aequidens* and *T. albacares* all exhibited evidence of recent population crashes and subsequent expansions, dating from the Last Glacial Maximum (Chapters 4.2, 4.3, 5.1). Interestingly, time since expansion for these large coastal fish populations was estimated at 30-25 KYA, which coincides with the timing of a reported crash in small pelagic fish species in the Benguela Current region (41-25 KYA, Grant & Bowen 2006), possibly related to a decrease in productivity in the region (Marlow et al. 2000; Jahn et al. 2003). Availability of prey is considered an important regulator of population dynamics (Mueter et al. 2007), and thus a crash in small pelagic populations may have led to a population decline in these larger predatory coastal species, as small pelagics currently compose their main dietary component (Griffiths & Hecht 1995b; Griffiths 1996; Kirchner 1998; Potts et al. 2010). Similar patterns of population decline and expansion during the Last Glacial Maximum have been proposed not only for coastal species, such as *Merluccius capensis* in the Benguela Current region (von der Heyden et al. 2010), *Lyphophrys pholis* in the northeastern Atlantic (Francisco et al. 2011), *Pleuragramma antarcticum* in the Antarctic (Zane et al. 2006) and *Diplodus sargus* in the northeastern Atlantic (Domingues et al. 2007), but also for other pelagic species such as *Engraulis* spp. (Grant & Bowen 2006) and *Thunnus obesus* (Gonzalez et al. 2008).

Although on different timescales, the evolutionary histories of *D. capensis* and *L. amia* were very similar to those reported for *Argyrosomus* spp. and *A. aequidens*. In both cases, there is clear genetic divergence between northern and southern Benguela populations, while each population exhibited evidence of past demographic expansions (Chapters 3 and 6). However, the estimated time since divergence was far more recent than suggested for *Argyrosomus* spp. and *A. aequidens*, and dated from the mid- to late Pleistocene (around 0.6-0.1 MYA). During the mid- and late Pleistocene, the Benguela Current entered a highly unstable mode, with multiple changes in sea surface temperature, sea levels and paleoproductivity due to worldwide climate-induced changes (Jahn et al. 2003). The most extreme changes occurred ~600 KYA, with severe decrease in sea surface temperatures and sea levels (Marlow et al. 2000; Jahn et al. 2003), followed by severe paleoproductivity decline (~300 KYA) due to the protrusion into the region of warm and nutrient-poor Angolan Current waters (Jahn et al. 2003).

Therefore, major climatic fluctuations during the mid- to late Pleistocene may have resulted in the isolation and decline of local populations of *D. capensis* and *L. amia*. The observed differences in estimates of time since expansion between the northern and southern *D. capensis* populations may be related to different palaeoceanographic changes in the northern and southern Benguela areas, in particular the effect of changes in sea level. The continental shelf in the Benguela Current region is narrower (20km) than that off southern South Africa (75km), due to the presence of the Agulhas Bank (Siesser & Dingle 1981): reported sea level drops of up to 100m in eastern Africa during this period (Siesser & Dingle 1981) would probably have had different impacts on availability of suitable habitat on either side of southern Africa.

An interesting issue was raised by the reconstruction of phylogenetic relationships among southern African *D. capensis*, using the related European species *D. sargus* and *D. vulgaris* as outgroups. Although as expected, the northern and southern *D. capensis* grouped in two different clades, with no shared haplotypes, the observed distance between these clades was far smaller than that between *D. capensis* and the two other sparids. This suggests that these populations of *D. capensis*, although genetically divergent are not yet differentiated enough to be recognised as two distinct species. Interestingly, two individuals caught (as *D. sargus*) in southern Europe grouped in the southern African *D. capensis* clade, implying that they were not *D. sargus* but *D. capensis*. Although further studies are required to address this issue, the obtained results suggest that there may be another, previously unrecognized population of *D. capensis* in northern Africa.

Therefore, as observed for other marine species (e.g. Grant & Bowen 2006; Zane et al. 2006; Domingues et al. 2007; Gonzalez-Wanguemert et al. 2008; Gonzalez et al. 2008; Shen et al. 2011), major climatic fluctuations during the Pleistocene appear to have influenced the evolutionary history of all study species. The benthopelagic species (*Argyrosomus* spp. and *A. aequidens*) are estimated to have diverged much earlier than the more pelagic dwelling species (*D. capensis* and *L. amia*). This result may be related with niches occupied by the different ecotypes, combined with changes in sea surface temperature and sea level at different times around the Pleistocene. During the lower Miocene there was an increase (compared to present day) in sea level by up to 542m in the Benguela Current region. By the upper Pliocene–lower Pleistocene boundary, however, multiple sea level regressions led to a decrease in depth to 80m below present levels (Siesser & Dingle 1981). The Namibian coast is characterized by the presence of

an oxygen-depleted layer at the depth of 100–150m, due to anaerobic decomposition of organic matter (Sakko 1998). Fall in sea levels during the Miocene-Pleistocene would have caused a narrowing of the Namibian continental shelf, but as it appears that there was no major impact in upwelling patterns (Kirst et al. 1999) it is likely that the oxygen-depleted layer remained at shallower depths during this time, where the benthopelagic species would normally occur. Thus, availability of suitable habitats may have decreased faster for benthopelagic species, such as *Argyrosomus* spp. and *A. aequidens*, than for coastal pelagics such as *D. capensis* and *L. amia*. A similar progression in divergence times was reported for snapping shrimps (*Alpheus* spp.) occurring on either side of the Isthmus of Panama (Knowlton & Weigt 1998). In this case, differences in genetic divergence were attributed to ecological differences; as different species occupied different habitats that did not change at exactly the same time, population differentiation was likely to have occurred at different times (Knowlton & Weigt 1998).

Grant and Bowen (1998) proposed a classification of species demographic history based on the diversity levels, namely haplotype and nucleotide diversity. According to the Grant and Bowen (1998) classification *A. coronus*, *A. inodorus* and both *A. aequidens* species exhibit long evolutionary histories with large and stable populations, whereas *D. capensis*, *L. amia* and *T. albacares* display evidence of shallow population histories with recent population contractions followed by rapid population growth. This different classification may also be related to estimated time since divergence: the sciaenids exhibit older divergence times both within and between populations/species, allowing more time for accumulation of mutations and hence an increase in diversity levels, when compared with *D. capensis*, *L. amia* and *T. albacares*.

8.3.2. Demographic history of the study species

As over-exploitation can result in severe losses of genetic diversity (Kenchington et al. 2003), assessment of recent demographic changes, using microsatellites, was conducted for *D. capensis* (Chapter 3), *A. coronus* (Chapter 4.3), *A. aequidens* (Chapter 5.1) and *T. albacares* (Chapter 7). In all cases genetic diversity levels were relatively high, suggesting an absence of recent (10s - 100s years) population crashes. Estimates of long-term effective population sizes (N_e), using an estimator based on linkage equilibrium, revealed high values as expected for marine fish (Hauser & Carvalho 2008). *Diplodus capensis* and *A. aequidens* exhibited the highest values of N_e , while *A.*

coronus and *T. albacares* the lowest. Although these results should be interpreted with caution, as obtained estimates depend on accurate identification of population sub-structuring, it is likely that these values reflect the species true effective population size (Waples & Do 2010). It is possible that the inability to accurately define population sub-structuring in the northern sub-system population of *D. capensis*, *A. aequidens* and in *T. albacares* may result from observed high levels of effective population size, that can retard the effects of genetic drift and thus limit detection of population isolation using neutral markers (e.g. Andre et al. 2011)

Although it was possible to detect signals of recent population crashes in *D. capensis* and *A. aequidens*, these conclusions were dependent on the microsatellite mutation model used. In all cases, bottlenecks were only identified under the Infinite Alleles Model (IAM), which is disputed as the most likely model of microsatellite evolution (Beebee & Rowe 2005). However, Piry et al. (1999) considered that it is easier to detect population crashes if microsatellite loci evolve under IAM than if they evolve under a strict Stepwise Mutation Model (SMM). Therefore, it is possible that the results produced using the IAM are indeed accurate, and that these species underwent recent population contractions. On the contrary, no evidence of recent population contractions was detected for *A. coronus* and *T. albacares*. Although, as stated above, this cannot completely exclude its occurrence, a recent study into *A. coronus* biological and life history features suggest that it is still in a healthy state, as it is not commonly targeted by the inshore artisanal fishery (Potts et al. 2010). Thus, it is possible that *A. coronus* does not yet show signs of over-exploitation. As suggested by Riccioni et al. (2010), the inability to detect recent population crashes may be due to the fact that current methods require severe losses of genetic diversity. Thus, smaller population crashes that would still have a severe impact on conservation may go undetected, particularly in species with such high effective population sizes.

8.4. Implications of climate change

On-going climate change is a potentially increasing threat to marine species (Briggs 2011; Dawson et al. 2011). As most fish exhibit specific temperature requirements for feeding, dispersal and spawning, climatic fluctuations can be predicted to have a severe impact throughout the world. How a species reacts to climate change will depend upon multiple factors, such as body size, trophic level and generation time (Lo Brutto et al. 2011). Thus, it is predicted that small pelagics, such as sardines and anchovies, will be more vulnerable to climate change than large-bodied species (Lo Brutto et al. 2011). As it is not easy to assess what will happen in the future, it may help to look back in time to see how species reacted in the past to climate-induced environmental changes.

Reconstruction of evolutionary histories for the study species revealed evidence of multiple historical population crashes and expansions that appeared to coincide in time with major climatic fluctuations in the Benguela Current. The generalized cooling indicated for the Pliocene-Pleistocene transition was followed by an intensification of the upwelling system and sea level regressions that may have influenced speciation events in *Argyrosomus* spp. and *A. aequidens*, while a more recent drop in sea surface temperatures during the mid-Pleistocene may have led to divergence of *D. capensis* and *L. amia* populations. Finally, the Last Glacial Maximum left clear signals of population contractions and expansion in all studied species. As such, it is likely that future climatic changes will influence population demography in these species.

The present work reports the first evidence of climate-induced population changes in the Benguela Current region. Analyses of relative abundance for *A. inodorus* in central Namibia (Chapter 4.2) revealed a recent increase in abundance of *A. coronus*, whereas the latter species' occurrence was thought to be negligible up to a decade ago (Kirchner 1998). The identified shift in species composition is likely to be related to a southwards expansion of the Angola-Benguela Front, due to an increase of almost 1°C in sea surface temperatures during the last few decades (Monteiro et al. 2008). In addition, population structure analyses of *A. coronus* revealed evidence of introgressive hybridization events with *A. inodorus* (Chapter 4.3). The majority of identified hybrids were backcrosses with parental *A. coronus*, which suggests that the F1 generation was at least partially viable. As *A. inodorus* spawning grounds are thought to be located in

southern Namibia, it is likely that the distribution of *A. coronus* goes further south than here described. Only a small percentage (3.64%) of individuals were identified as hybrids, suggesting that hybridization was sporadic. However, if sea surface temperatures in the region continue to increase observed hybridization events would most likely increase in frequency leading to the establishment of a hybrid zone. Buggs (2007) suggests that the occurrence of hybrid zones is likely to increase with climate change, as species that evolved in allopatry come into contact again.

Therefore, it is likely that contemporary climate-induced changes in the Benguela Current will have a severe impact in the genetic architecture of local fish species, as it has happened in the past.

8.5. Implications for fisheries and conservation

Due to the rapid increase in fishing pressure throughout the globe, it has become extremely important to establish accurate management units that allow species to maintain their evolutionary potential. As fisheries management is mainly based on the assumption that a unit has definable patterns of recruitment and mortality, and hence a sustainable yield (Carvalho & Hauser 1994), it is necessary to know a species' ecological and biological features, and to understand the evolution and population dynamics in time and space, in order to predict the impact of fishery exploitation.

Results obtained in the present work revealed evidence that despite previous considerations, *D. capensis*, *A. aequidens* and *L. amia* are not transboundary stocks across the Benguela Current region, and should not be managed as one unit. In fact South African, and most likely southern Namibian, populations either constitute a different species or are isolated from Angolan and northern Namibian populations. However, no differentiation was found between samples from northern Namibia and Angola, suggesting that these two countries need to coordinate efforts to ensure the establishment of sustainable harvesting practices.

In a first approach it is recommended that the two identified *D. capensis* and *L. amia* populations should be considered independent Evolutionary Significant Units (ESU *sensu* Mortiz 1994), based on observed mitochondrial divergence levels and complete lineage sorting. The absence of significant differentiation in the Angolan populations of inshore species could be beneficial for future management and conservation plans, since any given site can be replenished by individuals from any location.

Evidence of recent population bottlenecks in *D. capensis*, *A. aequidens* and *T. albacares* suggest that over-exploitation is reducing species genetic diversity levels. Therefore, it is necessary to regulate catches in the region to ensure that the species are harvested at sustainable levels, for maintaining their evolutionary potential.

Investigation of *T. albacares* population structure revealed a small differentiation between western Atlantic and Indian Ocean populations. Furthermore, no significant divergence was found within South Africa, and these populations appeared to be more closely related to the Indian Ocean than western Atlantic populations. In South Africa, the Western Cape province tuna fishery is at present regulated by the ICCAT (Atlantic Ocean Commission), whereas the Eastern Cape and KwaZulu-Natal fisheries are

regulated by the IOTC (Indian Ocean Tuna Commission). Based on the present findings it is suggested that all South African *T. albacares* stocks should be managed by IOTC, and should be considered part of the Indian Ocean stock.

Due to decades of unstable civil climate, Angolan fishery industries are not as developed as they used to be, or as fisheries are in South Africa (Potts et al. 2009). However, the Angolan inshore subsistence fishery has increased in the last decade (Potts et al. 2009; Richardson 2010), placing more pressure in this vulnerable ecosystem. Richardson (2010) estimated that subsistence fisheries have been responsible for an almost 80% decrease in *D. capensis* abundance, making this type of fishery an increasing threat to the conservation of inshore species.

One effective way to ensure the maintenance of marine species diversity and evolutionary potential, particularly in inshore species, is through the establishment of marine protected areas (MPAs – Lenfant 2003; Perez-Ruzafa et al. 2006; Arrieta et al. 2010; Briggs 2011). In Angola there are regions that function, at the moment, as informal marine protected areas due to the difficulty of access, such as Baía dos Tigres (near the Cunene River mouth), the Flamingo River mouth, and the rocky region between Lucira and Benguela, making these ideal candidates for future official MPAs. Establishment of MPAs should take into consideration larval dispersion routes, population connectivity and oceanographic processes (Briggs 2011; Dawson et al. 2011; Grantham et al. 2011). Thus, in order to ensure the establishment of suitable marine protected areas in Angola it is necessary to investigate larvae dispersion patterns and how they are influenced by the Benguela Current oceanography.

8.6. Future work

The present work brought new insights into the influence of the Benguela Current oceanographic features in the genetic sub-structuring and evolutionary history of several inshore and offshore commercially exploited marine fish species. However, like most molecular studies, it was only possible to focus in a small number of species, and at a small geographical scale.

In order to fully understand how the Benguela Current can influence different species, with different life histories, it is necessary to study other types of marine organisms in the region such as sharks that exhibit a slower rate of evolution, or molluscs, in which the dispersal phase is normally limited to the early life cycle, as well as other teleost species.

Future studies should also include sampling sites in central and southern Namibian and western coast of South Africa, as it is vital to understand where the geographical cut-off point is between the identified populations. Also, biological information is still lacking for most species occurring in the region. Contemporary patterns of genetic sub-structuring will greatly depend on a species life history features, therefore, biological and ecological information is necessary to help interpreting observed patterns.

Finally, Hauser & Carvalho (2008) called for a paradigm shift in fishery genetics, as local adaptation appears to be an important evolutionary mechanism shaping population structure of marine species. Therefore, adaptive loci (or loci under selection), should be used in future studies in the Benguela Current, to ensure the retrieval of accurate population sub-structuring patterns, and understand the mechanisms driving local adaptation in the region.

8.7. Conclusion

The present work was the first study done on the influence of the Benguela Current oceanographic features in population sub-structuring and evolutionary history of fish species, at a regional level, using multiple molecular approaches. No other study conducted so far has sampled from either side of the Lüderitz perennial upwelling cell, thus providing a clear picture of genetic structuring across the Benguela Current. Therefore, the main conclusions of the present work are:

- the Benguela Current oceanographic features appear to play a major role in shaping population genetic sub-structure and evolutionary history of multiple inshore fish species;
- mitochondrial and nuclear markers provided clear evidence for disruption of gene flow across the region in most inshore species;
- shallow differentiation was observed for the offshore pelagic *T. albacares*, suggesting that the Benguela Current is a permeable barrier for this species;
- no genetic differentiation was observed within each identified regional population, despite occurring in highly heterogeneous environments;
- 3 major demographic events were observed, that appeared to be connected with climatic fluctuations in the Benguela Current during the Pleistocene: speciation of *A. aequidens* and *Argyrosomus* spp., at the Pliocene-Pleistocene transition; divergence of *D. capensis* and *L. amia*, in the mid- to late Pleistocene; and population expansions in all species, at the end of the Last Glacial Maximum;
- observed divergence levels and different time estimates of demographic events appear to be linked to the species different life history features;
- influence of the Benguela Current oceanographic features varied from species to species, due to their life history features;
- reconstruction of evolutionary histories suggest that future climate change will have a severe impact in these species' distribution ranges and genetic architectures;
- evidence of distribution range shifts and introgressive hybridization events in *A. coronus* may be related to a reported increase in sea surface temperatures in the Benguela Current, and thus constitute the first evidences of climate-induced changes in the region.

BIBLIOGRAPHY

- Aboim MA, Mavarez J, Bernatchez L, Coelho MM (2010) Introgressive hybridization between two Iberian endemic cyprinid fish: a comparison between two independent hybrid zones. *Journal of Evolutionary Biology*, **23**, 817-828.
- Accioly IV, Molina WF (2008) Cytogenetic studies in Brazilian marine Sciaenidae and Sparidae fishes (Perciformes). *Genetics and Molecular Research*, **7**, 358-370.
- Aleman D, Acha EM, Iribarne O (2009) The relationship between marine fronts and fish diversity in the Patagonian Shelf Large Marine Ecosystem. *Journal of Biogeography*, **36**, 2111-2124.
- Alves-Costa FA, Martins C, de Matos FDC, Foresti F, Oliveira C, Wasko AP (2008) 5S rDNA characterization in twelve Sciaenidae fish species (Teleostei, Perciformes): Depicting gene diversity and molecular markers. *Genetics and Molecular Biology*, **31**, 303-307.
- Anderson EC, Thompson EA (2002) A model-based method for identifying species hybrids using multilocus genetic data. *Genetics*, **160**, 1217-1229.
- Andre C, Larsson LC, Laikre L, Bekkevold D, Brigham J, Carvalho GR, Dahlgren TG, Hutchinson WF, Mariani S, Mudde K, Ruzzante DE, Ryman N (2011) Detecting population structure in a high gene-flow species, Atlantic herring (*Clupea harengus*): direct, simultaneous evaluation of neutral vs putatively selected loci. *Heredity*, **106**, 270-280.
- Anisimova M, Gascuel O (2006) Approximate likelihood-ratio test for branches: A fast, accurate, and powerful alternative. *Systematic Biology*, **55**, 539-552.
- Antao T, Lopes A, Lopes RJ, Beja-Pereira A, Luikart G (2008) LOSITAN: A workbench to detect molecular adaptation based on a F-st-outlier method. *Bmc Bioinformatics*, **9**.
- Appleyard SA, Grewe PM, Innes BH, Ward RD (2001) Population structure of yellowfin tuna (*Thunnus albacares*) in the western Pacific Ocean, inferred from microsatellite loci. *Marine Biology*, **139**, 383-393.
- Apte S, Gardner JPA (2002) Population genetic subdivision in the New Zealand greenshell mussel (*Perna canaliculus*) inferred from single-strand conformation polymorphism analysis of mitochondrial DNA. *Molecular Ecology*, **11**, 1617-1628.
- Archangi B, Chand V, Mather PB (2009) Isolation and characterization of 15 polymorphic microsatellite DNA loci from *Argyrosomus japonicus* (mulloway), a new aquaculture species in Australia. *Molecular Ecology Resources*, **9**, 412-414.

- Arrieta JM, Arnaud-Haond S, Duarte CM (2010) What lies underneath: Conserving the oceans' genetic resources. *Proceedings of the National Academy of Sciences of the United States of America*, **107**, 18318-18324.
- Avice JC (2000) *Phylogeography: The History and Formation of Species*. Harvard University Press, Cambridge, Massachusetts, USA.
- Avice JC, Arnold J, Ball RM, Bermingham E, Lamb T, Neigel JE, Reeb CA, Saunders NC (1987) Intraspecific phylogeography - the mitochondrial DNA bridge between population genetics and systematics. *Annual Review of Ecology and Systematics*, **18**, 489-522.
- Avice JC, Walker D, Johns GC (1998) Speciation durations and Pleistocene effects on vertebrate phylogeography. *Proceedings of the Royal Society of London Series B-Biological Sciences*, **265**, 1707-1712.
- Balloux F, Lugon-Moulin N (2002) The estimation of population differentiation with microsatellite markers. *Molecular Ecology*, **11**, 155-165.
- Bandelt HJ, Forster P, Rohl A (1999) Median-joining networks for inferring intraspecific phylogenies. *Molecular Biology and Evolution*, **16**, 37-48.
- Bard FX, Scott EL (1991) Sept traversées transatlantiques d'álbacores marqués. Thons migrants ou sédentaires? *Collective Volume of Scientific Papers - ICCAT*, **36**, 205-222.
- Bargelloni L, Alarcon JA, Alvarez MC, Penzo E, Magoulas A, Palma J, Patarnello T (2005) The Atlantic-Mediterranean transition: Discordant genetic patterns in two seabream species, *Diplodus puntazzo* (Cetti) and *Diplodus sargus* (L.). *Molecular Phylogenetics and Evolution*, **36**, 523-535.
- Barton NH, Slatkin M (1986) A quasi-equilibrium theory of the distribution of rare alleles in a subdivided population. *Heredity*, **56**, 409-415.
- Bay LK, Crozier RH, Caley MJ (2006) The relationship between population genetic structure and pelagic larval duration in coral reef fishes on the Great Barrier Reef. *Marine Biology*, **149**, 1247-1256.
- Beaumont M, Nichols R (1996) Evaluating loci for use in the genetic analysis of population structure. *Proceedings of the Royal Society B*, **363**, 1619-1626.
- Beaumont MA (1999) Detecting population expansion and decline using microsatellites. *Genetics*, **153**, 2013-2029.

- Beebe T, Rowe G. (2005) *An Introduction to Molecular Ecology*. Oxford University Press, Oxford, UK.
- Belkhir K, Borsa P, Chiki L, Refaust N, Bonhomme F (2000) GENETIX 4.0.1; logiciel sous Windows pour la génétique des populations. Laboratoire Génome, Populations, Interactions, Université de Montpellier.
- Bennett P (2000) Desmystified... microsatellites. *Molecular Pathology*, **53**, 177-183.
- Benson G (1999) Tandem repeats finder: a program to analyze DNA sequences. *Nucleic Acids Research*, **27**, 573-580.
- Bermingham E, McCafferty SS, Martin, PP (1997) Fish biogeography and molecular clocks: perspectives from the Panamian Isthmus. In: *Molecular Systematics of Fishes* (ed. Kosher TDS, C.A.), San Diego, USA.
- Bernardi G (2000) Barriers to gene flow in *Embiotoca jacksoni*, a marine fish lacking a pelagic larval stage. *Evolution*, **54**, 226-237.
- Bernardi G, Lape J (2005) Tempo and mode of speciation in the Baja California disjunct fish species *Anisotremus davidsonii*. *Molecular Ecology*, **14**, 4085-4096.
- Bester-van der Merwe AE, Roodt-Wilding R, Volckaert FAM, D'Amato ME (2011) Historical isolation and hydrodynamically constrained gene flow in declining populations of the South-African abalone, *Haliotis midae*. *Conservation Genetics*, **12**, 543-555.
- Bianchi G, Carpenter KE, Roux JP, Molloy FJ, Boyer D, Boyer HJ (1999) *FAO species identification field guide for fishery purposes: the living resources of Namibia*. FAO, Rome, Italy.
- Bierne N, David P, Langlade A, Bonhomme F (2002) Can habitat specialisation maintain a mosaic hybrid zone in marine bivalves? *Marine Ecology-Progress Series*, **245**, 157-170.
- Bilgmann K, Moller LM, Harcourt RG, Gibbs SE, Beheregaray LB (2007) Genetic differentiation in bottlenose dolphins from South Australia: association with local oceanography and coastal geography. *Marine Ecology-Progress Series*, **341**, 265-276.
- Bowen BW, Bass AL, Muss A, Carlin J, Robertson DR (2006) Phylogeography of two Atlantic squirrelfishes (Family Holocentridae): exploring links between pelagic larval duration and population connectivity. *Marine Biology*, **149**, 899-913.
- Bowen BW, Bass AL, Rocha LA, Grant WS, Robertson DR (2001) Phylogeography of the trumpetfishes (*Aulostomus*): Ring species complex on a global scale. *Evolution*, **55**, 1029-1039.

- Bowen BW, Grant WS (1997) Phylogeography of the sardines (*Sardinops* spp): Assessing biogeographic models and population histories in temperate upwelling zones. *Evolution*, **51**, 1601-1610.
- Bowen BW, Kamezaki N, Limpus CJ, Hughes GR, Meylan AB, Avise JC (1994) Global phylogeography of the loggerhead turtle (*Caretta caretta*) as indicated by mitochondrial DNA haplotypes. *Evolution*, **48**, 1820-1828.
- Boyer D, Cole J, Bartholomae C (2000) Southwestern Africa: Northern Benguela Current region. *Marine Pollution Bulletin*, **41**, 123-140.
- Bremer JRA, Stequert B, Robertson NW, Ely B (1998) Genetic evidence for inter-oceanic subdivision of bigeye tuna (*Thunnus obesus*) populations. *Marine Biology*, **132**, 547-557.
- Bridle JR, Saldamando CI, Koning W, Butlin RK (2006) Assortative preferences and discrimination by females against hybrid male song in the grasshoppers *Chorthippus brunneus* and *Chorthippus jacobsi* (Orthoptera : Acrididae). *Journal of Evolutionary Biology*, **19**, 1248-1256.
- Briggs JC (1987) Antitropical distribution and evolution in the Indo-West Pacific Ocean. *Systematic Zoology*, **36**, 237-247.
- Briggs JC (2011) Marine extinctions and conservation. *Marine Biology*, **158**, 485-488.
- Brown GG, Simpson MV (1979) Intraspecific mtDNA polymorphism and the mechanism of maternal inheritance. *Journal of Supramolecular Structure*, 157-157.
- Brunelli JP, Steele CA, Thorgaard GH (2010) Deep divergence and apparent sex-biased dispersal revealed by a Y-linked marker in rainbow trout. *Molecular Phylogenetics and Evolution*, **56**, 983-990.
- Buggs RJA (2007) Empirical study of hybrid zone movement. *Heredity*, **99**, 301-312.
- Burridge CP (2002) Antitropicality of Pacific fishes: molecular insights. *Environmental Biology of Fishes*, **65**, 151-164.
- Caddy JF, Seij JC (2005) This is more difficult than we thought! The responsibility of scientists, managers and stakeholders to mitigate the unsustainability of marine fisheries. *Philosophical Transactions of the Royal Society B-Biological Sciences*, **360**, 59-75.
- Carcraft J (1983) Species concepts and speciation analysis. *Current Ornithology*, **1**, 159-187.

- Carcraft J (2000) Species concepts in theoretical and applied biology: a systematic debate with consequences. In: *Species Concepts and Phylogenetic Theory* (ed. Wheeler QDM, R.), pp. 1-14. Columbia University Press, New York.
- Cardenas L, Castilla JC, Viard F (2009) A phylogeographical analysis across three biogeographical provinces of the south-eastern Pacific: the case of the marine gastropod *Concholepas concholepas*. *Journal of Biogeography*, **36**, 969-981.
- Carlsson J, McDowell JR, Diaz-Jaimes P, Carlsson JEL, Boles SB, Gold JR, Graves JE (2004) Microsatellite and mitochondrial DNA analyses of Atlantic bluefin tuna (*Thunnus thynnus thynnus*) population structure in the Mediterranean Sea. *Molecular Ecology*, **13**, 3345-3356.
- Carvalho GR, Hauser L (1994) Molecular genetics and the stock concept in fisheries. *Reviews in Fish Biology and Fisheries*, **4**, 326-350.
- Chakraborty R (1992) Sample-size requirements for addressing the population genetic issues of forensic use of dna typing. *Human Biology*, **64**, 141-159.
- Chapuis MP (2006) Génétique des populations d'un insect pullulant, le croquet migrateur, *Locusta migratoria*. Montpellier II University, Montpellier.
- Chapuis MP, Estoup A (2007) Microsatellite null alleles and estimation of population differentiation. *Molecular Biology and Evolution*, **24**, 621-631.
- Chaves-Campos J, Johnson SG, de Leon FJG, Hulsey CD (2011) Phylogeography, genetic structure, and gene flow in the endemic freshwater shrimp *Palaemonetes suttkusi* from Cuatro Ciénegas, Mexico. *Conservation Genetics*, **12**, 557-567.
- Chen MT, Chang YP, Chang CC, Wang LW, Wang CH, Yu EF (2002) Late Quaternary sea-surface temperature variations in the southeast Atlantic: a planktic foraminifer faunal record of the past 600 000 yr (IMAGES II MD962085). *Marine Geology*, **180**, 163-181.
- Chen WJ, Bonillo C, Lecointre G (2003) Repeatability of clades as a criterion of reliability: a case study for molecular phylogeny of *Acanthomorpha* (Teleostei) with larger number of taxa. *Molecular Phylogenetics and Evolution*, **26**, 262-288.
- Chiba SN, Iwatsuki Y, Yoshino T, Hanzawa N (2009) Comprehensive phylogeny of the family Sparidae (Perciformes: Teleostei) inferred from mitochondrial gene analyses. *Genetic Systems*, **84**, 153-170.
- Chow S, Hazama K (1998) Universal PCR primers for S7 ribosomal protein gene introns in fish. *Molecular Ecology*, **7**, 1255-1256.

- Chow S, Ushiyama H (1995) Global population structure of albacore (*Thunnus alalunga*) inferred by RFLP analysis of the mitochondrial ATPase gene. *Marine Biology*, **123**, 39-45.
- Clark DL, Leis JM, Hay AC, Trnski T (2005) Swimming ontogeny of larvae of four temperate marine fishes. *Marine Ecology-Progress Series*, **292**, 287-300.
- Clark MR, Anderson OF, Francis R, Tracey DM (2000) The effects of commercial exploitation on orange roughy (*Hoplostethus atlanticus*) from the continental slope of the Chatham Rise, New Zealand, from 1979 to 1997. *Fisheries Research*, **45**, 217-238.
- Clark TB, Ma L, Saillant E, Gold JR (2004) Microsatellite DNA markers for population-genetic studies of Atlantic bluefin tuna (*Thunnus thynnus thynnus*) and other species of genus *Thunnus*. *Molecular Ecology Notes*, **4**, 70-73.
- Cochrane KL, Doullman DJ (2005) The rising tide of fisheries instruments and the struggle to keep afloat. *Philosophical Transactions of the Royal Society B-Biological Sciences*, **360**, 77-94.
- Colborn J, Crabtree RE, Shaklee JB, Pfeiler E, Bowen BW (2001) The evolutionary enigma of bonefishes (*Albula* spp.): Cryptic species and ancient separations in a globally distributed shorefish. *Evolution*, **55**, 807-820.
- Cole J, McGlade J (1998) Clupeoid population variability, the environment and satellite imagery in coastal upwelling systems. *Reviews in Fish Biology and Fisheries*, **8**, 445-471.
- Collin R (2003) Phylogenetic relationships among calyptraeid gastropods and their implications for the biogeography of marine speciation. *Systematic Biology*, **52**, 618-640.
- Conover DO, Clarke LM, Munch SB, Wagner GN (2006) Spatial and temporal scales of adaptive divergence in marine fishes and the implications for conservation. *Journal of Fish Biology*, **69**, 21-47.
- Conover DO, Munch SB (2002) Sustaining fisheries yields over evolutionary time scales. *Science*, **297**, 94-96.
- Corrigan S, Beheregaray LB (2009) A recent shark radiation: Molecular phylogeny, biogeography and speciation of wobbegong sharks (family: Orectolobidae). *Molecular Phylogenetics and Evolution*, **52**, 205-216.
- Costagliola D, Robertson DR, Guidetti P, Stefanni S, Wirtz P, Heiser JB, Bernardi G (2004) Evolution of coral reef fish *Thalassoma* spp. (Labridae). 2. Evolution of the eastern Atlantic species. *Marine Biology*, **144**, 377-383.

Coyle T (1997) Stock identification and fisheries management: the importance of using several methods in a stock identification study. In: *Taking stock: defining and managing shared resources* (ed. Hancock DA), pp. 173-179. Australian Society for Fish Biology and Fish and Aquatic Resource Management Association of Australasia, Darwin, Australia.

Cowley PD, Kerwath SE, Childs AR, Thorstad EB, Okland F, Naesje TF (2008) Estuarine habitat use by juvenile dusky kob *Argyrosomus japonicus* (Sciaenidae), with implications for management. *African Journal of Marine Science*, **30**, 247-253.

Dammannagoda ST, Hurwood DA, Mather PB (2008) Evidence for fine geographical scale heterogeneity in gene frequencies in yellowfin tuna (*Thunnus albacares*) from the north Indian Ocean around Sri Lanka. *Fisheries Research*, **90**, 147-157.

Dammannagoda ST, Hurwood DA, Mather PB (2011) Genetic analysis reveals two stocks of skipjack tuna (*Katsuwonus pelamis*) in the northwestern Indian Ocean. *Canadian Journal of Fisheries and Aquatic Sciences*, **68**, 210-223.

Dawson TP, Jackson ST, House JI, Prentice IC, Mace GM (2011) Beyond Predictions: Biodiversity Conservation in a Changing Climate. *Science*, **332**, 53-58.

de Queiroz K (1998) The general lineage concept of species, species criteria, and the process of speciation: a conceptual unification and terminological recommendations. In: *Endless forms: species and speciation* (ed. Howard DJB, S.H.), pp. 57-75. Oxford University Press, New York.

de Queiroz K (2007) Species concepts and species delimitation. *Systematic Biology*, **56**, 879-886.

DeSalle R, Amato G (2004) The expansion of conservation genetics. *Nature Reviews Genetics*, **5**, 702-712.

Di Finizio A, Guerriero G, Russo GL, Ciarcia G (2007) Identification of gadoid species (Pisces, Gadidae) by sequencing and PCR-RFLP analysis of mitochondrial 12S and 16S rRNA gene fragments. *European Food Research and Technology*, **225**, 337-344.

Diaz-Jaimes P, Uribe-Alcocer M (2006) Spatial differentiation in the eastern Pacific yellowfin tuna revealed by microsatellite variation. *Fisheries Science*, **72**, 590-596.

Diaz-Jaimes P, Uribe-Alcocer M, Rocha-Olivares A, Garcia-de-Leon FJ, Nortmoon P, Durand JD (2010) Global phylogeography of the dolphinfish (*Coryphaena hippurus*): The influence of large effective population size and recent dispersal on the divergence of a marine pelagic cosmopolitan species. *Molecular Phylogenetics and Evolution*, **57**, 1209-1218.

- Diester-Haass L, Meyers PA, Bickert T (2004) Carbonate crash and biogenic bloom in the late Miocene: Evidence from ODP Sites 1085, 1086, and 1087 in the Cape Basin, southeast Atlantic Ocean. *Paleoceanography*, **19**.
- Diester-Haass L, Meyers PA, Vidal L (2002) The late Miocene onset of high productivity in the Benguela Current upwelling system as part of a global pattern. *Marine Geology*, **180**, 87-103.
- Diester-Haass L, Meyers PA, Rothe P (1990) Miocene history of the Benguela Current and Antarctic ice volumes: evidence from rhythmic sedimentation and current growth across the Walvis Ridge (DSDP Sites 632 and 532). *Paleoceanography*, **5**, 685-707.
- Diester-Haass L, Heine K, Rothe P, Schrader H (1988) Late Quaternary history of continental climate and the Benguela current off southwest Africa. *Palaeogeography Palaeoclimatology Palaeoecology*, **65**, 81-91.
- Domingues VS, Santos RS, Brito A, Alexandrou M, Almada VC (2007) Mitochondrial and nuclear markers reveal isolation by distance and effects of Pleistocene glaciations in the northeastern Atlantic and Mediterranean populations of the white seabream (*Diplodus sargus*, L.). *Journal of Experimental Marine Biology and Ecology*, **346**, 102-113.
- Donaldson KA, Wilson RR (1999) Amphi-panamic geminates of snook (Percoidei : Centropomidae) provide a calibration of the divergence rate in the mitochondrial DNA central region of fishes. *Molecular Phylogenetics and Evolution*, **13**, 208-213.
- Drummond AJ, Ho SYW, Phillips MJ, Rambaut A (2006) Relaxed phylogenetics and dating with confidence. *Plos Biology*, **4**, 699-710.
- Drummond AJ, Rambaut A (2007) BEAST: Bayesian evolutionary analysis by sampling trees. *Bmc Evolutionary Biology*, **7**.
- Durand JD, Collet A, Chow S, Guinand B, Borsa P (2005) Nuclear and mitochondrial DNA markers indicate unidirectional gene flow of Indo-Pacific to Atlantic bigeye tuna (*Thunnus obesus*) populations, and their admixture off southern Africa. *Marine Biology*, **147**, 313-322.
- Ely B, Vinas J, Bremer JRA, Black D, Lucas L, Covello K, Labrie AV, Thelen E (2005) Consequences of the historical demography on the global population structure of two highly migratory cosmopolitan marine fishes: the yellowfin tuna (*Thunnus albacares*) and the skipjack tuna (*Katsuwonus pelamis*). *Bmc Evolutionary Biology*, **5**.
- Estoup A, Cornuet JM (1999) Microsatellite evolution: inferences from population data. In: *Microsatellites - Evolution and Applications* (ed. Schlötterer DBG), pp. 49-65. Oxford University Press, Oxford, UK.

- Etourneau J, Martinez P, Blanz T, Schneider R (2009) Pliocene-Pleistocene variability of upwelling activity, productivity, and nutrient cycling in the Benguela region. *Geology*, **37**, 871-874.
- Evanno G, Regnaut S, Goudet J (2005) Detecting the number of clusters of individuals using the software STRUCTURE: a simulation study. *Molecular Ecology*, **14**, 2611-2620.
- Evans BS, Sweijd NA, Bowie RCK, Cook PA, Elliott NG (2004) Population genetic structure of the perlemoen *Haliotis midae* in South Africa: evidence of range expansion and founder events. *Marine Ecology-Progress Series*, **270**, 163-172.
- Excoffier L, Laval G, Schneider S (2005) Arlequin (version 3.0): An integrated software package for population genetics data analysis. *Evolutionary Bioinformatics*, **1**, 47-50.
- FAO (2001) Second technical consultation on the suitability of the CITES criteria for listing commercially-exploited aquatic species. FAO, Windhoek, Namibia.
- FAO (2005a) Cultured aquatic species information programme - *Argyrosomus regius*. (ed. Stipa PA, M.). FAO Fisheries and Aquaculture Department, Rome.
- FAO (2005b) Review of the State of World Marine Fisheries Resources. In: *Technical Paper*. FAO.
- FAO (2009) Yellowfin tuna (*Thunnus albacares*) species fact sheets.
- Farmer EC, deMenocal PB, Marchitto TM (2005) Holocene and deglacial ocean temperature variability in the Benguela upwelling region: Implications for low-latitude atmospheric circulation. *Paleoceanography*, **20**.
- Fennel W (1999) Theory of the Benguela upwelling system. *Journal of Physical Oceanography*, **29**, 177-190.
- Filippelli GM, Flores J-A (2009) From the warm Pliocene to the cold Pleistocene: A tale of two oceans. *Geology*, **37**, 959-960.
- Floeter SR, Rocha LA, Robertson DR, Joyeux JC, Smith-Vaniz WF, Wirtz P, Edwards AJ, Barreiros JP, Ferreira CEL, Gasparini JL, Brito A, Falcon JM, Bowen BW, Bernardi G (2008) Atlantic reef fish biogeography and evolution. *Journal of Biogeography*, **35**, 22-47.
- Florin A-B, Hoglund J (2007) Absence of population structure of turbot (*Psetta maxima*) in the Baltic Sea. *Molecular Ecology*, **16**, 115-126.

- Fodrie FJ, Heck KL, Powers SP, Graham WM, Robinson KL (2010) Climate-related, decadal-scale assemblage changes of seagrass-associated fishes in the northern Gulf of Mexico. *Global Change Biology*, **16**, 48-59.
- Francisco SM, Faria C, Lengkeek W, Vieira MN, Velasco EM, Almada VC (2011). Phylogeography of shanny *Lyphophrys pholis* (Pisces: Blenniidae) in the NE Atlantic record signs of major expansion events older than the last glaciation. *Journal of Experimental Marine Biology and Ecology*, **403**, 14-20.
- Frankham R, Ballou JD, Briscoe DA (2002) *Introduction to Conservation Genetics*. Cambridge University Press, Cambridge, UK.
- Freon P, Drapeau L, David JHM, Moreno AF, Leslie RW, Oosthuizen WH, Shannon LJ, van der Lingen CD (2005) Spatialized ecosystem indicators in the southern Benguela. *Ices Journal of Marine Science*, **62**, 459-468.
- Frontana-Uribe S, De la Rosa-Velez J, Enriquez-Paredes L, Ladah LB, Sanvicente-Anorve L (2008) Lack of genetic evidence for the subspeciation of *Pisaster ochraceus* (Echinodermata : Asteroidea) in the north-eastern Pacific Ocean. *Journal of the Marine Biological Association of the United Kingdom*, **88**, 395-400.
- Fu YX (1997) Statistical tests of neutrality of mutations against population growth, hitchhiking and background selection. *Genetics*, **147**, 915-925.
- Fullard KJ, Early G, Heide-Jorgensen MP, Bloch D, Rosing-Asvid A, Amos W (2000) Population structure of long-finned pilot whales in the North Atlantic: a correlation with sea surface temperature? *Molecular Ecology*, **9**, 949-958.
- Gaggiotti OE, Bekkevold D, Jorgensen HBH, Foll M, Carvalho GR, Andre C, Ruzzante DE (2009) Disentangling the effects of evolutionary, demographic, and environmental factors influencing genetic structure of natural populations: Atlantic herring as a case study. *Evolution*, **63**, 2939-2951.
- Gaither MR, Toonen RJ, Robertson DR, Planes S, Bowen BW (2010) Genetic evaluation of marine biogeographical barriers: perspectives from two widespread Indo-Pacific snappers (*Lutjanus kasmira* and *Lutjanus fulvus*). *Journal of Biogeography*, **37**, 133-147.
- Galarza JA, Carreras-Carbonell J, Macpherson E, Pascual M, Roques S, Turner GF, Rico C (2009) The influence of oceanographic fronts and early-life-history traits on connectivity among littoral fish species. *Proceedings of the National Academy of Sciences of the United States of America*, **106**, 1473-1478.

- Gammelsrod T, Bartholomae CH, Boyer DC, Filipe VLL, O'Toole MJ (1998) Intrusion of warm surface water along the Angolan-Namibian coast in February-March 1995: The 1995 Benguela Nino. *South African Journal of Marine Science-Suid-Afrikaanse Tydskrif Vir Seewetenskap*, **19**, 41-56.
- Gante HF, Micael J, Oliva-Paterna FJ, Doadrio I, Dowling TE, Alves MJ (2009) Diversification within glacial refugia: tempo and mode of evolution of the polytypic fish *Barbus sclateri*. *Molecular Ecology*, **18**, 3240-3255.
- Garcia SM, Grainger RJR (2005) Gloom and doom? The future of marine capture fisheries. *Philosophical Transactions of the Royal Society B-Biological Sciences*, **360**, 21-46.
- Garroway CJ, Bowman J, Holloway GL, Malcolm JR, Wilson PJ (2011) The genetic signature of rapid range expansion by flying squirrels in response to contemporary climate warming. *Global Change Biology*, **17**, 1760-1769.
- Glenn TC, Schable NA (2005) Isolating microsatellite DNA loci. *Molecular Evolution: Producing the Biochemical Data, Part B*, **395**, 202-222.
- Gold JR, Pak E, DeVries DA (2002) Population structure of king mackerel (*Scomberomorus cavalla*) around peninsular Florida, as revealed by microsatellite DNA. *Fishery Bulletin*, **100**, 491-509.
- Gold JR, Richardson LR (1991) Genetic studies in marine fishes - 4. An analysis of population structure in the red drum (*Sciaenops ocellatus*) using mitochondrial DNA. *Fisheries Research*, **12**, 213-241.
- Gold JR, Richardson LR (1998) Mitochondrial DNA diversification and population structure in fishes from the Gulf of Mexico and western Atlantic. *Journal of Heredity*, **89**, 404-414.
- Gomez-Uchida D, Weetman D, Hauser L, Galleguillos R, Retamal M (2003) Allozyme and AFLP analyses of genetic population structure in the hairy edible crab *Cancer setosus* from the Chilean coast. *Journal of Crustacean Biology*, **23**, 486-494.
- Gonzalez EG, Beerli P, Zardoya R (2008) Genetic structuring and migration patterns of Atlantic bigeye tuna, *Thunnus obesus* (Lowe, 1839). *Bmc Evolutionary Biology*, **8**.
- Gonzalez-Quiros R, del Arbol J, Garcia-Pacheco MD, Silva-Garcia AJ, Naranjo JM, Morales-Nin B (2011) Life-history of the meagre *Argyrosomus regius* in the Gulf of Cadiz (SW Iberian Peninsula). *Fisheries Research*, **109**, 140-149.

- Gonzalez-Wanguemert M, Canovas F, Perez-Ruzafa A, Marcos C, Alexandrino P (2010) Connectivity patterns inferred from the genetic structure of white seabream (*Diplodus sargus* L.). *Journal of Experimental Marine Biology and Ecology*, **383**, 23-31.
- Gonzalez-Wanguemert M, Perez-Ruzafa A, Garcia-Charton JA, Marcos C (2006) Genetic differentiation and gene flow of two sparidae subspecies, *Diplodus sargus sargus* and *Diplodus sargus cadenati* in Atlantic and south-west Mediterranean populations. *Biological Journal of the Linnean Society*, **89**, 705-717.
- Gonzalez-Wanguemert M, Perez-Ruzafa A, Marcos C, Garcia-Charton JA (2004) Genetic differentiation of *Diplodus sargus* (Pisces : Sparidae) populations in the south-west Mediterranean. *Biological Journal of the Linnean Society*, **82**, 249-261.
- Gonzalez-Wanguemert N, Perez-Ruzafa A, Canovas F, Garcia-Charton JA, Marcos C (2007) Temporal genetic variation in populations of *Diplodus sargus* from the SW Mediterranean Sea. *Marine Ecology-Progress Series*, **334**, 237-244.
- Gopal K, Tolley KA, Groeneveld JC, Matthee CA (2006) Mitochondrial DNA variation in spiny lobster *Palinurus delagoae* suggests genetically structured populations in the southwestern Indian Ocean. *Marine Ecology-Progress Series*, **319**, 191-198.
- Goudet J (1995) FSTAT (Version 1.2): A computer program to calculate F-statistics. *Journal of Heredity*, **86**, 485-486.
- Grant WS, Bowen BW (1998) Shallow population histories in deep evolutionary lineages of marine fishes: Insights from sardines and anchovies and lessons for conservation. *Journal of Heredity*, **89**, 415-426.
- Grant WS, Bowen BW (2006) Living in a tilted world: climate change and geography limit speciation in Old World anchovies (Engraulis; Engraulidae). *Biological Journal of the Linnean Society*, **88**, 673-689.
- Grantham HS, Game ET, Lombard AT, Hobday AJ, Richardson AJ, Beckley LE, Pressey RL, Huggett JA, Coetzee JC, van der Lingen CD, Petersen SL, Merkle D, Possingham HP (2011) Accommodating dynamic oceanographic processes and pelagic biodiversity in marine conservation planning. *Plos One*, **6**.
- Graves JE (1998) Molecular insights into the population structures of cosmopolitan marine fishes. *Journal of Heredity*, **89**, 427-437.
- Graves JE, McDowell JR (2003) Stock structure of the world's istiophorid billfishes: a genetic perspective. *Marine and Freshwater Research*, **54**, 287-298.

Griffiths AM, Sims DW, Cotterell SP, El Nagar A, Ellis JR, Lynghammar A, McHugh M, Neat FC, Pade NG, Queiroz N, Serra-Pereira B, Rapp T, Wearmouth VJ, Genner MJ (2010) Molecular markers reveal spatially segregated cryptic species in a critically endangered fish, the common skate (*Dipturus batis*). *Proceedings of the Royal Society B-Biological Sciences*, **277**, 1497-1503.

Griffiths MH (1996) Life history of the dusky kob *Argyrosomus japonicus* (Sciaenidae) off the east coast of South Africa. *South African Journal of Marine Science-Suid-Afrikaanse Tydskrif Vir Seewetenskap*, **17**, 135-154.

Griffiths MH (1997a) The life history and stock separation of silver kob, *Argyrosomus inodorus*, in South African waters. *Fishery Bulletin*, **95**, 47-67.

Griffiths MH (1997b) Management of South African dusky kob *Argyrosomus japonicus* (Sciaenidae) based on per-recruit models. *South African Journal of Marine Science-Suid-Afrikaanse Tydskrif Vir Seewetenskap*, **18**, 213-228.

Griffiths MH, Hecht T (1995) On the life-history of *Atractoscion aequidens*, a migratory sciaenid off the east coast of southern Africa. *Journal of Fish Biology*, **47**, 962-985.

Griffiths MH, Heemstra PC (1995) A contribution to the taxonomy of the marine fish genus *Argyrosomus* (Perciformes: Sciaenidae), with description of two new species from southern Africa. *Ichthyological Bulletin of the J.L.B. Smith Institute of Ichthyology*, 1-40.

Guillot G, Foll M (2009) Correcting for ascertainment bias in the inference of population structure. *Bioinformatics*, **25**, 552-554.

Guillot G, Mortier F, Estoup A (2005) GENELAND: a computer package for landscape genetics. *Molecular Ecology Notes*, **5**, 712-715.

Guillot G, Santos F (2009) A computer program to simulate multilocus genotype data with spatially autocorrelated allele frequencies. *Molecular Ecology Resources*, **9**, 1112-1120.

Guillot G, Santos F, Estoup A (2008) Analysing georeferenced population genetics data with Geneland: a new algorithm to deal with null alleles and a friendly graphical user interface. *Bioinformatics*, **24**, 1406-1407.

Guindon S, Dufayard JF, Hordijk W, Lefort V, Gascuel O (2009) PhyML: Fast and Accurate Phylogeny Reconstruction by Maximum Likelihood. *Infection Genetics and Evolution*, **9**, 384-385.

Gyory J, Mariano AJ, Ryan EH (2005) The Benguela Current, in *Ocean Surface Currents – online database*. Available at: <http://oceancurrents.rsmas.miami.edu/atlantic/benguela.html>.

Hall BG (2008) *Phylogenetic trees made easy: a how-to manual*, 3rd edn. Sinauer Associates, Sunderland, USA.

Han ZQ, Gao TX, Yanagimoto T, Sakurai Y (2008) Deep phylogeographic break among white croaker *Pennahia argentata* (Sciaenidae, Perciformes) populations in North-western Pacific. *Fisheries Science*, **74**, 770-780.

Hansen MM, Hemmer-Hansen J (2007) Landscape genetics goes to sea. *Journal of biology*, **6**, 6.

Harpending HC (1994) Signature of ancient population growth in a low-resolution mitochondrial DNA mismatch distribution. *Human Biology*, **66**, 591-600.

Hauser L, Adcock GJ, Smith PJ, Ramirez JHB, Carvalho GR (2002) Loss of microsatellite diversity and low effective population size in an overexploited population of New Zealand snapper (*Pagrus auratus*). *Proceedings of the National Academy of Sciences of the United States of America*, **99**, 11742-11747.

Hauser L, Carvalho GR (2008) Paradigm shifts in marine fisheries genetics: ugly hypotheses slain by beautiful facts. *Fish and Fisheries*, **9**, 333-362.

He SP, Mayden RL, Wang XZ, Wang W, Tang KL, Chen WJ, Chen YY (2008) Molecular phylogenetics of the family Cyprinidae (Actinopterygii : Cypriniformes) as evidenced by sequence variation in the first intron of S7 ribosomal protein-coding gene: Further evidence from a nuclear gene of the systematic chaos in the family. *Molecular Phylogenetics and Evolution*, **46**, 818-829.

Hebert PDN, Ratnasingham S, deWaard JR (2003) Barcoding animal life: cytochrome c oxidase subunit 1 divergences among closely related species. *Proceedings of the Royal Society of London Series B-Biological Sciences*, **270**, S96-S99.

Hedrick PW (2005) *Genetics of Populations*, 3rd edn. Jones and Bartlett, USA.

Heemstra P, Heemstra E. (2004) *Coastal Fishes of Southern Africa*, 1st edn. NISC, SAIAB, Grahamstown, South Africa.

Heiser JB, Moura RL, Robertson DR (2000) Two new species of creole wrasse (Labridae: *Clepticus*) from opposite sides of the Atlantic. *Aqua Journal of Ichthyology and Aquatic Biology*, **4**, 67-76.

Hemmer-Hansen J, Nielsen EE, Gronkjaer P, Loeschcke V (2007) Evolutionary mechanisms shaping the genetic population structure of marine fishes; lessons from the European flounder (*Platichthys flesus* L.). *Molecular Ecology*, **16**, 3104-3118.

- Heymans JJ, Shannon LJ, Jarre A (2004) Changes in the northern Benguela ecosystem over three decades: 1970s, 1980s, and 1990s. *Ecological Modelling*, **172**, 175-195.
- Hickey AJR, Lavery SD, Hannan DA, Baker CS, Clements KD (2009) New Zealand triplefin fishes (family Tripterygiidae): contrasting population structure and mtDNA diversity within a marine species flock. *Molecular Ecology*, **18**, 680-696.
- Hill JK, Griffiths HM, Thomas CD (2011) Climate Change and Evolutionary Adaptations at Species' Range Margins. *Annual Review of Entomology, Vol 56*, **56**, 143-159.
- Ho SYW (2007) Calibrating molecular estimates of substitution rates and divergence times in birds. *Journal of Avian Biology*, **38**, 409-414.
- Ho SYW, Phillips MJ (2009) Accounting for Calibration Uncertainty in Phylogenetic Estimation of Evolutionary Divergence Times. *Systematic Biology*, **58**, 367-380.
- Hoarau G, Boon E, Jongma DN, Ferber S, Palsson J, Van der Veer HW, Rijnsdorp AD, Stam WT, Olsen JL (2005) Low effective population size and evidence for inbreeding in an overexploited flatfish, plaice (*Pleuronectes platessa* L.). *Proceedings of the Royal Society B-Biological Sciences*, **272**, 497-503.
- Hubbs CL (1952) Antitropical distribution of fishes and other organisms. In: *Symposium on the Problems of Bipolarity and of Pantemperate Faunas*, pp. 324-329. Proceeding of the Seventh Pacific Science Congress (Pacific Science Association).
- Huelsenbeck JP, Ronquist F (2001) MRBAYES: Bayesian inference of phylogenetic trees. *Bioinformatics*, **17**, 754-755.
- Hutchings JA, Gerber L (2002) Sex-biased dispersal in a salmonid fish. *Proceedings of the Royal Society of London Series B-Biological Sciences*, **269**, 2487-2493.
- Hutchings JA, Reynolds JD (2004) Marine fish population collapses: Consequences for recovery and extinction risk. *Bioscience*, **54**, 297-309.
- Hutchings L, van der Lingen CD, Shannon LJ, Crawford RJM, Verheye HMS, Bartholomae CH, van der Plas AK, Louw D, Kreiner A, Ostrowski M, Fidel Q, Barlow RG, Lamont T, Coetzee J, Shillington F, Veitch J, Currie JC, Monteiro PMS (2009) The Benguela Current: An ecosystem of four components. *Progress in Oceanography*, **83**, 15-32.
- Hutton T, Griffiths MH, Sumaila UR, Pitcher TJ (2001) Cooperative versus non-cooperative management of shared linefish stocks in South Africa: an assessment of alternative management strategies for geelbek (*Atractoscion aequidens*). *Fisheries Research*, **51**, 53-68.

Ingram T (2011) Speciation along a depth gradient in a marine adaptive radiation. *Proceedings of the Royal Society B-Biological Sciences*, **278**, 613-618.

IUCN (2010) IUCN Red List of Threatened Species. Version 2010.4.

Jackson JBC (1995) Constancy and change of life in the sea. *Extinction rates*, 45-54.

Jahn B, Donner B, Muller PJ, Rohl U, Schneider RR, Wefer G (2003) Pleistocene variations in dust input and marine productivity in the northern Benguela Current: Evidence of evolution of global glacial-interglacial cycles. *Palaeogeography Palaeoclimatology Palaeoecology*, **193**, 515-533.

Janko K, Lecointre G, DeVries A, Coulloux A, Cruaud C, Marshall C (2007) Did glacial advances during the Pleistocene influence differently the demographic histories of benthic and pelagic Antarctic shelf fishes? - Inferences from intraspecific mitochondrial and nuclear DNA sequence diversity. *Bmc Evolutionary Biology*, **7**.

Joyeux JC, Floeter SR, Ferreira CEL, Gasparini JL (2001) Biogeography of tropical reef fishes: the South Atlantic puzzle. *Journal of Biogeography*, **28**, 831-841.

Jukes T, Cantor C (1969) Evolution of protein molecules. In: *Mammalian Protein Metabolism* (ed. Munro H), pp. 21-132. New York: Academic Press, New York.

Kaouèche M, Bahri-Sfar L, Gonzalez-Wanguemert M, Perez-Ruzafa A, Ben Hassine OK (2011) Allozyme and mtDNA variation of white seabream *Diplodus sargus* populations in a transition area between western and eastern Mediterranean basins (Siculo-Tunisian Strait). *African Journal of Marine Science*, **33**, 79-90.

Karl SA, Castro ALF, Lopez JA, Charvet P, Burgess GH (2011) Phylogeography and conservation of the bull shark (*Carcharhinus leucas*) inferred from mitochondrial and microsatellite DNA. *Conservation Genetics*, **12**, 371-382.

Kelly RP, Eernisse DJ (2007) Southern hospitality: A latitudinal gradient in gene flow in the marine environment. *Evolution*, **61**, 700-707.

Kenchington E, Heino M, Nielsen EE (2003) Managing marine genetic diversity: time for action? *Ices Journal of Marine Science*, **60**, 1172-1176.

Kenchington EL, Harding GC, Jones MW, Prodohl PA (2009) Pleistocene glaciation events shape genetic structure across the range of the American lobster, *Homarus americanus*. *Molecular Ecology*, **18**, 1654-1667.

- Kim JK, Kim YH, Kim MJ, Park JY (2010) Genetic diversity, relationships and demographic history of the small yellow croaker, *Larimichthys polyactis* (Pisces: Sciaenidae) from Korea and China inferred from mitochondrial control region sequence data. *Animal Cells and Systems*, **14**, 45-51.
- Kirchner CH (1998) Population dynamics and stock assessment of the exploited silver kob (*Argyrosomus inodorus*) in Namibian waters. University of Port Elizabeth, Port Elizabeth, South Africa.
- Kirchner CH, Beyer JE (1999) Estimation of total catch of silver kob *Argyrosomus inodorus* by recreational shore-anglers in Namibia using a roving-roving creel survey. *South African Journal of Marine Science-Suid-Afrikaanse Tydskrif Vir Seewetenskap*, **21**, 191-199.
- Kirchner CH, Holtzhausen JA (2001) Seasonal movements of silver kob, *Argyrosomus inodorus*, (Griffiths and Heemstra) in Namibian waters. *Fisheries Management and Ecology*, **8**, 239-251.
- Kirst GJ, Schneider RR, Muller PJ, von Storch I, Wefer G (1999) Late Quaternary temperature variability in the Benguela Current System derived from alkenones. *Quaternary Research*, **52**, 92-103.
- Klopper AW (2005) Intraspecific genetic variation in the percoid teleosts, *Argyrosomus japonicus* (Temminck & Schlegel, 1843) and *Pomadasys commersonii* (Lacepede, 1801) as inferred from the mitochondrial control region. University of Pretoria, Pretoria, South Africa.
- Knowlton N (2000) Molecular genetic analyses of species boundaries in the sea. *Hydrobiologia*, **420**, 73-90.
- Knowlton N, Weigt LA (1998) New dates and new rates for divergence across the Isthmus of Panama. *Proceedings of the Royal Society of London Series B-Biological Sciences*, **265**, 2257-2263.
- Koblmuller S, Egger B, Sturmbauer C, Sefc KM (2007) Evolutionary history of Lake Tanganyika's scale-eating cichlid fishes. *Molecular Phylogenetics and Evolution*, **44**, 1295-1305.
- Krammer R, Baumann KH, Hennich R (2006) Middle to late Miocene fluctuations in the incipient Benguela Upwelling System revealed by calcareous nannofossil assemblages (ODP Site 1085A). *Palaeogeography Palaeoclimatology Palaeoecology*, **230**, 319-334.
- Kumar S, Nei M, Dudley J, Tamura K (2008) MEGA: A biologist-centric software for evolutionary analysis of DNA and protein sequences. *Briefings in Bioinformatics*, **9**, 299-306.

- Lakra WS, Goswami M, Gopalakrishnan A (2009) Molecular identification and phylogenetic relationships of seven Indian Sciaenids (Pisces: Perciformes, Sciaenidae) based on 16S rRNA and cytochrome c oxidase subunit I mitochondrial genes. *Molecular Biology Reports*, **36**, 831-839.
- Lakra WS, Goswami M, Mohindra V, Lal KK, Punia P (2007) Molecular identification of five Indian sciaenids (Pisces: Perciformes, Sciaenidae) using RAPD markers. *Hydrobiologia*, **583**, 359-363.
- Lamberth SJ, van Niekerk L, Hutchings K (2008) Comparison of, and the effects of altered freshwater inflow on, fish assemblages of two contrasting South African estuaries: the cool-temperate Olifants and the warm-temperate Breede. *African Journal of Marine Science*, **30**, 311-336.
- Lankford TE, Targett TE, Gaffney PM (1999) Mitochondrial DNA analysis of population structure in the Atlantic croaker, *Micropogonias undulatus* (Perciformes : Sciaenidae). *Fishery Bulletin*, **97**, 884-890.
- Larmuseau MHD, Raeymaekers JAM, Hellemans B, Van Houdt JKJ, Volckaert FAM (2010) Mito-nuclear discordance in the degree of population differentiation in a marine goby. *Heredity*, **105**, 532-542.
- Lass HU, Mohrholz V (2005) On the fluctuations and vertical structure of the shelf circulation off Walvis Bay, Namibia. *Continental Shelf Research*, **25**, 1473-1497.
- Lass HU, Schmidt M, Mohrholz V, Nausch G (2000) Hydrographic and current measurements in the area of the Angola-Benguela front. *Journal of Physical Oceanography*, **30**, 2589-2609.
- Lavoue S, Sullivan JP, Hopkins CD (2003) Phylogenetic utility of the first two introns of the S7 ribosomal protein gene in African electric fishes (Mormyroidea : Teleostei) and congruence with other molecular markers. *Biological Journal of the Linnean Society*, **78**, 273-292.
- Lechanteur Y, Griffiths CL (2003) Diets of common suprabenthic reef fish in False Bay, South Africa. *African Zoology*, **38**, 213-227.
- Lecomte F, Grant WS, Dodson JJ, Rodriguez-Sanchez R, Bowen BW (2004) Living with uncertainty: genetic imprints of climate shifts in East Pacific anchovy (*Engraulis mordax*) and sardine (*Sardinops sagax*). *Molecular Ecology*, **13**, 2169-2182.
- Leduc G, Herbert CT, Blanz T, Martinez P, Schneider R (2010) Contrasting evolution of sea surface temperature in the Benguela upwelling system under natural and anthropogenic climate forcings. *Geophysical Research Letters*, **37**.

- Lemaire C, Versini JJ, Bonhomme F (2005) Maintenance of genetic differentiation across a transition zone in the sea: discordance between nuclear and cytoplasmic markers. *Journal of Evolutionary Biology*, **18**, 70-80.
- Lenfant P (2003) Demographic and genetic structures of white sea bream populations (*Diplodus sargus*, Linnaeus, 1758) inside and outside a Mediterranean marine reserve. *Comptes Rendus Biologies*, **326**, 751-760.
- Lenfant P, Planes S (1996) Genetic differentiation of white sea bream within the Lion's Gulf and the Ligurian Sea (Mediterranean sea). *Journal of Fish Biology*, **49**, 613-621.
- Lessios HA, Kane J, Robertson DR (2003) Phylogeography of the pantropical sea urchin *Tripneustes*: Contrasting patterns of population structure between oceans. *Evolution*, **57**, 2026-2036.
- Lessios HA, Kessing BD, Pearse JS (2001) Population structure and speciation in tropical seas: Global phylogeography of the sea urchin *Diadema*. *Evolution*, **55**, 955-975.
- Lessios HA, Kessing BD, Robertson DR, Paulay G (1999) Phylogeography of the pantropical sea urchin *Eucidaris* in relation to land barriers and ocean currents. *Evolution*, **53**, 806-817.
- Lett C, Veitch J, van der Lingen CD, Hutchings L (2007) Assessment of an environmental barrier to transport of ichthyoplankton from the southern to the northern Benguela ecosystems. *Marine Ecology-Progress Series*, **347**, 247-259.
- Lo Brutto S, Arculeo M, Grant AS (2011) Climate change and population genetic structure of marine species. *Chemistry and Ecology*, **27**, 107-119.
- Mabuchi K, Nakabo T, Nishida M (2004) Molecular phylogeny of the antitropical genus *Pseudolabrus* (Perciformes: Labridae): evidence for a Southern Hemisphere origin. *Molecular Phylogenetics and Evolution*, **32**, 375-382.
- Mallet J (2005) Hybridization as an invasion of the genome. *Trends in Ecology & Evolution*, **20**, 229-237.
- Mallet J (2007) Species concepts. In: *Evolutionary Genetics* (ed. Fox CW, Wolf JB), pp. 367-373. Oxford University Press, Oxford.
- Mann BQ, Buxton CD (1997) Age and growth of *Diplodus sargus capensis* and *D. cervinus hottentotus* (Sparidae) on the Tsitsikamma Coast, South Africa. *Cybium*, **21**, 135-147.
- Mann BQ, Buxton CD (1998) The reproductive biology of *Diplodus sargus capensis* and *D. cervinus hottentotus* (Sparidae) off the south-east Cape coast, South Africa. *Cybium*, **22**, 31-47.

- Marlow JR, Lange CB, Wefer G, Rosell-Mele A (2000) Upwelling intensification as part of the Pliocene-Pleistocene climate transition. *Science*, **290**, 2288.
- Matthee CA, Cockcroft AC, Gopal K, von der Heyden S (2007) Mitochondrial DNA variation of the west-coast rock lobster, *Jasus lalandii*: marked genetic diversity differences among sampling sites. *Marine and Freshwater Research*, **58**, 1130-1135.
- Matthee CA, Fourie F, Oosthuizen WH, Meyer MA, Tolley KA (2006) Mitochondrial DNA sequence data of the Cape fur seal (*Arctocephalus pusillus pusillus*) suggest that population numbers may be affected by climatic shifts. *Marine Biology*, **148**, 899-905.
- Mayr E (1942) *Systematics and the Origin of Species*. Columbia University Press, New York.
- McCairns RJS, Bernatchez L (2008) Landscape genetic analyses reveal cryptic population structure and putative selection gradients in a large-scale estuarine environment. *Molecular Ecology*, **17**, 3901-3916.
- McCartney MA, Keller G, Lessios HA (2000) Dispersal barriers in tropical oceans and speciation in Atlantic and eastern Pacific sea urchins of the genus *Echinometra*. *Molecular Ecology*, **9**, 1391-1400.
- McDowell JR, Diaz-Jaimes P, Graves JE (2002) Isolation and characterization of seven tetranucleotide microsatellite loci from Atlantic northern bluefin tuna *Thunnus thynnus thynnus*. *Molecular Ecology Notes*, **2**, 214-216.
- McKeown NJ, Shaw PW (2008) Polymorphic nuclear microsatellite loci for studies of brown crab, *Cancer pagurus* L. *Molecular Ecology Resources*, **8**, 653-655.
- Mehner T, Freyhof J, Reichard M (2011) Summary and perspective on evolutionary ecology of fishes. *Evolutionary Ecology*, **25**, 547-556.
- Meyer A, Salzburger W, Scharl M (2006) Hybrid origin of a swordtail species (Teleostei: *Xiphophorus clemenciae*) driven by sexual selection. *Molecular Ecology*, **15**, 721-730.
- Miethe T, Dytham C, Dieckmann U, Pitchford JW (2010) Marine reserves and the evolutionary effects of fishing on size at maturation. *Ices Journal of Marine Science*, **67**, 412-425.
- Mohrholz V, Schmidt M, Lutjeharms JRE, John HC (2004) Space-time behaviour of the Angola-Benguela Frontal Zone during the Benguela Nino of April 1999. *International Journal of Remote Sensing*, **25**, 1337-1340.

- Monteiro PMS, van der Plas AK, Melice JL, Florenchie P (2008) Interannual hypoxia variability in a coastal upwelling system: Ocean-shelf exchange, climate and ecosystem-state implications. *Deep-Sea Research Part I-Oceanographic Research Papers*, **55**, 435-450.
- Moritz C (1994) Defining Evolutionarily Significant Units for conservation. *Trends in Ecology & Evolution*, **9**, 373-375.
- Mueter FJ, Boldt JL, Megrey BA, Peterman RM (2007) Recruitment and survival of Northeast Pacific Ocean fish stocks: temporal trends, covariation, and regime shifts. *Canadian Journal of Fisheries and Aquatic Sciences*, **64**, 911-927.
- Near TJ, Cheng CHC (2008) Phylogenetics of notothenioid fishes (Teleostei : Acanthomorpha): Inferences from mitochondrial and nuclear gene sequences. *Molecular Phylogenetics and Evolution*, **47**, 832-840.
- Neethling M, Matthee CA, Bowie RCK, von der Heyden S (2008) Evidence for panmixia despite barriers to gene flow in the southern African endemic, *Caffrogobius caffer* (Teleostei: Gobiidae). *Bmc Evolutionary Biology*, **8**.
- Nielsen EEG, Bach LA, Kotlicki P (2006) HYBRIDLAB (version 1.0): a program for generating simulated hybrids from population samples. *Molecular Ecology Notes*, **6**, 971-973.
- Nielsen EE, Hemmer-Hansen J, Larsen PF, Bekkevold D (2009) Population genomics of marine fishes: identifying adaptive variation in space and time. *Molecular Ecology*, **18**, 3128-3150.
- Nye JA, Link JS, Hare JA, Overholtz WJ (2009) Changing spatial distribution of fish stocks in relation to climate and population size on the Northeast United States continental shelf. *Marine Ecology-Progress Series*, **393**, 111-129.
- Oosthuizen CJ (2007) Genetic variation within the Cape Stumpnose *Rhabdosargus holubii* Steindachner (Teleostei: Sparidae). University of Pretoria, Pretoria, South Africa.
- Ostrowski M, da Silva JCB, Bazik-Sangolay B (2009) The response of sound scatterers to El Niño- and La Niña-like oceanographic regimes in the southeastern Atlantic. *Ices Journal of Marine Science*, **66**, 1063-1072.
- Paine MA, McDowell JR, Graves JE (2008) Specific identification using COI sequence analysis of scombrid larvae collected off the Kona coast of Hawaii Island. *Ichthyological Research*, **55**, 7-16.
- Palumbi SR (1992) Marine speciation on a small planet. *Trends in Ecology & Evolution*, **7**, 114-118.

- Palumbi SR (2004) Fisheries science - Why mothers matter. *Nature*, **430**, 621-622.
- Palumbi SR (2009) Speciation and the evolution of gamete recognition genes: pattern and process. *Heredity*, **102**, 66-76.
- Palumbi SR, Martin A, Romano S, McMillan WO, Stice L, Grabowski G (2002) The simple fool's guide to PCR version 2.0. Department of Zoology, Kewalo Marine Laboratory, University of Hawaii, Honolulu.
- Pardinas AF, Campo D, Pola IG, Miralles L, Juanes F, Garcia-Vazquez E (2010) Climate change and oceanic barriers: genetic differentiation in *Pomatomus saltatrix* (Pisces: Pomatomidae) in the North Atlantic Ocean and the Mediterranean Sea. *Journal of Fish Biology*, **77**, 1993-1998.
- Patarnello T, Volckaert F, Castilho R (2007) Pillars of Hercules: is the Atlantic-Mediterranean transition a phylogeographical break? *Molecular Ecology*, **16**, 4426-4444.
- Patrick P, Strydom NA (2009) Swimming abilities of wild-caught, late-stage larvae of *Diplodus capensis* and *Sarpa salpa* (Pisces: Sparidae) from temperate South Africa. *Estuarine Coastal and Shelf Science*, **85**, 547-554.
- Perez L, Infante C, Ponce M, Crespo A, Zuasti E, Funes V, Catanese G, Manchado M (2008) Characterization of eight microsatellite markers in the white sea bream, *Diplodus sargus* (Teleostei, Sparidae). *Molecular Ecology Resources*, **8**, 1291-1293.
- Perez-Losada M, Nolte MJ, Crandall KA, Shaw PW (2007) Testing hypotheses of population structuring in the Northeast Atlantic Ocean and Mediterranean Sea using the common cuttlefish *Sepia officinalis*. *Molecular Ecology*, **16**, 2667-2679.
- Perez-Ruzafa A, Gonzalez-Wanguemert M, Lenfant P, Marcos C, Garcia-Charton JA (2006) Effects of fishing protection on the genetic structure of fish populations. *Biological Conservation*, **129**, 244-255.
- Pinera JA, Bernardo D, Blanco G, Vazquez E, Sanchez JA (2007) Usefulness of microsatellite markers developed from *Pagellus bogaraveo* to genetically study five different species of Sparidae. *Marine Ecology-an Evolutionary Perspective*, **28**, 184-187.
- Piry S, Alapetite A, Cornuet JM, Paetkau D, Baudouin L, Estoup A (2004) GENECLASS2: A software for genetic assignment and first-generation migrant detection. *Journal of Heredity*, **95**, 536-539.

- Piry S, Luikart G, Cornuet JM (1999) BOTTLENECK: A computer program for detecting recent reductions in the effective population size using allele frequency data. *Journal of Heredity*, **90**, 502-503.
- Pisias NG, Moore TC (1981) The evolution of Pleistocene climate - a time-series approach. *Earth and Planetary Science Letters*, **52**, 450-458.
- Portnoy DS, McDowell JR, Heist EJ, Musick JA, Graves JE (2010) World phylogeography and male-mediated gene flow in the sandbar shark, *Carcharhinus plumbeus*. *Molecular Ecology*, **19**, 1994-2010.
- Posada D (2008) jModelTest: Phylogenetic model averaging. *Molecular Biology and Evolution*, **25** (7), 1253-1256.
- Potts WM, Childs AR, Sauer WHH, Duarte ADC (2009) Characteristics and economic contribution of a developing recreational fishery in southern Angola. *Fisheries Management and Ecology*, **16**, 14-20.
- Potts WM, Sauer WHH, Childs AR, Duarte ADC (2008) Using baseline biological and ecological information to design a Traffic Light Precautionary Management Framework for leerfish *Lichia amia* (Linnaeus 1758) in southern Angola. *African Journal of Marine Science*, **30**, 113-121.
- Potts WM, Sauer WHH, Henriques R, Sequesseque S, Santos CV, Shaw PW (2010) The biology, life history and management needs of a large sciaenid fish, *Argyrosomus coronus*, in Angola. *African Journal of Marine Science*, **32**, 247-258.
- Pritchard JK, Stephens M, Donnelly P (2000) Inference of population structure using multilocus genotype data. *Genetics*, **155**, 945-959.
- Puchnick-Legat A, Levy JA (2006) Genetic structure of brazilian populations of white mouth croaker *Micropogonias furnieri* (Perciformes : Sciaenidae). *Brazilian Archives of Biology and Technology*, **49**, 429-439.
- Quero JC, Vayne JJ (1985) Le Maigre, *Argyrosomus regius* (Asso, 1801) (Pisces, Perciformes, Sciaenidae) du Golf de Gascogne et des eaux plus septentrionales. *Revue des Travaux de l'Institute des Peches Maritimes*, **49**, 35-66.
- Quinteiro J, Vidal R, Rey-Mendez M (2000) Phylogeny and biogeographic history of hake (genus *Merluccius*), inferred from mitochondrial DNA control-region sequences. *Marine Biology*, **136**, 163-174.
- Rambaut A (2009) FigTree v.1.3.1. Available at <http://tree.bio.ed.ac.uk/software>

- Rambaut A, Drummond AJ (2007) Tracer v1.4. Available at <http://tree.bio.ed.ac.uk/software>
- Ramsay PJ, Cooper JAG (2002) Late Quaternary sea-level change in South Africa. *Quaternary Research*, **57**, 82-90.
- Randall JE (1981) Examples of anti-tropical and anti-equatorial distribution of Indo-West Pacific fishes. *Pacific Science*, **35**, 197-209.
- Ravago-Gotanco RG, Magsino RM, Juinio-Menez MA (2007) Influence of the North Equatorial Current on the population genetic structure of *Tridacna crocea* (Mollusca: Tridacnidae) along the eastern Philippine seaboard. *Marine Ecology-Progress Series*, **336**, 161-168.
- Raymond M, Rousset F (1995) GENEPOP (version 1.2) - Population genetics software for exact tests and ecumenicism. *Journal of Heredity*, **86**, 248-249.
- Reeb CA (2010) Genetic discontinuity of big fish in a small sea. *Proceedings of the National Academy of Sciences of the United States of America*, **107**, 2377-2378.
- Reeves PA, Richards CM (2011) Species delimitation under the General Lineage Concept: an empirical example using wild North American hops (Cannabaceae: *Humulus lupulus*). *Systematic Biology*, **60**, 45-59.
- Riccioni G, Landi M, Ferrara G, Milano I, Cariani A, Zane L, Sella M, Barbujani G, Tinti F (2010) Spatio-temporal population structuring and genetic diversity retention in depleted Atlantic Bluefin tuna of the Mediterranean Sea. *Proceedings of the National Academy of Sciences of the United States of America*, **107**, 2102-2107.
- Rice WR (1989) Analyzing tables of statistical tests. *Evolution*, **43**, 223-225.
- Richardson TJ (2010) The taxonomy, life-history and population dynamics of blacktail, *Diplodus capensis* (Perciformes: Sparidae), in southern Angola. In: *Department of Ichthyology and Fishery Sciences*, p. 157. Rhodes University, Grahamstown.
- Riginos C, Nachman MW (2001) Population subdivision in marine environments: the contributions of biogeography, geographical distance and discontinuous habitat to genetic differentiation in a blennioid fish, *Axoclinus nigricaudus*. *Molecular Ecology*, **10**, 1439-1453.
- Roberts DG, Ayre DJ (2010) Panmictic population structure in the migratory marine sparid *Acanthopagrus australis* despite its close association with estuaries. *Marine Ecology-Progress Series*, **412**, 223-230.
- Rocha LA, Robertson DR, Roman J, Bowen BW (2005) Ecological speciation in tropical reef fishes. *Proceedings of the Royal Society B-Biological Sciences*, **272**, 573-579.

- Rocha-Olivares A, Rosenblatt RH, Vetter RD (1999) Molecular evolution, systematics, and zoogeography of the rockfish subgenus *Sebastomus* (Sebastes, Scorpaenidae) based on mitochondrial cytochrome b and control region sequences. *Molecular Phylogenetics and Evolution*, **11**, 441-458.
- Roff DA (1988) The evolution of migration and some life-history parameters in marine fishes. *Environmental Biology of Fishes*, **22**, 133-146.
- Rogers SM, Bernatchez L (2006) The genetic basis of intrinsic and extrinsic post-zygotic reproductive isolation jointly promoting speciation in the lake whitefish species complex (*Coregonus clupeaformis*). *Journal of Evolutionary Biology*, **19**, 1979-1994.
- Ronquist F, Huelsenbeck JP (2003) MrBayes 3: Bayesian phylogenetic inference under mixed models. *Bioinformatics*, **19**, 1572-1574.
- Roques S, Galarza JA, Macpherson E, Turner GF, Rico C (2007) Isolation and characterization of nine polymorphic microsatellite markers in the two-banded sea bream (*Diplodus vulgaris*) and cross-species amplification in the white sea bream (*Diplodus sargus*) and the saddled bream (*Oblada melanura*). *Molecular Ecology Notes*, **7**, 661-663.
- Rozen S, Skalestky HJ (1998) PRIMER 3. (ed. Whitehead Institute for Biomedical Research C, Massachusetts), Massachusetts.
- Rundell RJ, Price TD (2009) Adaptive radiation, nonadaptive radiation, ecological speciation and nonecological speciation. *Trends in Ecology & Evolution*, **24**, 394-399.
- Rundle HD, Nosil P (2005) Ecological speciation. *Ecology Letters*, **8**, 336-352.
- Runge JA, Kovach AI, Churchill JH, Kerr LA, Morrison JR, Beardsley RC, Berlinsky DL, Chen CS, Cadrin SX, Davis CS, Ford KH, Grabowski JH, Howell WH, Ji RB, Jones RJ, Pershing AJ, Record NR, Thomas AC, Sherwood GD, Tallack SML, Townsend DW (2010) Understanding climate impacts on recruitment and spatial dynamics of Atlantic cod in the Gulf of Maine: Integration of observations and modeling. *Progress in Oceanography*, **87**, 251-263.
- Ruzzante DE, Walde SJ, Macchi PJ, Alonso M, Barriga JP (2011) Phylogeography and phenotypic diversification in the Patagonian fish *Percichthys trucha*: the roles of Quaternary glacial cycles and natural selection. *Biological Journal of the Linnean Society*, **103**, 514-529.
- Saavedra C, Stewart DT, Stanwood RR, Zouros E (1996) Species-specific segregation of gender-associated mitochondrial DNA types in an area where two mussel species (*Mytilus edulis* and *M. trossulus*) hybridize. *Genetics*, **143**, 1359-1367.

- Sachs JP, Anderson RF, Lehman SJ (2001) Glacial surface temperatures of the southeast Atlantic Ocean. *Science*, **293**, 2077-2079.
- Sakko AL (1998) The influence of the Benguela upwelling system on Namibia's marine biodiversity. *Biodiversity and Conservation*, **7**, 419-433.
- Sambrook J, Fritscher EF, Maniatis T (1989) *Molecular cloning: a laboratory manual*. Cold Spring Harbor Laboratory Press, New York, USA.
- Sanders KL, Lee MSY (2007) Evaluating molecular clock calibrations using Bayesian analyses with soft and hard bounds. *Biology Letters*, **3**, 275-279.
- Sandoval-Castellanos E, Uribe-Alcocer M, Diaz-Jaimes P (2007) Population genetic structure of jumbo squid (*Dosidicus gigas*) evaluated by RAPD analysis. *Fisheries Research*, **83**, 113-118.
- Santos S, Hrbek T, Farias IP, Schneider H, Sampaio I (2006) Population genetic structuring of the king weakfish, *Macrodon ancylodon* (Sciaenidae), in Atlantic coastal waters of South America: deep genetic divergence without morphological change. *Molecular Ecology*, **15**, 4361-4373.
- Sasaki K (1989) Phylogeny of the family Sciaenidae, with notes on its zoogeography (Teleostei, Perciformes). *Memoirs of the Faculty of Fisheries, Hokkaido University*, **36**, 1-137.
- Schluter D (2009) Evidence for ecological speciation and its alternative. *Science*, **323**, 737-741.
- Schmieder F, von Dobeneck T, Bleil U (2000) The Mid-Pleistocene climate transition as documented in the deep South Atlantic Ocean: initiation, interim state and terminal event. *Earth and Planetary Science Letters*, **179**, 539-549.
- Schulte PM (2001) Environmental adaptations as windows on molecular evolution. *Comparative Biochemistry and Physiology B-Biochemistry & Molecular Biology*, **128**, 597-611.
- Scoles DR, Graves JE (1993) Genetic analysis of population structure of yellowfin tuna, *Thunnus albacares*, from the Pacific Ocean. *Fishery Bulletin US*, **91**, 690-698.
- Scoles DR, Collette BB, Graves JE (1998) Global phylogeography of mackerels of the genus *Scomber*. *Fishery Bulletin (Washington D C)*, **96**, 823-842.
- Selkoe KA, Toonen RJ (2006) Microsatellites for ecologists: a practical guide to using and evaluating microsatellite markers. *Ecology Letters*, **9**, 615-629.
- Sevilla RG, Diez A, Noren M, Mouchel O, Jerome M, Verrez-Bagnis V, van Pelt H, Favre-Krey L, Krey G, Bautista JM, Fishrace C (2007) Primers and polymerase chain reaction conditions

for DNA barcoding teleost fish based on the mitochondrial cytochrome b and nuclear rhodopsin genes. *Molecular Ecology Notes*, **7**, 730-734.

Shannon LV (1985) The Benguela ecosystem - 1. Evolution of the Benguela, physical features and processes. *Oceanography and Marine Biology*, **23**, 105-&.

Shaw PW, Arkhipkin AI, Al-Khairulla H (2004) Genetic structuring of Patagonian toothfish populations in the Southwest Atlantic Ocean: the effect of the Antarctic Polar Front and deep-water troughs as barriers to genetic exchange. *Molecular Ecology*, **13**, 3293-3303.

Shen KN, Jamandre BW, Hsu CC, Tzeng WN, Durand JD (2011) Plio-Pleistocene sea level and temperature fluctuations in the northwestern Pacific promoted speciation in the globally-distributed flathead mullet *Mugil cephalus*. *Bmc Evolutionary Biology*, **11**.

Shillington FA, Reason CJC, Duncombe RCM, Florenchie P, Penven P (2004) Large scale physical variability of the Benguela Current Large Marine Ecosystem (BCLME). In: *Benguela: Predicting a Large Marine Ecosystem* (ed. Shannon V, Gotthilf H, Malanotte-Rizzoli P, Moloney C, Woods J), p. 410. Elsevier, Amsterdam, The Netherlands.

Siesser WG (1980) Late Miocene origin of the Benguela upwelling system off northern Namibia. *Science*, **208**, 283-285.

Siesser WG, Dingle RV (1981) Tertiary sea-level movements around southern Africa. *Journal of Geology*, **89**, 523-536.

Silberschneider V, Gray CA (2008) Synopsis of biological, fisheries and aquaculture-related information on mulloway *Argyrosomus japonicus* (Pisces: Sciaenidae), with particular reference to Australia. *Journal of Applied Ichthyology*, **24**, 7-17.

Simpson GG (1951) The species concept. *Evolution*, **5**, 285-298.

Sinnock P (1975) Wahlund effect for 2-locus model. *American Naturalist*, **109**, 565-570.

Sivasundar A, Palumbi SR (2010) Life history, ecology and the biogeography of strong genetic breaks among 15 species of Pacific rockfish, *Sebastes*. *Marine Biology*, **157**, 1433-1452.

Slatkin M (1994) An exact test for neutrality based on the ewens sampling distribution. *Genetical Research*, **64**, 71-74.

Sowman M, Hauck M, van Sittert L, Sunde J (2011) Marine Protected Area management in South Africa: new policies, old paradigms. *Environmental Management*, **47**, 573-583.

Stephens M, Smith NJ, Donnelly P (2001) A new statistical method for haplotype reconstruction from population data. *American Journal of Human Genetics*, **68**, 978-989.

- Stepien CA, Rosenblatt RH (1996) Genetic divergence in antitropical pelagic marine fishes (*Trachurus*, *Merluccius*, and *Scomber*) between North and South America. *Copeia*, 586-598.
- Summerer M, Hanel R, Sturmbauer C (2001) Mitochondrial phylogeny and biogeographic affinities of sea breams of the genus *Diplodus* (Sparidae). *Journal of Fish Biology*, **59**, 1638-1652.
- Sunnucks P (2000) Efficient genetic markers for population biology. *Trends in Ecology & Evolution*, **15**, 199-203.
- Swofford DL (1993) PAUP - a computer program for phylogenetic inference using maximum parsimony. *Journal of General Physiology*, **102**, A9-A9.
- Tajima F (1989) Statistical method for testing the neutral mutation hypothesis by DNA polymorphism. *Genetics*, **123**, 585-595.
- Tamura K, Nei M (1993) Estimation of the number of nucleotide substitutions in the control region of mitochondrial DNA in humans and chimpanzees. *Molecular Biology and Evolution*, **10**, 512-526.
- Tang QY, Liu HZ, Mayden R, Xiong BX (2006) Comparison of evolutionary rates in the mitochondrial DNA cytochrome b gene and control region and their implications for phylogeny of the *Cobitoidea* (Teleostei: Cypriniformes). *Molecular Phylogenetics and Evolution*, **39**, 347-357.
- Tatarenkov A, Healey CIM, Avise JC (2010) Microgeographic population structure of green swordtail fish: genetic differentiation despite abundant migration. *Molecular Ecology*, **19**, 257-268.
- Taylor MS, Hellberg ME (2005) Marine radiations at small geographic scales: speciation in neotropical reef gobies (*Elacatinus*). *Evolution*, **59**, 374-385.
- Teske PR, Cherry MI, Matthee CA (2003) Population genetics of the endangered Knysna seahorse, *Hippocampus capensis*. *Molecular Ecology*, **12**, 1703-1715.
- Teske PR, Forget FRG, Cowley PD, von der Heyden S, Beheregaray LB (2010) Connectivity between marine reserves and exploited areas in the philopatric reef fish *Chrysoblephus laticeps* (Teleostei: Sparidae). *Marine Biology*, **157**, 2029-2042.
- Teske PR, McQuaid CD, Froneman PW, Barker NP (2006) Impacts of marine biogeographic boundaries on phylogeographic patterns of three South African estuarine crustaceans. *Marine Ecology-Progress Series*, **314**, 283-293.

- Thompson JD, Gibson TJ, Plewniak F, Jeanmougin F, Higgins DG (1997) The CLUSTAL_X windows interface: flexible strategies for multiple sequence alignment aided by quality analysis tools. *Nucleic Acids Research*, **25**, 4876-4882.
- Tobler M, Riesch R, Tobler CM, Schulz-Mirbach T, Plath M (2009) Natural and sexual selection against immigrants maintains differentiation among micro-allopatric populations. *Journal of Evolutionary Biology*, **22**, 2298-2304.
- Triantafyllidis A, Leonardos I, Bista I, Kyriazis ID, Stoumboudi MT, Kappas I, Amat F, Abatzopoulos TJ (2007) Phylogeography and genetic structure of the Mediterranean killifish *Aphanius fasciatus* (Cyprinodontidae). *Marine Biology*, **152**, 1159-1167.
- Vähä J, Primmer C (2006) Efficiency of model-based Bayesian methods for detecting hybrid individuals under different hybridisation scenarios and with different numbers of loci. *Molecular Ecology*, **15**, 63-72.
- van der Bank H, Kirchner C (1997) Biochemical genetic markers to distinguish two sympatric and morphologically similar Namibian marine fish species, *Argyrosomus coronus* and *A. inodorus* (Perciformes: Sciaenidae). *Journal of African Zoology*, **111**, 441-448.
- van der Elst RP, Govender A, Chater SA (1992) The biology and status of garrick (*Lichia amia*). In: *Fish, Fishers and Fisheries - Second South African Marine Linefish Symposium* (ed. Beckley LE, van der Elst RP), pp. 28-31. Special publication of the Oceanographic Research Institute, Durban.
- van Hal R, Smits K, Rijnsdorp AD (2010) How climate warming impacts the distribution and abundance of two small flatfish species in the North Sea. *Journal of Sea Research*, **64**, 76-84.
- van Oosterhout C, Weetman D, Hutchinson WF (2006) Estimation and adjustment of microsatellite null alleles in nonequilibrium populations. *Molecular Ecology Notes*, **6**, 255-256.
- van Valen L (1976) Ecological species multi species and oaks. *Taxon*, **25**, 233-239.
- Verissimo A, McDowell JR, Graves JE (2010) Global population structure of the spiny dogfish *Squalus acanthias*, a temperate shark with an antitropical distribution. *Molecular Ecology*, **19**, 1651-1662.
- Vinas J, Perez-Serra A, Vidal O, Bremer JRA, Pla C (2010) Genetic differentiation between eastern and western Mediterranean swordfish revealed by phylogeographic analysis of the mitochondrial DNA control region. *Ices Journal of Marine Science*, **67**, 1222-1229.
- Vincze T, Posfai J, Roberts RJ (2003) NEBcutter: a program to cleave DNA with restriction enzymes. *Nucleic Acids Research*, **31**, 3688-3691.

- Vinson C, Gomes G, Schneider H, Sampaio I (2004) Sciaenidae fish of the Caete River estuary, Northern Brazil: mitochondrial DNA suggests explosive radiation for the Western Atlantic assemblage. *Genetics and Molecular Biology*, **27**, 174-180.
- von der Heyden S, Lipinski MR, Matthee CA (2007) Mitochondrial DNA analyses of the Cape hakes reveal an expanding, panmictic population for *Merluccius capensis* and population structuring for mature fish in *Merluccius paradoxus*. *Molecular Phylogenetics and Evolution*, **42**, 517-527.
- von der Heyden S, Lipinski MR, Matthee CA (2010) Remarkably low mtDNA control region diversity in an abundant demersal fish. *Molecular Phylogenetics and Evolution*, **55**, 1183-1188.
- von der Heyden S, Prochazka K, Bowie RCK (2008) Significant population structure and asymmetric gene flow patterns amidst expanding populations of *Clinus cottoides* (Perciformes, Clinidae): application of molecular data to marine conservation planning in South Africa. *Molecular Ecology*, **17**, 4812-4826.
- Waples RS (1998) Separating the wheat from the chaff: Patterns of genetic differentiation in high gene flow species. *Journal of Heredity*, **89**, 438-450.
- Waples RS (2006) A bias correction for estimates of effective population size based on linkage disequilibrium at unlinked gene loci. *Conservation Genetics*, **7**, 167-184.
- Waples RS, Do C (2008) LDNE: a program for estimating effective population size from data on linkage disequilibrium. *Molecular Ecology Resources*, **8**, 753-756.
- Waples RS, Do C (2010) Linkage disequilibrium estimates of contemporary N_e using highly variable genetic markers: a largely untapped resource for applied conservation and evolution. *Evolutionary Applications*, **3**, 244-262.
- Ward R, Bowers K, Hensley R, Mobley B, Belouski E (2007) Genetic variability in spotted seatrout (*Cynoscion nebulosus*), determined with microsatellite DNA markers. *Fishery Bulletin*, **105**, 197-206.
- Ward RD (1995) Population genetics of tunas. *Journal of Fish Biology*, **47**, 259-280.
- Ward RD (2000) Genetics in fisheries management. *Hydrobiologia*, **420**, 191-201.
- Ward RD, Elliott NG, Grewe PM, Smolenski AJ (1994a) Allozyme and mitochondrial DNA variation in yellowfin tuna (*Thunnus albacares*) from the Pacific ocean. *Marine Biology*, **118**, 531-539.

- Ward RD, Elliott NG, Innes BH, Smolenski AJ, Grewe PM (1997) Global population structure of yellowfin tuna, *Thunnus albacares*, inferred from allozyme and mitochondrial DNA variation. *Fishery Bulletin*, **95**, 566-575.
- Ward RD, Woodwark M, Skibinski DOF (1994b) A comparison of genetic diversity levels in marine, freshwater, and anadromous fishes. *Journal of Fish Biology*, **44**, 213-232.
- Ward RD, Zemlak TS, Innes BH, Last PR, Hebert PDN (2005) DNA barcoding Australia's fish species. *Philosophical Transactions of the Royal Society B-Biological Sciences*, **360**, 1847-1857.
- Watanabe K, Kawase S, Mukai T, Kakioka R, Miyazaki JI, Hosoya K (2010) Population divergence of *Biwia zezera* (Cyprinidae: Gobioninae) and the discovery of a cryptic species, based on mitochondrial and nuclear DNA sequence analyses. *Zoological Science*, **27**, 647-655.
- Waters JM, Roy MS (2003) Global phylogeography of the fissiparous sea-star genus *Coscinasterias*. *Marine Biology*, **142**, 185-191.
- Waters JM, Roy MS (2004) Phylogeography of a high-dispersal New Zealand sea-star: does upwelling block gene-flow? *Molecular Ecology*, **13**, 2797-2806.
- Weir BS (1986) *Genetic data analysis II*. Sinauer Associates. Sunderland, Massachusetts.
- White C, Selkoe KA, Watson J, Siegel DA, Zacherl DC, Toonen RJ (2010) Ocean currents help explain population genetic structure. *Proceedings of the Royal Society B-Biological Sciences*, **277**, 1685-1694.
- Whitlock MC, McCauley DE (1999) Indirect measures of gene flow and migration: F_{ST} not equal $1/(4Nm+1)$. *Heredity*, **82**, 117-125.
- Wilson CC, Bernatchez L (1998) The ghost of hybrids past: fixation of arctic charr (*Salvelinus alpinus*) mitochondrial DNA in an introgressed population of lake trout (*S. namaycush*). *Molecular Ecology*, **7**, 127-132.
- Winnepenninckx B, Backeljau T, Dewachter R (1993) Extraction of high-molecular-weight DNA from mollusks. *Trends in Genetics*, **9**, 407-407.
- Wirtz P (1999) Mother species-father species: unidirectional hybridization in animals with female choice. *Animal Behaviour*, **58**, 1-12.
- Worheide G, Epp LS, Macis L (2008) Deep genetic divergences among Indo-Pacific populations of the coral reef sponge *Leucetta chagosensis* (Leucettidae): Founder effects, vicariance, or both? *Bmc Evolutionary Biology*, **8**.

Wright S (1965) The interpretation of population structure by F-statistics with special regard to the systems of mating. *Evolution*, **19**, 395-420.

Wu GCC, Chiang HC, Chou YW, Wong ZR, Hsu CC, Chen CY, Yang HY (2010) Phylogeography of yellowfin tuna (*Thunnus albacares*) in the Western Pacific and the Western Indian Oceans inferred from mitochondrial DNA. *Fisheries Research*, **105**, 248-253.

York KL, Blacket MJ, Appleton BR (2008) The Bassian Isthmus and the major ocean currents of southeast Australia influence the phylogeography and population structure of a southern Australian intertidal barnacle *Catomerus polymerus* (Darwin). *Molecular Ecology*, **17**, 1948-1961.

Zakas C, Binford J, Navarrete SA, Wares JP (2009) Restricted gene flow in Chilean barnacles reflects an oceanographic and biogeographic transition zone. *Marine Ecology-Progress Series*, **394**, 165-177.

Zane L, Marcato S, Bargelloni L, Bortolotto E, Papetti C, Simonato M, Sarotto V, Pattarnello T (2006) Demographic history and population structure of the Antarctic silver fish *Pleuragramma antarcticum*. *Molecular Ecology*, **15**, 4499-4511.

Zardi GI, McQuaid CD, Teske PR, Barker NP (2007) Unexpected genetic structure of mussel populations in South Africa: indigenous *Perna perna* and invasive *Mytilus galloprovincialis*. *Marine Ecology-Progress Series*, **337**, 135-144.

Zarraonaindia I, Angel Pardo M, Iriondo M, Manzano C, Estonba A (2009) Microsatellite variability in European anchovy (*Engraulis encrasicolus*) calls for further investigation of its genetic structure and biogeography. *ICES Journal of Marine Science*, **66**, 2176-2182.

Zemlak TS, Ward RD, Connell AD, Holmes BH, Hebert PDN (2009) DNA barcoding reveals overlooked marine fishes. *Molecular Ecology Resources*, **9**, 237-242.